PB86-167152

# Symposium on the Transfer and Utilization of Particulate Control Technology (5th). Volume 1

Research Triangle Inst.
Research Triangle Park, NC

Prepared for

Environmental Protection Agency
Research Triangle Park, NC

Feb 86

U.S. Department of Commerce
National Technical Information Service
NTIS

PB86-167152

EPA/600/9-86/008a
February 1986

# Proceedings: Fifth Symposium on the Transfer and Utilization of Particulate Control Technology

Volume 1

Franklin A. Ayer, Compiler

Research Triangle Institute
P.O. Box 12194
Research Triangle Park, North Carolina 27709

EPA Cooperative Agreement CR810152

EPA Project Officer:
Dale L. Harmon
Air and Energy Engineering Research Laboratory
Research Triangle Park, NC 27711

EPRI Project Manager:
R. F. Altman
Air Quality Control Program
Coal Combustion Systems Division
Palo Alto, California 94304

REPRODUCED BY
NATIONAL TECHNICAL INFORMATION SERVICE
U.S. DEPARTMENT OF COMMERCE
SPRINGFIELD, VA. 22161

AIR AND ENERGY ENGINEERING RESEARCH LABORATORY
OFFICE OF RESEARCH AND DEVELOPMENT
U.S. ENVIRONMENTAL PROTECTION AGENCY
RESEARCH TRIANGLE PARK, NC 27711

## TECHNICAL REPORT DATA
*(Please read Instructions on the reverse before completing)*

| | | |
|---|---|---|
| 1. REPORT NO.<br>EPA/600/9-86/008a | 2. | 3. RECIPIENT'S ACCESSION NO.<br>PB86 167152/AS |
| 4. TITLE AND SUBTITLE<br>Proceedings: Fifth Symposium on the Transfer and Utilization of Particulate Control Technology, Volume 1 | | 5. REPORT DATE<br>February 1986<br>6. PERFORMING ORGANIZATION CODE |
| 7. AUTHOR(S)<br>Franklin A. Ayer, Compiler | | 8. PERFORMING ORGANIZATION REPORT NO.<br>EPRI CS-4404, V1-4 |
| 9. PERFORMING ORGANIZATION NAME AND ADDRESS<br>Research Triangle Institute<br>P.O. Box 12194<br>Research Triangle Park, North Carolina 27709 | | 10. PROGRAM ELEMENT NO.<br>11. CONTRACT/GRANT NO.<br>CR810152 |
| 12. SPONSORING AGENCY NAME AND ADDRESS<br>EPA, Office of Research and Development*<br>Air and Energy Engineering Research Laboratory<br>Research Triangle Park, NC 27711 | | 13. TYPE OF REPORT AND PERIOD COVERED<br>Proceedings; August 1984<br>14. SPONSORING AGENCY CODE<br>EPA/600/13 |

15. SUPPLEMENTARY NOTES AEERL project officer is Dale L. Harmon, Mail Drop 61, 919/541-2429. EPA-600/9-84-025a, b, and c were proceedings for the fourth symposium. (*) Cosponsored by EPRI.

16. ABSTRACT The proceedings document the Fifth Symposium on the Transfer and Utilization of Particulate Control Technology, held August 27-30, 1984, in Kansas City, MO. The symposium was sponsored by EPA's Air and Energy Engineering Research Laboratory (formerly the Industrial and Environmental Research Laboratory), located in Research Triangle Park, NC, and EPRI's Coal Combustion Systems Division, in Palo Alto, CA. The symposium provided for the exchange of knowledge and to stimulate new ideas for particulate control with the goal of extending the technology and aiding its diffusion among designers, users, and educators. Fabric filters and ESPs received the major attention, but novel concepts and advanced technologies were also explored. Volume 1 covered the plenary session, advanced energy applications, economics, and novel concepts. Volume 2 was devoted to electrostatic precipitators. Volume 3 dealt with fabric filters. Volume 4 described fugitive emissions, dry SO2, and operation and maintenance.

17. KEY WORDS AND DOCUMENT ANALYSIS

| a. DESCRIPTORS | | b. IDENTIFIERS/OPEN ENDED TERMS | c. COSATI Field/Group | |
|---|---|---|---|---|
| Pollution | Economics | Pollution Control | 13B | 05C |
| Particles | Processing | Stationary Sources | 14G | 13H |
| Aerosols | Leakage | Particulate | 07D | |
| Electrostatic Precipitators | | Fabric Filters | 13I | |
| Filtration | | Fugitive Emissions | | |
| Fabrics | | | 11E | |

| | | |
|---|---|---|
| 18. DISTRIBUTION STATEMENT<br>Release to Public | 19. SECURITY CLASS *(This Report)*<br>Unclassified | 21. NO. OF PAGES<br>286 |
| | 20. SECURITY CLASS *(This page)*<br>Unclassified | 22. PRICE |

EPA Form 2220-1 (9-73)

# NOTICE

This document has been reviewed in accordance with U.S. Environmental Protection Agency policy and approved for publication. Mention of trade names or commercial products does not constitute endorsement or recommendation for use.

## ORDERING INFORMATION

Requests for copies of this report should be directed to Research Reports Center (RRC), Box 50490, Palo Alto, CA 94303, (415) 965-4081. There is no charge for reports requested by EPRI member utilities and affiliates, U.S. utility associations, U.S. government agencies (federal, state, and local), media, and foreign organizations with which EPRI has an information exchange agreement. *

(*) Copies of this report are available to the public through the National Technical Information Service, Springfield, Virginia 22161.

**Copyright © 1986, EPRI CS-4404, V1-4, "Proceedings: Fifth Symposium on the Transfer and Utilization of Particulate Control Technology, Volumes 1-4." Since this work was, in part, funded by the U.S. Government, the Government is vested with a royalty-free, non-exclusive, and irrevocable license to publish, translate, reproduce, and deliver that information and to authorize others to do so.**

NOTICE

This report was prepared by the Electric Power Research Institute, Inc. (EPRI). Neither EPRI, members of EPRI, nor any person acting on their behalf (a) makes any warranty, express or implied, with respect to the use of any information, apparatus, method, or process disclosed in this report or that such use may not infringe privately owned rights; or (b) assumes any liabilities with respect to the use of, or for damages resulting from the use of, any information, apparatus, method, or process disclosed in this report; or (c) is responsible for statements made or opinions expressed by individual authors.

# ABSTRACT

These proceedings are of the Fifth Symposium on the Transfer and Utilization of Particulate Control Technology, held August 27 to 30, 1984, in Kansas City, Missouri. The symposium was sponsored by EPA's Air and Energy Engineering Research Laboratory (formerly Industrial Environmental Research Laboratory), located in Research Triangle Park, North Carolina, and the EPRI Coal Combustion Systems Division, located in Palo Alto, California.

The objective of the symposium was to provide for the exchange of knowledge and to stimulate new ideas for particulate control with the goal of extending the technology and aiding its diffusion among designers, users, and educators. Fabric filters and electrostatic precipitators were the major topics, but novel concepts and advanced technologies were also explored. The organization of sessions was as follows:

- Day 1
  - --Plenary session
  - --ESP: Performance Estimating (Modeling)
  - --FF: Practical Considerations
  - --Economics
  - --Novel Concepts
- Day 2
  - --ESP: Performance Enhancement I
  - --FF: Full-Scale Studies I (Coal-Fired Boilers)
  - --Fugitive Emissions I
  - --ESP: Performance Enhancement II
  - --FF: Full-Scale Studies II (Coal-Fired Boilers)
  - --Fugitive Emissions II
- Day 3
  - --ESP: Advanced Technology I
  - --FF: Fundamentals/Measurement Techniques

--Dry $SO_2$ Removal I

--ESP: Advanced Technology II

--FF: Advanced Concepts

--Dry $SO_2$ Removal II

- Day 4

--ESP: Fundamentals I

--FF: Pilot-Scale Studies (Coal-Fired Boilers)

--Operation and Maintenance I

--ESP: Fundamentals II

--Advanced Energy Applications

--Operations and Maintenance II

Volume 1 contains 19 papers presented at the Plenary, Advanced Energy Applications, Economics and Novel Concepts Sessions.

Volume 2 contains 33 papers presented at the ESP: Performance Estimating (Modeling), ESP: Performance Enhancement I and II, ESP: Advanced Technology I and II, and ESP: Fundamentals I and II Sessions, plus one unpresented paper.

Volume 3 contains 24 papers presented at the FF: Practical Considerations, FF: Full-Scale Studies I and II (Coal-Fired Boilers), FF: Fundamentals/Measuring Techniques, FF: Advanced Concepts, and FF: Pilot-Scale Studies (Coal-Fired Boilers) Sessions.

Volume 4 contains 29 papers presented at the Fugitive Emissions I and II, Dry $SO_2$ Removal I and II, and Operations Maintenance I and II.

# PREFACE

These proceedings for the Fifth Symposium on the Transfer and Utilization of Particulate Control Technology constitute the final report submitted to EPA's Air and Energy Engineering Research Laboratory (AEERL), Research Triangle Park, North Carolina, and to the Coal Combustion Systems Division, EPRI, Palo Alto, California. The symposium was conducted at the Hyatt Regency Hotel at the Crown Center in Kansas City, Missouri, August 27-30, 1984.

This symposium (the first jointly sponsored by EPA and EPRI) was designed to provide a forum for the exchange of knowledge and to stimulate new ideas for particulate control with the goal of extending technology and aiding its diffusion among designers, users, educators, and researchers. In the opening session, an address was given on the regulatory framework for future particulate technology needs followed by a series of addresses on the impact of coming particulate requirements on the utility industry and the iron and steel industry as well as the viewpoint of large and small manufacturers. There were subsequent technical sessions on electrostatic precipitator performance estimating (modeling), ESP performance enhancement, ESP advanced technology, ESP fundamentals, practical considerations for fabric filters, fabric filter full-scale studies (coal-fired boilers), fabric filter fundamentals/measurement techniques, fabric filter pilot-scale studies (coal-fired boilers), fugitive emissions, dry $SO_2$ removal, operation and maintenance, and advanced energy applications. Participants represented electric utilities, equipment and process suppliers, state environmental agencies, coal and petroleum suppliers, EPA and other Federal agencies, educational institutions, and research organizations.

The following persons contributed their efforts to this symposium:

- Dale L. Harmon, Chemical Engineer, Particulate Technology Branch, Utilities and Industrial Power Division, U.S. EPA, AEERL, Research Triangle Park, North Carolina, was a symposium co-general chairman and EPA project officer.

- Ralph F. Altman, Ph.D., Project Manager, Coal Combustion Systems Division, EPRI, Chattanooga, Tennessee, was a co-general chairman and EPRI project manager.

- Franklin A. Ayer, Consultant, Research Triangle Institute, Research Triangle Park, North Carolina, was the overall symposium coordinator and compiler of the proceedings.

## TABLE OF CONTENTS

VOLUME 1, PLENARY, ADVANCED ENERGY APPLICATIONS, ECONOMICS, AND NOVEL CONCEPTS

VOLUME 2, ELECTROSTATIC PRECIPITATION

VOLUME 3, FABRIC FILTRATION

VOLUME 4, FUGITIVE EMISSIONS, DRY $SO_2$, AND OPERATION AND MAINTENANCE

## VOLUME 1
## PLENARY, ADVANCED ENERGY APPLICATIONS, ECONOMICS, AND NOVEL CONCEPTS

Page

Session 1: PLENARY SESSION . . . . . . . . . . . . . . . . . . . . 1
Everett L. Plyler, Chairman

The Regulatory Framework for Future Particulate Technology Needs . . . . . . . . . . . . . . . . . . . . 2
Sheldon Meyers

The Impact of Coming Particulate Control Requirements on the Utility Industry . . . . . . . . . . . . . . . . . . . . 9
George T. Preston

The Impact of Coming Particulate Control Requirements on the Iron and Steel Industry. . . . . . . . . . . . . . . . . . . . 16
Earle F. Young, Jr.

The Impact of Particulate Control Requirements: Large Manufacturer's Viewpoint . . . . . . . . . . . . . . . . . . . . 22
Herbert H. Braden
Paper presented by Gary R. Gawreluk

Future Particulate Regulations: The View of the Small Manufacturer . . . . . . . . . . . . . . . . . . . . 33
Sidney R. Orem

Session 2: ADVANCED ENERGY APPLICATIONS. . . . . . . . . . . . . . 36
George A. Rinard, Chairman

Page

High-Temperature, High-Pressure Electrostatic Precipitation, Current Status . . . . . . . . . . . . . . . . . . 37
P. L. Feldman* and K. S. Kumar

Test Results of a Precipitator Operating at High-Temperature and High-Pressure Conditions . . . . . . . . . . . . . . . . . . 50
Donald E. Rugg*, George Rinard, Michael Durham, and James Armstrong

Evaluation and Development of Candidate High Temperature Filter Devices for Pressurized Fluidized Bed Combustion. . . . 64
T. E. Lippert*, D. F. Ciliberti, S. G. Drenker, and O. J. Tassicker

High Temperature Gas Filtration with Ceramic Filter Media: Problems and Solutions . . . . . . . . . . . . . . . . . 79
Ramsay Chang

The Development and High Temperature Application of a Novel Method for Measuring Ash Deposits and Cake Removal on Filter Bags. . . . . . . . . . . . . . . . . . 92
David F. Ciliberti*, Thomas E. Lippert, Owen J. Tassicker, and Steven Drenker

Session 3: ECONOMICS . . . . . . . . . . . . . . . . . . . . . . 107
John S. Lagarias, Chairman

Economics of Electrostatic Precipitators and Fabric Filters . . . . . . . . . . . . . . . . . . . . . . 108
Victor H. Belba*, Fay A. Horney, Robert C. Carr, and Walter Piulle

Estimating the Benefits of $SO_3$ Gas Conditioning on the Performance of Utility Precipitators When Burning U.S. Coals . . . . . . . . . . . . . . . . . . . . . . . . 126
Peter Gelfand

Microcomputer Models for Particulate Control . . . . . . . . . 135
A. S. Viner*, D. S. Ensor, and L. E. Sparks

The Impact of Proposed Acid Rain Legislation on Power Plant Particulate Control Equipment. . . . . . . . . . . . . 142
William H. Cole

Session 4: NOVEL CONCEPTS. . . . . . . . . . . . . . . . . . . . 158
Dale L. Harmon, Chairman

*Denotes speaker

Page

Particle Charging with an Electron Beam Precharger . . . . . . 159
J. S. Clements*, A. Mizuno, and R. H. Davis

Charging of Particulates by Evaporating Charged Water Droplets . . . . . . . . . . . . . . . . . . . . . . . . . . 175
G. S. P. Castle*, I. I. Inculet, and R. Littlewood

Role of Electrostatic Forces in High Velocity Particle Collection Devices . . . . . . . . . . . . . . . . . . . . . . . 187
H. C. Wang, J. J. Stukel*, K. H. Leong, and P. K. Hopke

Hot-Gas Fabric Filtration 500° F - 1500° F, No Utopia but Reality. . . . . . . . . . . . . . . . . . . . . . . . . . . . . 201
Lutz Bergmann

The Prediction of Plume Opacity from Stationary Sources. . . . 211
David S. Ensor*, Ashok S. Damle, Philip A. Lawless, and Leslie E. Sparks

APPENDIX: Attendees . . . . . . . . . . . . . . . . . . . . . . . 234

VOLUME 2
ELECTROSTATIC PRECIPITATION

Session 5: ESP: PERFORMANCE ESTIMATING (MODELING) . . . . . . . 267
Leslie E. Sparks, Chairman

Microcomputer Programs for Precipitator Performance Estimates. . . . . . . . . . . . . . . . . . . . . . . . . . . . 268
M. G. Faulkner*, J. L. DuBard, R. S. Dahlin, and Leslie E. Sparks

Analysis of Error in Precipitator Performance Estimates. . . . 283
J. L. DuBard* and R. F. Altman

Use of a Mobile Electrostatic Precipitator for Pilot Studies. . . . . . . . . . . . . . . . . . . . . . . . . . . . . 299
Robert R. Crynack* and John D. Sherow

Prediction of Voltage-Current Curves for Novel Electrodes--Arbitrary Wire Electrodes on Axis. . . . . . . . . 314
Phil A. Lawless* and L. E. Sparks

Numerical Computation of the Electrical Conditions in a Wire-Plate Electrostatic Precipitator Using the Finite Element Technique. . . . . . . . . . . . . . . . . . . . . . 328
Gregory A. Kallio* and David E. Stock

*Denotes speaker

Page

Session 6: ESP: PERFORMANCE ENHANCEMENT I . . . . . . . . . . . . 345
Ralph F. Altman, Chairman

A Field Study of a Combined $NH_3$-$SO_3$ Conditioning System on a Cold-Side Fly Ash Precipitator at a Coal-Fired Power Plant. . . . . . . . . . . . . . . . . . . . . . . . . 346
Robert S. Dahlin*, John P. Gooch, Guillaume H. Marchant, Jr., Roy E. Bickelhaupt, D. Richard Sears, and Ralph F. Altman

Conditioning of Power Station Flue Gases to Improve Electrostatic Precipitator Efficiency. . . . . . . . . . . . . . 362
Gernot Mayer-Schwinning* and J. D. Riley

Pilot-Scale Study of a New Method of Flue-Gas Conditioning with Ammonium Sulfate. . . . . . . . . . . . . . . . . . . . . 375
Edward B. Dismukes*, E. C. Landham, Jr., John P. Gooch, and Ralph F. Altman

Power Plant Plume Opacity Control. . . . . . . . . . . . . . . . 390
J. Martin Hughes* and Kai-Tien Lee

Pulse Energization System of Electrostatic Precipitator for Retrofitting Application . . . . . . . . . . . . . . . . . . 404
Senichi Masuda* and Shunsuke Hosokawa

Session 7: ESP: PERFORMANCE ENHANCEMENT II. . . . . . . . . . . . 419
B. G. McKinney, Chairman

Practical Implications of Pulse Energization of Electrostatic Precipitators. . . . . . . . . . . . . . . . . . . 420
H. Milde*, J. Ottesen, and C. Salisbury

Laboratory and Full-Scale Characteristics of Electrostatic Precipitators with Rigid Mast Electrodes . . . . . . . . . . . 437
H. Krigmont*, R. Allan, R. Triscori, and H. W. Spencer, III

Full Scale Experience with Pulsed Energization of Electrostatic Precipitators. . . . . . . . . . . . . . . . . . . 458
K. Porle* and K. Bradburn

New Life for Old Weighted Wire Precipitators: Rebuilding with Rigid Electrodes. . . . . . . . . . . . . . . . . . . . . . . 479
Peter J. Aa* and Gary R. Gawreluk*

*Denotes speaker

Page

Pulsing on a Cold-Side Precipitator, Florida Power Corporation, Crystal River, Unit 1 . . . . . . . . . . . . . . . . 495
Joseph W. Niemeyer*, Robert A. Wright, and Wayne Love

Session 8: ESP: ADVANCED TECHNOLOGY I . . . . . . . . . . . . . . 499
Norman Plaks, Chairman

Field Study of Multi-Stage Electrostatic Precipitators . . . . 500
Michael Durham, George Rinard, Donald Rugg, Theodore Carney, James Armstrong*, and Leslie E. Sparks

Optimizing the Collector Sections of Multi-Stage Electrostatic Precipitators. . . . . . . . . . . . . . . . . . . . . 513
George Rinard*, Michael Durham, Donald Rugg, and Leslie Sparks

Ceramic-Made Boxer-Charger for Precharging Applications. . . . 525
Senichi Masuda*, Shunsuke Hosokawa, and Shuzo Kaneko

Precipitator Performance Enhancement with Pulsed Energization . . . . . . . . . . . . . . . . . . . . . . . . . . 539
E. C. Landham, Jr.*, James L. DuBard, Walter R. Piulle, and Leslie Sparks

Aerosol Particle Charging in a Pulsed Corona Discharge . . . . 554
James L. DuBard* and Walter R. Piulle

Session 9: ESP: ADVANCED TECHNOLOGY II. . . . . . . . . . . . . 569
Walter R. Piulle, Chairman

Performance of Large-Diameter Wires as Discharge Electrodes in Electrostatic Precipitators. . . . . . . . . . . 570
P. Vann Bush*, Duane H. Pontius, and Leslie E. Sparks

Technical Evaluation of Plate Spacing Effects on Fly Ash Collection in Precipitators. . . . . . . . . . . . . . 586
Ralph F. Altman*, Gerald W. Driggers, Ronald W. Gray, and James L. DuBard, and E. C. Landham, Jr.

Electrical Characteristics of Large-Diameter Discharge Electrodes in Electrostatic Precipitators. . . . . . . . . . . 599
Kenneth J. McLean* and Leslie E. Sparks

Laboratory Analysis of Corona Discharge Electrodes and Back Corona Phenomena. . . . . . . . . . . . . . . . . . . . 610
P. Vann Bush* and Todd R. Snyder

*Denotes speaker

Page

Session 10: ESP: FUNDAMENTALS I . . . . . . . . . . . . . . . . . . . 627
Grady B. Nichols, Chairman

The Onset of Electrical Breakdown in Dust Layers . . . . . . . . 628
Ronald P. Young*, James L. DuBard, and Leslie E. Sparks

Bipolar Current Probe for Diagnosing Full-Scale Precipitators. . . . . . . . . . . . . . . . . . . . . . . . . . . . 643
Senichi Masuda*, Toshifumi Itagaki, Shigeyuki Nohso, Osamu Tanaka, Katsuji Hironaga, and Nobuhiko Fukushima

A Method for Predicting the Effective Volume Resistivity of a Sodium Depleted Fly Ash Layer . . . . . . . . . . . . . . 658
Roy E. Bickelhaupt* and Ralph F. Altman

Analysis of Air Heater-Fly Ash-Sulfuric Acid Vapor Interactions . . . . . . . . . . . . . . . . . . . . . . . . . . 676
Norman W. Frisch

Session 11: ESP: FUNDAMENTALS II. . . . . . . . . . . . . . . . . . 698
Philip A. Lawless, Chairman

Experimental Studies of Space Charge Effects in an ESP . . . . 699
D. H. Pontius* and P. V. Bush

An Electrostatic Precipitator Facility for Turbulence Research . . . . . . . . . . . . . . . . . . . . . . . . . . . 714
J. H. Davidson* and E. J. Shaughnessy

On the Static Field Strength in Wire-Plate Electrostatic Precipitators with Profiled Collecting Electrodes by an Experimental Method. . . . . . . . . . . . . . . . . . . . . . . . 730
C. E. Akerlund

The Fluid Dynamics of Electrostatic Precipitators: Effects of Electrode Geometry. . . . . . . . . . . . . . . . . 741
E. J. Shaughnessy*, J. H. Davidson, and J. C. Hay

VOLUME 3
FABRIC FILTRATION

Session 12: FF: PRACTICAL CONSIDERATIONS. . . . . . . . . . . . 751
Wallace B. Smith, Chairman

Fabric Screening Studies for Utility Baghouse Applications . . 752
Larry G. Felix* and Randy L. Merritt

*Denotes speaker

Page

Tensioning of Filter Bags in Reverse Air Fabric Filters. . . . 769
Robert W. Tisone* and Gregory L. Lear

Sound of Energy Savings. . . . . . . . . . . . . . . . . . . . . . . . 784
N. D. Phillips* and J. A. Barabas

Solving the Pressure Drop Problem in Fabric Filter Bag Houses . . . . . . . . . . . . . . . . . . . . . . . . . 797
Carl V. Leunig

Session 13: FF: FULL-SCALE STUDIES (COAL-FIRED BOILERS) . . . . 807
Robert P. Donovan, Chairman

Emission Reduction Performance and Operating Characteristics of a Baghouse Installed on a Coal-Fired Power Plant . . . . . . . . . . . . . . . . . . . . . . 808
David S. Beachler*, John W. Richardson, John D. McKenna, John C. Mycock, and Dale Harmon

Evaluation of Sonic-Assisted, Reverse-Gas Cleaning at Utility Baghouses . . . . . . . . . . . . . . . . . . . . . 823
Kenneth M. Cushing*, Larry G. Felix, Anthony M. LaChance, and Stephen J. Christian

Sonic Horn Application in a Dry FGD System Baghouse. . . . . . 839
Yang-Jen Chen*, Minh T. Quach, and H. W. Spencer III

Full Scale Operation and Performance of Two New Baghouse Installations . . . . . . . . . . . . . . . . . . . . 853
C. B. Barranger

Session 14: FF: FULL-SCALE STUDIES II (COAL-FIRED BOILERS). . . 867
Robert C. Carr, Chairman

Performance of Baghouses in the Electric Generating Industry . . . . . . . . . . . . . . . . . . . . . . . . . . . 868
Wallace B. Smith* and Robert C. Carr

Flue Gas Filtration: Southwestern Public Service Company's Experience in Design, Construction, and Operation. . . . . . . . . . . . . . . . . . . . . . . . . . 893
John Perry

Start-Up and Operation of a Reverse-Air Fabric Filter on a 550 MW Boiler . . . . . . . . . . . . . . . . . . . . . 902
R. A. Winch and L. J. Pflug, Jr.*

*Denotes speaker

Page

Update on Australian Experience with Fabric Filters on Power Boilers . . . . . . . . . . . . . . . . . . . . . . . . 920
F. H. Walker

Session 15: FF: FUNDAMENTALS/MEASUREMENT TECHNIQUES . . . . . . 937
David S. Ensor, Chairman

Modeling Baghouse Performance. . . . . . . . . . . . . . . . . . . 938
David S. Ensor*, Douglas W. VanOsdell, Andrew S. Viner, Robert P. Donovan, and Louis S. Hovis

Measurement of the Spatial Distribution of Mass on a Filter . . . . . . . . . . . . . . . . . . . . . . . . . . . 952
Andrew S. Viner*, R. P. Gardner, and L. S. Hovis

Laboratory Studies of the Effects of Sonic Energy on Removal of a Dust Cake from Fabrics. . . . . . . . . . . . . 964
B. E. Pyle*, S. Berg, and D. H. Pontius

Cleaning Fabric Filters. . . . . . . . . . . . . . . . . . . . . 981
G. E. R. Lamb

Session 16: FF: ADVANCED CONCEPTS . . . . . . . . . . . . . . . 994
John K. McKenna, Chairman

Modeling Studies of Pressure Drop Reduction in Electrically Stimulated Fabric Filtration . . . . . . . . . . . . . . . . . . 995
Barry A. Morris*, George E. R. Lamb, and Dudley A. Saville

Flow Resistance Reduction Mechanisms for Electrostatically Augmented Filtration . . . . . . . . . . . . . . . . . . . . .1007
D. W. VanOsdell*, R. P. Donovan, and Louis S. Hovis

Laboratory Studies of Electrically Enhanced Fabric Filtration . . . . . . . . . . . . . . . . . . . . . . . . . .1020
Louis S. Hovis*, Bobby E. Daniel, Yang-Jen Chen, and and R. P. Donovan

Pressure Drop for a Filter Bag Operating with a Lightning-Rod Precharger . . . . . . . . . . . . . . . . . . . .1034
George E. R. Lamb* and Richard I. Jones

New High Performance Fabric for Hot Gas Filtration . . . . . .1048
J. N. Shah
Paper presented by Peter E. Frankenburg

*Denotes speaker

Page

Session 17: FF: PILOT-SCALE STUDIES (COAL-FIRED BOILERS). . . .1059
Louis S. Hovis, Chairman

The Influence of Coal-Specific Fly Ash Properties Upon Baghouse Performance: A Comparison of Two Extreme Examples . . . . . . . . . . . . . . . . . . . . . . . . . . .1060
Stanley J. Miller* and D. Richard Sears

Top Inlet Baghouse Evaluation at Pilot Scale . . . . . . . . .1081
Gary P. Greiner* and Dale A. Furlong

Development of Woven Electrode Fabric and Preliminary Economics for Full-Scale Operation of Electrostatic Fabric Filtration. . . . . . . . . . . . . . . . . . . . . . . .1082
James J. Spivey*, Richard L. Chambers, and Dale L. Harmon

ESFF Pilot Plant Operation at Harrington Station . . . . . . .1101
Richard L. Chambers*, James J. Spivey, and Dale L. Harmon

## VOLUME 4
## FUGITIVE EMISSIONS, DRY $SO_2$, AND OPERATION AND MAINTENANCE

Session 18: FUGITIVE EMISSIONS I . . . . . . . . . . . . . . . . .1119
Chatten Cowherd, Jr., Chairman

Technical Manual on Hood Capture Systems to Control Process Fugitive Particulate Emissions . . . . . . . . . . . .1120
E. R. Kashdan*, J. J. Spivey, D. W. Coy,
H. Goodfellow, T. Cesta, and D. L. Harmon

Pilot Demonstration of Air Curtain Control of Buoyant Fugitive Emissions . . . . . . . . . . . . . . . . . . . .1132
Michael W. Duncan*, Shui-Chow Yung, Ronald G. Patterson,
William B. Kuykendal, and Dale L. Harmon

Characterization of Fugitive Particulate Emissions from Industrial Sites . . . . . . . . . . . . . . . . . . . . . . . .1147
K. S. Basden

Evaluation of an Air Curtain Secondary Hooding System. . . . .1161
John O. Burckle
Paper presented by William F. Kemner

*Denotes speaker

Page

Session 19: FUGITIVE EMISSIONS II. . . . . . . . . . . . . . . . . . .1172
Michael J. Miller, Chairman

Technical Manual on the Identification, Assessment, and Control of Fugitive Emissions. . . . . . . . . . . . . . . . .1173
Chatten Cowherd, Jr.*, John S. Kinsey, and William B. Kuykendal

Quantification of Roadway Fugitive Dust at a Large Midwestern Steel Mill. . . . . . . . . . . . . . . . . . . . . . .1188
Keith D. Rosbury and William Kemner*

Evaluation of Street Sweeping as a Means of Controlling Urban Particulate. . . . . . . . . . . . . . . . . . . . . . . . .1200
T. R. Hewitt

Windbreak Effectiveness for the Control of Fugitive-Dust Emissions from Storage Piles--A Wind Tunnel Study. . . . . . .1210
Barbara J. Billman

Evaluation of Chemical Stabilizers and Windscreens for Wind Erosion Control of Uranium Mill Tailings. . . . . . . . .1227
Monte R. Elmore* and James N. Hartley

Session 20: DRY $SO_2$ REMOVAL I. . . . . . . . . . . . . . . . . . . .1245
Richard G. Rhudy, Chairman

Modeling of $SO_2$ Removal in Spray-Dryer Flue Gas Desulfurization System . . . . . . . . . . . . . . . . . . . . . .1246
Ashok S. Damle* and Leslie E. Sparks

Fabric Filter Operation Downstream of a Spray Dryer: Pilot and Full-Scale Results . . . . . . . . . . . . .1275
Richard G. Rhudy and Gary M. Blythe*

Novel Design Concepts for an 860 MW Fabric Filter Used with a Dry Flue Gas Desulfurization System. . . . . . . .1303
Michael F. Skinner, Steven H. Wolf, John M. Gustke*, and Donald O. Swenson

Start-Up and Operating Experience with a Reverse Air Fabric Filter as Part of the University of Minnesota Dry FGD System . . . . . . . . . . . . . . . . . . . . . . . . .1315
J. C. Buschmann*, J. Mills, and W. Soderberg

*Denotes speaker

Page

Spray Dryer/Baghouse Experiences on a 1000 ACFM Pilot Plant. . . . . . . . . . . . . . . . . . . . . . . . . . .1325
Wayne T. Davis*, Gregory D. Reed, and Tom Lillestolen

Session 21: DRY $SO_2$ REMOVAL II . . . . . . . . . . . . . . . . . . .1337
Theodore G. Brna, Chairman

Design and Operation of the Baghouse at Holcomb Station, Unit No. 1. . . . . . . . . . . . . . . . . . . . . . . .1338
B. R. McLaughlin* and R. D. Emerson

An Update of Dry-Sodium Injection in Fabric Filters. . . . . .1357
Richard G. Hooper*, Robert C. Carr, G. P. Green, V. Bland, L. J. Muzio, and R. Keeth

Removal of Sulfur Dioxide and Particulate Using E-SOX. . . . .1366
Leslie E. Sparks*, Geddes H. Ramsey, Richard E. Valentine, and Cynthia Bullock

Comparison of Dry Injection Systems at Normal and High Flue Gas Temperatures . . . . . . . . . . . . . . . . . . . . .1382
Robert M. Jensen*, William Dunlop, George C. Y. Lee, and Duane Folz

Acid Rain Control Options - Impact on Precipitator Performance. . . . . . . . . . . . . . . . . . . . . . . . . .1397
Victor H. Belba*, Fay A. Horney, and Donald M. Shattuck

Session 22: OPERATIONS AND MAINTENANCE I . . . . . . . . . . . .1412
Richard D. McRanie, Chairman

Comparison of U.S. and Japanese Practices in the Specification and Operation and Maintenance of Electrostatic Precipitators. . . . . . . . . . . . . . . . . . . . . . .1413
Michael F. Szabo*, Charles A. Altin, and William B. Kuykendal

Operation and Maintenance Manuals for Electrostatic Precipitators and Fabric Filters . . . . . . . . . . . . . . .1427
Michael F. Szabo*, Ronald D. Hawks, Fred D. Hall, and Gary L. Saunders

An Update of the Performance of the Cromby Station Fabric Filter. . . . . . . . . . . . . . . . . . . . . . . . . . .1448
M. Gervasi*, J. R. Darrow, and J. E. Manogue

*Denotes speaker

Page

Critical Electrostatic Precipitator Purchasing Concepts. . . . .1463
Charles A. Altin* and Ralph F. Altman

Reducing Electrostatic Precipitator Power Consumption. . . . .1481
Joseph P. Landwehr* and George Burnett

Session 23: OPERATIONS AND MAINTENANCE II. . . . . . . . . . . . .1494
Peter R. Goldbrunner, Chairman

Design Considerations to Avoid Common Fly Ash Conveying Problems . . . . . . . . . . . . . . . . . . . . . . . . .1495
Gus Monahu* and Walter Piulle

Feasibility of Using Parameter Monitoring as an Aid in Determining Continuing Compliance of Particulate Control Devices. . . . . . . . . . . . . . . . . . . . . . . . .1510
Joseph Carvitti*, Michael F. Szabo, and William Kemner

Air Pollution Control: Maintenance Cost Savings from the Washing, Patching and Reuse of Bags Used in Fabric Filters. . . . . . . . . . . . . . . . . . . . . . . .1530
Frank L. Cross, Jr.
Paper presented by Lutz Bergmann

Optimizing the Performance of a Modern Electrostatic Precipitator by Design Refinements . . . . . . . . . . . . . .1537
Donald H. Rullman* and Franz Neulinger

Weighted Discharge Electrodes - A Solution to Mechanical Fatigue Problems. . . . . . . . . . . . . . . . . . .1567
John A. Knapik

PAPER PRESENTED AT THE FOURTH SYMPOSIUM ON THE TRANSFER AND UTILIZATION OF PARTICULATE CONTROL TECHNOLOGY BUT NOT PUBLISHED IN PROCEEDINGS

Measurement of the Electrokinetic Transport Properties of Particles in an Electrostatic Precipitator. . . . . . . . .1584
Wallace T. Clark III*, Robert L. Bond, and Malay K. Mazumder

UNPRESENTED PAPER

Electrostatic Precipitator Bus Section Failure: Operation and Maintenance. . . . . . . . . . . . . . . . . . . . . . . . .1596
Louis Theodore, Joseph Reynolds, Francis Taylor, Alan Filippi, and Steve Errico

*Denotes speaker

# Session 1: PLENARY SESSION

Everett L. Plyler, Chairman
U.S. Environmental Protection Agency
Air and Energy Engineering Research Laboratory
Research Triangle Park, NC

# THE REGULATORY FRAMEWORK FOR FUTURE PARTICULATE TECHNOLOGY NEEDS

By

Sheldon Meyers
Deputy Assistant Administrator
Office of Air and Radiation
Environmental Protection Agency
Washington, D.C.

My talk today is entitled "The Regulatory Framework for Future Particulate Technology Needs." The discussion can also be characterized as a "primer on particulates" or if you will, "particulates 101." And it naturally follows that there will be a short quiz at the end of the session, so I hope you will be taking notes.

I would like to see if in examining the Regulatory Framework mentioned in my assigned topic, we can talk about the particulate proposal itself and see if I can suggest why it took the form that it did. I also want to point to some of the basic questions raised in the proposal, and finally I want to urge you to think about approaches which may help us over some of the genuine difficulties associated with the proposal.

Our text today is the Federal Register notice of March 20, 1984. That document consists of the proposed standard itself; the Monitoring, Reference and Equivalent Methods; and proposed rules for ambient air quality surveillance. Addendum I is the Executive Summary of the staff paper that accompanied the new P.M. critria document, and Addendum II is the CASAC (Clean Air Scientific Advisory Committee) "closure" document, that is the CASAC review of the EPA staff document, its scientific conclusions and evaluations. The documents stand out, as far as I'm concerned, because of the clarity and simplicity of the language which distinguishes this proposal from lots of other EPA documents I've read over the years because of those characteristics.

I'll start with a brief review, but first, some definitions, then some law.

Particulate matter in the generic sense covers a wide class of chemically and physically diverse substances that can be viewed as discrete particles. They come from a wide range of stationary and mobile sources. They can be emitted directly into the atmosphere or they can come into existence as gaseous emissions like sulfur oxides or NOx or volatile organic substances and be transformed in the atmosphere. We estimate that man-made emissions of particulate matter today in the United States amount to somewhere between 100 and 400 million metric tons a year. They come from the burning of fossil fuels, other industrial processes, and activities that stir up dust and dirt e.g., construction, mining activities, highway traffic.

The physical and chemical properties vary according to time, place, meteorology and the source of the emission. From the point of view of public health, the major worry has to do with fine particles - particles with dimensions below 10 micrometers. These fine fractions include gaseous transformation products such as sulfuric acid, ammonium, sulfates, nitrates, some organics, as well as directly emitted substances like carbon, polycyclic organics, trace elements of metals such as arsenic and lead. In high concentrations, the major effects on human health have to do with the breathing and respiratory system: they can aggravate existing heart and lung disorders, reduce the body's defense mechanisms against foreign materials, damage lung tissue and even lead to premature mortality. In lower concentrations of the kind we experience in many U.S. cities today, it is difficult to evaluate effects or to determine if any or all of those effects observed at high concentrations occur at lower concentrations. Sensitive population groups we have to watch out for when it comes to particulate matter are people with chronic obstructive lung or heart disease, individuals with influenza, asthmatics, the elderly, small children, smokers, and people who tend to breathe through the mouth.

Two sections of the Clean Air Act come into play in this discussion. Section 108 says the Administrator shall identify those pollutants which "may reasonably be anticipated to endanger public health and welfare." Having identified such pollutants, the Administrator is required to issue air quality criteria for them. These criteria, the Act says, should reflect the latest scientific information showing the kind and extent of all identifiable effects which may flow from this pollutant, effects on both public health and welfare which can be expected from the presence of this pollutant in the ambient air. That's section 108.

Section 109 directs the Administrator to propose and promulgate primary and secondary national ambient air quality standards for the criteria pollutants identified under section 108. The primary standard is, of course, intended to protect public health. It must be based on the criteria and must allow for an adequate margin of safety.

The secondary standard is one which is sufficient to protect the public welfare from "any known or anticipated adverse effects" associated with the presence of that criteria pollutant in the ambient air. Section 302(h) defines these welfare effects as effects on soils, waters, crops, vegetation, wildlife, animals, man-made materials, weather, climate, visibility, damage to property, deterioration of property, hazards to transportation, effects on economic values and effects on personal comfort and well-being.

The courts have interpreted "the adequate margin of safety" language to mean that the Congress intended EPA to somehow address the uncertainties that exist because of inconclusive scientific information available at the time we set the standard. It also was intended, the courts have said, to give reasonable protection against hazards which research has not yet identified. In other words, it is anticipatory as well as cautionary.

The courts have also held, as you know, that the economic and technological feasibility can play no function in the Administrator's decision to set a primary standard. Public health is the only criteria for setting a primary standard.

The original standards were set back in April 1971 for particulate matter and for five other "criteria" pollutants - oxides of nitrogen, sulfur oxides, carbon dioxide, hydrocarbons, oxidants or ozone. Since 1971 we have rescinded one standard - hydrocarbon, and added one - lead.

The reference method for measuring attainment of the particulate matter standard in 1971 is the "high volume" sampler which collects particulate matter up to a nominal size of 25 to 45 micrometers - this is the so-called "total suspended particulate" or TSP.

The 1971 primary standards measured as TSP are 260 micrograms per cubic meter averaged over a period of 24 hours - and not to be exceeded more than once a year; and 75 micrograms per cubic meter annual geometric mean. The secondary standard is 150 micrograms per cubic meter, averaged over a period of 24 hours and not to be exceeded more than once a year. The original criteria document on which these standards were based was published by the old Department of Health, Education and Welfare back in 1969.

The 1977 amendments directed EPA to review and, if appropriate, revise the air quality criteria and the ambient standards every five years. This particulate matter revision is the latest in that effort. So far we have proposed or promulgated revisions for ozone, hydrocarbons, carbon monoxide and nitrogen dioxide. Sulfur dioxide is in the works.

The particulate matter revision proposed last March has several important elements.

First, we propose to change the way particulate matter is measured for the primary standard. We propose to abandon the so-called TSP or total suspended particulates method in favor of a method that includes only particles small enough to penetrate to the more sensitive parts of the human respiratory tracts. The new indicator would be particles of 10 micrometers or less, called $PM_{10}$.

Next, the standards themselves: we want to establish new concentration levels for the primary standards. For the 24 hour standard, a new level would be a number from the range 150 to 250 micrograms per cubic meter. For the annual standard, a new level would be a number from the range of 50 to 65 micrograms per cubic meter.

We proposed replacing the current 24 hour secondary standard with an annual TSP secondary standard from the range of 70 to 90 micrograms per cubic meter. For the secondary standard, the particulate matter would continue to be measured by the high volume air sampler which, as we mentioned before, measures TSP.

Why the ranges? Why not a specific number?

Perhaps the best way to answer that question is briefly to go over the process that got us this far. The process has evolved much and expanded considerably since the first standards were set in 1971. The new process, like the old one, begins with a review of all relevant literature and information on the subject. This information is assembled, organized and weighed in the criteria document. For $PM_{10}$, the criteria document consists of 1400 pages and refers to 2900 scientific papers, reports or studies. We have been working on it in earnest since 1979.

CASAC reviews the document prior to publication and takes views and comments from the public, from interest groups, environmental groups, business representatives, and so forth, in public meetings held around the country. OAQPS then prepares a staff paper which evaluates and interprets the available information to identify the factors which must be considered in revising the standard. A big part of this work is also to spot the uncertainties which exist in the literature and the gaps in our knowledge of the pollutant and its effects. The staff paper then undergoes its own review by the CASAC. It is also opened to public scrutiny at this time. CASAC makes its recommendations about what the standard should be.

All that has been done here. We have the criteria document, the staff paper, the closure letter, the public meetings, the reviews of written comments and so on.

What we don't have is unanimity or even consensus about what the numerical stringency of the 24 hour primary standard ought to be. The best that we can get from the scientific review is a relatively broad range of numbers from which the standard should be chosen — the 150 to 250 micrograms per cubic meter which I mentioned earlier. The CASAC cautioned EPA that a primary 24 hour standard at or above 350 micrograms could involve serious adverse health effects and it would provide little or no margin of safety. The EPA staff recommended, and the Administrator agreed, that the upper bound should be 250 micrograms for a 24 hour standard.

Now comes one of the many serious problems: the statute lacks a clear guide for the Administrator to use in settling on "an adequate margin of safety" so the question becomes: how much of a margin of safety is adquate to protect the most vulnerable groups in our population? Because the Act is precautionary, Administrator Ruckelshaus has publicly stated that he is "inclined to select a final primary standard from among the lower range of these numbers."

He has stipulated that a reasonable person could choose any one of several numbers within the proposed range. He finds this particularly troubling because once a number is selected it sets in motion a whole parcel of actions by EPA and States which can be cumbersome, costly and prolonged. The inability of the Administrator to take into consideration the practical problems that States and localities, industries and business may have in putting the standard into practice poses, as Bill Ruckelshaus says, "grave problems" and can lead to "potential dramatic confrontations". Remember also, that the States under the law must revise their SIP's and do a myriad of other things within nine months of final promulgation of the standards. We all know that that is a difficult goal as spelled out by the statute.

The whole landscape is cluttered with what Bill Ruckelshaus calls "real world problems," as distinguished from theoretical exercises. They comprise some of the most time consuming and controversial issues facing the regulatory community. How, for example, do you deal with rural dust and agricultural dust? How do you deal with mother nature? The decision, as the Administrator says, "to scope/modify/upgrade" a TSP control strategy which is now deemed necessary to demonstrate attainment of a small particulate standard is a tough one. Additional measures like paving parking lots, plant and access roads may now be necessary to bring an industrial area up to $PM_{10}$ attainment.

How do you factor in local conditions - topographical conditions, meteorology, and that elusive factor - local economic vitality?

"What may be a straightforward and quick solution for one area," Bill Ruckelshaus has said, "may require extraordinary effort and a great deal of time to solve in another." Our proposal solicits comments on what, if any, considerations we may take into account in setting and implementing the primary standards.

EPA has spent over a million dollars in looking at the potential impact these standards will have on the national economy, as well as the practical problems States, localities and businesses will likely have in putting the standards into effect. But the Administrator is precluded from using that information in setting the standard or even reading the studies which estimate these costs because of the language of the Act itself and the decisions of various courts which say that health effects are the only criteria on which his decision may be based.

One document the Administrator will not be reviewing, therefore, is the RIA - the Regulatory Impact Analysis - required by Executive Order 12291. It estimates that a primary standard at the lower end of the range - for example, an annual $PM_{10}$ standard of 50 micrograms per cubic meter - and a 24 hour standard of 150 could result in capital costs of $4.4 billion and annualized charges of $740 million. Numbers in the upper range, on the other hand, would give us costs approximately one-third as great - $1.4 billion capital, and $240 million annual.

As to the elusive benefits side of the equation which is always softer than the costs side, our people have come up with these numbers: depending on the value you assign to estimated risk reductions, and depending on the number of benefit categories you consider, the benefits from the lower end of the primary standard range would be at least $3 billion and could go as high as $110 billion. That is, as I'm sure you will note, a very wide spread indeed.

As I mentioned before, the March 20 proposal suggests replacing the current 24 hour secondary TSP standard with an annual TSP standard in the range of 70 to 90 migrograms per cubic meter. It is designed to protect against welfare effects such as soiling and nuisance effects. But particles larger than 90 micrograms can also contribute to the same adverse effects. So in the proposal we are inviting comment on whether it is possible to adequately protect the public welfare with an appropriately selected secondary standard in the range of 70 to 90 micrograms per cubic meter.

The March 20 proposal also defers a decision on secondary standards for fine particulates - that is particulates of less than 2.5 micron size, so that we can consider such a standard as part of a longer, more detailed future look at regional air problems - such as visibility and acid deposition. A special study group has been set up to tackle this issue and those results can be expected to be available by the end of the year.

One of the things that I personally would like to see subjected to scrutiny during this public comment period is the feasibility - and if feasible, the desirability of multiple secondary standards. Should we have a TSP secondary for soiling and nuisance and a different secondary for visibility and acid deposition which I would call a "PM two point five secondary"? It is an idea that certainly is worthy of a serious close-up examination by the scientists, by industry and environmental groups.

That concludes my lecture this morning. The proposals are important ones that have many long term and serious consequences flowing from them. A great deal of time and expense are involved for all parties. I hope that the public comment period can be used for a serious examination which will lead to a greater measure of public understanding of the problems and possible solutions. It is our job to help lead this discussion and make these admittedly complex and often obscure distinctions understandable to the public. I hope that this symposium will contribute to that important goal.

Thank you for your attention and consideration. Because your conduct was so exemplary, I will forego today's quiz, but please be prepared to discuss these issues with one another in the days ahead.

# THE IMPACT OF COMING PARTICULATE CONTROL REQUIREMENTS ON THE UTILITY INDUSTRY

By: George T. Preston
Electric Power Research Institute

The impact that particulate control requirements have on electric utilities is important because electricity is such a critical element of our energy picture. In 1950 electricity provided 15% of our national energy demand; electricity accounts for one-third of our energy today; and it will provide the bulk of our energy growth up through the year 2000, when electricity is projected to represent 45% of our national energy demand.

To consider the likely impact of particulate control requirements that may be coming in the near future, we really have to reflect on how we got where we are today. We don't have to go very far back to do this. I'm going to refer this morning to three regulatory "eras":

1. The era of no regulation
2. The Clean Air Act era
3. 1985 and beyond

Each of these regulatory eras is characterized by distinct impacts on, and responses by, the electric utility industry:

- Collection efficiency requirement - how much particulate emission do we have to control, and can we do it, technically?
- Cost of the hardware - how can we develop technology that will hold down the increasing cost of more stringent control requirements?
- Operability and reliability of the hardware - how do we insure that environmental control is compatible with the ability of the power plant to produce kilowatts?

## THE ERA OF NO REGULATION

Particulate control has come a long way since the 1920s. Utility coal-fired boiler operators then were using mechanical collectors (cyclone separators) for a little emission control and to cut down erosion of their induced draft fans. As boilers grew larger, there was a move toward electrostatic precipitators to achieve a higher degree of particulate collection and to keep operating and maintenance costs down.

## THE CLEAN AIR ACT

Passage of the Clean Air Act and its amendments led to the imposition of particulate control requirements on large stationary sources. The early emissions limits were based on stack opacity, and subsequently mass emission rate. In particular, the Clean Air Act Amendments of 1970 and 1977 changed the picture drastically for coal-fired utilities, due to the advent of the technology-forcing concepts of New Source Performance Standards and Best Available Control Technology. The current NSPS limit of 0.03 lb particulate emission/MBtu is equivalent to about 99.7% particle collection efficiency — in other words, the allowable particulate emissions were reduced by a factor of 30 in a 20-year period.

### What Were the Impacts on the Electric Utility Industry?

In the early and mid-1970s, electrostatic precipitators were the predominant control device for particulate emissions. Two things happened:

- Tightening limits on mass emissions and stringent stack opacity standards required the ESP to collect larger fractions of the fine particles (<2 microns).

- Fuel switching by many utilities to low-sulfur coals to comply with 1971 NSPS $SO_2$ limits resulted in high resistivity fly ash that was harder to collect in the ESP. (This proved troublesome even for new units, where you would suppose we could design the ESP bigger to compensate for the high resistivity. It turned out precipitators didn't scale up as we thought they would.)

The results of these two developments were reduced reliability, increased costs, and (in some cases) an inability to achieve compliance.

### How Has the Utility Industry Responded Technologically to Current Regulations?

A variety of technologies have been implemented — many of them just in the last decade — some successfully and others not. I'd like to highlight just three of the prominent and promising technologies, because I expect that they will play important roles in the industry's response to future regulatory developments as well.

- Flue gas conditioning (FGC) is the most promising technology now commercially available for improving ESP performance. Research programs and full-scale utility tests conducted over the past six years have established FGC as a legitimate technology that utilities can choose with a clear understanding of how well it will work in a given application. I would term this technology fully commercial for retrofit application, although there is still substantial resistance to designing FGC into new ESP application.

- Even more recently, tests at EPRI's Arapahoe Test Facility have demonstrated that pulsed power supplies can improve ESP performance over a broad range of operating conditions, especially when the ESP's initial baseline efficiency is low. Although pulsed power supplies have been offered and sold commercially, they have not yet achieved wide acceptance in the industry.

- Utilities began to apply fabric filters (baghouses) for particulate collection in the late 1970s. The pioneering efforts of a few utilities, and an intensive, results-oriented research program over the past decade, have brought fabric filtration to full commercial status in the utility industry for particulate control in low-sulfur coal applications. Specifically, the importance of good gas and dust distribution in the baghouse, optimized bag cleaning techniques, and a knowledgeable tradeoff between capital cost (size) and operating cost (pressure drop) are now recognized.

## 1985 AND BEYOND

I would like to highlight two of the regulatory initiatives mentioned in earlier talks, because they would be likely to have a strong impact on utilities' technology choices for particulate control. These are:

- The proposed $PM_{10}$-based standard for particulate emissions

- Proposed acid rain legislation calling for retrofit $SO_2$ controls on existing coal-fired boilers.

### What Would Be the Impacts of an Inhalable Particulate Standard?

EPA has proposed to change the primary National Ambient Air Qualtiy Standard from a Total Suspended Particulate base to a standard based on particles smaller than 10 microns -- that is, focusing on the inhalable fraction of the particulate emissions. If such a standard were reflected in tighter requirements under revised NSPS and BACT, it could impact the design and operation of particulate control systems for new and/or existing plants. Even without knowing what specific new regulations might be proposed, we can make a few general observations. It is safe to say that the technology to achieve acceptably low particulate emissions probably already exists. However, the cost to achieve the required levels could be quite large, particularly if retrofit improvements are called for.

- For newer units built under the 1979 NSPS (0.03 lb/MBtu) there would be little or no impact, since these units already can collect particles smaller than 10 microns with fairly high efficiency (95% or more), using baghouses or efficient ESPs.

- On the other hand, for units built under the 1971 NSPS and earlier, promulgation of a size-dependent control requirement could have serious technical and economic implications.

- For one thing, these units operate under widely differing emission limits.
- Second, over 90% of these units are equipped with ESPs, and extensive field studies have shown that ESPs are extremely sensitive to flue gas and fly ash conditions when forced to operate in the high efficiency ranges.

Consequently, if an inhalable particulate standard were to be applied to these older existing units, each ESP would have to be evaluated case by case to determine if upgrading were needed and economically feasible. The major options would be:

- Improve the performance of the existing ESP
- Enlarge the existing ESP
- Replace with a baghouse
- Retire the plant (especially likely for the older, smaller units)

There are already examples of each of these courses being adopted by utilities in complying with regulations now in effect.

## What Would Be the Impacts of Retrofit $SO_2$ Controls?

There is growing interest in total atmospheric loading issues -- the current ones, for example, are acid deposition, long-range transport, and visibility -- and this could result in requirements for retrofit $SO_2$ controls on existing coal-fired power plants. While many utilities may choose wet $SO_2$ scrubbing to comply with any such requirements, EPRI, EPA and several individual utilities are carrying out some significant R&D programs to develop less costly dry $SO_2$ control processes. In addition, AFBC is being developed as an $SO_2$ control alternative to conventional pulverized coal-fired boilers. If they are implemented, any of these technologies could have a significant impact on the performance of existing particulate controls and on the design of new control systems.

For existing plants equipped with baghouses, the good news is that none of the retrofit $SO_2$ control methods is likely to have a major effect on particulates control. The bad news is that very few of the existing units that might be affected by acid rain retrofit legislation are equipped with baghouses. Most of these units have ESPs, and most of the ESPs are relatively small ones designed for low resistivity ash (i.e. high- and medium-sulfur coal) applications.

Let me now list some of the specific retrofit $SO_2$ control options and how they may impact ESP performance.

o Fuel switching to low-sulfur coal. Switching from 3%-sulfur coal to 1.5%-sulfur coal will result in an order of magnitude increase in fly ash resistivity — for example, from 5 x $10^{10}$ ohm-cm (not too difficult to collect) to 5 x $10^{11}$ ohm-cm (marginal). Without any ESP modifications or performance upgrading, this could at least double the particulate emission from the ESP in a typical situation.

- Coal cleaning would decrease the ash loading going to the ESP, because some of the ash is removed in the cleaning; but the dominant effect would be a higher resistivity ash due to the lower sulfur content, leading to a net increase in particulate emissions as the likely result.

- The overall impact of spray-drying on the particulate collection performance (outlet particulate emissions) of an ESP is not clear, because there are several competing effects:
    - The resistivity of the particulate mixture being collected is low due to the moisture content of the flue gas and its lower temperature (improves ESP performance).
    - The lower gas temperature decreases the gas volume and thus increases the precipitator's specific collecting area (improves ESP performance).
    - The particulate loading to be collected increases by a factor of 2 to 5 (degrades ESP performance).

Furnace sorbent injection $SO_2$ control is where a sorbent material (e.g. limestone) is injected into the boiler to capture $SO_2$ as it is generated or soon after it is generated. Since this process is at an early stage of development, there are few data; but the data so far suggest that the solids loading to the ESP will increase by a factor of 2 or more, and the fly ash resistivity may increase 1-2 orders of magnitude. The particle size distribution reaching the ESP may also change substantially. The overall effect is expected to be a degradation of precipitator performance. (In fact, in contrast to two years ago when we were most concerned about slagging and fouling in the boiler, particulate collection and disposal is one of the biggest technical issues associated with the furnace sorbent injection approach now.)

Fluidized bed combustion will be retrofit to some existing pulverized coal-fired boilers. Although the technology itself is well along toward commercialization with three commercial-size utility projects in engineering now, the effects on particulate collection performance on an ESP are much less well known. The solids loadings and resistivity are likely to be substantially higher, as with furnace sorbent injection — and therefore we need to be similarly concerned as to whether particulate collection issues could inhibit the implementation of this technology.

## What Control Technologies Will the Industry Use in Response?

Having looked at possible impacts, let's look at what particulate control technologies might be considered by the utility industry to respond to regulatory initiatives such as the two I've mentioned.

- Both flue gas conditioning and pulsed power supplies are commercially available, and would be two of the first options considered for upgrading the performance of existing ESPs, due to their low cost ($5-7/kW) and high potential for ESP performance improvement. FGC in particular is viewed as a promising option because it directly addresses the key issue affecting ESP performance -- namely, high resistivity of the particulate.

- If neither conditioning nor pulsing can produce satisfactory performance, then rebuilding or enlarging the existing ESP would have to be considered, at a significantly higher cost ($20-50/kW). In this case, increasing the spacing between the collecting plates to 18 inches or more may save money. This technology is still at the pilot stage of development, by EPRI and others.

- Converting an existing precipitator to two-stage operation is another option that might be considered to upgrade ESP performance. This concept has been investigated by several teams, for example EPA's current studies of a temperature-controlled particle precharger.

- Even though there are a number of new methods to improve existing ESP performance commercially available or under development, in some instances retrofitting a fabric filter may be the best means of particulate control for an existing plant subject to new control requirements. Such action is not without precedent: of the 110 baghouses now operating or being installed in the utility industry, about 50% have been retrofit. Advanced baghouse concepts that have been looked at to maintain low fabric filter pressure drops and thus minimize operating costs include shake/deflate cleaning, sonic assisted reverse gas cleaning, novel fabrics, and electrically augmented dustcake formation.

## CONCLUSION

Looking at the evolution of regulatory requirements and control technology over the past 40 years or so, it's clear that further reductions in particulate emissions are much harder technologically than the reductions we have achieved so far, and that to progress further the technologies we rely on will have to offer cost improvements as well as collection efficiency improvements. Looking at the achievements of the utility industry and others' research programs over the past 10 years, I'm optimistic that we will successfully meet that challenge.

## ACKNOWLEDGEMENT

I am grateful for the contributions of Ralph F. Altman and Robert C. Carr during preparation of these remarks.

The work described in this paper was not funded by the U.S. Environmental Protection Agency and therefore the contents do not necessarily reflect the views of the Agency and no official endorsement should be inferred.

# THE IMPACT OF COMING PARTICULATE CONTROL REQUIREMENTS ON THE IRON AND STEEL INDUSTRY

by: Earle F. Young, Jr.
American Iron and Steel Institute
Washington, D. C. 20036

## ABSTRACT

The steel industry has made major strides in control of particulate emissions. The controls now in use are examined in light of proposed new standards that will emphasize control of PM10 rather than Total Suspended Particulate matter.

For the iron and steel industry, air pollution control and particulate pollution control are almost interchangeable terms. The steel industry has four characteristics that give it potential for being a major source of particulate emissions:

- It is a big industry, handling up to 300 million tons per year of materials in the production and shipment of up to 100 million tons of steel per year.
- The materials it handles are impure: rough, solid materials like ore and coal and limestone, not clean, pure, chemical substances.
- Our operations are hot, involving the heat reactions of these millions tons of impure raw materials at temperatures up to 3300°F.
- Many of our operations are cyclic since steelmaking is essentially a batch process.

Because of these factors, the steel industry has always been and always will be a major potential source of particulate emissions. The industry has recognized this problem for a long time, and has for many years -- dating well back before the passage of the Clean Air Act -- been working hard and investing heavily in the control of particulate pollution.

One measure of this effort would be the records of what the industry has spent on equipment for particulate pollution control. AISI records of pollution control capital expenditures go back to 1951. Since then, the industry has invested over $3.6 billion in facilities for control of air pollution, of which about 95 percent, or $3.3 billion, was spent on particulate pollution controls. These investments have been effective: it is estimated that there is in place equipment and facilities to control well over 96% of the emissions from our manufacturing processes.

In March 1984, the EPA announced its intent to revise the National Ambient Air Quality Standards for particulate matter, to consider PM10 - material smaller than 10 microns in diameter, instead of TSP, Total Suspended Particulate Matter, the measurement made by a high volume sampler. Thus, the future emphasis on control of particulate matter emissions will be on small particles rather than on all particles.

The level of the new standard has not yet been selected, so it is impossible as yet to predict quantitatively the effect of the new standards on any industry, including the steel industry. Nevertheless, an examination of the steel industry - its processes, their emissions and controls - in light of these changing standards may be useful.

Steel making is not one operation. It is a complex series of operations progressing from raw materials through pyrometallurgical processes to establish the composition of the product to a series of mechanical, thermal and chemical processes to establish the form, physical and surface properties of the product. It is in the pyrometallurgical processes that the potential exists for particulate emissions.

There are basically two types of steel plants. The integrated facility which starts with basic raw materials utilizes the blast furnace to make iron from iron ore, coal and limestone. It generally includes coke plants for making of coke from coal and frequently sinter plants for agglomeration of raw materials. Steel is made in basic oxygen process furnaces or open hearth furnaces utilizing the hot metal from the blast furnace along with scrap.

The nonintegrated facility, sometimes called a cold metal shop, makes steel completely from scrap utilizing the electric furnace. Many mills use this type of operation, and in addition, electric furnace shops are frequently included in integrated plants to provide supplemental steel making capacity.

This examination of the steel industry will consider the full integrated facility. Since our primary interest is particulate emissions, per se, I will not talk about the coke ovens since coke oven emissions, even though they include a significant amount of particulate matter, are considered something different from normal particulate emissions and are generally regulated as "coke ovens" rather than as particulate emission sources.

The first major process other than coke ovens is the blast furnace. In a blast furnace thousands of tons a day of iron ore, coke and limestone are passed countercurrently to 100,000 cubic feet per minute or more of air to produce molten iron and slag. Although we think of the blast furnace today as a relatively clean operation, it has the potential to emit huge quantities of particulates. The steel industry learned years ago, however, that the off gas from a blast furnace contains significant fuel value. Today all this gas is captured and used, for heating the stoves which preheat the air to the furnace, for generating steam in boilers, and for process heating in the plant. In order to be used as fuel this gas has to be cleaned. So the industry has installed multi-stage gas cleaners on all its blast furnaces. Generally technology for this clean-up is dust catchers to remove the coarsest particles, then high energy wet scrubbers to clean the gas to a very high degree of cleanliness. So today's blast furnace is a clean operation.

There are, however, fugitive emissions from the blast furnace. When the furnace is tapped, molten iron is drawn from the bottom of the furnace and run through troughs into ladles in which it is taken off to the steel making processes. Frankly, until the major processes in the steel mills were brought under control, no one even considered this to be a pollution source. But as mills have become much cleaner, it is obvious that are intermittently some significant emissions from a cast house. In the building of new furnaces today, in recognition of this intermittent emission source, cast houses are completely enclosed. Fumes are ducted off to bag houses and collected. However, older furnaces weren't designed with the idea that cast houses could be enclosed. Nonetheless, at least two techniques and combinations of these techniques are being developed and installed today to control these emissions where they are a problem. One of these is the installation of localized hoods around the tap hole of the furnace and other major emission points. The other is a technique known as fume suppression, which involves both the covering of runners where the hot metal is exposed and gas shrouding of the metal to prevent it coming in contact with air. Both of these techniques have proven effective and, where necessary, they can give control almost as good as that of the total enclosure on new blast furnaces.

Moving on to steel making, the Bessemer furnace is a creature of the past. The last one was shut down about 15 years ago. A look at an old Bessemer, however, shows that steel's major source of particulate emissions is the making of steel. The reaction of oxygen with the impurities in the steel and with iron itself leads to the generation of 20 - 40 lbs. of dust for every ton of steel produced. In basic oxygen steel making, the primary steel production method in integrated plants today, oxygen is blown directly into the molten bath of iron either through lances from the top of the furnace or through tuyeres at the bottom of the furnace in a modification known as QBOP. The dust laden gases discharging from the furnace at a temperature of about 3000 degrees Fahrenheit are immediately collected in either open or closed hoods and cleaned very effectively in either electrostatic precipitators or, more commonly today, high energy wet scrubbers. Emissions from these gas collectors are so much less than discharges from older steel making processes that we are in a totally different world of control.

Again, it was only after these major emissions were controlled that attention turned to other emissions connected with the process. The charging of the furnace, in which molten iron is poured into the furnace on top of the scrap charge, can be a source of significant emissions, particularly if the scrap charge happens to be oily. There are emissions even when the furnace is just turned down to permit taking the temperature of the steel. There are emissions from tapping. Recognition of these problems has lead to the installation of secondary fume control systems. Many of these consist of supplementary hoods over various parts of the operation with ducts leading to bag houses. Some consist of duct work guiding fugitive emissions into the primary control systems. Some go as far as to completely enclose the furnace with complex secondary control systems. These are effective. We have come a long way.

The electric furnace is the ubiquitous steel making operation. There are electric furnaces in some of the integrated plants as supplemental steel making facilities. There are many mills and minimills which produce steel directly from scrap in electric furnaces. All of the speciality steel industry producing stainless and high alloy and other specialty steels relies on electric furnaces for steel making.

The electric furnace has potential for particulate emissions comparable to that of other processes. Molten metal being refined just naturally fumes. Many electric furnaces use significant quantities of oxygen to speed the refining process. One of the first and a reasonably effective means of controlling the emissions during the refining process, is what we call direct extraction. A fourth hole is put in the roof of the furnace and a negative pressure duct system carries the fumes into a bag house for collection. While this system is effective for capture and collection of the fumes during the refining period in the furnace, it is not effective throughout the steel making cycle. An electric furnace is moving equipment. The roof of the furnace is removed to permit the charging of the furnace, so that a direct extraction system cannot collect any of the fumes generated during charging. The furnace is tipped during the tapping process, which again results in the direct extraction system being disconnected and ineffective. Two additional approaches have been used. One is the canopy hood above the furnace. The fumes being hot tend to rise, and capture hoods installed above and around the furnaces have proved quite effective for capture of these fumes. In some cases, it's proven more effective simply to use the roof of the building as an enclosure and to ventilate the entire building to a bag house, thus preventing escape of fumes. In a few cases, the furnaces have been totally enclosed within the building with the totally ventilated exposures going to bag houses. At times these various systems are used in combination. All in all, between direct extraction, canopy hoods and total enclosures, today's electric furnace has become almost emission free.

In addition to the iron and steel making furnaces themselves, there are auxiliary metallurgical operations ranging from desulfurization of the hot metal between blast furnace and steel making operation to argon-oxygen refining as a final step in the production of electric furnace steel teeming. Basically, these today are controlled by the same methodologies used for capturing fugitive emissions from the furnaces themselves. The fumes are similar, the capture systems are similar and the bag house collection systems are effective.

In addition to the process emissions from the iron and steel making processes, there is one other source of emissions from a steel plant that we should consider. A steel plant handles vast quantities of material, much of it in bulk but also much of it by truck and rail movement within plants. Control of the basic processes has reached the point where today in many cases these wind blown fugitive emissions are significantly greater than remaining process emissions in the plants. Particularly where plants have been considered under the bubble, control of these emissions has been shown feasible. By such simple procedures as installation of sprays on raw materials piles, sweeping of paved roads and the spraying of unpaved roads, significant emission reductions have been made in steel plants.

Basically, the steel plant of today is a clean installation with low particulate emissions.

It is against this background that we're trying to look at the new particulate standards to determine what impact they will have on our industry. The new standards will be based on control of fine particulates. Basically the steel industry's particulate emissions are fine particulates. The majority of particulate matter from steel making operations is not only less than 10 microns, it is less than 1 micron. We are controlling that fine particulate matter today and controlling it quite effectively.

To really assess the impact of coming particulate control requirements on the iron and steel industry requires more knowledge of the new standards than I have, possibly than anyone has at present. It's been said that the new standards may be more stringent than the present standards. It's also been said they may be less stringent. We won't know until a final standard is promulgated and test methods specified for the measurement of this fine particulate, and then a great deal of monitoring done to determine what areas are and what areas aren't in compliance with these new standards. It may well be that some areas today classed as nonattainment will be found to be in attainment of a new standard because much of what makes them nonattainment today is coarse material that won't be picked up by the new measuring technique. On the other hand, there may be areas which are considered attainment today, which have such high fine particulate concentrations that they'll become nonattainment. Only when these determinations are made, will we really be in a position to say that in some areas, at some operations, some additional controls will be required. What type of controls these will be will depend on the data generated over the coming years.

I have attempted to show you that the steel industry has great potential for particulate emissions, that the industry has recognized these problems and has taken positive and very expensive steps to bring particulate emissions under control. We started this before current requirements were established, we have worked diligently and productively to get where we are today. We are now looking at a future where the standards will be changed and there may be new requirements. I can assure you that we will work diligently to meet these new requirements.

To give you my best thought on the impact of coming particulate control requirements on the iron and steel industry, I can summarize my position today in three simple words, I don't know.

# THE IMPACT OF PARTICULATE CONTROL REQUIREMENTS: LARGE MANUFACTURER'S VIEWPOINT

by: Herbert H. Braden
Research-Cottrell, Inc.
Somerville, New Jersey 08876

## ABSTRACT

The traditional role of the manufacturer in the air pollution control business is to develop the applications base required to permit the sale of equipment with acceptable performance guarantees backed up by financial penalties. At the present, in anticipation of more stringent Federal regulations in the area of fine particulate emissions and in anticipation of acid rain legislation which will affect the particulate collection capability of existing equipment, ourselves and others are conducting extensive testing programs to develop a reliable applications base.

It is not anticipated that new and advanced technology is needed or is being developed to address these areas. Properly designed and constructed precipitators and fabric filters from conventional designs can meet the collection performance demanded by the proposed new requirements.

There is adequate production capacity in place to meet the market demand for new particulate collection equipment on almost any conceivable schedule.

# THE IMPACT OF PARTICULATE CONTROL REQUIREMENTS: LARGE MANUFACTURER'S VIEWPOINT

I represent a single manufacturer in this discussion and while I cannot speak for others in the industry, I believe our situations are similar. I hope that information to supplement this presentation will be brought forth during the public discussion.

## GENERAL

Before I can discuss the specifics of the proposed regulations, I would like to comment on the general role of the supplier of air pollution control equipment to the power industry and large industrial companies.

Contracts for these large air pollution control systems are awarded only if the supplier is in a position to provide performance guarantees and to back up these guarantees with contingent liabilities. The extent of the guarantees and potential liabilities are a matter of negotiation with the owner.

During negotiations, the supplier is required to provide extensive technical and cost information to the owner and his agent, the architect and engineer, during the conceptual development of the project and the preparation of equipment specifications. In addition, the equipment supplier submits with his bid not only prices, conceptual designs and guarantees, but detailed engineering information on all elements of the proposed system. The marketing costs associated with a single negotiation for a large total air quality system may exceed one million dollars, and this expense is borne simultaneously by several suppliers in the negotiation competition. This marketing and proposal expense may collectively be a greater number than the profits realized by the successful bidder on the job. Thus, the industry as a whole loses money on the negotiation.

The technical role of the equipment supplier has moved from a developer of technology to that of providing applications and engineering skills. Therefore, the bulk of the funding of technological development for this industry has now been passed on to others, e.g. EPA, EPRI, DOE and the utilities, working in conjunction with equipment suppliers. As a consequence, I am not in a position to discuss technological breakthroughs available to address the proposed new fine particulate regulations and the anticipated acid rain regulations. Although more efficient and cost-effective products are being developed, to my knowledge new and advanced technology is not being developed by the manufacturer to address the proposed regulations for three primary reasons:

First, existing technology appears to be in place, which will address all of the applications requirements which we currently anticipate.

Second, the exact timing and language of the proposed regulations is not known. There is, therefore, no sound business reason to commit scarce development money into a situation where it is impossible to place priorities. Uncertainties will kill investment.

Third, the profit levels now realized in the air pollution control business cannot support ambitious new technology development programs.

Those of you who follow the industry are aware that within the last five years, sixteen large air pollution control businesses have sold out, discontinued major product lines, or have gone out of business entirely. Published net operating income levels before taxes on air pollution control equipment are typically under 10%.

Therefore, to the manufacturer has fallen the chores of accepting performance risks and developing reliable and conservative applications bases. The financial return is not available to support the commercial and technical risk of developing new technology. Competition in the industry keeps the equipment offerings very cost-effective.

## FINE PARTICULATES

Based on our perception of the proposed regulations, it appears that conventional technology is in place which will handle the technical requirements of higher collection efficiencies on inhalable particulates. There is not a large body of published data to conclusively indicate the most cost-effective equipment selection in a variety of cases. However, our experience would indicate that a properly sized precipitator or fabric filter will meet the requirements of the proposed rules.

An interesting study was done by William Lane and Anup Khosla of Bechtel and presented at the Joint Power Generation Conference in Indianapolis in 1983. Their study covered the performance of 30 baghouses and electrostatic precipitators on fine particulates, trace elements and total emissions.

Figure 1 indicates the collection efficiency of 8 hot and cold side precipitators plotted against particle diameter. The range of collection efficiency ranges from about 90% to 99.9% in the range down to one micron.

Figure 2 compares the collection efficiency of five baghouses studied with the conditioned cold side precipitator at Pleasant Prairie. Note that although the collection efficiency of fine particulates is consistently higher for the baghouses, the single conditioned precipitator has the best performance overall of the 13 units studied. See Figure 3.

We are continuing to refine our own considerable applications base in this area. However, we are confident that we can provide equipment with commercial guarantees to meet the emission requirements of the proposed regulations.

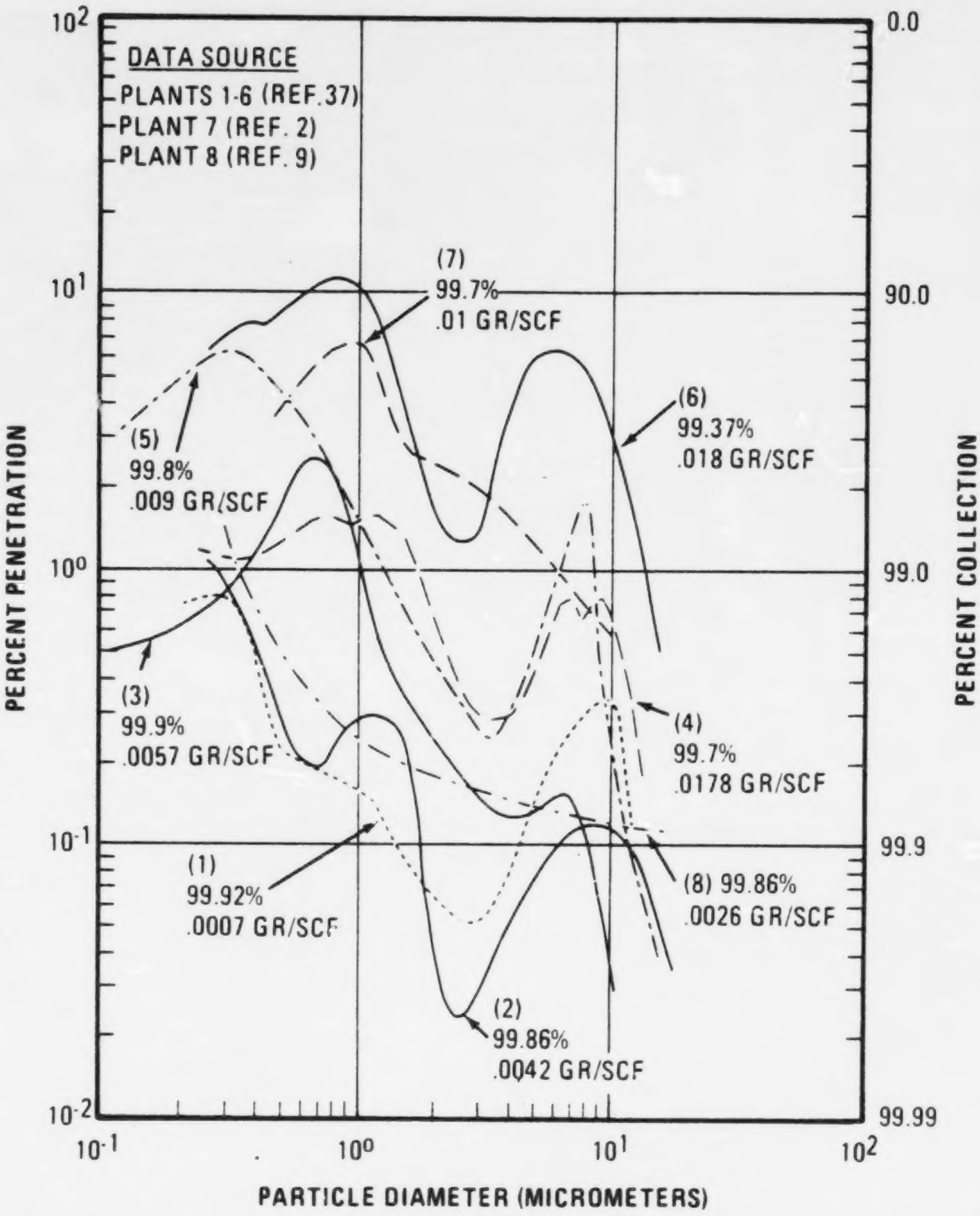

**PLANT NOTES:**

| | |
|---|---|
| 1. WESTERN, COLD, LOW SULFUR | 5. WESTERN COLD, LOW SULFUR |
| 2. EASTERN, COLD, LOW SULFUR | 6. WESTERN HOT, LOW SULFUR |
| 3. EASTERN, COLD, HIGH SULFUR | 7. WESTERN COLD |
| 4. EASTERN, HOT, LOW SULFUR | 8. NORTH DAKOTA LIGNITE |

Figure 1. Fine Particulate Collection in Electrostatic Precipitators.

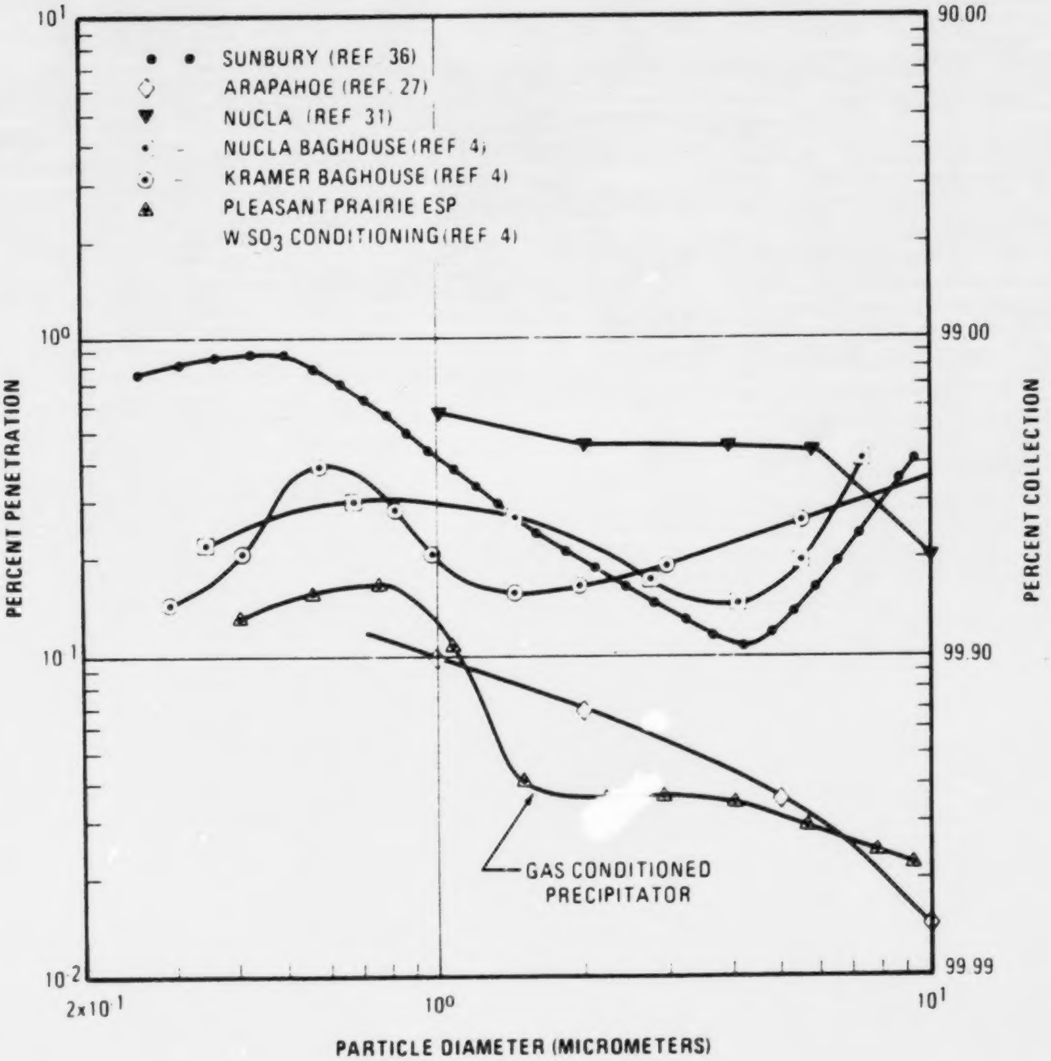

Figure 2. Fine Particulate Collection Baghouses and Precipitator with Gas Conditioning.

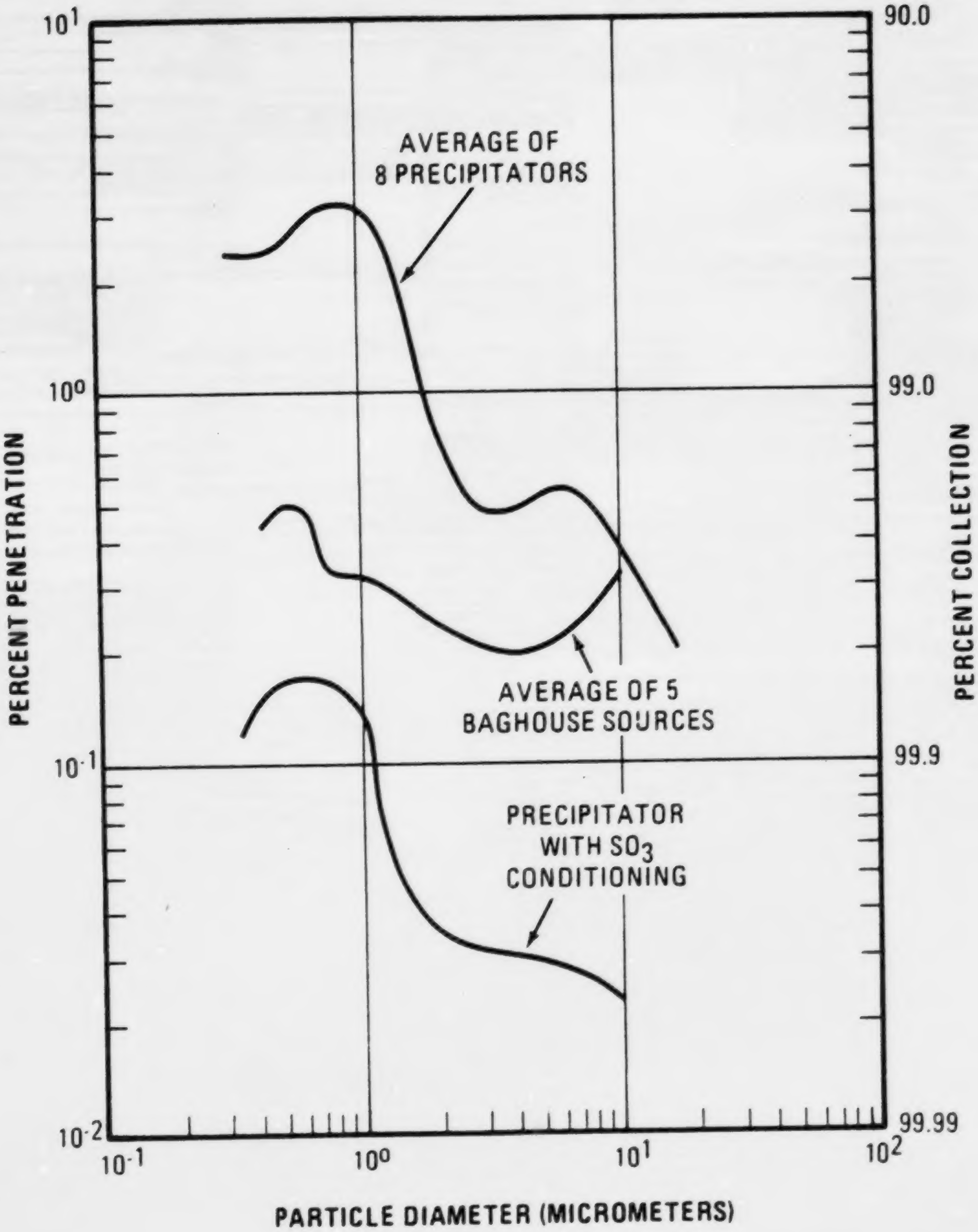

Figure 3. Summary of Fine Particulate Collection.

## ACID RAIN

The proposed acid rain regulations will have an effect on the particulate collection device in three areas:

1. Fuel switching. A primary strategy (if allowed in the regulations), that of switching to lower sulfur coal, will produce an ash with a higher resistivity and therefore an application which must be accommodated in the sizing and design of the ESP. Note that fabric filter collectors are insensitive to ash resistivity.

The industry is experienced in providing precipitator upgrades, additional capacity or new installations to accommodate fuel switching. Many new installations currently have precipitators in place sized to accommodate the ash from low sulfur coal.

2. LIMB. Furnace injection of limestone as a compliance strategy will produce higher grain loadings and higher resistivity ash than the base fuel. Again, the compliance strategy may involve gas conditioning, precipitator upgrades or the installation of additional particulate collection equipment.

Figure 4 indicates the stoichiometry and therefore, the grain loading increases anticipated for 2-4% sulfur fuels. You will note from the example in Figure 5 that at a stoichiometry of 2, the grain loading will double and the resistivity is expected to increase by one order of magnitude.

Research-Cottrell and others are currently involved in full scale testing of this technology for the purpose of developing a satisfactory applications base.

3. FGD retrofits. This will be the last choice of the utilities, but may involve in excess of 20,000 MW of existing generating capacity. Wet FGD backfits may not have an effect on the existing particulate collection device, but dry FGD backfits placed in front of the particulate collecting device will most certainly require a complete modification or supplement to existing particulate control equipment to accommodate the different ash -- both chemically and quantity, as well as the reagent recycle requirement.

## ABILITY OF THE INDUSTRY TO RESPOND TO THE NEW REGULATIONS

The appropriate question now to ask is "what is the ability of the industry to respond to the demand that may be created by new regulations -- fine particulates and acid rain?"

We have every confidence that the increased demands, estimated to be as much as 40,000 MW over fifteen years, will not exceed the capabilities of the industry to produce on almost any conceivable schedule. The demand noted above for particulate collection devices is considerably below the demand levels existing in the early and mid-1970's from the backfit market resulting from enactment of the Clean Air Act, together with a high level of grassroots plants activity in the period.

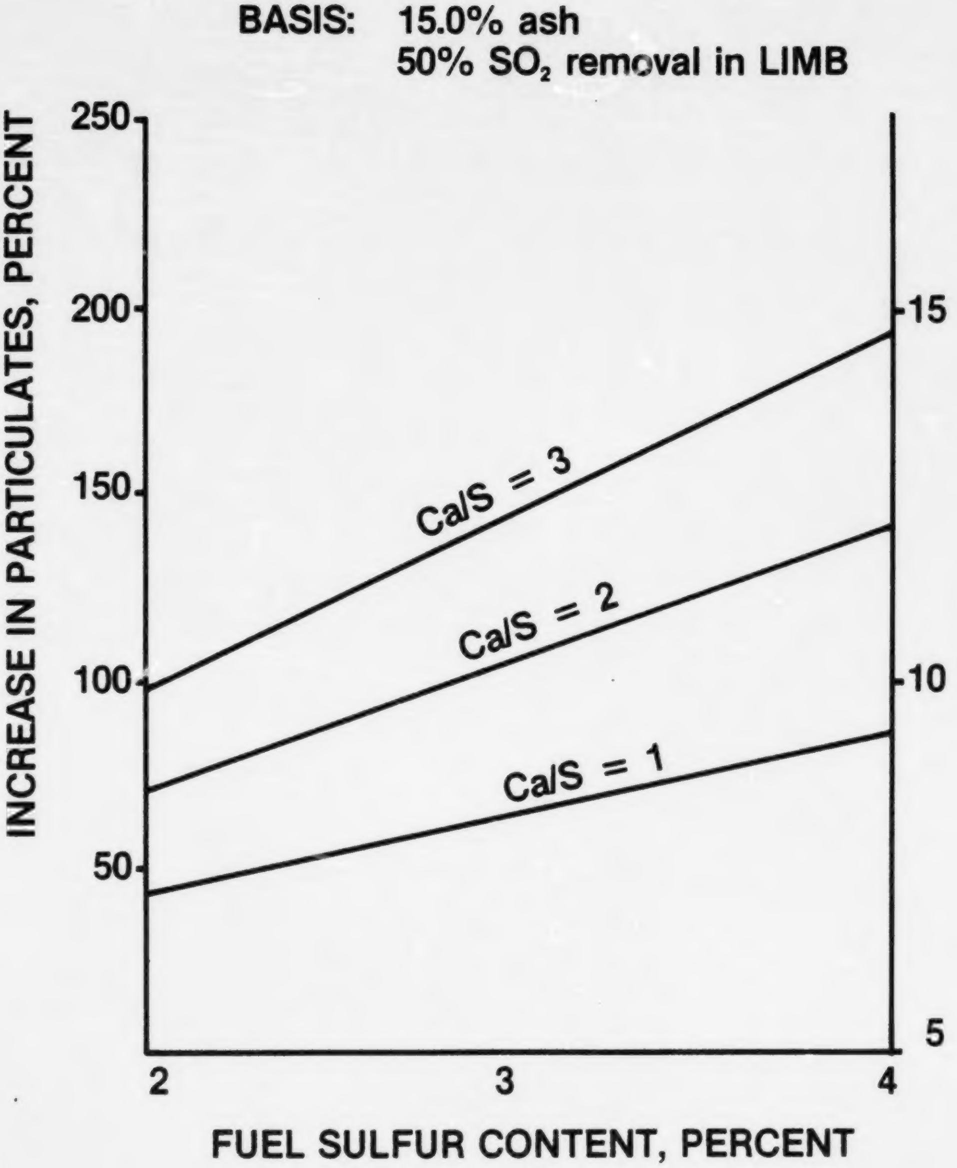

Figure 4. Effect of Limestone Injection on Particulate Loading to ESP.

**BASIS:** 500 MW = $1.02 \times 10^6$ SCFM
50% $SO_2$ removal in LIMB
200 SCA @ T = 300

| BOILER PROCESS CONDITIONS | BASE CASE | LIMB RETROFIT | |
|---|---|---|---|
| Limestone Stoichiometry | 0 | 1 | 2 |
| Resistivity Ohm-cm | $2 \times 10^{11}$ | $2 \times 10^{12}$ | $2 \times 10^{12}$ |
| ESP Inlet Loading, GR/SCF | 5.0 | 8.8 | 11.2 |
| ESP Outlet Loading, GR/SCF | 0.3 | 0.7 | 0.8 |
| ESP Efficiency, % | 94.8 | 92.5 | 92.5 |

Figure 5. Effect of Limestone Injection on ESP Performance.

The following Figure 6 indicates a peak year in 1974 in which 31,000 MW of precipitator capacity was purchased for a combination of new plants and low-sulfur-fuel-switching backfits. In the fiteen year period, 1971-1984, over 228,000 MW of precipitator capacity in the U.S. was purchased. The average market in the decade of the 1970's was 21,000 MW annually. The projected 1984 market is less than 5% of the average 1970's figure and 1985 is projected to rise only slightly from this figure. You could therefore, correctly conclude that we are operating at less than 10% of capacity in the air pollution control industry at this time, and are certainly capable of meeting the requirements of the proposed legislation.

In conclusion, my viewpoint as an employee of a major air pollution manufacturer is that:

1. The technology is in place to meet the projected particulate regulations. Both ESP's and fabric filters may be utilized. Therefore, no major technical development is needed nor underway on this program at this time.

2. It is the primary responsibility of the manufacturer to develop an applications base to permit the negotiation of contracts with commercial guarantees for both fine particulates and the particulate control applications on acid rain.

3. There is adequate capacity in the air pollution control industry to meet any anticipated market for particulate control equipment.

The work described in this paper was not funded by the U.S. Environmental Protection Agency and therefore the contents do not necessarily reflect the views of the Agency and no official endorsement should be inferred.

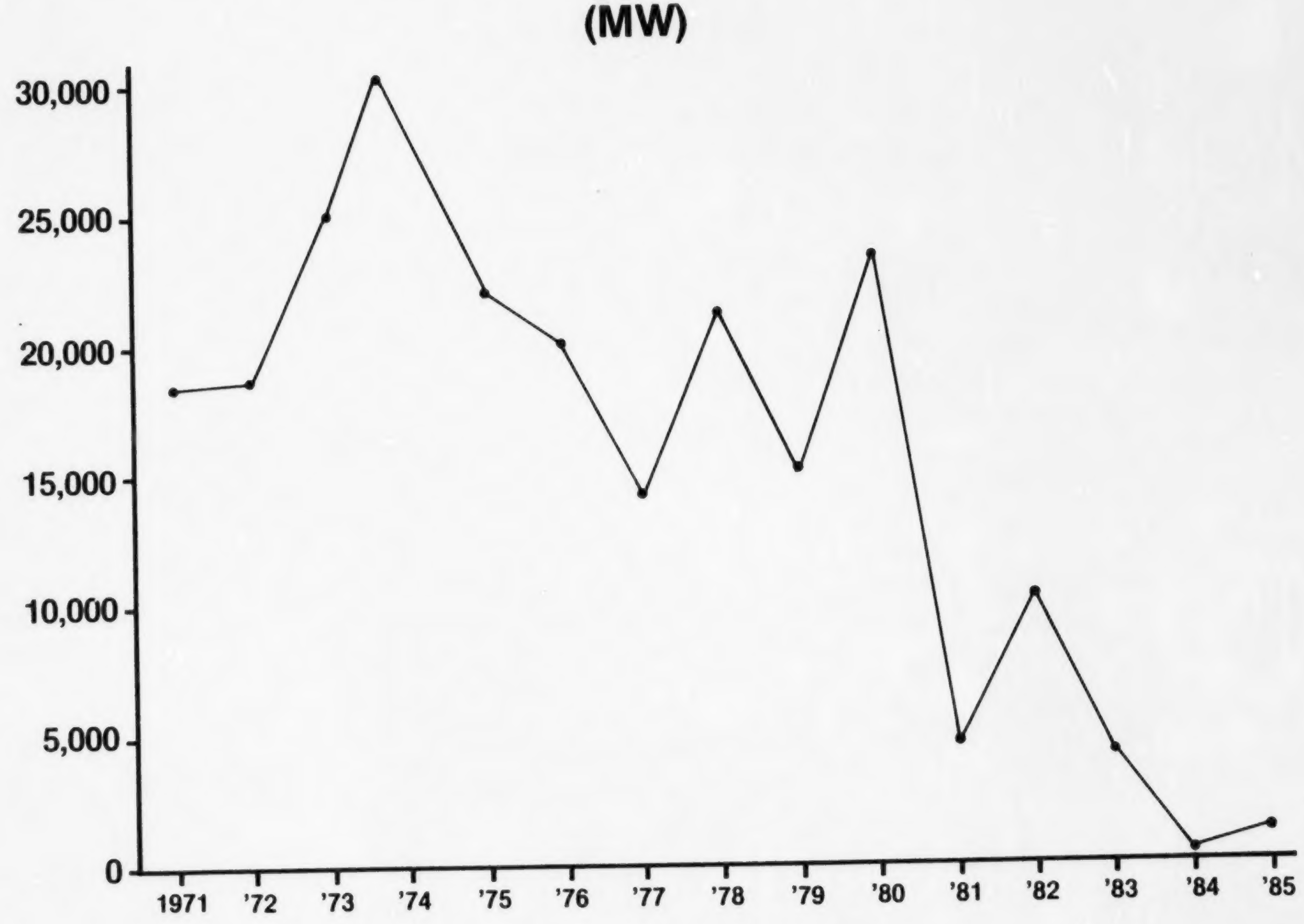

Figure 6. Utility Particulate Bookings.

# FUTURE PARTICULATE REGULATIONS

## THE VIEW OF THE SMALL MANUFACTURER

by: Sidney R. Orem
Executive Director
Industrial Gas Cleaning Institute
Alexandria, Virginia 22314

Good morning. I am honored to have been invited to join the prior panel of distinguished speakers. As the last of five speakers on the same broad topic, is there really something left to say?

All manufacturers of particulate control apparatus, small and large, have genuine concerns influenced by evolving policies in the near term. Some of these are:

(1) PM10 - Fine Particle Standards
(2) Acid Deposition Control - What Form?
(3) Industrial Boiler NSPS
(4) Requirements of Fluid-Bed Combustion
(5) Increasing Complexity of Doing Business
  (a) With More Vigorous Competition
  (b) With Increasing Cost of More Elaborate Proposals

### PM10 - FINE PARTICLE STANDARDS

When a PM10 ambient air quality standard is put in force, OAQPS will be required in due course to modify emission control regulations to insure maintenance of limits on PM10 levels. Control manufacturers, for the most part, do not possess a sufficient data base on less than 10 micrometer performance to make knowledgeable guarantees. Obviously, we must acquire more hands on capability with cascade impactors and other fine particle measurement techniques. To date, data from these sophisticated tools have largely been developed and used by EPA laboratories, agency contractors and testing contractors.

## ACID DEPOSITION CONTROL - WHAT FORM?

When we face the scientific facts and adopt acid deposition controls in the U.S., as we certainly will, the form and rigidity of the requirements will have special meaning to particulate control manufacturers. For example, any significant switching to very low sulfur coals will require retrofitting of many ESP's to maintain performance or more widespread flue gas conditioning. Alternately, it will also mean some total replacement of existing particulate controls, perhaps with fabric filters and in some cases, coupled with a spray dryer as part of a dry scrubbing system.

## INDUSTRIAL BOILER NSPS

The Federal Register of June 19 last contained the first Industrial Boiler NSPS, particulate and NOx standards for industrial boilers 100 to 250 MM BTU/hr. heat input. The 0.05 #/MM BTU requirement will indeed generate some much needed business in ESP's and fabric filters. An SOx regulation is under study and if, as many expect, the federal court in current litigation orders issuance of an SOx standard sooner, rather than later, it is conceivable such a standard may be on the street within six months.

The small manufacturer particularly faces problems with the purchase of smaller capacity FGD systems (as opposed to electric utility sizes). Witness the recent invitation to bid on an industrial FGD system for a major industrial, the specification and invitation having been prepared by a well known A&E accustomed to working on utility jobs. The protest from the small manufacturers could be heard from the East Coast to Kansas City! "If I bid this job by the book, the cost of bid preparation will be larger than the potential profit, even if I am lucky enough to win the job!" After much talk, a compromise on a less complex proposal evolved.

## REQUIREMENTS OF FLUID-BED COMBUSTION

Several smaller particulate control manufacturers have indicated a high percentage of their current small-capacity boiler bids involving FBC units, where neither the boiler manufacturer or the control equipment manufacturer has available as much "products of combustion" data as they would like. These uncertainties include dust particle size distribution, dust concentration, density, etc. Start-up and testing of additional units will surely begin to build a more adequate data base. With circulating PBC, it appears we will be facing higher dust loadings of much finer particle sizes -- not an easier particulate control problem.

## COMPLEXITY OF DOING BUSINESS

As the buyer becomes more knowledgeable, he hires more sophisticated A&E firms and the result is more elaborate proposal requirements and more difficult business judgments. Few jobs are let any more on "seat of the pants" specifications.

This is all as it should be provided specs do not grow in complexity just for the sake of more "weight and thickness" to the book. Our trade association, the Industrial Gas Cleaning Institute, hopes to try to develop an improved understanding with the A&E firms, as well as our ultimate customers on the specification/contract complexity problem.

## Session 2: ADVANCED ENERGY APPLICATIONS

George A. Rinard, Chairman
Denver Research Institute
Denver, CO

# HIGH-TEMPERATURE, HIGH-PRESSURE ELECTROSTATIC PRECIPITATION, CURRENT STATUS

By: P. L. Feldman
Research-Cottrell, Inc.
Somerville, NJ 08876

K. S. Kumar
Research-Cottrell, Inc.
Somerville, NJ 08876

## ABSTRACT

The development of the technologies of pressurized fluidized bed combustion and coal gasification brings new challenges to particulate control technology. Removal of particulate from gas streams at conditions of high temperature and high pressure requires a reevaluation of the criteria for choosing and sizing particulate control equipment.

This paper presents the theory of electrostatic precipitation as it applies to the special case of high temperature and high pressure. The effects of temperature and gas density on electrical energization and particle migration are discussed and conclusions are drawn concerning the viability of electrostatic precipitation and its comparison to other control methods. Precipitator design considerations and previous precipitator experience at conditions of high temperature and high pressure are also presented.

## BACKGROUND

Pressurized fluidized bed combustion (PFBC) and coal gasification are technologies which are being developed to be used in combined cycle electric power generation. This method of power generation uses gases at high temperature and pressure to drive a gas turbine for electrical power generation in addition to that generated by the steam turbine. The viability of both of these processes depends on efficient and reliable particulate removal from the gases ahead of the gas turbine blades.

The temperature of the gas to be treated for particulate removal is typically about 1600°F for both the gasification and PFBC processes. Pressure may be typically 20 atmospheres for gasification and 6 to 10 atmospheres for the PFBC processes. An important exception in the PFBC processes is the low-temperature PFBC process in which the temperature of the combustion gas to be treated is about 800°F. In this case there is no net power generation by the gas turbine but the energy generated by the turbine is used to compress the air to the fluidized bed. The power generating efficiency of this process is somewhat lower than the higher temperature process, but the low-temperature process has the advantage of allowing simpler and more economical design and choice of materials for equipment downstream of the combustor.

Figure 1 shows the requirments on the hot gas cleanup system (HGCS) for particulate removal prior to the turbine (1). The figure shows the particle size distributions in terms of cumulative ppm greater than a given size versus particle diameter in microns. The turbine tolerance line represents the maximum concentration-size relationship that the gas turbine can accept. The "bed efflux" line shows the particulate concentration at the outlet of a typical PFBC. The HGCS must at least remove particulate as represented by the difference between these two lines. However, the particulate removal requirement to satisfy EPA emission standards is more stringent, requiring a maximum total emission corresponding to 22 ppm.

It can be seen from the figure that a 3-stage cyclone system barely satisfies the turbine requirement but falls short of satisfying the EPA requirement. This is because cyclone collection efficiency drops off rapidly for particles below 10 microns in size. Thus, if the 3-stage cyclone system is used as the HGCS, an additional downstream particulate collector, such as an electrostatic precipitator (ESP) or fabric filter at atmospheric pressure, would be required to satisfy EPA requirements.

However, use of a high-efficiency particulate collection device such as an ESP at conditions of high temperature and high pressure (HTHP) ahead of the gas turbine allows satisfaction of both the EPA and turbine tolerance requirements as shown in Figure 1. The ESP line in the figure assumes use of a HGCS consisting of a single stage cyclone operating at 85% efficiency followed by an ESP at 99.3% efficiency. There are several advantages to the use of a high-efficiency HGCS over the 3-stage cyclone approach:

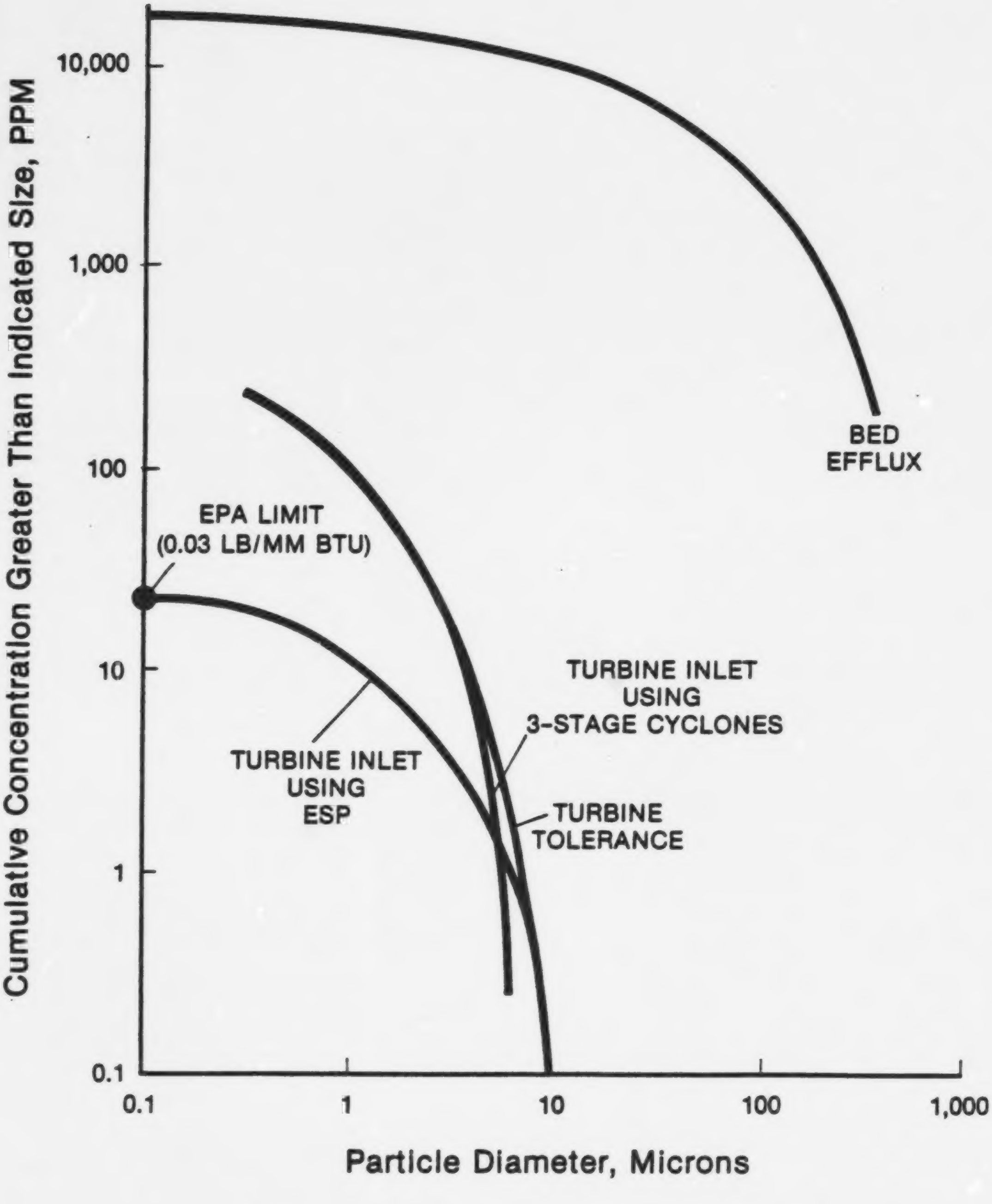

FIGURE 1. PFBC SYSTEM SIZE DISTRIBUTION

1. The need for a large atmospheric pressure downstream collector is eliminated.

2. Because the high-efficiency HGCS exceeds the turbine tolerance requirement, turbine blade life can be extended significantly.

3. Very low particulate concentration to the turbine allows close-to-design power output for a longer period of time.

The economics of the high-efficiency HGCS as compared to 3-stage cyclones have been studied (2) and a significant advantage was reported for the high efficiency HGCS.

Particulate collectors which qualify for consideration in the HGCU are the ESP and barrier filters such as ceramic filters or gravel bed filters. These are all in various stages of development for the HTHP application. However, at the present time the ESP is further advanced in its development, and shows fewer potential technical problems than the filtration devices. Barrier filters are prone to plugging depending on particulate properties at high-temperature operations or during process upsets. Also, filter materials are largely undeveloped at this time. An additional and important point in favor of the HTHP ESP is that the physics of electrostatic precipitation predicts significant performance improvement at HTHP conditions whereas the filtration mehanisms of impaction and diffusion become less effective at HTHP conditions.

The remainder of this paper will discuss the present status of development of the HTHP ESP, the theory of its performance, and conceptual design considerations.

## PRESENT STATUS OF HTHP PRECIPITATOR DEVELOPMENT

Research-Cottrell has been active in the development of HTHP electrostatic precipitation since the early 1960's. During this time pilot precipitators were designed and operated under a variety of conditions of temperature and pressure in the following applications:

(1) Union Carbide Olefins Co. - Pilot PFBC
(2) Texaco - Pilot Pressurized Gasifier
(3) Bureau of Mines - Simulated PFBC
(4) Combustion Power Co. - Pilot Pressurized Combustion
(5) Texas Gas Transmission Co. - Natural Gas Pipeline
(6) Curtiss-Wright - Pilot PFBC

In addition Research-Cottrell conducted a parametric study of the feasibility of corona generation over a wide range of temperature and pressure for EPA in the mid-1970's.

Details of the operation of these pilot precipitators have been reported before[3,4] and are summarized briefly here:

1. Union Carbide : A HTHP pilot precipitator was supplied in 1963 to Union Carbide Olefins Co. to remove particulate from a pilot PFBC at 1300°F and pressures up to 100 psig prior to a gas turbine. Over 100 tests were run demonstrating consistent high-efficiency removal of a fine particulate size distribution. Of particular note in these tests was the ability to operate at high electric field strengths, often exceeding 20 kV/in, and the strongly beneficial effect of the high field strength on collection efficiency.

2. Texaco : In 1960 Texaco operated a pilot synthesis gas generator which generated very fine carbon particulate. Research-Cottrell supplied a pilot precipitator designed to reduce the carbon concentration from 400 ppm to less than 5 ppm. Precipitator temperature was only 350°F but pressure was high at 350 psig. A wet-wall precipitator was supplied for these conditions. Again the beneficial effect of gas density was seen as the precipitator operated at high field strength and consistently maintained carbon emission below the 5 ppm level. It was also seen during this program that negative discharge polarity was much superior to positive for high efficiency precipitation.

3. Bureau of Mines : In the mid-1960's the Bureau of Mines ran tests on a pilot-scale electrostatic precipitator using flue gas generated by burning natural gas with reinjected fly ash particles. Typical operating conditions were 1500°F and 80 psig. Although operating problems were encountered due to tube distortions, reasonably high collection efficiencies were reported. Again the superiority of negative discharge over positive was demonstrated.

4. Combustion Power : In the mid-1960's Combustion Power Company ran a program for HEW to test electrostatic precipitation at 1600-1700°F with pressures around 150 psig. A methanol burner generated flue gas into which alumina or redispersed flyash was injected. Because of the relatively long discharge wires used, wire oscillation problems limited the field strength and, hence, collection efficiency was limited in the mid 90% range. However, the test program again showed the correlation of collection efficiency with field strength and the advantage of negative over positive discharge polarity.

5. Texas Gas Transmission : In 1965 Research-Cottrell worked with Texas Gas Transmission Co. to develop a high pressure precipitator for removing oil mist from a compressed natural gas pipeline. The operating temperature was 110°F but the pressure was very high at 850 psig. The precipitator operated very successfully for a year in steady operation achieving collection efficiencies over

99% while collecting the very fine oil mist of 0.7 micron mean diameter. Because of the very high gas density (relative density = 55) it was possible to achieve very high field strengths. In fact it was found that for field strength greater than 50 kV/inch the electrostatic forces were great enough to actually pull the oil from the collecting surfaces. Thus 50 kV/inch was a practical operating limitation.

6. Curtiss-Wright : The largest pilot HTHP precipitator test to date was carried out in a DOE sponsored program in 1982-1983 at the Curtiss-Wright PFBC facility in New Jersey. Successful tests were carried out at 1400-1500°F and 70 psig showing collecting efficiencies up to 99.5% for the actual PFBC particulate. It was intended to test at 1600°F and 80 psig but control upsets in the PFBC facility caused water flooding and consequent damage and misalignment of the internals in the electrostatic precipitator. Even in the damaged condition the precipitator was capable of collection efficiencies in the 75-85% range. Rigid discharge electrodes were used in the design to avoid oscillation problem such as seen at Combustion Power.

7. EPA Corona Feasibility Study : In the mid-1970's Research-Cottrell conducted a laboratory program to study the feasibility of corona generation over a wide range of temperature and pressure from ambient conditions to 2000°F and 500 psig. Current voltage characteristics for both negative and positive corona were measured with several discharge wire diameters in dry air, a simulated combustion gas and a simulated fuel gas. It was shown that, subject to appropriate choice of polarity and pressure, stable corona discharge can be achieved at all temperatures.

## HTHP ELECTROSTATIC PRECIPITATION THEORY

In order to understand the advantages of electrostatic precipitation for particulate collection in HTHP applications such as PFBC and coal gasification, it is necessary to examine the theory of electrostatic precipitation. Several of the parameters which influence the sizing and collection efficiency of electrostatic precipitators are dependent on gas temperature and pressure. It is through understanding of these dependences that an appreciation of the unique applicability of electrostatic precipitators to high gas density conditions can be gotten.

It has been shown (6) that the collection efficiency of an electrostatic precipitator can be expressed in the form:

$$\eta = 1 - e^{-(w_k A/Q)^m} \qquad (1)$$

where is the fraction of inlet dust collected in the precipitator, A is precipitator collecting area, Q is the volumetric flow rate, $w_k$ is a modified particle collection velocity or migration velocity and m is an exponent dependent on the precipitator inlet particle size distribution and the molecular mean free path of the gas. The term (A/Q) is known as the specific collecting area (SCA).

Thus, precipitator efficiency increases as the specific collecting area, A/Q, increases and as the modified collecting velocity increases. It can be shown that the modified migration velocity can be represented by:

$$w_k = C_2 \varepsilon_o E_o E_p \, d/\mu \qquad (2)$$

where $C_2$ is a second constant dependent on inlet particle size distribution and the mean free path, $\varepsilon_o$ is the permittivity of free space, $E_o$ is the particle charging field strength, $E_p$ is the particle collecting field strength, d is the inlet mass median particle diameter, and $\mu$ is the gas viscosity.

The key controllable parameters in the expression for $w_k$ are the charging and collecting field strengths. To be precise, these fields differ from each other and depend on several factors including applied voltage, particulate space charge and ionic space charge. However, a very useful approximation is gotten by considering both $E_o$ and $E_p$ to be equal to the applied voltage divided by the discharge to collecting electrode spacing:

$$E_o \simeq E_p \simeq V_o/S \qquad (3)$$

Then:

$$w_k = (C_2 \varepsilon_o d/\mu S^2) V_o^2 \qquad (4)$$

or, for a given application the collecting velocity increases with the square of the applied voltage. It is for this reason that electrostatic precipitators are designed to operate at maximum voltage, allowing $w_k$ to be maximized and, consequently, collecting area minimized. The maximum voltage that can be applied in any given application is that corresponding to electrical breakdowns in the precipitator such as sparking or back corona. The electrical breakdown voltage is dependent, among other things, on gas density, and it is this dependence which is the key to the success of electrostatic precipitation to high gas density applications.

Figure 2 shows electric field strength vs. relative gas density (relative to density at 70°F and 1 atm). The data points shown are taken from Research-Cottrell's previous experience in high temperature high pressure pilot precipitator operation. The field strengths shown in the figure are maximum field strength limited by sparking in the pilot precipitators. The 1300°F data are taken from the Union Carbide and Curtiss-Wright PFBC operations, the 1500°F data are from Curtiss-Wright and the Bureau of Mines PFBC facility, and the 1650°F data are from the Combustion Power program.

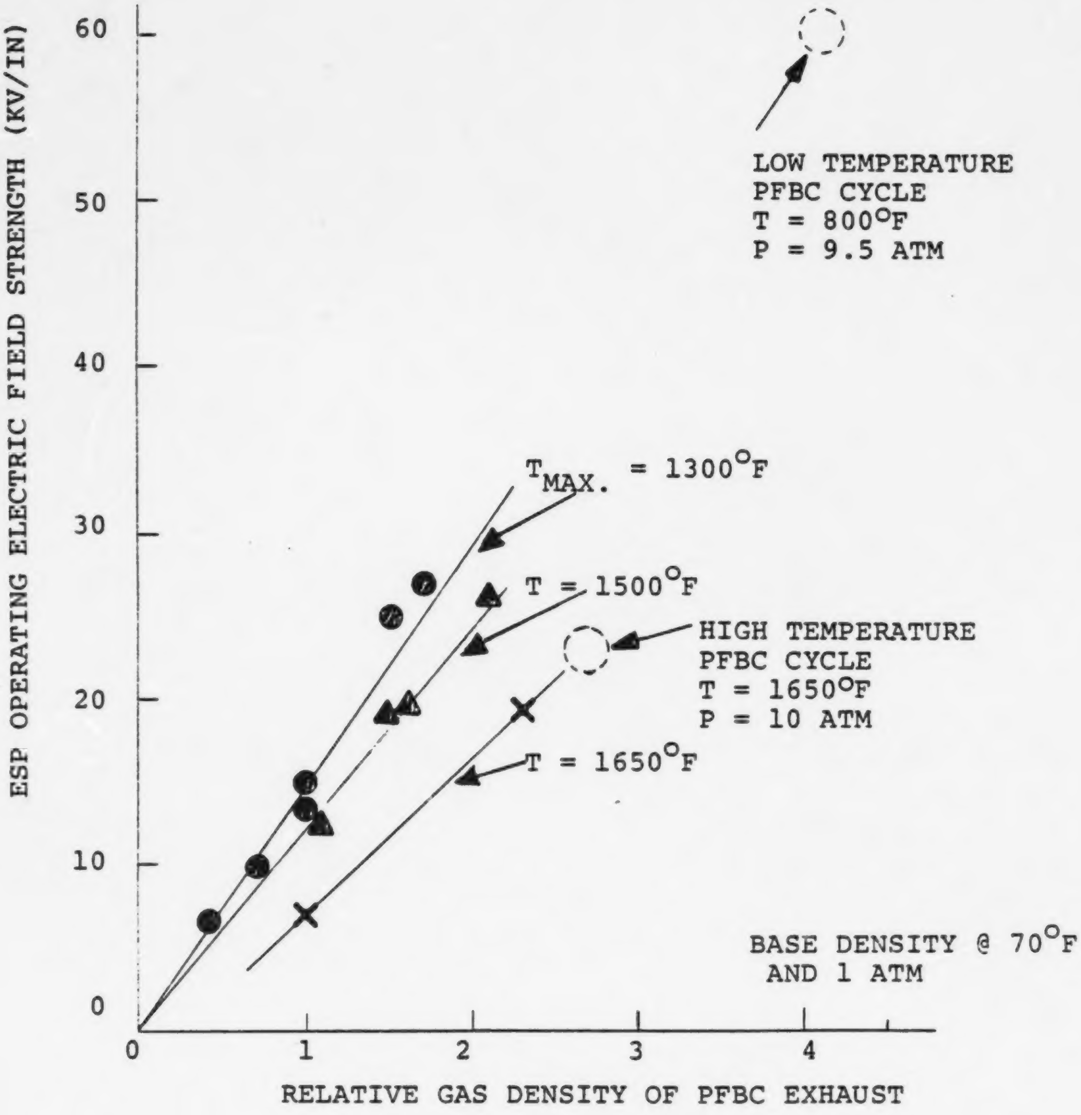

FIGURE 2. HTHP ESP OPERATING FIELD STRENGTH AS A FUNCTION OF GAS DENSITY

It is seen from Figure 2 that for the 1300$^{o}$F case the field strength is directly proportional to the gas density, increasing at a rate of 15 kV/in per unit of density. This is similar to the field strength rate of increase expected at lower temperatures for normal precipitator geometries. The 1500$^{o}$F and 1650$^{o}$F lines, however, show an increase with density at somewhat lower rates. Apparently an independent temperature effect is promoting electrical breakdowns at lower field strengths for temperatures over 1300$^{o}$F. Nevertheless, in all cases the increase in field strength with gas density is significant and the resultant impact on the particle collection velocity, $w_k$, is very favorable because of the square relationship of field strength to $w_k$.

It must be remembered when estimating the effects of increasing temperature and pressure on $w_k$ to account for the gas viscosity change with temperature. Gas viscosity increases with temperature roughly to the 0.6 power of temperature. This is a negative effect on $w_k$ and, to a small extent, affects some of the large advantage of the higher field strength discussed above.

Additional negative effects of increased gas density are found in the constants, $C_2$ and m, in equations (1) and (2). These constants depend on gas density to the extent that gas density reduces the gas phase molecular mean free path and affects diffusion charging and transport of the sub-micron portion of the particle size distribution. Again, although this is a negative effect of gas density, it is greatly overridden by the strong positive effect of the higher field strength.

An additional advantage of higher gas density is the reduction of the volume of gas treated in the precipitator. Precipitators are sized based on the actual volume of gas handled. Thus, after accounting for the previously mentioned density effects, an additional reduction in collecting area directly proportional to gas density can be taken.

Accounting for all the above considerations, the following example illustrates the strong beneficial effect of gas density on precipitator size. Consider, as a basis, a conventional power boiler precipitator operating at 300$^{o}$F and 1 atmosphere (relative density = 0.7) at a field strength of 10 kV/inch. At these conditions, using appropriate values of the constants in equation (1) and (2), an SCA of about 248 square feet per 1000 acfm of flue gas is calculated to achieve 99% collection efficiency.

If we now consider PFBC conditions at 1650$^{o}$F and 10 atmospheres (relative density = 2.5), Figure 2 shows that the precipitator can now operate at a field strength of 23 kv/inch. Again using the appropriate values of the constants for these conditions, we can calculate an SCA requirement of 124 square feet per 1000 acfm to achieve 99% collection efficiency. This represents a 50% reduction in theoretically required SCA over the conventional case. In terms of actual precipitator area required the additional savings due to the volume reduction must be taken into account. The volume reduction is the ratio of the gas densities, i.e. 0.7/2.5 = 0.28. Therefore the collecting area required for the 1650°F, 10 atmosphere PFBC case is only 0.5 x 0.28 = 14% of that required for the conventional precipitator.

For higher gas densities, the benefits become even greater, especially in situations where the gas density is higher at lower temperature, e.g. the low temperature PFBC process which operates about 800°F and 9.5 atmospheres (relative density = 4). For cases such as this, the calculated precipitator size becomes unrealistically small and the extent of potential size saving which can be realized is limited by practical considerations as will be discussed below.

The important point to be learned from the above is that, because of favorable electrical effects at higher gas densities, the sizing and/or performance of an electrostatic precipitator becomes much more favorable as compared to conventional precipitator operation. Except for the positive electrical effects, the impact of other physical parameters such as gas viscosity and mean free path on particle collection at high temperature and pressure is adverse. In the precipitator the electrical effect overrides these negative effects. However, in other devices relying on inertial and diffusional collection the trend in particulate collection at higher temperature and pressure is toward poorer performance.

## HTHP ESP CONCEPTUAL DESIGN CONSIDERATIONS

Although precipitation theory indicates that the precipitator collection area requirement becomes very small at high gas density, practical precipitator design criteria limit the extent to which the small indicated size can be realized. For example, gas velocity through the precipitator must be limited at some reasonable maximum value in order to avoid excessive particulate reentrainment; the specification of the limiting velocity sets a minimum cross sectional area for flow in the precipitator.

Aspect ratio is another design parameter which must be reasonably specified in order to provide sufficient precipitator length in relation to its height so that collected particulate can be moved to the hopper area without excessive loss. Rapping segregation and electrical sectionalization are other considerations tending to limit the extent to which precipitator size can be reduced.

From the above it can be seen that the specification of minimum velocity determines precipitator flow cross section, or height and width, and aspect ratio determines a minimum precipitator length. Thus, a minimum precipitator size is dictated by these two parameters alone. Any theoretically indicated size below this minimum cannot be realized without reconsideration of the velocity and aspect ratio criteria. For example, considering a HTHP ESP for a 125 MW PFBC handling about 100,000 acfm of gas at 1650°F and 10 atmospheres pressure, if a maximum velocity of 5 feet per second and an aspect ratio of 1.3 is specified, the minimum ESP SCA is 150 $ft^2$/1000 acfm. This SCA is more than theoretically required for 99%

efficiency particulate collection, which indicates that precipitators used for this application will necessarily be oversized, resulting in a highly redundant, highly reliable system. This is not undesirable because the precipitator is not only a pollution control device but is also an in-line process component whose job is to protect the gas turbine from erosion.

As mentioned previously the HGCS using an ESP, or for that matter a barrier filter, would probably retain a single-stage cyclone operating at about 85% efficiency upstream of the ESP. In the case of the precipitator the reasons for the cyclone are to reduce particulate loading so that corona suppression is not a problem and so that the rapping frequency can be minimized. However, because of the built-in excess collection efficiency in the ESP, the cyclone is not required in order to meet an overall efficiency objective. Thus the conceived requirement for the cyclone may be waived as experience is gained with HTHP ESP's in the future.

The conceived configuration of the ESP itself is a horizontal-flow, plate-type ESP using rigid discharge electrodes and contained in a horizontal cylindrical pressure vessel. All of the previous pilot experience descirbed before, except for the Texas Gas Transmission case, used vertical tube-type ESP's. This choice was primarily for better flow containment required by the relatively small size of the systems. However, for full-scale HTHP ESP's, the horizontal flow, plate-type arrangement is preferred because of the considerations shown in Table 1.

TABLE 1. CONSIDERATIONS IN CHOICE OF HORIZONTAL FLOW ESP

- Electrical Sectionalization
- Rapping Segregation
- Electrode Alignment
- Flow Distribution
- Flow Direction

The first area of consideration is electrical sectionalization. Maximum electric sectionalization is very important in applications in which the reliability of high-efficiency particulate collection is critical. PFBC and gasifier applications fit this category because the precipitator is in-line to protect the downstream turbine. With the horizontal flow design, there is normal freedom in selecting the number of electrical sections in a given flow length. With vertical pipes, on the other hand, it is not feasible to consider more than one section per vessel. Although schemes can be devised to increase the sectionalization in vertical vessels, they are at the expense of flow velocity through the vessel, pressure drop and design reliability. The only way remaining to achieve sectionalization in vertical flow is through the use of multiple vessels which is economically unfeasible.

Rapping segregation is another problem with the vertical flow design. With vertical pipes the entire length is rapped at one time which means that all collected ash is dislodged at the same time resulting in the potential for undue particulate carryover in the rapping puff. With horizontal flow it is possible to rap individual sections or even individual plates so as to minimize the amount of particulate that can be entrained by a single rap.

Electrode alignment is another potential problem in the vertical design because the discharge electrode is hung through the entire flow length. In the horizontal design the discharge electrodes are perpendicular to the flow length and can therefore be shorter than in the vertical design. The longer electrode coupled with the possibility of tube sheet deformation make electrode misalignment more likely with the vertical design than with the horizontal design.

Flow distribution and pressure drop are also more easily dealt with in the horizontal design where standard precipitator design features can be employed with no change in flow direction and minimum pressure drop through the precipitator. In the vertical flow design, however, the flow must be brought into and leave the precipitator in the horizontal direction. The resulting changes in direction add to the precipitator pressure drop and proper management of uniform flow through each tube is difficult.

Although the above considerations are enough to make the decision for horizontal over vertical flow, there are additional considerations which are equally important and in favor of horizontal flow. They have to do with the direction of the flow itself. If the direction of the vertical flow is upward, it opposes the movement of ash to the hoppers after rapping and increases the probability of large particle reentrainment which can be damaging to the downstream turbine. With upflow there is also the problem of aggravated corona suppression because of the high concentration of particulate at the bottom of the precipitator tube where ash falling upward the hopper from the entire tube meets the incoming gas with its high particulate concentration.

If the direction of the vertical flow is downward, then there is the problem of reentrainment from the hopper or the need for extra precipitator length and baffling to try to avoid that problem. This is also an undesirable arrangement because the rapped ash can easily be reentrained in the outlet flow stream as it falls to the hopper.

With horizontal flow no such problems exist because the flow is perpendicular to the movement of ash flow to the hopper which is within normal precipitator experience.

## ESP DEVELOPMENT NEEDS

Considerable progress has been made in the development of high temperature, high pressure electrostatic precipitators for particulate control. In addition to successful performance, key hardware components have been succesfully demonstrated such as high voltage insulators, rigid discharge electrodes, internally located rappers, and materials selection. However, the application of all these successes into one single program where the precipitator has been designed with scale-up in mind is yet to be accomplished. Thus, demonstration of a horizontal flow ESP, integrating all previously gained component knowledge, under actual PFBC conditions is needed on a pilot or sub-pilot scale.

Following such a program, the operating characteristics of a commercial-design ESP will be known and can be taken into account in an accurate scaled-up design. If commercial feasibility is indicated following the scale-up studies, then a larger-scale, long-term demonstration of a prototype HTHP ESP will be in order.

## REFERENCES

1. P. Suter, D. K. Mukherjee, Particle Distribution and Expected Erosion Rate in a Gas Turbine Driven by Pressurized Fluidized Bed Flue Gas, 7th International Conference on Fluidized Bed Combustion, 1982.
2. R. Zaharchuk, et al, Cost Evaluation of Four PFBC Hot Gas Cleanup Devices , 7th International Conference on Fluidized Bed Combustion, 1982.
3. P. L. Feldman, K. S. Kumar, High Temperature High Pressure Electrostatic Precipitation , Fine Particle Society 13th Annual Meeting, April 1982.
4. K. S. Kumar, Testing and Evaluation of ESP at Curtiss-Wright ,3rd Annual Contractor's Meeting, Proceedings: Contaminant Control in Hot Coal Derived Gas Streams, December, 1983.
5. J. R. Bush, P. L. Feldman, M. Robinson, Development of a High Temperature High Pressure Electrostatic Precipitator , EPA-600/7-77/132, November 1977.
6. P. L. Feldman, Effects of Particle Size Distribution on the Performance of Electrostatic Precipitators , APCA 68th Annual Meeting, June 1975.

The work described in this paper was not funded by the U.S. Environmental Protection Agency and therefore the contents do not necessarily reflect the views of the Agency and no official endorsement should be inferred.

# TEST RESULTS OF A PRECIPITATOR OPERATING AT HIGH-TEMPERATURE AND HIGH-PRESSURE CONDITIONS

by

Donald E. Rugg, George Rinard, Michael Durham and James Armstrong
Denver Research Institute
P. O. Box 10127
Denver, Colorado 80210

## ABSTRACT

The results of pilot scale tests on an ESP operating at Pressurized Fluidized Bed Combustor (PFBC) conditions are presented. The tests were performed at the Denver Research Institute's Hot Gas Test Facility in Denver, Colorado at a constant flow rate of .056 $m^3$/sec (118 acfm) on a single tube cylindrical ESP with an SCA of 36 sec/m (183 $ft^2$/kacfm). Dust conditions were simulated by reentrainment of fly ash obtained from the Curtiss-Wright Small Gas Turbine Test Rig, and mass collection efficiencies were determined by simultaneous inlet and outlet dust concentration measurements. Tests were performed for different corona electrode designs, at temperatures of 760° and 900°C (1400° and 1650°F), and pressures of 6.4 and 10 atm. The effect of the parameters on collection efficiency is discussed. While no signs of thermal ionization were apparent at even the highest temperature, the addition of fly ash did cause an unexpected increase in corona current. The importance of the design on the corona electrode in determining a practical operating region is discussed.

The results are important, for hot gas cleanup not only for combined cycle PFBC applications, but also for turbo-charged PFBC systems and coal gasifiers.

## DISCLAIMER

The work described in this paper was not funded by the U. S. Environmental Protection Agency and therefore the contents do not necessarily reflect the views of the Agency and no official endorsement should be inferred.

## INTRODUCTION

The electrostatic precipitator (ESP) is being considered as a candidate device for final particle cleanup in combined cycle pressurized fluidized bed combustor (PFBC) power plants. Typical operating conditions for the ESP in this type system would be 900°C (1650°F) and 1 MPa (10 atm). Pilot scale tests on an ESP operating at these high-temperature and high-pressure (HTHP) conditions are being performed at the Denver Research Institute's Hot Gas Test Facility. The HTHP-ESP system and the particle sampling procedures that have been developed are discussed. Test results at temperatures of 760°C (1400°F) and 900°C (1650°F) and pressures of 640 kPa (6.4 atm) and 1 MPa (10 atm) are presented. Electrical characteristics and performances at the different operating conditions are compared.

## DESCRIPTION OF THE HTHP-ESP SYSTEM

The HTHP-ESP system at the Denver Research Institute was designed to simulate a wide range of PFBC operating conditions for the evaluation of electrostatic precipitation at high temperatures and pressures. A schematic of the HTHP-ESP and associated equipment is shown in Figure 1. The specifications of the system are given in Table 1. Compressors have been added to the system to provide the capability of delivering 0.47 $Nm^3/s$ (1000 scfm) of gas to the ESP at temperatures up to 980° (1800°F) and pressures up to 1 MPa (10 atm). Dust injection is provided immediately following the burner. Inlet particle sampling of the flue gas is conducted before the gas enters the main pressurized vessel containing the ESP and the outlet particle sampling is conducted in the outlet duct upstream of the orifice meter and throttle valve which monitors and controls the flow through the ESP.

TABLE 1. HTHP-ESP SYSTEM SPECIFICATIONS

MAXIMUM CONDITIONS

| | | |
|---|---|---|
| Electrical | | |
| Corona Voltage | 150 kV | |
| Corona Current | 50 mA | |
| Gas Conditions | | |
| Flow Rate | 0.47 $Nm^3/s$ | 1000 scfm |
| Pressures | 1.1 MPa | 11 atm |
| Temperature | 980°C | 1800°F |
| Collector Size | | |
| Active Tube Length | 2.1 m | 6.9 ft |
| Tube Diameter | 0.3 m | 1.0 ft |
| Tube Area | 2.0 $m^2$ | 21.7 $ft^2$ |
| Burner | | |
| Heat Capacity | 264 kW | 0.9 MBTU/hr |
| Fuel | Methanol | |

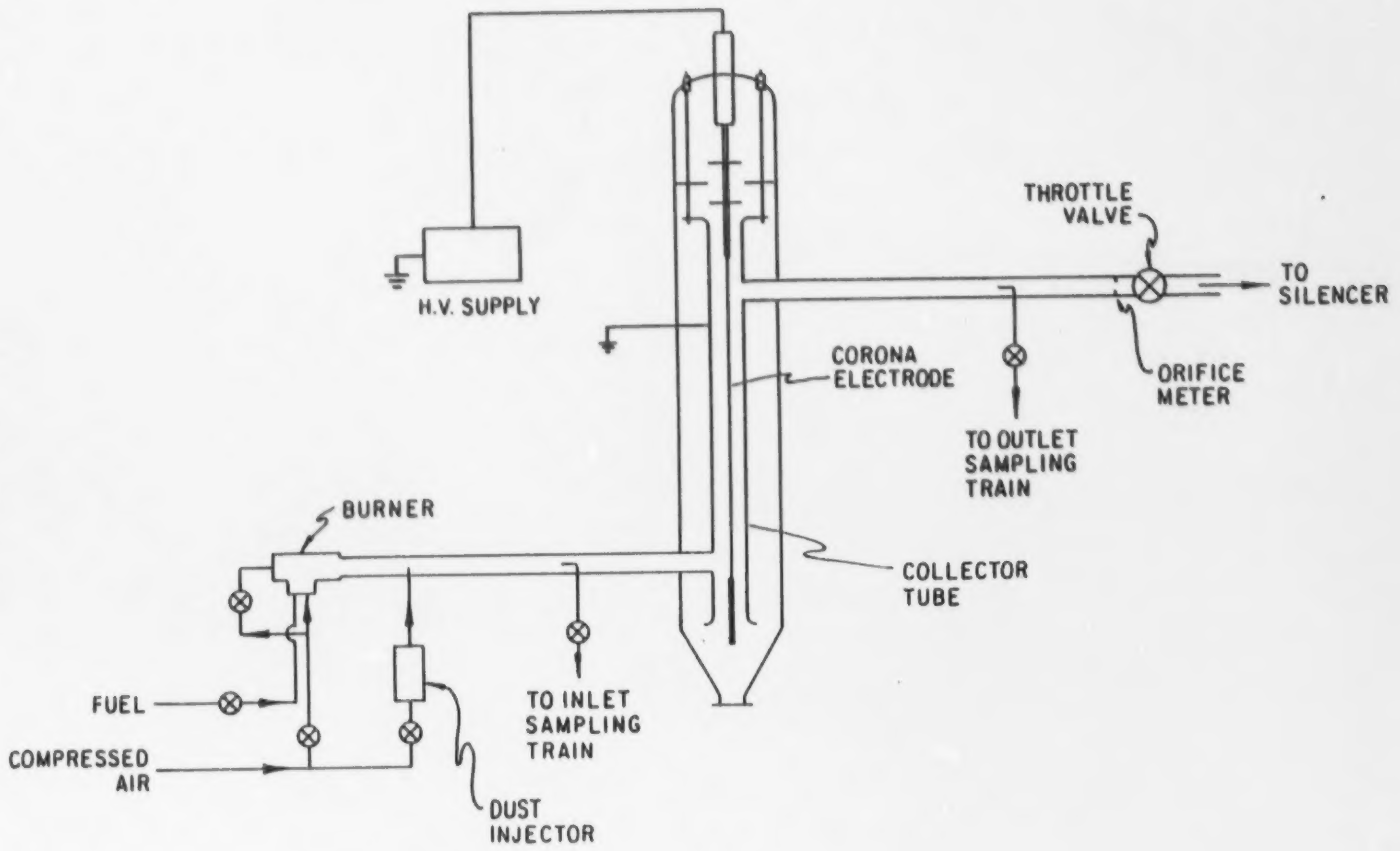
H.V. SUPPLY
THROTTLE VALVE
TO SILENCER
CORONA ELECTRODE
ORIFICE METER
TO OUTLET SAMPLING TRAIN
BURNER
COLLECTOR TUBE
FUEL
TO INLET SAMPLING TRAIN
COMPRESSED AIR
DUST INJECTOR

FIGURE 1. SCHEMATIC OF HIGH TEMPERATURE HIGH PRESSURE ESP TEST FACILITY

## CORONA ELECTRODES

Three types of corona electrodes, shown in Figure 2, have been used in the HTHP-ESP tests to determine electrical characteristics and ESP performance at various temperatures and pressures. Wire or smooth electrodes up to 15.9 mm (.625 inches) in diameter were used since this electrode should produce a minimum of corona current. The scalloped electrode should produce the maximum amount of corona current while the wide vaned electrode should produce an intermediate amount of corona current. The latter two electrodes are rigid electrode designs by Research Cottrell.

## DUST INJECTION SYSTEM

The dust injection system is housed in a separate pressure vessel and connected to the injection nozzle by delivery lines. Compressed air to the dust injection vessel is preheated to about 120°C (250°F) to prevent moisture condensation in the system. The gas flow rate through the dust injection system is maintained at 2.4 l/s (5 acfm) which maintains a slightly higher pressure than the ESP. Initially, a fluidized bed aerosol generator fed by a K-TRON twin screw dust feeder was used to redisperse the dust. However, with a flow rate of only 2.4 l/s (5 acfm) through the bed it was not possible to redisperse dust at a rate high enough to achieve an Inlet dust loading of 2.3 g/Nm$^3$ (1 gr/scfm) at the ESP inlet. The fluidized bed was replaced by a metal block which has a slot the width of the twin screws and is attached to the ends of the screwfeeder. Air passing through the slot at about 60 m/s (200 ft/s) carried the dust from the screwfeeder to transport lines at a uniform rate. A counter on the screwfeeder and the control for the screwfeeder motor are used to set the dust feed rate. Also there are bypass lines and valves which allow the gas to bypass the dust injection system and go directly to the dust injection nozzle which permits the dust to be shut off without disturbing the flow in the ESP.

## SAMPLING PROCEDURES

Capabilities have been designed into the system for simultaneous sampling of particles at the inlet and outlet of the ESP. A sketch of the inlet sampling system is shown in Figure 3. At the inlet sampling nozzle, the gas temperature can be as high as 980°C (1800°F), requiring that the gas be cooled in the sampling line before it reaches the high pressure valve which has a maximum operating temperature of 540°C (1000°F) and the filter holders which operate up to 230°C (450°F). At the outlet sampling port, the gas temperature is less than 540°C (1000°F), so no cooling other than radiation is required.

A 17.8 cm (7 inch) long tube inlet filter and a 6.35 cm (2.5 inch) long tube outlet filter were used to provide sufficient collection surface so that both tests could be run simultaneously for one hour without overloading. To ensure that no leakage occurs around the tube filters, 47 mm disk backup filters are used. Downstream of the filters, the gas stream is cooled and dried and the moisture content of the gas is determined. A laminar flow element and dry gas meter are used to maintain isokinetic sampling conditions at the nozzles.

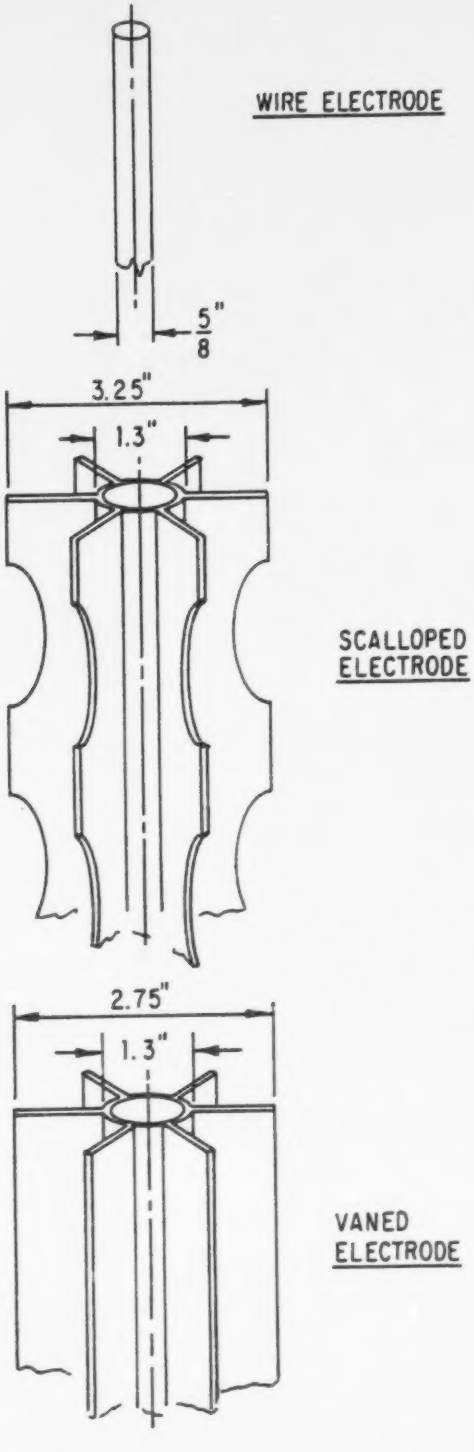
WIRE ELECTRODE
5"/8
3.25"
1.3"
SCALLOPED ELECTRODE
2.75"
1.3"
VANED ELECTRODE

FIGURE 2. CORONA ELECTRODES

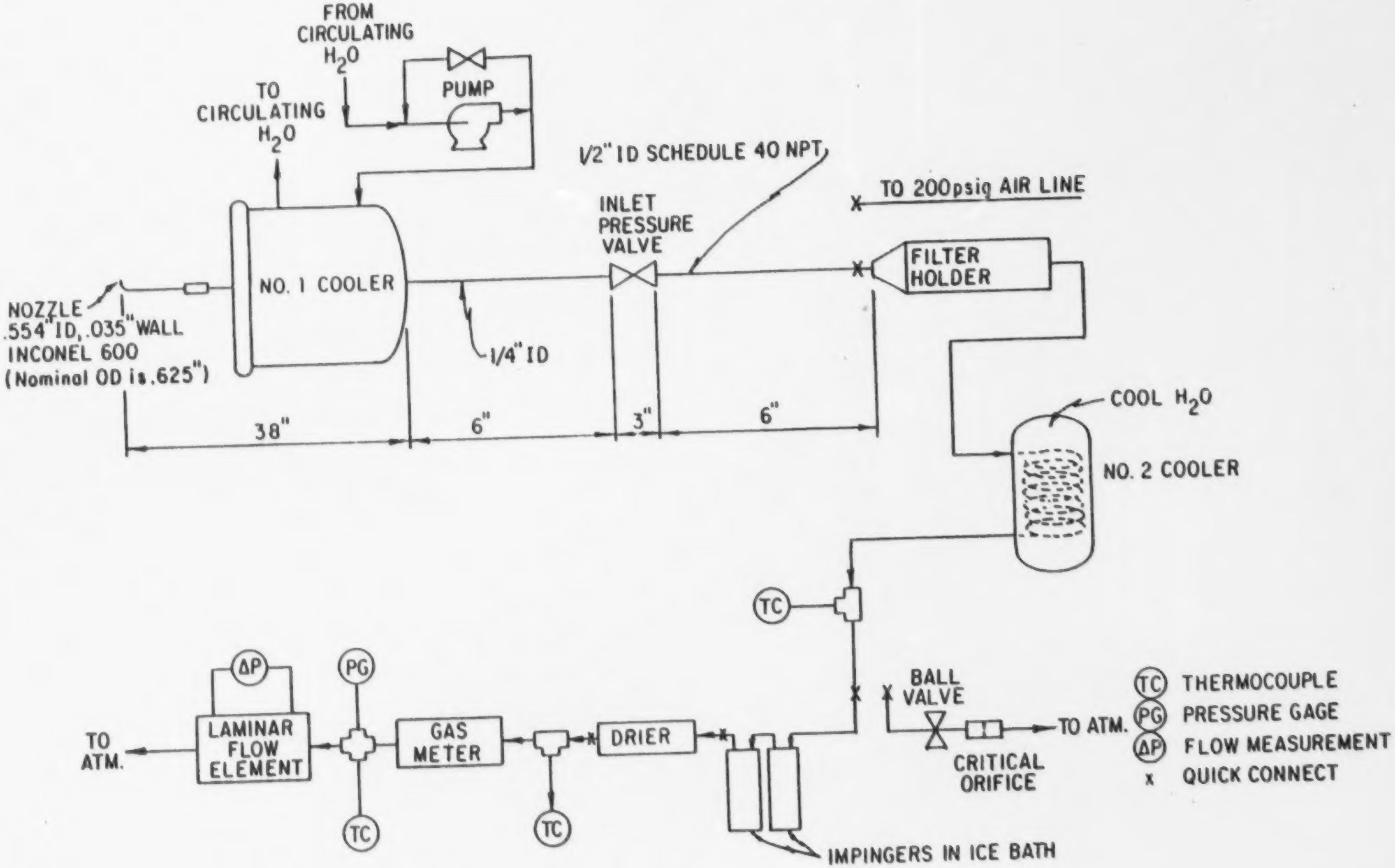
FROM CIRCULATING H2O
TO CIRCULATING H2O
PUMP
NOZZLE .554" ID, .035" WALL INCONEL 600 (Nominal OD is .625")
NO. 1 COOLER
1/4" ID
1/2" ID SCHEDULE 40 NPT
INLET PRESSURE VALVE
TO 200psig AIR LINE
FILTER HOLDER
38"
6"
3"
6"
COOL H2O
NO. 2 COOLER
TC
BALL VALVE
TO ATM.
CRITICAL ORIFICE
TC THERMOCOUPLE
PG PRESSURE GAGE
ΔP FLOW MEASUREMENT
x QUICK CONNECT
ΔP
PG
TO ATM.
LAMINAR FLOW ELEMENT
GAS METER
DRIER
TC
TC
IMPINGERS IN ICE BATH

FIGURE 3. HTHP INLET SAMPLING SYSTEM

To avoid an expensive traversing system the sampling nozzles were designed to be a fixed part of the precipitator system. This makes it impossible to either turn the nozzle downstream when not in use or to clean out the pressure valve and sample lines between tests. Therefore, sampling procedures were developed to ensure that the pressure valve, the sampling line upstream of the valve and the nozzle were clean before a run was started.

Because of large losses in the sample lines during a run, 30-60%, it was necessary to develop a procedure to recover this material as a part of each run. A series of inlet and outlet mass measurements were made in which the nozzle, line and valve were purged after the test, with the high pressure gas from within the ESP. Then the system was shut down, the valve, line and nozzle were removed and washed. The dust collected on the filter during the run, the dust removed by the air purge and the dust removed by the wash were weighed separately. The gas velocity that was required in the purge to remove the dust that collected in the nozzle, line and valve during a run was determined. The sample train was disconnected at the impingers during the purge and connected to a ball valve and critical orifice as shown in Figure 3. To purge the probe assembly, the pressure valve upstream of the filters was fully opened while the ball valve downstream of the filters was closed. Then the ball valve was quickly opened and after about 5 seconds was closed. This was repeated three times and the flow rate through the probe assembly was controlled by the diameter of the critical orifice since the gas velocity is sonic through the orifice. It was found that a velocity of about 30 m/s (100 ft/s) would clean the nozzle, line and valve. If the probe assembly is purged without the critical orifice, the gas velocity through the sampling nozzle can be extremely high and dust which has collected on the inside of the duct can be pulled into the nozzle and cause an error in determining mass concentration.

During the tests to establish the proper sampling techniques and procedures, it was found that during an inlet mass sample run, 50% of the mass reached the filters and 50% was caught in the nozzle, line and valve which could be removed by the purge. At the outlet, 65% of the mass was on the filter and 35% was caught in the probe assembly. Such large amounts of fallout in the sampling probe assembly makes particle sizing by impactor measurements almost meaningless since only the size distribution of the particles that reach the impactor would be determined while the size distribution of the particles caught in the probe assembly would not be known. Sizing the particles caught on the filters and in the probe by Coulter Counter analysis appears to be one means of determining the approximate size distribution of particles at the inlet and outlet of the ESP.

Since the sampling nozzles cannot be turned downstream when not in use, dust can be caught in the nozzles at the start of a mass sample. To solve this problem, a 1.5 MPa (200 psig) filtered air line is connected to the sampling system just downstream of the pressure valve as shown in Figure 3. Immediately before a test is started, the pressure valve is opened and the probe assembly is cleaned by blowing the dust into the ESP duct. Then the air line is removed, and the filter holder is connected.

## CHARACTERISTICS OF HOT GAS STREAM

To simulate dust collection in an actual PFBC system, fly ash from the Curtiss-Wright PFBC was redispersed in the hot gas stream in the HTHP-ESP at the Denver Research Institute. The ash had been collected in the second cyclone of the Curtiss-Wright system and the Research Cottrell precipitator that was tested at Curtiss-Wright. The size distribution of the ash, as determined by Coulter Counter analysis, was approximately log-normal with a mass median diameter of 8 micrometers and a geometric standard deviation of 2.1. For the tests made in 1984 at the Denver Research Institute, the ash was ground in a fluid mill. The ground ash had a mass median diameter of 3.5 micrometers and a geometeric standard deviation of 2.18 as determined by Coulter Counter analysis.

Laboratory measurements of the resistivity of Curtiss-Wright fly ash were made in a parallel plate resistivity cell. A 0.44 cm thick layer of ash was placed between plates which had a cross sectional area of 2.84 $cm^2$. The temperature of the cell was varied from 980°C (1800°F) to 316°C (600°F) and the applied voltage and current were measured. The resistivity for this temperature range is shown in Figure 4. At 760°C (1400°F) the resistivity is about $2.5 \times 10^6$ ohm-cm and drops to about $2 \times 10^5$ ohm-cm at 900°C (1650°F).

The flue gas has a moisture content of about 10% $H_2O$ by volume. The burning of the methanol fuel to heat the gas produces the $H_2O$. The $O_2$ and $CO_2$ contents are about 11.5% and 3% by volume, respectively. The values depend upon the temperature to which the gas is being heated since more fuel is required for higher temperatures. The amount of excess air is about equal to the amount required to burn the fuel.

The amount of $NO_x$ present in the flue gas was analyzed using ion chromatography of a grab sample. The results obtained with this procedure showed about 10 ppmv of $NO_x$ on a dry basis. This level of $NO_x$ should not affect the electrical characteristics or performance of the HTHP-ESP.

Because of the importance of temperature on the operating characteristics of an HTHP-ESP, several series of tests were made to measure temperatures of the gas stream. To determine the temperature profile inside the ESP, the corona electrode was replaced by a tube containing six shielded thermocouples along its length. The ESP was then operated over a large range of temperatures and pressures and the temperatures inside the ESP were correlated with the measured inlet temperature and mass flow rate. In general, the temperature gradient along the tube varied from 55° - 110°C (100° - 200°F) with the higher gradients occurring at the higher temperatures and lower flow rates. The temperature at the mid-point of the tube is considered to be the ESP operating temperature and can be calculated from the inlet temperature and mass flow rate using the correlation determined during the temperature measurements.

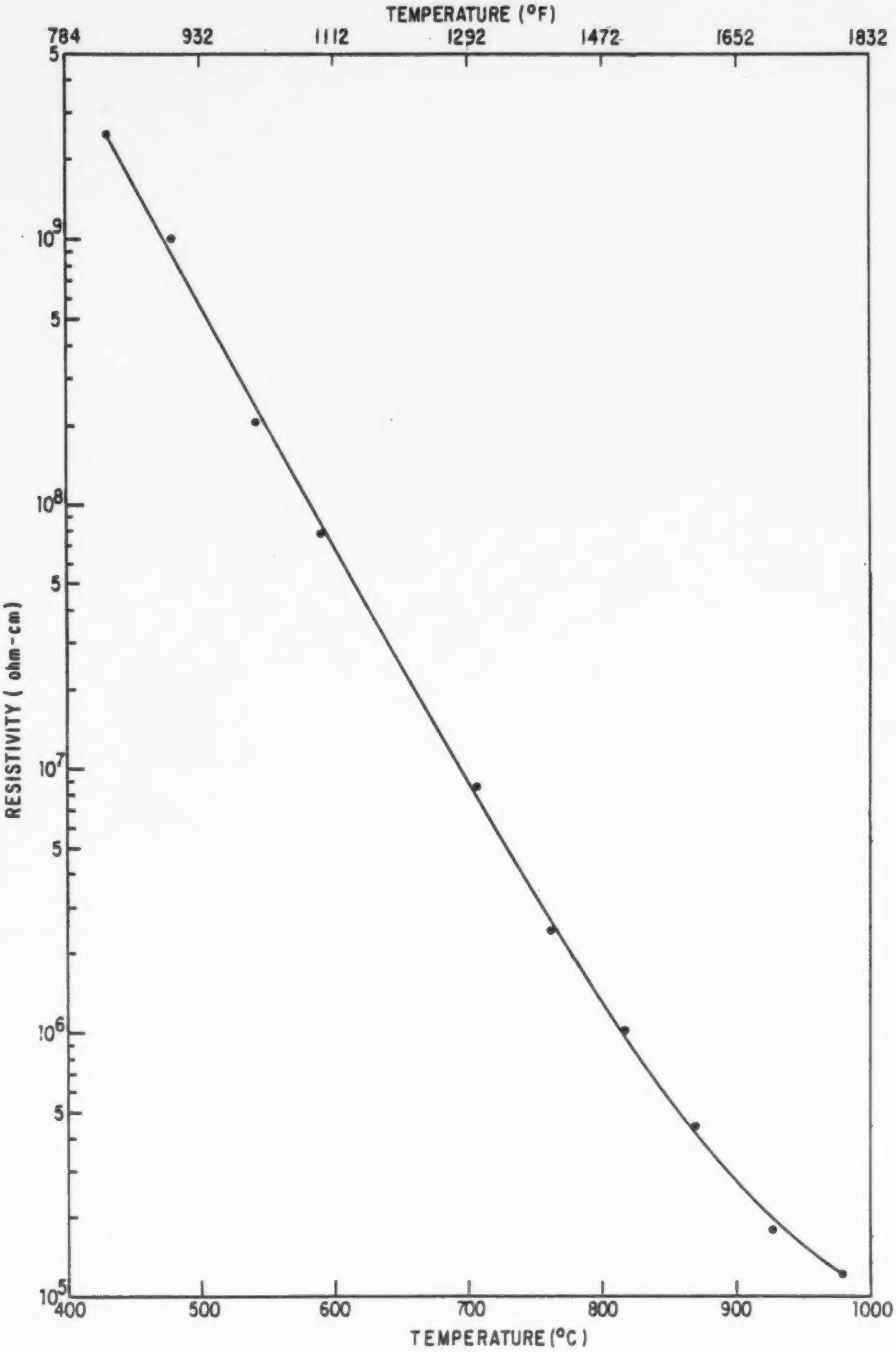

FIGURE 4. RESISTIVITY OF CURTISS-WRIGHT PFBC ASH

# RESULTS

## CHARACTERISTICS OF THE HTHP-ESP AT 760°C (1400°F)

The electrical characteristics and the performance of the HTHP-ESP at 760°C (1400°F) were measured for two different pressures, 640 kPa (6.4 atm) and 1 MPa (10 atm). To maintain a temperature of 760°C (1400°F) at the mid-point of the collector tube, the temperatures in the inlet duct were 838°C (1540°F) and 821°C (1510°F) for 640 kPa (6.4 atm) and 1 MPa (10 atm), respectively.

The electrical characteristics of the scalloped electrode at the two different pressures are shown in Figure 5. There are distinct corona onset voltages at about 50 kV and 70 kV for 640 kPa (6.4 atm) and 1 MPa (10 atm), respectively. The increase in pressure causes a decrease in current for a given voltage and also allows operation at a higher voltage before sparking occurs.

The average voltage-current (VI) operating points during performance measurements are shown in Figure 5 and the results are presented in Table 2. During these tests the gas velocity was 0.76 m/s (2.5 ft/s), the volume flow rate was 0.056 $m^3/s$ (118 acfm) and the SCA was 36 s/m (183 $ft^2$/kacfm). The penetration, defined as the ratio of outlet to inlet mass concentration, was less than 1% at both pressures. The slightly higher penetration at the higher pressure may not be significant since even with the dust injection off, outlet mass concentrations which corresponded to several tenths of a percent penetration were measured. Therefore, the accuracy of penetration measurements decreases at values of less than one percent.

As the data shows, an ESP is very effective in removing particles over a wide range of pressures at a temperature of 760°C (1400°F). However, the power consumption during these tests was high, being about 14.8 kW-s/$Nm^3$ (7W/scfm) of a gas treated. The operating voltage level was just below sparking which produced minimum penetration but is not necessarily the most economical operating point. For example, it may be possible to reduce the power input by a factor of two with only a slight increase in penetration.

TABLE 2
PERFORMANCE OF HTHP-ESP WITH SCALLOPED ELECTRODE AT 760°C (1400°F)

| | | |
|---|---|---|
| Pressure | 640 kPa (6.4 atm) | 1 MPa (10 atm) |
| Voltage | 97 kV | 134 kV |
| Current | 16 mA | 17 mA |
| Avg. E Field | 8.7 kV/cm | 12.1 kV/cm |
| Current Density | 8 mA/$m^2$ | 8.5 mA/$m^2$ |
| Power Density | .78 kW/$m^2$ | 1.14 kW/$m^2$ |
| Power/Std.Vol. | 15.3kW-s/$Nm^3$(7.2W/scfm) | 14.3kW-s/$Nm^3$(6.8W/scfm) |
| SCA | 36s/m(183$ft^2$/kacfm) | 36m/s(183$ft^2$/kacfm) |
| Penetration | 0.6% | 0.9% |
| Efficiency | 99.4% | 99.1% |

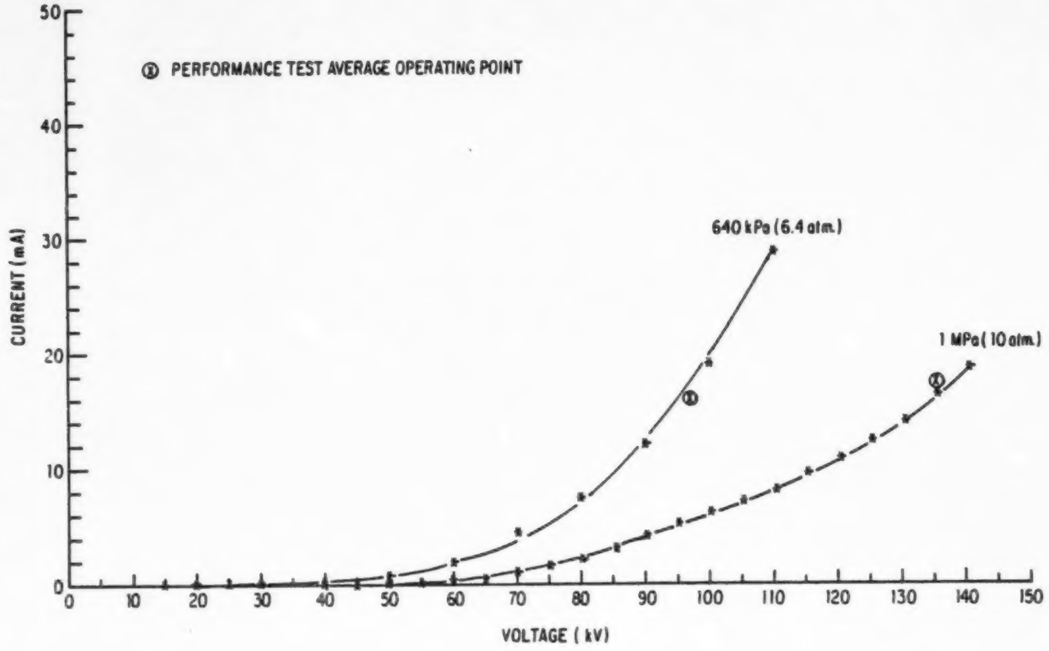

FIGURE 5. THE HTHP V-I CHARACTERISTICS AT 760°C (1400°F) WITH SCALLOPED ELECTRODE

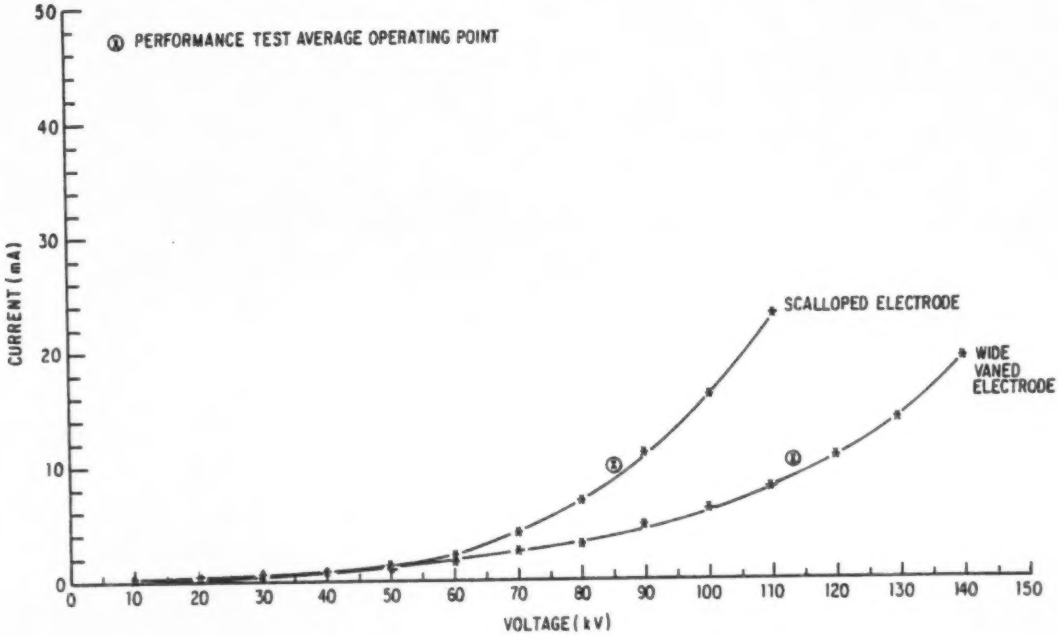

FIGURE 6. THE HTHP V-I CHARACTERISTICS AT 900°C (1650°F) AND 1 MPa (10 atm)

## CHARACTERISTICS OF THE HTHP-ESP AT 900°C (1650°F) AND 1 MPa (10 atm)

Since the typical temperature and pressure for a combined cycle PFBC system are about 900°C (1650°F) and 1 MPa (10 atm), this operating condition is of primary interest. For tests at these conditions, the gas velocity was 0.76 m/s (2.5 ft/s), the volume flow rate was 0.056 $m^3$/s (118 acfm) and the SCA was again 36 s/m (183 $ft^2$/kacfm). An inlet duct temperature of 985°C (1805°F) is required to maintain an operating ESP temperature of 900°C (1650°F). The test results show that there is a significant difference in the electrical characteristic and in the performance of the ESP at 900°C (1650°F) and at 760°C (1400°F).

The electrical characteristics of the scalloped electrode and the wide vaned electrode are shown in Figure 6. The scalloped electrode produced more corona current than the wide vaned electrode and the wide vaned electrode could be operated at higher voltages. The corona onset voltage was not distinct at 900°C (1650°F) as it was at 760°C (1400°F).

The results of the performance test with each electrode are presented in Table 3 and the average VI operating points during the two tests are shown in Figure 6. The current density for both tests was 5 mA/$m^2$. This operating level was considerably below sparkover for both electrodes. For the wide vaned electrode, the average field strength between vane and collector tube was 9.6 kV/cm and for the scalloped electrode, 7.6 kV/cm. However, the penetration with the wide vaned electrode was higher than with the scalloped electrode. In another test where the wide vaned electrode voltage was reduced to about 85 kV, the value on the scalloped electrode, the current density decreased to 2.5 mA/$m^2$ and the penetration increased to 15%. These results indicated that the wide vaned electrode did not charge the particles to the same extent as the scalloped electrode or that reentrainment was higher since for equal or higher field strengths the penetration was higher. This suggests that the current distribution was not uniform with the wide vaned electrode.

TABLE 3
PERFORMANCE OF HTHP-ESP AT 900°C (1650°F) AND 1 MPa (10 atm)

| Electrode | Scalloped | Wide Vaned |
|---|---|---|
| Voltage | 85 kV | 113 kV |
| Current | 10 mA | 10 mA |
| Avg. E Field | 7.6 kV/cm | 9.6 kV/cm |
| Current Density | 5 mA/$m^2$ | 5 mA/$m^2$ |
| Power Density | .43 kW/$m^2$ | .57 kW/$m^2$ |
| Power/Std.Vol. | 6.1kW-s/$Nm^3$(2.9W/scfm) | 8.1kW-s/$Nm^3$(3.8W/scfm) |
| SCA | 36s/m(183$ft^2$/kacfm) | 36s/m(183$ft^2$/kacfm) |
| Penetration | 5.4% | 8.1% |
| Efficiency | 94.6% | 91.9% |

The penetration at 900°C (1650°F) and 1 MPa (10 atm) was 5 to 10 times higher than the values measured at 760°C (1400°F) and 640 kPa (6.4 atm). This change does not appear to be due to the field strength alone since the field strength with the scalloped electrode only changed from 8.7 to 7.6 kV/cm while the penetration increased from 0.5% to 5.4%. This definitely indicates that particle charging and collection are more difficult at 900°C (1650°F) and 1 MPa (10 atm) than at 760°C (1400°F) and 640 kPa (6.4 atm).

The electrical characteristics were not stable at 900°C (1650°F). For example, with the scalloped electrode, the electrical operating point was about 80 kV and 20 mA/$m^2$ during several mass collection efficiency runs. In another series of measurements, with the voltage again 80 to 85 kV, the current was 5 mA/$m^2$. The penetration was about the same although power consumption had decreased by a factor of 4. The reasons for the variation in the electrical characteristics were not positively identified. However, one reason may be dust build-up on the electrodes that is not consistently removed by rapping.

To further investigate the V-I characteristics at 900°C (1650°F) and 1 MPa (10 atm), a smooth wire electrode 1.58 cm (5/8 inch) in diameter was used. At these conditions the relative gas density was 2.5 and the theoretical corona onset voltage was about 200 kV. Therefore, it should be possible to determine the characteristics of the current that had been observed at low voltages with the other two electrodes.

Figure 7 shows the negative and positive V-I curves for two dust conditions. The curves labeled 1 were recorded after the collector tube and electrode had been rapped and the system had been at temperature and pressure for about two hours without dust injection. The negative V-I curve appeared normal except for a small amount of current which was detectable at about 20 kV. The positive current was detectable at about 10 kV and increased until about 60 kV and remained reasonably constant until about 120 kV. Below 130 kV the positive current was considerably larger than the negative current. The curves labeled 2 were recorded immediately after dust had been injected into the ESP for 15 minutes. The negative current increased for voltages up to 120 kV. The positive current increased abruptly for voltages above 10 kV and remained larger than the negative current for all voltages. This large amount of current at voltages less than 100 kV does not appear to be corona current. It does not appear to be thermal ionization because of the difference in the positive and negative V-I curves. Both positive and negative currents decreased as temperature decreased. The variation in current as a function of temperature could not be accurately determined because the dust conditions on the electrodes could not be kept constant. The polarity of the charge carriers in the gas for the low-voltage currents has not been determined and the origin of the currents has not been identified.

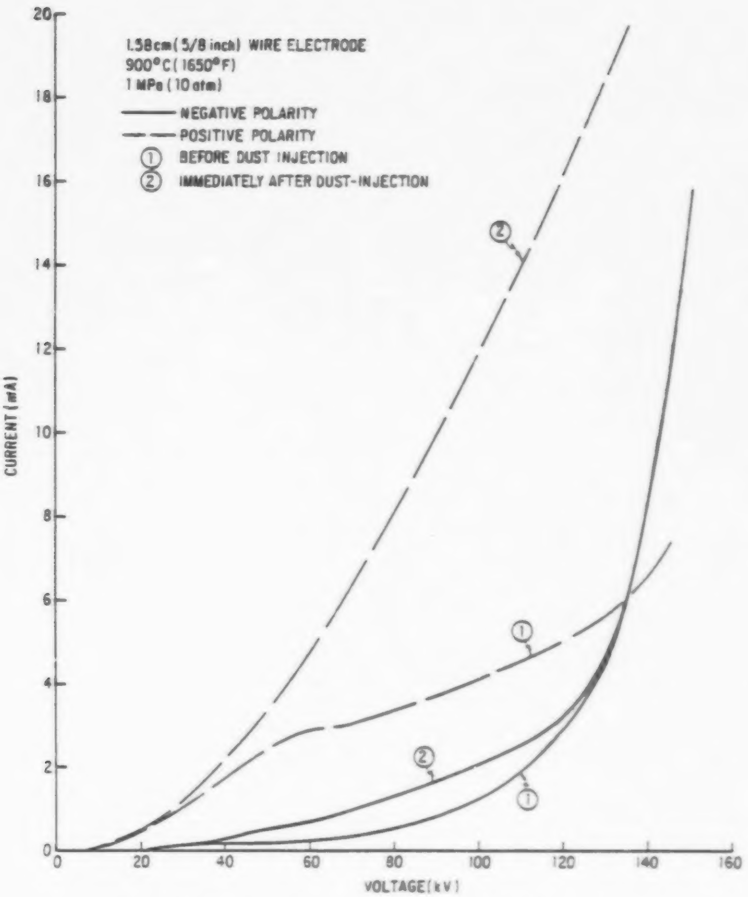

FIGURE 7. ELECTRICAL CHARACTERISTICS OF SMOOTH WIRE ELECTRODE

## CONCLUDING REMARKS

The HTHP-ESP system at the Denver Research Institute can simulate a wide range of PFBC operating conditions. Sampling techniques and procedures have been developed for measuring mass concentration in a high-pressure system.

Performance tests at 760°C (1400°F) and 900°C (1650°F) showed that particle charging and collection were more difficult at the higher temperature. At 900°C (1650°), all of the current in the ESP does not appear to be produced by corona. Also, the results showed that ESP performance could not be predicted from only the electrical characteristics. The design of the electrode and system temperature and pressure must also be considered.

Tests are continuing to determine the sensitivity of ESP performance to voltage, current, pressure and temperature near the operating conditions of 900°C (1650°F) and 1 MPa (10 atm).

# EVALUATION AND DEVELOPMENT OF CANDIDATE HIGH TEMPERATURE FILTER DEVICES FOR PRESSURIZED FLUIDIZED BED COMBUSTION

by: T. E. Lippert and D. F. Ciliberti
Westinghouse Electric Corp.
Pittsburgh, PA 15235

S. G. Drenker and O. J. Tassicker
Electric Power Research Institute
Palo Alto, CA 94303

## ABSTRACT

The Electric Power Research Institute (EPRI) and Department of Energy (DOE) have sponsored work at Westinghouse to evaluate and develop particle filtration technology for Pressurized Fluidized Bed Combustion (PFBC). This work has included testing granular beds woven ceramic bag and two different rigid porous ceramic filters, the ceramic candle and ceramic cross-flow filter. The cross-flow filter has also been tested at the Argonne National Laboratory on the effluent from a small PFBC combustor. Results of test work on these candidate devices are summarized.

To date no filter device has been demonstrated for PFBC. The woven ceramic bag filters appear attractive for early PFBC demonstration because of their potential for easy cleaning and high performance and have been tested at a filter size that should be easily scaleable to pilot operation. The porous ceramic candle and cross flow filters are attractive candidates because of their high performance characteristics and the ability to operate these filters over a wide range of conditions. The cleanability of these filters over a long term basis and methods for mechanical support are uncertainties that need to be evaluated and demonstrated to minimize risk in pilot plant operation.

The shallow, granular bed filter (GBF) system originally under development by Ducon for lower temperature industrial application has been modified for PFBC. The revised design has been successfully tested on a bench scale, single bed configuration. Further work is needed to optimize bed media selection and cleaning cycle.

The work described in this paper was not funded by the U.S. Environmental Protection Agency and therefore the contents do not necessarily reflect the views of the agency and no official endorsement should be inferred.

## INTRODUCTION AND BACKGROUND

The successful removal of particulates from high temperature and pressure gas streams is a goal that is important to many advanced coal conversation technologies both from an operational process point of view and for environmental considerations. The economics of processes such as electric power production from low-Btu coal gasification could be greatly enhanced by a viable hot gas cleaning system, while the commercial development of power production from pressurized fluid-bed combustion critically depends on an effective hot gas cleaning system that will result in adequate turbine life. As such the hot gas cleaning problem has been identified as a key technological barrier to the commercial development of PFBC.

Over the past five or six years Westinghouse has been involved in evaluating high temperature gas cleaning technologies for particulate removal. This work has included subpilot scale and bench scale testing and analysis of various filter devices including

- Granular beds
- Woven ceramic bags
- Batted ceramic bags
- Rigid porous ceramic tube
- Powdered sintered metal
- Rigid ceramic cross-flow

A summary and review is provided in this paper of the testing and evaluations of several of these devices.

## TEST FACILITIES

In support of the high temperature gas cleaning work, Westinghouse under DOE and EPRI support have developed and operated two high pressure and temperature particulate control test facilities. One facility is a flexible bench-scale unit for the development of novel concepts or single element testing. The other facility is a subpilot-scale test facility intended for evaluating advanced concepts at significant scale. Both facilities are PFBC simulators in that pressurized air (11 atm) is heated to 870°C (1600°F) through an in-line combustor and PFBC ash is redispersed into the hot gas stream. The hot dusty gas then enters a pressure vessel containing the filter unit.

The bench-scale test facility was constructed by Westinghouse in conjunction with the DOE-sponsored program to develop a ceramic cross-flow filter and later upgraded by EPRI to allow filter bag testing. This test facility, shown schematically in Figure 1, can be operated to mass flows of .09 kg/s (0.2 lb/s), 11 atm and 900°C (1650°F). Test articles as large as 0.3 m (1 ft) diameter and 1.5 m (5 ft) long can be tested.

Westinghouse has also operated a subpilot scale PFBC simulator capable of gas flows to 5.4 kg/s (12 lb/s), 870°C (1600°F) and 15 atm. This facility, shown schematically in Figure 2, can accommodate filter equipment up to 1.37 m (4.5 ft) diameter and 2.4 m (8.0 ft) long. The high pressure air flows from the compressor building to the laboratory, where it can be heated to

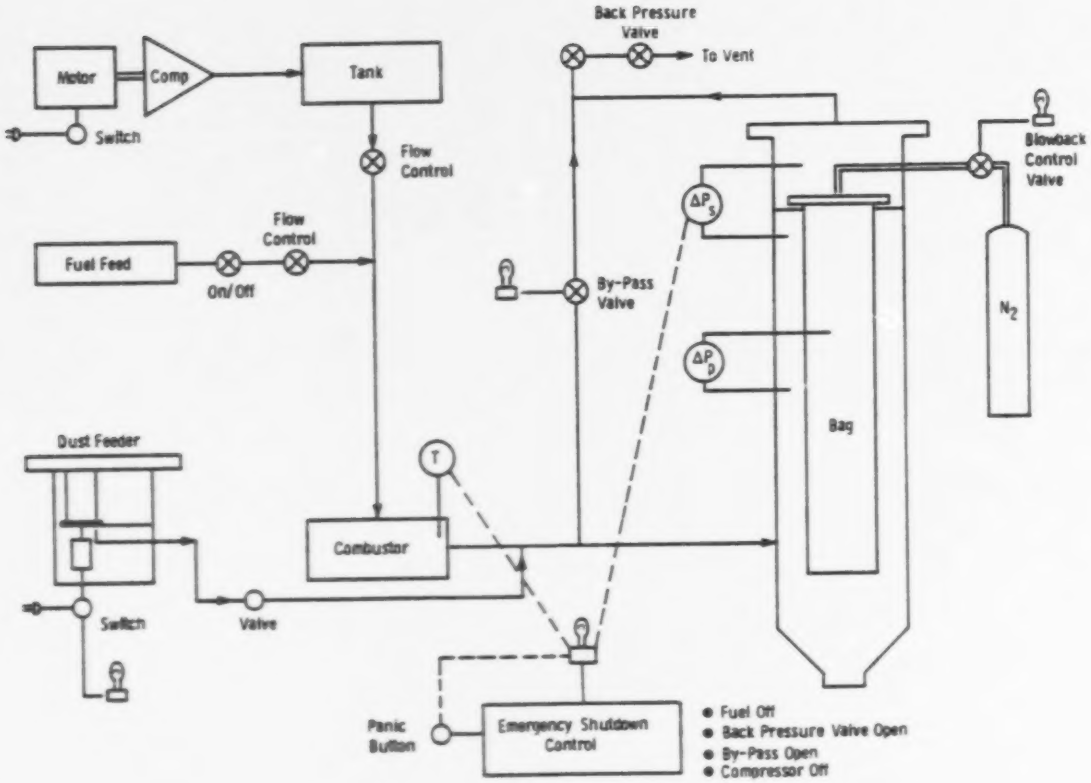
Back Pressure Valve
To Vent
Motor
Comp
Tank
Switch
Flow Control
Blowback Control Valve
Flow Control
Fuel Feed
On/Off
$\Delta P_s$
By-Pass Valve
$N_2$
$\Delta P_D$
Bag
Dust Feeder
T
Combustor
Switch
Valve
Panic Button
Emergency Shutdown Control
● Fuel Off
● Back Pressure Valve Open
● By-Pass Open
● Compressor Off

Figure 1. Bench scale PFBC test facility.

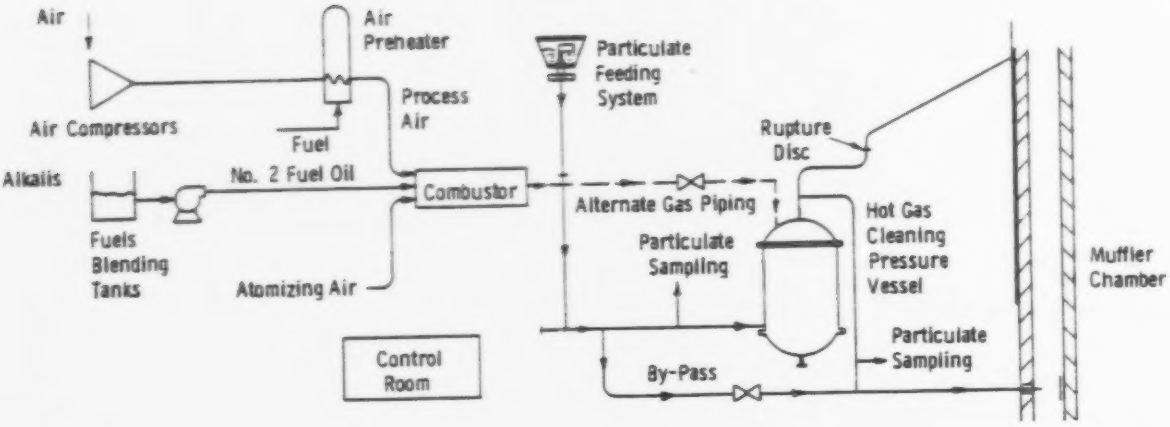
Air
Air Preheater
Particulate Feeding System
Process Air
Air Compressors
Fuel
Rupture Disc
Alkalis
No. 2 Fuel Oil
Combustor
Alternate Gas Piping
Hot Gas Cleaning Pressure Vessel
Fuels Blending Tanks
Particulate Sampling
Muffler Chamber
Atomizing Air
Control Room
By-Pass
Particulate Sampling

Figure 2. Schematic of subpilot scale PFBC simulator.

temperatures up to 650°C by either of two natural-gas-fired air preheaters. The air then flows through a combustor where No. 2 fuel is burned to raise the gases to the desired temperature. The combustor fuel is pumped from the fuel-blend building where several tanks are available for blending either corrosion inhibitors or promoters (combustible alkali organometallic compounds). From the combustor the hot pressurized gases enter the test passage piping. The passage piping and valving are arranged to allow a great deal of flexibility in the manner in which the gases are introduced to and exit from the pressure vessel, allowing virtually any device that will fit in the pressure vessel to be tested.

## SUMMARY OF FILTER TESTING

### GRANULAR BED FILTER

Westinghouse, under DOE contract has evaluated the Ducon shallow bed, granular filter concept for application in PFBC for particulate and alkali removal. The subpilot scale GBF test unit is shown in Figure 3 and consisted of six rectangular filter elements of the design illustrated with each element containing four filter beds. Total filter area was 1.1m$^2$ (12 ft$^2$).

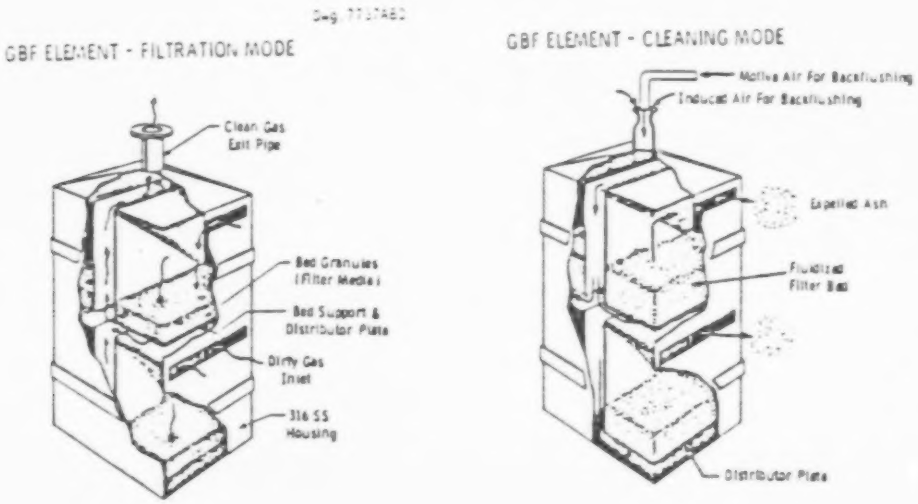
Dwg. 7737A82
GBF ELEMENT - FILTRATION MODE
Clean Gas Exit Pipe
Bed Granules (Filter Media)
Bed Support & Distributor Plate
Dirty Gas Inlet
316 SS Housing
GBF ELEMENT - CLEANING MODE
Motive Air For Backflushing
Induced Air For Backflushing
Expelled Ash
Fluidized Filter Bed
Distributor Plate

Figure 3. Schematic representation of Ducon GBF element.

In the Ducon concept the basic filter compartment consisted of a shallow (.5 to 3 inch) bed of fine sand (620 μm diameter) that was supported on a perforated and screen covered distributor plate. Dust laden gases would enter the filter compartment through screen covered openings provided above the filter bed, flow downward through the fine granular bed depositing dust onto the filter media. The filter beds were cleaned online by reverse flushing air or clean flue gas back through the beds, fluidizing the sand and dislodging accumulated dust. The dislodged dust would then be carried back-through the filter compartment inlet opening located above the bed and collected at the bottom of the pressure vessel.

To clean the GBF at PFBC conditions, precise control of the backflush flow must be maintained to operate between the minimum fluidization velocity and the velocity where the bed media begins to elutriate. In addition, distributing the backflush flow uniformly between beds operating in parallel requires equal flow resistance through each distributor and bed. Results from the subpilot scale testing showed that dust will reach the distributor and some plugging of the distributor plate assembly occurs which can cause a non-uniform distribution of the backflush flow between filter beds and elutriation of bed media.

A summary of test results is given in Table 1. Measured collection efficiency varied between tests and in those tests where problems were encountered with backflushing, performance decreased with operating time. Test Phase III showed the most consistent performance level for the GBF where collection efficiency averaged 99.2% at a filter face velocity of 50 ft/min. An important consequence of this test phase was identifying and quantifying the apparent adverse effect that fluidizing on backflush has on collection efficiency. Dust sampling on the clean gas side of the filter taken during the filtration portion of the operating cycle showed, when compared to similar samples taken over the backflush cycle (and a short period after backflush), that nearly 80 percent of the total dust that penetrated the filter could be accounted for on the backflush samples. Backflushing without fluidizing, i.e., static bed backflush was developed as an approach to improve GBF collection efficiency. Test Phase V conducted on a single bed, bench-scale unit focused on investigating static bed backflush as a basis for improved GBF operation at high temperature and high pressure PFBC conditions. Results of these tests are shown in Table 2.

TABLE 1. SUMMARY OF GBF TEST RESULTS

| | **Phase I** | **Phase II** | **Phase III** | **Phase IV** |
|---|---|---|---|---|
| **Test Unit Configuration** | **Rectangular – 4 Beds/Element Alumina** | **Rectangular – 4 Beds/Element Alumina** | **Rectangular – 1 Bed/Element Sand** | **Cylindrical – 1 Bed/Elemnt S.S. Shot/Alumina** |
| **Filter Face Velocity** | **40 To 50** | **40** | **50**<br>**75**<br>**100** | **45** |
| **Time At Conditions (Hrs)** | **50** | **50** | **71** | **50** |
| **Operating Cycles** | **103** | **90** | **282** | **140** |
| **Collection Efficiency (%)** | **98.8 To 99.4** | **98.9 To 80.8** | **99.2**<br>**98.5**<br>**96.0** | **99.8 To 80** |
| **Backflush Mode** | **On-Line** | **On-Line** | **Off-Line** | **On-Line** |

## TABLE 2. SUMMARY OF BENCH SCALE GBF TESTS -- PHASE V

| | Test Series 3 | Test Series 4 |
|---|---|---|
| Bed Design | 1-3/4" Layer - 1370 $\mu m$ Alumina<br>2" Layer - Alumina Chips | Same as 3 |
| Test Conditions | 75°F and 65 psi | 1200 to 1550°F and 165 psi |
| Backflush | 1.5 ft/s for 15 sec | 1.1 ft/s for 15 sec |
| Test Duration | 33 Cycles (24 Hours) | 20 Cycles (10 Hours) |
| Performance | • $\eta$ = 99.9% at 17 ft/min, 1590 ppm<br>99.9% at 17 ft/min, 7630 ppm<br>98.2% at 34 ft/min, 3980 to 4450 ppm | • $\eta$ = 97.3% at 20 ft/min, 8320 ppm<br>= 96 to 98.3% at 50 ft/min, 3700 ppm |
| | • Baseline $\Delta p$ Steady<br>4 in $H_2O$ at 17 ft/min<br>15 in $H_2O$ at 34 ft/min | • Baseline $\Delta p$ Steady<br>7 in $H_2O$ at 20 ft/min<br>22 in $H_2O$ at 50 ft/min |

NOTE: All Tests Conducted Using Redispersed PFBC Flyash, $\bar{d}_{50}$ = 12.7 $\mu m$

Both high temperature, high pressure (HTHP) and ambient temperature, low pressures (LTLP) tests were conducted with the filter bed comprising dual alumina media. In one of the LTLP test series the filter was operated over 33 cycles for a cumulative 24 hour test at filter velocities of 40 and 17 ft/min. Collection efficiencies were measured at 98.2 and 99.9% respectively. Baseline pressure drop remained constant and backflush was accomplished without fluidizing the bed. Tests at 50 ft/min (HTHP) and over 20 cycles showed lower collection efficiencies 96 to 98%. In these tests, backflush was reduced to about 1.2 ft/s to avoid bed fluidization. This velocity however may be to low to effectively elutriate dust cake. Post test examination showed that some accumulation of dust had occurred in the filter with evidence of flow channeling through the cake. No bed media was lost in either the LTLP or HTHP bench scale testing.

For application of the shallow bed, granular filter to high temperature, high pressure, further optimization of the bed media is needed. To backflush and effectively elutriate the dust agglomerates would appear to require elutriation velocities greater than 1.2 ft/s. Small media size is necessary to achieve high collection efficiency. Therefore, to effect backflush without fluidizing the bed yet efficiently elutriate the dust will require high density bed media. Test data also indicates trade-off of efficiency with media size and filter face velocity.

For PFBC, further development of the shallow bed granular filter is needed to demonstrate that the static bed reverse flush cleaning and modified bed and distributor design will result in significantly improved filter performance and stable filter operation. An ultra high density media is needed that permits relatively fine media size for good particle capture but allows for backflush velocities sufficiently high to effectively clean the bed without fluidizing.

## WOVEN CERAMIC BAG FILTERS

The testing of filter bags woven from yarns of ceramic fiber was accomplished through the cooperative effort of the 3M Company and Westinghouse under EPRI sponsorship. Testing has been carried out on subpilot scale using a 19-bag array and on the bench scale facility using single filter bags. Woven ceramic filter bags of different ceramic material, different weave and seam construction and of different geometry have all been evaluated. Considerable progress has been made in the design, construction and operation of these filter bags for high temperature gas cleaning.

Initial work conducted by Westinghouse on the woven ceramic bag was on a subpilot scale basis using a 19-bag array. Each bag was approximately 15.2 cm diameter by 1.4 m long (6 inch x 4.6 ft) and each fitted over a perforated metal mandrel to provide support. The filter bags were woven from 3M ceramic fibers of an alumina, borea, silica composite (NEXTEL 312) in an 8-harness weave. These fibers are nonoxidizing, nonconductive, and can tolerate temperatures in excess of 1090°C. In the 19-bag arrangement, the bags were pulsed-jet cleaned in groups of two or three. Hot-gas tests were conducted at two temperature conditions, 800°F (427°C) and 1500°F (815°C) and with filter velocity (air to cloth ratio) ranging from 0.85 to 1.71 m/min (2.8 to 5.6 ft/min), Table 3. Measured outlet dust loadings corresponding to the indicated collection efficiencies over the 50 hr operating period ranged from 26 to less than 1 ppm. Tests were halted subsequent to the 50 hours, when one of the filter bags failed at the sewn seam. Inspection of the filter bags by 3M Co. indicated that the top layer of Nextel fabric in the double-stitched French Feld seam broke at the crease and that numerous warp thread crossings in the eight-harness weave fabric showed fiber breakage in the form of tufts of fluffy protrusions at the point of each crossover of felt yarn by warp yarn.

Subsequent test work by Westinghouse has been on the bench scale facility utilizing the single bag assembly illustrated previously in Figure 1. Two different approaches to improve filter bag seam construction have now been evaluated. One approach that improved seam integrity was to overstitch the original Astroquartz thread with a Nextel thread. The second approach was to eliminate the seam and construct (weave) a seamless tube configuration. Test runs of 100 hours duration were conducted at 1500°F (815°C) and 11 atm on two different woven ceramic fibers (in bag and tube configuration) without any observed failure in material or construction in either the overstitched seam or in the seamless tube configuration. One of the filters (seamless tube) was the alumina, borea, silica composite material (Nextel 312). The other filter (bag configuration) was a zirconia, silica (ZS11) composition.

Table 4 summarizes results from three separate test runs at simulated PFBC conditions using three different woven ceramic fiber filters. As indicated from the results, overall particle collection efficiencies of 99.9% and better have been measured at a nominal filter face velocity. (air to cloth ratio) of 1 m/min (3.3 ft/min). Time averaged outlet dust loadings were 15 ppm or less, sufficiently below PFBC requirements to meet NSPS. In these test runs, the filter bags could be cleaned by pulse-jet method and were operated over low pressure drop.

## TABLE 3. SUMMARY OF WOVEN BAG TESTS 19-BAG ARRAY

| Test Series | Conditions | Overall Performance |
|---|---|---|
| 1 | T = 800°F<br>v = 2.8 ft/min<br>ΔP = 1.6 to 6.5 in $H_2O$ | 99.6% to 99.9% |
| 2 | T = 800°F<br>v = 5.6 ft/min<br>ΔP = 4.5 to 6.2 in $H_2O$ | 99.6% |
| 3 | T = 1500°F<br>v = 3.2 ft/min<br>ΔP = 3.9 in $H_2O$ | 99.9% |
| 4 | T = 1500°F<br>v = 6.5 ft/min<br>ΔP = 5.8 to 8.2 in $H_2O$ | 99.2% |
|  | Total Operating Time = 50 hrs |  |

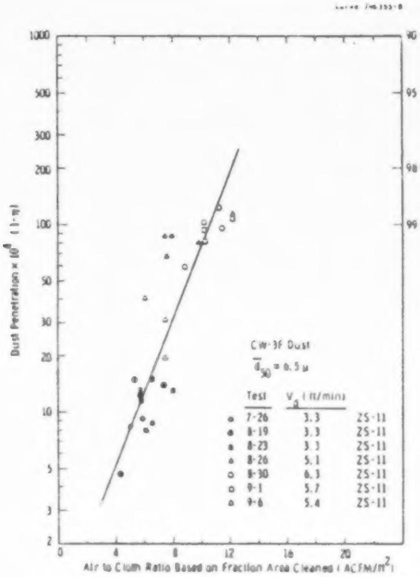

Figure 4. Trend in dust penetration with Bag cleaning effectiveness.

## TABLE 4. SUMMARY OF WESTINGHOUSE HTHP WOVEN CERAMIC FILTER BAG TESTS (815°C, 11 ATM)

| Bag | Nominal Filter Velocity (ft/min) | Pressure Drop (in $H_2O$) | Outlet-Time Avg Dust Conc (ppm) | Overall Dust Collection Eff., η % | Time At Conditions (Hr) |
|---|---|---|---|---|---|
| NEXTEL-312 Seamed 6" x 5' | 3.3$^{(1)}$ | 1.6 to 5 | <10 | 99.9 | 40 |
| ZS-11 Oversewn Seam 6" x 5' | 3.3$^{(2)}$ | 5 to 20 | <5 | 99.95 | 60 |
|  | 3.3$^{(3)}$ | 10 | <10 | 99.9 | 20 |
|  | 4.7 to 6.3$^{(3)}$ | 10 to 16 | 24 to <5 | 99.0 to 99.9 | 20 |
| NEXTEL-312 Seamless 4" x 5' | 3.3$^{(4)}$ | 10 | <15 | 99.95 | 53 |
|  | 7.9 to 8.5$^{(4)}$ | 16 | 200 to 60 | 96.5 to 99.0 | 32 |

(1) PFBC Ash $\bar{d}_{50}$ = 15 µm

(2) PFBC Ash $\bar{d}_{50}$ = 12.7 µm

(3) PFBC Fine Ash $\bar{d}_{50}$ = 6.5 µm

(4) PFBC Coarse $\bar{d}_{50}$ = 20 µm + 10% of PFBC Fine Ash $\bar{d}_{50}$ = 5 µm

At higher filter face velocities ranging from 1.8 to 2.6 m/min (6 to 8.5 ft/min) filter bag performance was observed to decrease in some test runs. The lower performance in these tests have been correlated to poorer filter bag cleaning and to the significantly higher local filter velocities that can result. Figure 4 shows a correlation of measured filter bag dust penetration with face velocity (based on actual cleaned area) that illustrates the sensitivity of the woven filter bags to high local filter face velocity.

Continued development of the woven ceramic fiber filters appears warranted based on the thus far encouraging test results. The woven ceramic bag filter is an attractive system for PFBC because high overall collection efficiency can be achieved and the filter can be easily and reliably cleaned by simple pulse-jet methods. Major improvements in the construction of the bags have been made that has promise for significantly improved filter bag durability. The performance of the woven bags however is sensitive to filter face velocity which in turn may limit design and system economics. For PFBC, based on conceptual design studies, filter face velocities of about 8 ft/min would be optimum while test results show high performance can be maintained in the 3 to 6 ft/min operating regime. Current work is now focused on evaluating filter bag weave and fiber designs that would provide lower filter permeability and permit high velocity operation. In addition long term testing is needed to confirm the overall operation, performance and materials durability in actual PFBC environment.

## POROUS CERAMIC CANDLE FILTERS

The porous ceramic tube filters tested were manufactured by Schumacher'sche Fabrik of Bieligheim, West Germany, and are denoted as candle filters. These filters are formed by incorporating very small pockets of pure mineral fibers in a dense matrix of silicon carbide. The interconnecting pockets of these small diameter (3 μm) fibers gives rise to very reasonable pressure drops in spite of the rather thick and rugged wall of the tube. The tubular filters tested were nominally 50 cm long with an OD of 6 cm and ID of 4 cm. The active filter area was estimated as 0.072 $m^2$, based on the outer area. Candle filters of up to 1.5 m long are available and are currently under evaluation. Two candle filters have been tested. One was a relatively porous element that had an ambient air resistance to flow of 0.25 kPa at a face velocity of 0.67 m/min and a relatively dense element that had essentially twice that resistance to flow at the same velocity.

During the first series of tests with the more porous filter candle, the test temperature and pressure were constant at 775°C and 11 atm. During this series seven tests were conducted accumulating a total of about 35 hours of actual filtration time and slightly more than 100 operating cycles (blow back sequences). The filter face velocities examined ranged from 2.5 to 5.3 m/min. The test dust used was a redispersed ash from the Curtiss-Wright PFBC and had a mass mean diameter of approximately 10 μm. Dust concentrations were in the range from 2700 to 3300 ppm. The results of these tests are summarized in Table 5. The performance shown here is typical of the behavior observed throughout this period of testing. During testing, a gradual shortening of cycle time and slowly increasing base line pressure drop was observed. The cleaning regimen employed for these tests was 0.5 sec reverse pulse of air from a 2.1ℓ reservoir charged to a pressure of 35 atm and discharged through a 0.75 cm diameter nozzle centered above the clean side of this filter element. Posttest examination of the filter revealed that a thin "cratered" deposit of dust remained on the filter surface. This dust layer was not sticky or hard and was easily removed. It is hypothesized that the nonuniformity in the dust

## TABLE 5. SUMMARY OF CERAMIC CANDLE TESTS

| Test No. | Test Time hr | Flow kg/min | Filter Velocity m/min | Dust Concentration Inlet, ppm | Measured Dust Collection Efficiency, % |
|---|---|---|---|---|---|
| Series 1 - Porous Element | | | | | * |
| 1 | 2.0 | 0.72 | 2.52 | 2,707 | 99.90 |
| 2 | 4.0 | 1.44 | 5.35 | 3,811 | 99.98 |
| 3 | 4.0 | 1.44 | 5.20 | 3,329 | 99.97 |
| 4 | 9.8 | 1.44 | 5.13 | 2,807 | 99.99 |
| 5 | 5.0 | 1.44 | 5.10 | 3,010 | 99.99 |
| 6 | 1.0 | 1.44 | 5.31 | 3,151 | 99.99 |
| 7 | 8.5 | 0.72 | 2.65 | 6,302 | 99.99 |
| Series 2 - More Dense Element | | | | | |
| 1 | 4.0 | 0.83 | 3.35 | 5,206 | 99.97 |
| 2 | 4.0 | 0.83 | 3.35 | 5,149 | 99.96 |
| 3 | 5.5 | 0.83 | 3.35 | 5,499 | 99.35* |
| 4 | 9.0 | 0.83 | 3.35 | 5,468 | 99.98 |

---

*Leaks in gasket seal

cake arises from the Local areas of high porosity at the imbedded fiber pocket surface sites.

In addition, a series of tests were carried out with the more dense high pressure drop element. The only system modifications were the insertion of a venturi section in the outlet of the candle in an effort to improve cleaning and an increase in the pulse accumulator volume to 8.4ℓ. The test pressure and temperature remained essentially the same as in previous tests, but the dust concentration was somewhat higher at 5100 to 5500 ppm. Approximately 25 hours of actual filter test time and 95 cleaning cycles were accumulated over four test days with the more dense filter candle. The results of these tests are also summarized in Table 5, where it can again be observed that the filter elements behaved essentially as absolute filters. As in the previous tests the pressure drop/time curves generated revealed a gradual shortening of cycle time and a slowly increasing baseline pressure drop. The inclusion of the venturi section and the larger pulse reservoir did not seem to significantly alter the pressure rise in the filter during blowback, and cleaning remained somewhat incomplete.

Figure 5 focuses on the observed cleaning uncertainty. This figure presents a measure of the cleaned filter permeability (filter velocity divided by the freshly cleaned baseline pressure drop) as a function of operating cycles. Both elements are gradually becoming less permeable at an apparently constant rate of about 0.0024 (m/min-kPa-cycle) for the more dense element and at 1.4 times that rate for the more porous element. It is apparent that if this constant decrease in permeability persists in spite of any operating modifications, then the filter system would not be viable. It should be emphasized that not enough operating time has been accumulated nor have a wide

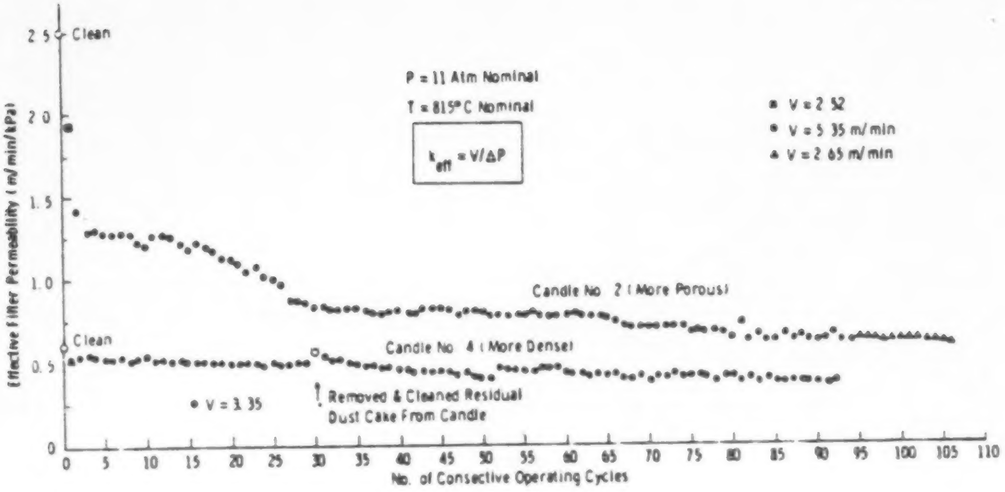

Figure 5. Effective permeability of ceramic candle in HTHP simulation tests.

enough range of operating parameters been explored to conclude that the system will not provide adequate life. The candle filter appears as an attractive device for PFBC because of its overall high collection efficiency (nearly absolute) that is basically insensitive to test operating conditions, i.e., velocity, inlet loading or pressure drop. Preliminary conceptual design studies show that an operating filter velocity from 3 to 4.5 m/min (10 to 15 ft/min) would be economically optimum for PFBC. Long term operation of the candle filter at these conditions needs to be conducted to demonstrate cleaning cycle stability, long term mechanical strength and resistance to thermal shock.

## CROSS FLOW FILTER

The cross-flow geometry is demonstrated by reference to Figure 6. The filter consists of a series of thin, gas permeable flate ceramic plates that are laid-up in block form and separated by a series of corrugations that form flow channels. The flow channels are perpendicularly oriented in each successive layer. One face of the element is sealed to gas flow and the opposing face manifolded to a clean gas plenum section. The element operates as a filter in the following manner: the dirty gas flows through the corrugations parallel to the sealed face. It then permeates the flat sheets separating the corrugations and flows out through the corrugations oriented perpendicularly to the inlet channels. Dust is deposited on the high-pressure side of the permeable separator sheets, forming a cake. The cake is removed periodically by a burst of reverse flow, high-pressure, clean air. One of the primary benefits of ceramic filters of this general configuration is their very high surface-area-to-volumes ratio, an important consideration for high-pressure applications where the minimization of the number and size of the pressure vessels required to house the filtration system is of great consequence. This is illustrated in Figure 7 which demonstrates the manner in which many individual filter elements can be mounted on a single plenum to comprise a module. Modules can then be installed in a pressure vessel forming a cross flow filter unit. To demonstrate compact nature of the cross flow filter system it should be noted that the flow accommodated by a single filter unit is equivalent to that processed by a normal high efficiency cyclone system housed in roughly the same size pressure vessel. Development of the cross-flow filter has been under DOE support at bench scale using both the Westinghouse PFBC simulator and with recent tests conducted on the Argonne National Laboratory (ANL) small pressurized fluidized bed coal combustor facility. Table 6 shows an overall summary of test results.

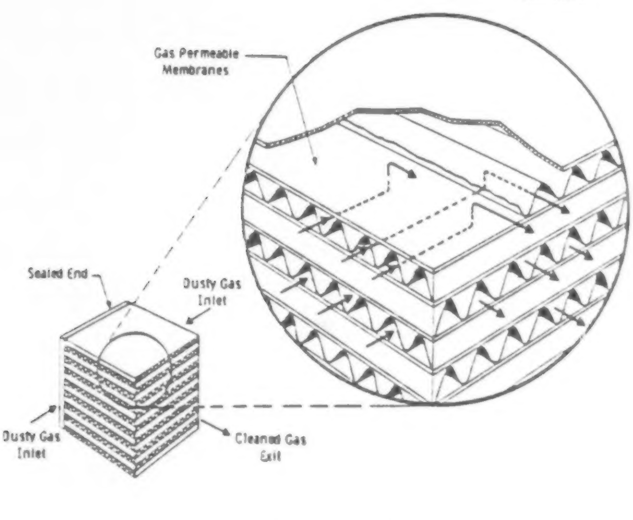
Dwg. 3359A91
Gas Permeable Membranes
Sealed End
Dusty Gas Inlet
Dusty Gas Inlet
Cleaned Gas Exit

Figure 6. Cross-flow ceramic membrane filter.

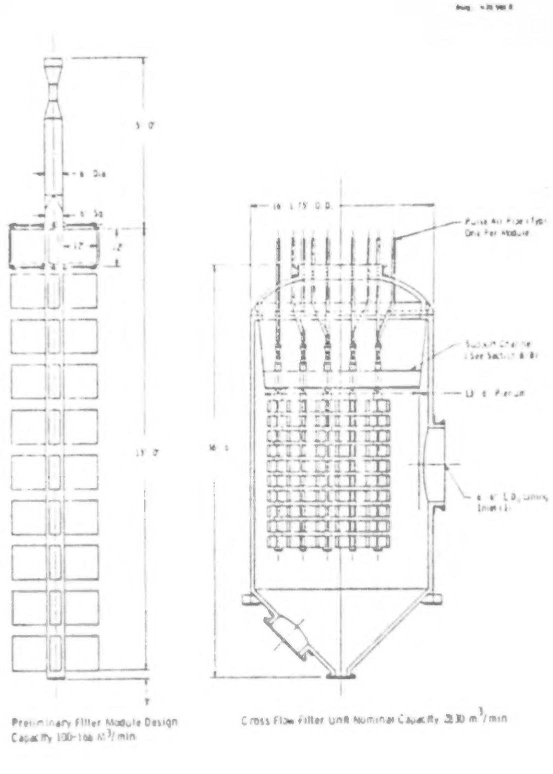
5' 0"
6" Dia
12"
12"
13' 0"
Pulse Air Pipe (Typ) One Per Module
Support Channel (See Section B-B)
Plenum
Preliminary Filter Module Design Capacity 100-166 M³/min
Cross Flow Filter Unit Nominal Capacity 2300 m³/min

Figure 7. Cross-flow filter module and unit.

In the course of bench scale testing of single elements in a HTHP test facility at the Westinghouse R&D Center a total of seven different filter types were investigated. Nominal pore sizes ranged from 10 to 144 μm and filter flat thicknesses from 1 to 3 mm. Approximately 450 hours of actual test time were logged during a series of 48 different test periods. Most of

TABLE 6. SUMMARY OF WESTINGHOUSE CROSS FLOW FILTER TESTING AT HTHP

| Test Program | No of Elements Tested | Filter Velocity (ft/min) | Pressure Drop (in $H_2O$) | Collection Efficiency (%) | Time (Hrs) |
|---|---|---|---|---|---|
| W Bench Scale<br>PFBC Simulator<br>(1500°F, 11 atm) | 7 | 6 | 4 to 20 | 99.99<br>(99.5 to 99.9*) | 450 |
| | | (Inlet Dust Loading 3000 to 5000 ppm) | | | |
| ANL-Small<br>PFBC Combustor<br>Phase I<br>(1340°F, 9 atm) | 1 | 12.4 | 15 to 25 | ~100 | 20 |
| | | (Inlet Dust Loading 300 to 1000 ppm - Upsets to 24,000 ppm) | | | |
| ANL-Small<br>PFBC Combustor<br>Phase II<br>(1340°F, 9 atm) | 1 | 6.3 to 12.4 | 12 | ~100 | 70 |
| | | (Inlet Dust Loading 3000 to 5000 ppm) | | | |

*With Delamination

the testing was carried out at a temperature of 1088 K, at a system pressure of 1114 kpa and with an inlet dust concentration ranging from 1555 to 4666 ppm. The range of filter velocities investigated was from 1.6 to 5.4 m/min, with most of the testing carried out at about 1.7 m/min.

At filter velocities around 2 m/min, the more porous elements gave pressure drops of about 1 to 2 kpa while the less porous filters had resistances that were typically 6 to 8 kpa. It was found that under these conditions filters were essentially absolute barriers to the redispersed PFBC test dust used with measured overall efficiencies of 99.9+%. A longer duration test was carried out in this facility on an element with 100 mm pore size and 1.5 mm thick filter flats. During this test 80 hours of essentially continuous operation was achieved. Operating at 1.7 m/min with an inlet concentration of 3,900 ppm of dust, the filter settled into virtually stable operation within a few hours. In the conditioned state the base-line pressure drop was 1 kPa and would rise to the blow back trigger pressure drop of 3 kPa over a constant 45 minute period.

The only recurrent experimental difficulty experienced has been a tendency for some of the filters to delaminate at one of the bonded layer interfaces. Dense, low-porosity elements were much more prone to failures of this type. Very large pore size elements, on the other hand, appeared to become too weak and to fail across filter flats. Working with the Coors Porcelain Co. (supplier of the ceramic block), significant gains in filter element design and fabrication techniques have been made which have minimized this problem.

Field testing of a single cross flow filter element was conducted at the Argonne National Laboratory's small-scale pressurized fluid bed combustion test loop. The flow loop arrangement at ANL allowed the flexibility to operate the filter over virtually the whole range of combustor flows by varying the split between the filter leg and the existing ANL test leg. The actual testing of the cross-flow filter at ANL occurred in two phases. This happened because of an in-bed heat exchanger failure in the PFBC system during the first test. Testing resumed after repair of the system.

In the ANL test program, the cross flow filter element was operated for over 110 hours, through 91 filter cycles at gas conditions that were nominally 1340°F. The filter face velocity was varied from 6.3 to 12.4 ft/min with inlet dust loading varying and typically ranging from less than 110 ppm to about 600 ppm. During the course of testing, various upsets occurred that resulted in transient inlet dust loading as high as 61,000 ppm. Throughout the test sequence the filter operated in a steady manner with recoverable pressure drop characteristics, reasonable operating cycle time and with measured dust collection efficiency that exceeded 99.99%. Figure 8 shows the pressure drop-time characteristics measured for the filter during the second test series and representing about 70 hours of actual test operation. For a short operating period at the end of the test program, a water cooled methane injection probe was installed on the filter inlet to boost operating temperature. During this 10 hour test sequence (bottom of Figure 8) there was no evidence that the higher operating temperature of the filter made cleaning more difficult or less effective. When the filter system was disassembled after testing, the absolute filtration determined by outlet sampling was confirmed by the total absence of PFBC ash on the clean side liner surfaces. Upon removal of the filter holder from the pressure vessel housing, nothing abnormal was observed, however, when some of the exterior dust was removed evidence of a crack was revealed. When the filter element was removed from its holder, it became apparent that the filter had delaminated in two places where the cracks were observed. This was somewhat puzzling since similar failures in past testing had resulted in a small but measurable penetration of dust. No such dust penetration was measured in the ANL test suggesting that the crack may have resulted during shutdown or disassembly.

The X-flow filter represents for PFBC potentially an extremely economic and effective high temperature particulate filter. Single element, bench scale tests have been conducted under simulated PFBC and tests on an actual (small) PFBC combustor show filter collection efficiencies that are greater than 99.99% with low system pressure drop. Continued development of the X-flow filter is needed to improve mechanical design and to demonstrate its operation (cleanability) in a multielement arrangement.

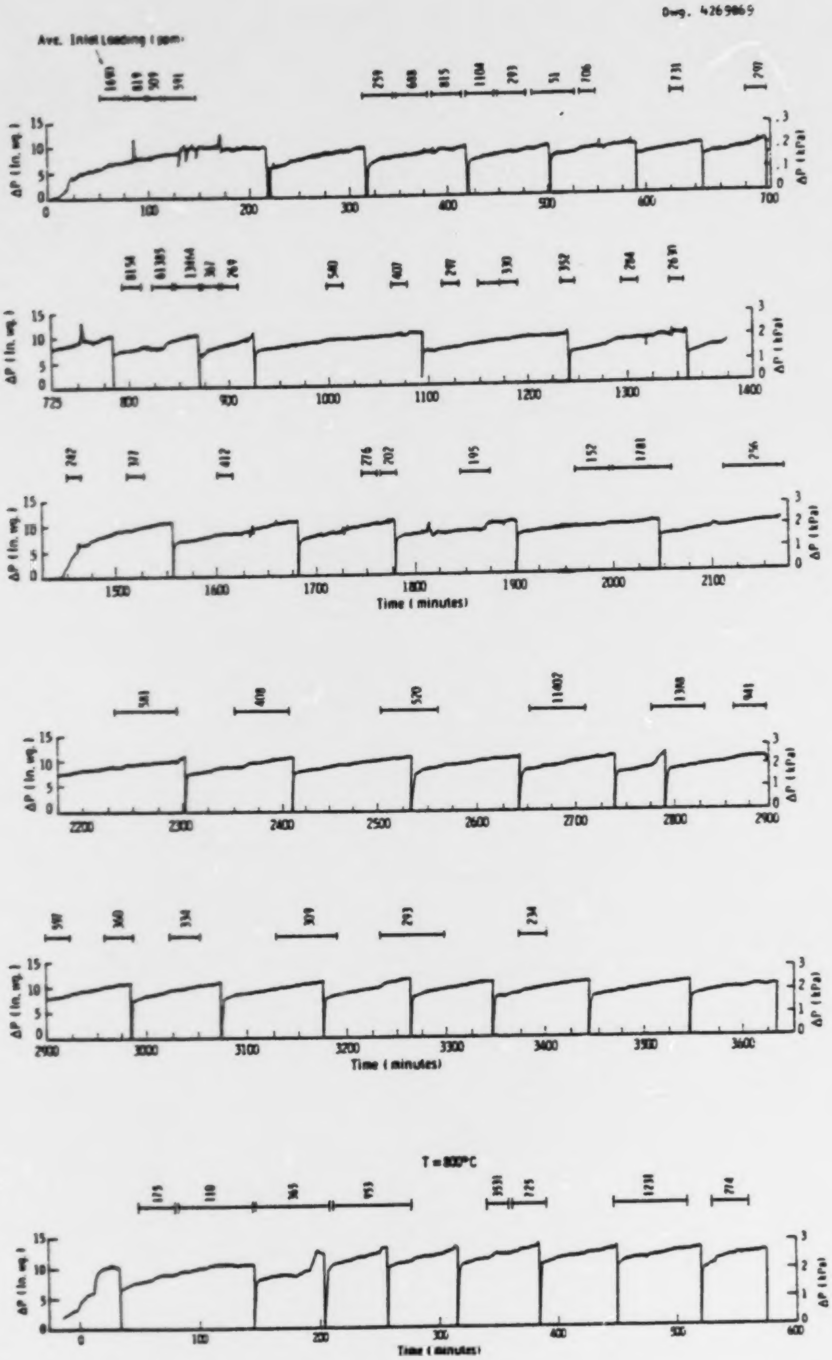

Figure 8. Pressure drop versus time for ceramic cross flow filter tests at ANL with T = 1340°F, P = 120 psig, V = 6.3 ft/min.

# HIGH TEMPERATURE GAS FILTRATION WITH CERAMIC FILTER MEDIA: PROBLEMS AND SOLUTIONS

Ramsay Chang
Acurex Corporation
555 Clyde Avenue
P.O. Box 7555
Mountain View, California 94309

## ABSTRACT

Filter media suitable for use at temperatures greater than 550°F, employing ceramic fibers in their construction, have been under development for several years. These filter media are intended for application in advanced energy processes such as pressurized, fluidized bed combustion and gasification as well as many diverse industrial processes with temperatures ranging from 600° to 1,600°F. The severe environment existing in these processes and the fragile nature of ceramic media pose a unique set of problems requiring special solutions. Ceramic media development work to date has shown significant progress toward achievement of a commercially viable high-temperature filter.

This paper will summarize the results of various hot gas cleanup applications using different ceramic filters, the problems encountered, and the solutions achieved.

## ACKNOWLEDGEMENT

This work is partially supported by Contract DE-AC21-83MC20110 and Contract DE-AC21-80ET17092 from the Department of Energy, Morgantown, West Virginia and Contract RP-1336-4 from the Electric Power Research Institute, Palo Alto, California.

## INTRODUCTION

The early development of hot gas filters at Acurex was made in response to an identified need for hot gas cleaning devices in advanced coal conversion processes. One process of particular interest is the direct combustion of coal in a pressurized, fluidized bed and subsequent expansion of the hot flue gas through a gas turbine for power generation. Commercially proven techniques are available for removal of the particulates from the gas stream before passing through the turbine. However, to work effectively, the temperature must be lowered then reheated, which results in a significant reduction in system energy efficiency. Under Department of Energy (DOE) and Electric Power Research Institute (EPRI) sponsorship, several hot gas cleanup techniques are being investigated for direct particulate removal at temperatures up to 1,700°F and pressures up to 10 atm. These include electrocycles, granular bed filters, eletrostatic precipitators, and ceramic filters (both rigid and flexible).

With the continued development of these high-temperature particulate removal devices, potential applications unrelated to advanced coal conversion processes are emerging. For these applications high-temperature particulate removal from a gas stream offers promise for energy savings, product recovery, product improvement, equipment protection, and emissions compliance. Some examples are given in table 1.

In shale retorting, for example, vapor phase particulate removal of retorting fines could produce a clean shale oil stream requiring very little liquid phase solid removal, which is difficult and expensive. In fluidized catalytic cracking, the catalyst is recycled using a series of cyclones. In some cases, the hog gas is then expanded across a heavy turbine called an "expander" for energy recovery. An efficient particulate removal device could offer better product recovery and extended turbine life.

In summary, the emergence of these options for removing particulates from hot gas streams has the potential for significant impact on the general chemical process industry.

## THE USE OF CERAMIC FILTER MEDIA

Fabric filters have been used successfully over the past several decades for high-efficiency particulate removal from gas streams. The application temperature is typically limited to less than 500°F, because standard filter media, such as Nomex, Teflon, glass, and a variety of synthetic and natural fibers deteriorate rapidly at higher temperatures. For glass fabrics, the coating on the fibers become unstable at high temperatures. Without this coating, the glass fibers have almost no abrasion resistance and break easily. A variety of fiber materials are now available that can be used at temperatures exceeding 550°F. These are ceramic or metallic materials that

TABLE 1. EXAMPLES OF HOT GAS FILTER APPLICATIONS

| | |
|---|---|
| Fluidized bed combustion | -- Turbine blade protection |
| Shale oil retort vapor | -- Vapor phase particulate removal |
| Wood/peat gasifiers | -- Particulate removal |
| Catalytic cracking | -- Product recovery, "expander" protection |
| Chemical processing | -- Dust removal from hot process gas |
| Iron and steel industry | -- Waste heat recovery |

can be configured into filtration media. Several types of ceramic filters are currently under development, including woven, matted, and rigid structures. These are made from silica, alumina, zirconia, boria, magnesia, and silicon carbide-based materials with use temperatures exceeding 2,000°F.

Most of the ceramic materials available are produced for the aerospace and insulation markets. To be useful as hot gas filters, each material must satisfy the three basic performance criteria of high particulate collection: efficiency, cleanability, and long-term durability. Each material must therefore be developed, fabricated, and tested with the goal of achieving these basic filter performance criteria before they become viable candidates for commercial hot gas cleanup systems.

## TEST RESULTS

### NONWOVEN FILTERS

The U.S. Department of Energy (DOE) has funded research to develop concepts and components of a particle collection device that uses bag filters composed of matted ceramic fibers as the filtration media, as shown in figure 1 (1). The bags are constructed of three layers of material. The primary filter is a nonwoven ceramic blanket placed between two layers of woven ceramic (or metal) screens for support. This filter has been tested at temperatures up to 1,500°F and pressures up to 10 atm with an overall mass collection efficiency generally greater than 99.9 percent. The nonwoven filter media construction is cleanable using reverse pulsing techniques. In accelerated high-temperature life tests, no damage is detectable after 100,000 cleaning pulses. Because this media uses small diameter (approximately 3-μm) fibers, collection efficiency is nearly absolute (90 percent collection of 0.3-μm Dioctylphtalate (DOP) smoke particles when clean). With this high initial collection efficiency, dustcakes (which further improve the efficiency) build up on the media surface where they are more easily removed during the cleaning cycle.

Further evaluation of the filter was conducted on a larger scale 520 ACFM at Westinghouse under simulated PFBC conditions (150 psia, 1,500°F) using redispersed flyash. The unit contained five filters, 8 in. in diameter

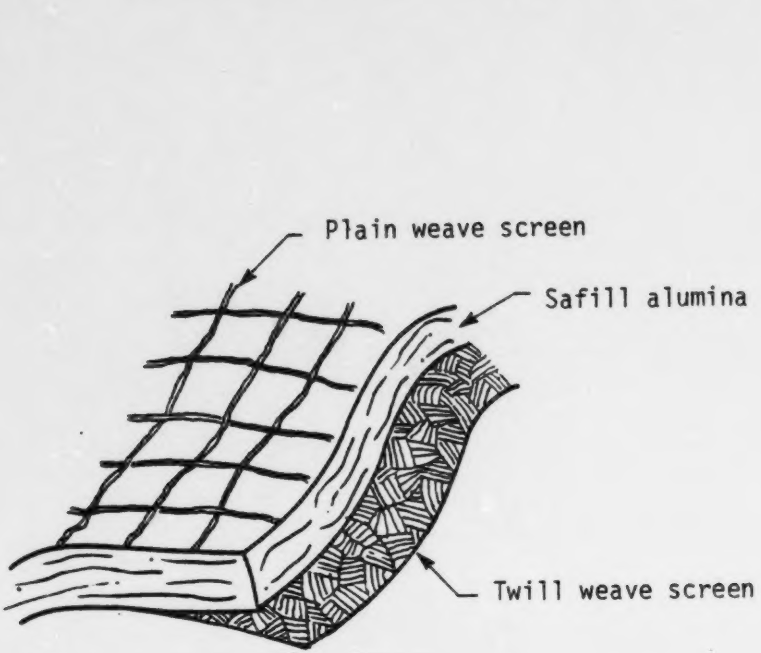

Figure 1. Example of Acurex filter.

by 5 ft in length, and was operated under dust loadings of 1 to 2 gr/ACF and face velocities 8 to 15 ft/min.

Cleanability of the filters was generally good over a total of 77 hr of test time. An overall baseline pressure drop of about 8 in. $H_2O$ was achieved from a pressure drop set point for cleaning 15 in. of $H_2O$. Overall collection efficiencies were initially high (greater than 99.9 percent) but dropped after about 20 hr of testing. Still, the collection efficiency stayed above 95 percent throughout most of the test. At the conclusion of the test it was found that in many places along the filters the Saffil filter media had been blown away. It was determined that a combination of overpulsing and large outer screen openings was the major cause of Saffil blowout. The pulse duration was set at 250 msec, the shortest possible setting on the timer but still significantly higher than normal settings of about 50 msec. This caused excessive high-pressure backflow during pulsing. The large outer screen openings also did not help to retain the fibers of the mat. The inner screen held up quite well and was the primary reason why a relatively high collection efficiency still could be maintained.

A subpilot filter unit, consisting of 15 filters 6 in. in diameter by 8 ft in length, was tested under actual PFBC conditons at Curtiss-Wright (Wood Ridge, NJ).

The PFBC was started with preheat air followed by kerosene addition and then coal. A final temperature of about 1,460°F and pressure of about 71 psig was achieved at a gas flow of about 940 ACFM to the filter vessel. The filters operated quite well during the first 70 hr of overall operation, including 20 hr on coal, and then seemed to fail abruptly. In terms of particulate collection, the filters were >99.6 percent efficient on the average before failure. The pressure drop characteristics of the filter showed also that they have good cleanability. At a set point of cleaning 25 in. of $H_2O$, the baseline $\Delta P$ seemed to be maintained at rather steady levels. During preheat, baseline was kept at 2 to 3 in. $H_2O$, while during the coal feed operations, the baseline was around 7 in. $H_2O$.

A detailed examination of the filters indicated that patches of Saffil very similar to those observed during the tests at Westinghouse were missing from the filter. In addition, patches of the woven inner screen were missing at various locations on the filter. Examination of the data indicated that the abrupt failure coincided with a disturbance in PFBC operation which caused a surge in air flow and perhaps also fuel flow. Scanning electron microscopy analysis around areas where fabric failure had occurred indicated that ash fusion had taken place in these areas which could have embrittled the fabric. A number of possibilities existed for the observed filter bag failures:

- Local ash fusion from combustion on the media surface, causing fabric embrittlement
- Cyclic crushing loads caused by $\Delta P$ buildup. The dustcake may have crushed the media between cleaning cycles causing the long fibers in the mat to break into shorter fibers which could not be held in place by the woven support fabric.
- Excessive cleaning pulse duration could have caused high-velocity gas jets to flow through weak spots around large pores, dragging fibers out of this media
- Open space in the outer "net-like" ceramic fabric support layer may have been too large to support the filtration mat layer of fine diameter fibers. Although the original openings were reduced in size for the tests at Curtiss-Wright, it was not possible to perform optimization tests to quantify the effect of outer screen opening size.
- Fundamental change in mechanical characteristics of Saffil. Earlier EPA-sponsored tests had used Saffil fibers produced by the pilot-scale production facility which ICI had used to develop Saffil alumina fibers. The facility was later dismantled and a full-scale production line was built which produced the fibers used in the DOE-sponsored filtration tests. Visual examinations of the Saffil from both facilities indicated that the production run material was not as flexible or as strong as the pilot-run material. ICI was not able to quantify these apparent differences because Saffil is used for refractory insulation application and these mechanical properties were not important.
- Stresses caused by unequal support cage and filter bag expansion. The ceramic filter is clamped at both ends of the metal cage; consequently, the metal elongates with temperature; the filter is stretched, and it finally tears.

- The possibility of chemical reaction between components in the PFBC gas stream or ashes and the ceramic filter material cannot be ruled out. For example, some of the alkali vapors present in the gas stream may interact with the silica/alumina present in the ceramic fibers.

To prevent some of the potential problems from occurring, various changes in the design of the filter system and filter bags were proposed:

- To prevent surges in flow and temperatures that could damage the filter bags, a bypass line is incorporated into the filter vessel design. Flow to the baghouse would be diverted to the bypass line when the gas flow or gas temperature to the baghouse exceeds some preset upper limit.

- Stresses caused by unequal expansion between the filter bag and cage at high temperatures has been alleviated by the design of a telescoping bottom piece (figure 2) which enables the cage to expand longitudinally at high temperatures without stretching the filter itself. This design also helps to tension the filter bag to prevent creasing along the bag length.

- To hold the ceramic mat in place more securely, various screen sizes and weaves have been proposed and tested, but no optimum has been found. The use of a knitted or biased weave which can be fitted snugly against the fiber mat has been suggested but so far has not been tested extensively. In early versions of the nonwoven filter bag, knitted metal wire support screens were used and no failure of the filter bags due to fiber blowout was observed. In conventional filters, the mat material is generally needled together or needled to a suporting scrim of woven cloth, which helps to stablilze the individual fibers. The technology of needling for ceramic fibers to form a stable structure is still being developed.

- More attention is being paid to ensure that the filter bag material and construction meet specifications and to devise small-scale tests to screen potential filter material before testing at larger scales. Acurex has an ongoing program with DOE on the testing of ceramic fabric filter media (2). The objectives of this project are to provide rapid testing procedures that can be used to quantitatively assess ceramic filter fabric properties to evaluate their potential as bag filter media for hot gas cleanup, compare various ceramic fabrics in terms of selected performance properties, and ensure good quality control of fabrics from batch to batch.

  The program is divided into two phases. In phase 1 standard methods for evaluating textile fabrics will be modified and adapted to the evaluation of ceramic fabrics. Conceptual designs of additional special test procedures and apparatus for assessment of ceramic fabrics will also be made. Two approaches are used for the development of special procedures and apparatus.

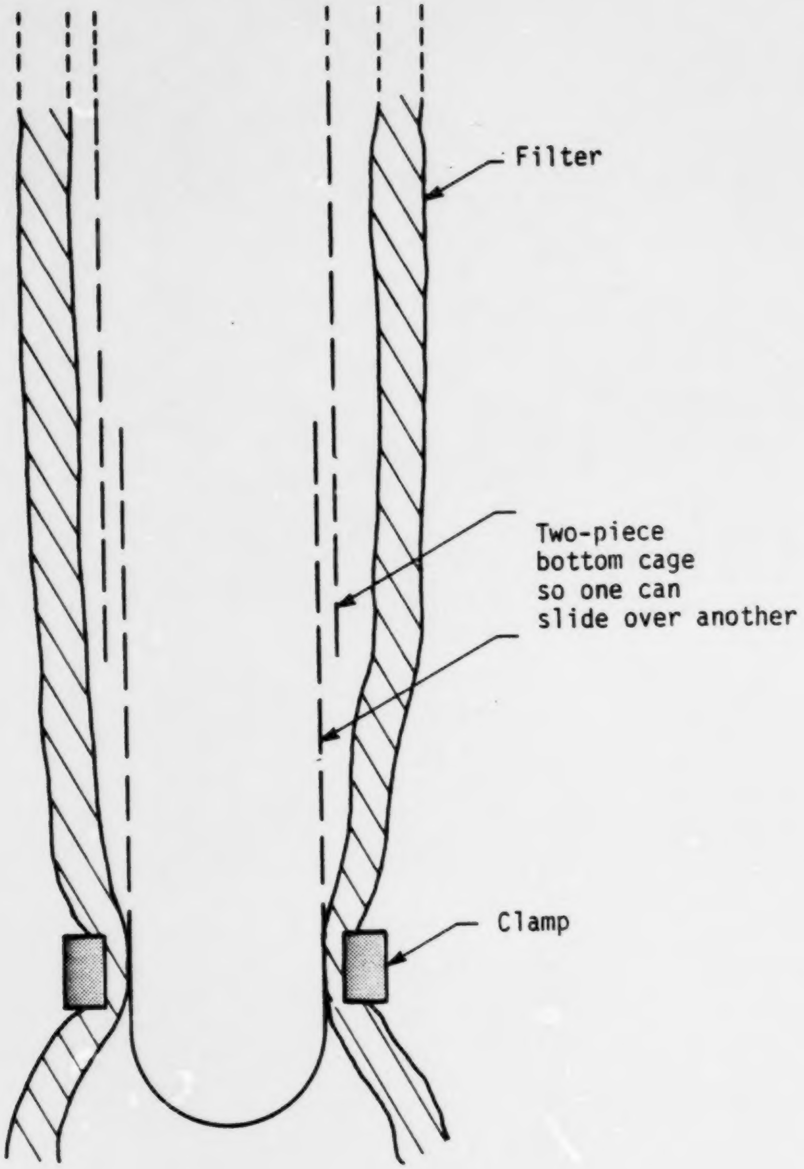
Filter
Two-piece bottom cage so one can slide over another
Clamp

Figure 2. Telescoping cage bottom.

In the first approach fabric mechanical properties such as tensile strength, Mullen burst, and MIT flex resistance will be measured before and after preconditioning in an environment that simulates specific aspects of field use in order to assess any loss in strength before and after exposure.

In the second approach specific fabric properties are measured in-situ in an environment simulating field conditions. Three types of in-situ tests are planned. In the heat flex test the material is to be flexed at high temperature to measure the effect of temperature on its durability. Another planned test is the cyclic crush test in which a heavy load is added cyclically to the middle of the sample to simulate cyclic stress forces.

To evaluate overall filter performance, including collection efficiency and cleanability (pressure drop characteristics), a bench-scale test cell is being constructed (figure 3). The test cell can test small pieces of filter fabric at temperatures up to 1,600°F. Pulse cleaning is used to remove dust periodically from the filter surface. By measuring the filter pressure drop characteristics as a function of time and the amount of dust penetration through the filter, the filter media collection efficiency, dustcake resistivity, and cleanability characteristics at high temperatures could be determined. This apparatus could also provide an assessment of the short-term durability of the filter media at high temperatures.

In phase 2 the development test methods and apparatus will be implemented, tested, and performed on a select group of fabric material.

## WOVEN FILTERS

Under contract to EPRI, Acurex has engaged in the development of woven ceramic filters. The effort focuses on the evaluation of ceramic filters for the cleanup of PFBC exhaust gas. A 13-filter test facility was erected to assess the long-term durability of woven filters. Nominal test conditions are given in table 2.

The first filter material chosen for durability testing was 3M Nextel AB312 ceramic fiber with an eight-harness weave construction. This material and construction was chosen because of encouraging collection efficiency and cleanability results obtained in earlier, short-term evaluations by Westinghouse and Buell Envirotech (3, 4). During the early stages of testing it was found that the Astroquartz thread used to sew the filter seams became brittle on exposure to the hot gas stream and was not strong enough to hold the seams together. Nextel AB312 thread was subsequently used to sew the seams. The filters were exposed for a total of 500 hr to hot gases (800°F) of which 170 hr were tested in the presence of injected flyash. Collection efficiencies for the PFBC flyash were comparable to those obtained

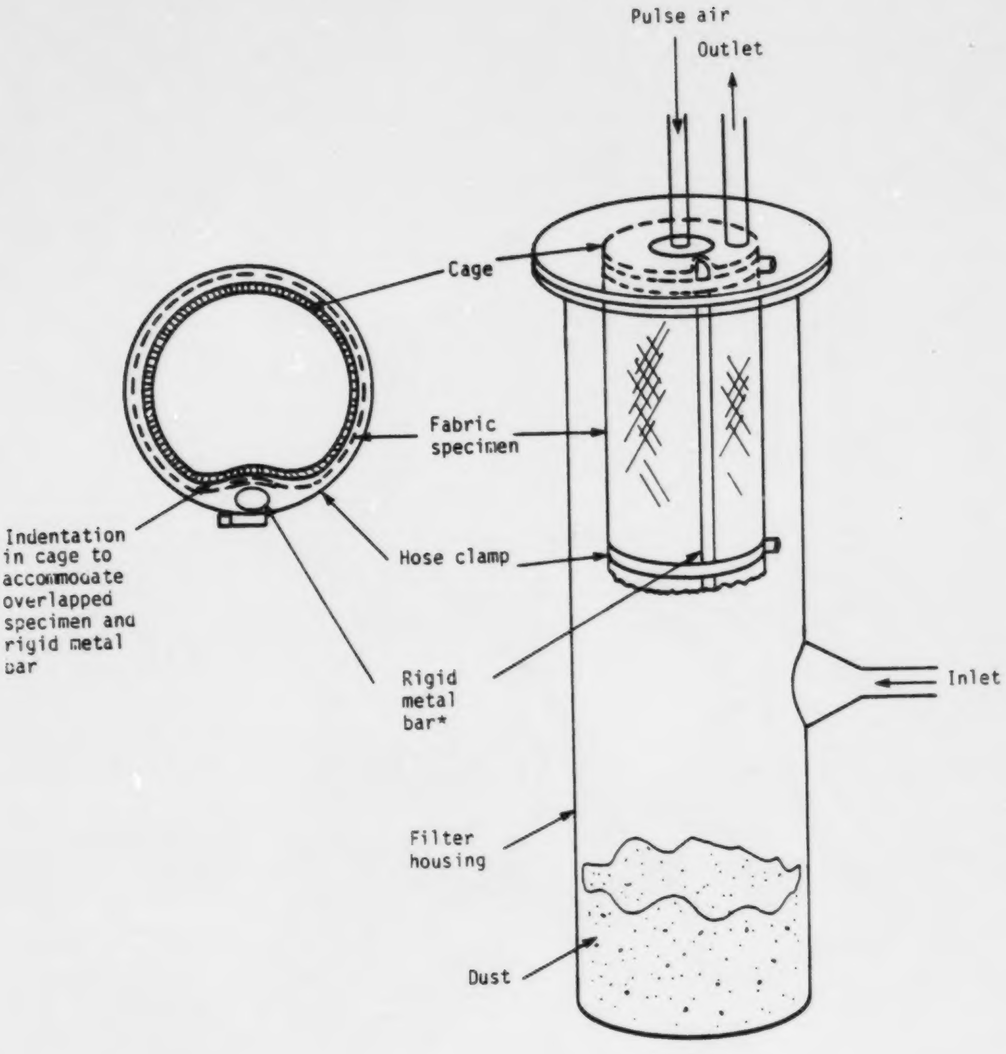
Pulse air
Outlet
Cage
Fabric specimen
Indentation in cage to accommodate overlapped specimen and rigid metal bar
Hose clamp
Rigid metal bar*
Inlet
Filter housing
Dust

* If bag is seamless rigid metal bar would not be used.

Figure 3. Bench-scale filter fabric evaluation test cell.

TABLE 2. NOMINAL TEST CONDITIONS FOR DURABILITY RIG

| Property | Value |
|---|---|
| Temperature | 800°F |
| Pressure | Atmospheric |
| Filter face velocity | 5 to 8 ft/min |
| Ash feedrate | 2 to 5 grains/ACF |
| $\Delta P$ cleaning setpoint | 5 to 10 in. $H_2O$ |
| Cleaning pressure | 90 psig |
| Dust type | Second-stage cyclone catch, PFBC flyash from Curtiss-Wright (25.5-μm mass median diameter) |

previously, averaging 99.2 percent with a high of 99.8 percent. The filters were pulse cleaned online effectively. At a face velocity of 5 ft/min the baseline pressure drop across the filter was maintained at less than 1 in. $H_2O$. At the end of 500 hr it was found that two seam failures had occurred. The first failure occurred at the french-felled side seam where the crease along the seam split apart. The second failure occurred at the bottom seam of the filter where the bottom filter piece split away from the tubular filter. Apart from the seam design problems, the filters performed well overall.

Other tests on woven ceramic filters were also conducted in a single-filter test facility at Acurex. A variety of weave patterns, seam designs, and fabric material were used. The first filter tested in the single-filter facility had the same weave (eight-harness), material (Nextel AB312), and seam structure (french-felled) as the filter selected for testing in the durability rig; however, Inconel wire was used as the sewing thread. Effective online cleaning could be achieved with a pulse pressure of 75 psig. The baseline pressure drop stabilized at 1.3 in. $H_2O$. The collection efficiency of this filter for the finer dust was around 97.9 percent after 117 hr of testing, which is significantly lower than the 99.2 percent for 25.5-μm in the durability rig. This shows that tighter weave structures should be used for fine dust. At the conclusion of testing, the eight-harness filter was visually inspected. The Inconel sewing thread appeared undamaged, although some fabric breakage around the Inconel wires was observed. Slight fabric breakage was also observed on the edges of the french-felled seam.

Due to the difficulty encountered in developing proper seams and sewing thread, attempts were made to weave seamless tubes. A seamless tubular filter in a five-harness weave was tested. A five-harness weave was chosen because earlier results from flat sheet dust loading tests showed that the five-harness weave has a better overall mass collection efficiency compared to an eight-harness weave. The bottom of the filter was sewn shut. Since some of the earlier bottom seam failures may have occurred due to stresses produced by the sand being distributed unevenly, no sand was placed at the bottom to tension the filter.

Two dust distributions were used to evaluate filter performance. The first dust was flyash collected by the second-stage cyclone at the Curtiss-Wright PFBC facility with a mass median diameter of 25.5-μm. The second dust was (mass median diameter 8.3-μm) collected at the same facility by a high-temperature electrostatic precipitator. About 105 hr of testing was accumulated using the coarse fraction. At the end of testing with the coarse dust, the filter was cleaned thoroughly by several pulses of air and testing was resumed using the fine dust. The five-harness filter was readily cleaned using a reservoir pressure of 80 psig. Baseline pressure drops were maintained at 1.5 to 1.7 in. $H_2O$. At 3 to 3.7 ft/min face velocity dust collection efficiencies were high (up to 99.8 percent) and there did not seem to be significant differences between the dust fractions. Collection efficiencies immediately after cleaning were lower (98.7 to 98.9 percent) as significant dust penetration generally occurred after pulse cleaning. Although the five-harness weave had good collection efificiencies, better fabrics and weaves need to be developed to improve operation at higher face velocities and to enable pulse cleaning without significant dust penetration. Some of the problems observed in the different tests were:

- Seam failures have occurred. There is evidence of two types of seam failures:
    - -- Sewing thread failure. Early designs used Astroquartz (glass) thread coated with Teflon. Teflon decomposition products and heat may have weakened the thread resulting in seam failure. This problem has been addressed through attempts to replace the glass sewing thread with ceramic or metal threads.
    - -- Fabric failure at the sharp (180°) crease in the typical french-felled seam. Recent tests at Acurex have shown that this failure may have been previously interpreted as a sewing thread failure. After fabric failure at the crease, the seam pulls apart.
- Dust penetration through woven filters can be a problem, especially during pulse cleaning. The most successful tests in terms of collection efficiency (>99 percent, eight-harness weave) have occurred using coarser dust fractions. Dust with a heavy concentration of fines cannot bridge over the large pores often present in a woven fabric, especially those made from smooth continuous filament yarns. The problem is that the woven filters, unlike the mat filters, are not inherently good particle filters. It is the cake eventually formed by dust depositing on the fabric and bridging over the pores that acts as the filtration barrier (5). The pores through woven fabrics form at the yarn intersections and, for continuous (smooth) filament yarns, provide a large pathway for dust penetration. This is one of the main reasons woven fabrics

generally operate at lower face velocities than felts. It also explains why pulse cleaning is seldom used with woven fabrics made of smooth yarns, since significant penetration occurs immediately after a cleaning pulse.

- Fabric embrittlement during long-term exposure to hot gases. At the Curtiss-Wright PFBC tests (1) for example, several holes formed in the inner woven support screen of the Acurex filters. Pieces of woven support screen were found to be considerably weaker (in tensile and flex properties) after the PFBC tests compared to a new piece of similar fabric. As discussed in the previous sections, this embrittlement could be due to ash fusion around the fibers or direct chemical attack by components in the gas stream.

- Filter-cage-related and media support wear problems. Movement of the media with respect to the cage support surface during the cleaning pulse creates a potential for abrasive wear. In a hot gas filter the large thermal expansion of the cage with respect to the media creates a more difficult fit problem than that which occurs in conventional filtration. Acurex has also noted signs of wear at the bottom of the bag where its excess length below the metal cage crumpled as a result of pressure differences.

To resolve some of the observed problems with woven filters, new bag designs have been proposed:

- The filters are now woven in a seamless tubular construction to eliminate the need for sewing thread and seams. A variety of weave patterns are possible. The bottom seam is eliminated by using a telescoping piece suggested earlier.

- The operating face velocity and collection efficiency can be increased significantly by using stapled or texturized yarns that contain a substantial amount of small, protruding fibers. These new fibers stick out and serve as dust collection centers. New fabrics are being developed that contain "fuzzy" yarns. Recent tests show that these "fuzzy" fabrics have a significantly improved collection efficiency over "smooth" fabrics even at high face velocities and for fine dust distributions.

  Another approach to improve collection efficiency with smooth yarns is to modify the yarn structure and the weave pattern. For example, smaller diameter yarns enable the fabric to be woven tighter with small pore openings. Flat yarns also decrease the size of the openings at the yarn intersections. Acurex is developing special weave patterns to create more tortuosity for the dust path so that there will be less direct dust penetration.

- Problems with ash fusion are addressed by keeping the filter operating temperature below ash fusion points. This is done by monitoring the filter vessel or filter bag temperature closely and bypassing the vessel if the temperature exceeds a preset limit. The bypass line will also be used in case of upset conditions, such as flow surges, that can cause fuel carryover.

The various tests on woven and nonwoven ceramic bag filters discussed above have illustrated the performance of these filters for hot gas cleanup applications. These tests also pointed out the problems which can be encountered during high-temperature applications and the various solutions which have been proposed. The development of ceramic filters has progressed significantly since these tests with the incorporation of the numerous innovations in filter system and filter bag design. These will need more in-situ long-term filter performance evaluations to bridge the gap between product development and final commercialization.

The work described in this paper was not funded by the U.S. Environmental Protection Agency and therefore the contents do not necessarily reflect the view of the Agency and no official endorsement should be inferred.

## REFERENCES

1. Shackleton, M. et al., "High-Temperature, High-Pressure Gas Cleanup With Ceramic Bag Filters," DOE/ET/17092-1504, January 1984.

2. Chang, R., "Ceramic Fabric Material Testing," DOE Draft Interim Report Tr-84-157/EE, April 1984.

3. Ciliberti, D. F. and T. E. Lippert, "Gas Cleaning Technology for High-Temperature, High-Pressure Gas Streams," EPRICS-3197, August 1983.

4. Furlong, D. A. and T. S. Shevlin, "Fabric Filtration at High Temperature," Chemical Engineering Progress, p. 89, January 1981.

5. Billings, C. E., J. Wilder, "Handbook and Fabric Filter Technology," Volume I, EPA No. APTD0690, December 1970.

# THE DEVELOPMENT AND HIGH TEMPERATURE APPLICATION OF A NOVEL METHOD FOR MEASURING ASH DEPOSITS AND CAKE REMOVAL ON FILTER BAGS

by: David F. Ciliberti
Thomas E. Lippert

Westinghouse Electric Corporation
Pittsburgh, PA 15235

and

Owen J. Tassicker
Steven Drenker

Electric Power Research Institute
Palo Alto, CA

## ABSTRACT

This paper presents theoretical development and experimental confirmation of a novel capacitance based measurement technique for the on-line determination of dust cake build-up and removal, on pulse jet cleaned bag filters. Ambient testing results indicate that a resolution of approximately .05 $kg/m^2$ is easily attainable with the transducer.

The method has been applied to filtration at ambient conditions and extended to operation at temperatures in excess of 800°C and at pressures at 11 atm. This method has been further expanded to allow axial resolution of dust cake deposits along the bag and has allowed a better understanding of the mechanics involved in dust cake release and subsequent build-up.

## INTRODUCTION

Traditionally the effectiveness of filter bag cleaning has been judged by the level of the baseline pressure drop just after a cleaning episode. It can easily be shown, however, that this pressure drop is a rather insensitive measure of cleaning effectiveness for filters which tend to clean in a "patchy" fashion. Many types of porous rigid filters and particularly woven filter bags frequently demonstrate this patchy cleaning behavior. An accurate means of quantifying cleaning effectiveness is important in the establishment of a cleaning regimen that optimizes bag life, efficiency and pressure drop characteristics. These considerations have been of paramount importance in our current efforts to develop high temperature and pressure ceramic bag filters for advanced energy conversion technologies since these bags are composed of ceramic fibers which are more subject to damage during cleaning than are conventional lubricated glass fibers. To this end a new capacitance measurement technique has been developed that is capable of on line filter cake mass measurement. The device can be used to give estimates of overall filter cake removal efficiencies as well as the axial distribution of dust cake on the filter.

A brief overview of the concept is illustrated in Figure 1 and described here as applied to a woven bag filter.

The device measures the capacitance of a system consisting of two concentric electrodes. The bag filter is fitted over the inner electrode and when dust cake forms on the bag between the two electrode elements, the capacitance of the system is increased. In Figure 1 the inner perforated bag former (H) and the outer metal container (L) are the two principal electrodes. The upper and lower guards (N) eliminate end effects and define the capacitance (C).

## THEORETICAL DEVELOPMENT

In order to proceed with the development of the filter cake mass detector (FCMD) it was necessary to first derive the working equations that describe the system and then to investigate the sensitivity of transducer to various operating parameters.

## WORKING EQUATIONS FOR FCMD

The working equation for the FCMD are developed using Figure 2 as a reference and for nomenclature. As can be noted from this figure the inner electrode can be segmented by electrically isolating adjacent sections. This allows the capacitance to be measured for each section and gives a

Dwg. 9364A14

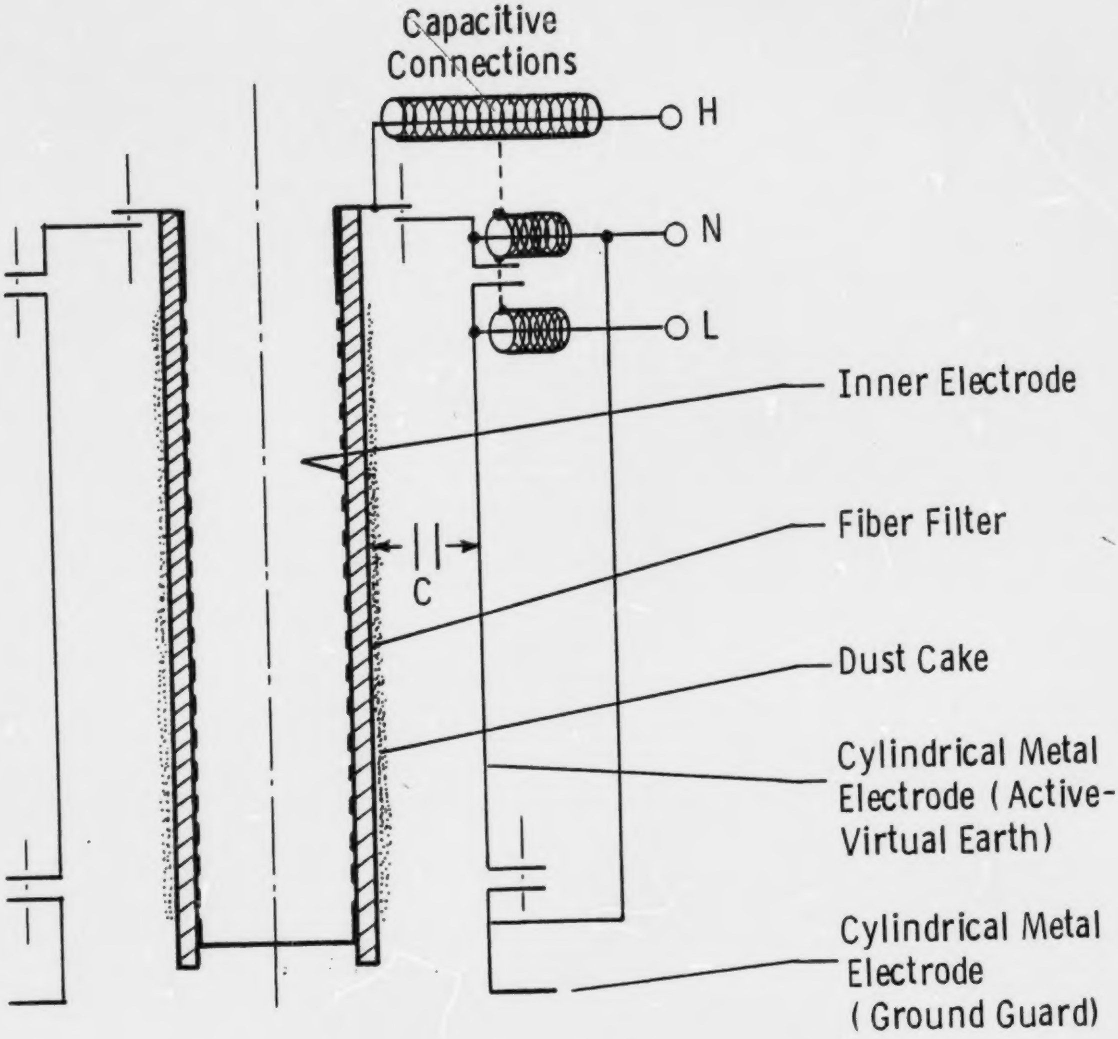
Capacitive Connections
H
N
L
Inner Electrode
Fiber Filter
C
Dust Cake
Cylindrical Metal Electrode ( Active-Virtual Earth)
Cylindrical Metal Electrode ( Ground Guard)

Figure 1. Determination of Dust Deposit by Capacitance

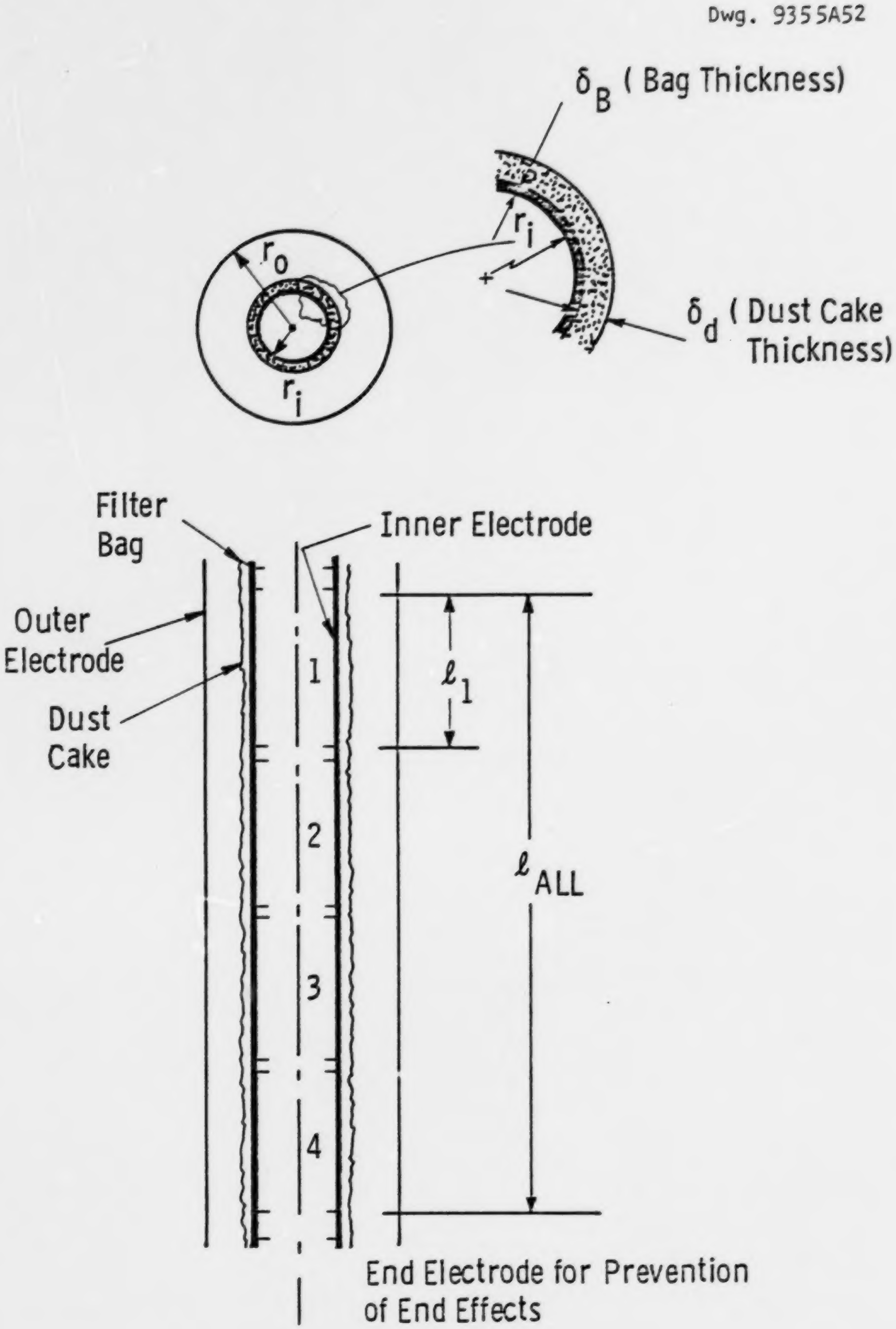
Dwg. 9355A52
$\delta_B$ ( Bag Thickness)
$r_o$
$r_i$
$r_i$
+
$\delta_d$ ( Dust Cake Thickness)
Filter Bag
Inner Electrode
Outer Electrode
Dust Cake
1
2
3
4
$\ell_1$
$\ell_{ALL}$
End Electrode for Prevention of End Effects

Figure 2. - Geometry and Nomenclature for Segmented Filter Cake Mass Detector

means for axial resolution of the distribution of dust on the filter. The equations for the capacitance ($C_j$) of any of these sections is determined as follows. For capacitors in series, the total capacitance is written

$$\frac{1}{C_j} = \frac{1}{C_1} + \frac{1}{C_2} + \cdots\cdots \frac{1}{C_N} \tag{1}$$

For coaxial electrodes, the expression for capacitance is written

$$C_j = \varepsilon_j \varepsilon_o \frac{2\pi \ell_j}{\ln\,(r_o/r_i)} \tag{2}$$

where $\varepsilon_j$ is the relative permittivity (dielectric constant) of the material between the electrodes, $\varepsilon_o$ is the permittivity constant, $r_i$ and $r_o$ the inner and outer radius of the coaxial capacitor, respectively, and $\ell_j$ the active length of segment j.

For any segment of the FCMD depicted the Figure 2, the capacitance between the inner and outer electrode is written

$$\frac{1}{C_j} = \frac{1}{2\pi\ell_j \varepsilon_o \varepsilon_b} \ln\left(\frac{r_i + \delta_b}{r_i}\right) + \frac{1}{2\pi\ell_j\, \varepsilon_o \varepsilon_d} \ln\left(\frac{r_i + \delta_b + \delta_d}{r_i + \delta_b}\right) + \frac{1}{2\pi\ell_j\, \varepsilon_o} \ln\,\left(\frac{R}{r_i + \delta_b + \delta_d}\right) \tag{3}$$

where the subscripts b and d refer to bag and dust cake, respectively. The change in the capacitance measured between the electrodes due to the accumulation of dust cake is

$$2\pi\varepsilon_o \ell_j\left(\frac{1}{C_o} - \frac{1}{C_j}\right) = \ln\left[\frac{\frac{1}{r_i + \delta_b}}{\left(\frac{r_i + \delta_b + \delta_d}{r_i + \delta_b}\right)^{1/\varepsilon_d} \left(\frac{1}{r_i + \delta_b + \delta_d}\right)}\right] \tag{4}$$

where $C_o$ is the system capacitance without dust cake and $C_j$ the system capacitance with dust cake. Rearranging the above equation and solving for $\delta_d$, dust cake thickness, gives

$$\delta_d = (r_i + \delta_b)\left\{e^{\left(\frac{2\pi\varepsilon_o \ell_j \left(\frac{1}{C_o} - \frac{1}{C_j}\right)}{(\varepsilon_d - 1)/\varepsilon_d}\right)} - 1\right\} \tag{5}$$

The mass of dust on the $j^{th}$ section of the bag is calculated from

$$M_j = \pi\, \delta_d \ell_j \rho_d \left[ 2\left(r_i + \delta_b\right) + \delta_d \right] \qquad (6)$$

Where $\delta_d$ is the bulk density of the dust deposit

## SENSITIVITY OF THE THICKNESS MEASUREMENT TO UNCERTAINTY IN DUST DIELECTRIC CONSTANT

A potential difficulty in using this technique for dust cake thickness measurements arises from the fact that the dielectric properties of the ash deposit are functions of temperature, ash composition and bulk density. It is clear that calibration at conditions as near as possible to actual operating conditions is desirable, however, it is also likely that variations in all of the parameters above will occur in the course of actual use. To investigate the impact of these variations on the measured deposit thickness the following analysis was performed.

The change in indicated deposit thickness $\Delta\delta$ with variations in dielectric constant $\Delta\varepsilon$ can be determined from

$$\Delta\delta = \left(\frac{\partial\delta}{\partial\varepsilon}\right) \Delta\varepsilon \qquad (7)$$

Using equation (5) and performing the indicated operations the following result is obtained

$$\left(\frac{\Delta\delta}{\delta}\right) = -\left(\frac{\Delta\varepsilon_d}{\varepsilon_d}\right) \left(\frac{1}{(\varepsilon_d - 1)}\right) \left(\frac{x}{1 - e^{-x}}\right) \qquad (8)$$

where

$$x = 2\pi\varepsilon_o \ell \left(\frac{C - C_o}{CC_o}\right) \left(\frac{\varepsilon_d}{\varepsilon_d - 1}\right) \qquad (9)$$

For the experimental device under consideration dust cake dielectric constant ranged over a factor of 2 from $\varepsilon = 5$ to 10.

The expected range of values of x is

$$o < x < .034$$

For these small values of x, the exponential term in equation (8) can be approximated

$$e^x \sim 1 + x$$

so that the expression for $(\Delta\delta/\delta)$ becomes

$$\left(\frac{\Delta\delta}{\delta}\right) = \left(\frac{\Delta\varepsilon}{\varepsilon}\right) \frac{1}{(\varepsilon - 1)} \tag{10}$$

In this form the fractional uncertainty in cake thickness can be seen to be a very rapidly decreasing function of $\varepsilon$. In the range of values observed

$$\frac{\Delta\varepsilon}{(10)\,(9)} < \frac{\Delta\delta}{\delta} < \frac{\Delta\varepsilon}{(5)\,(4)} \quad \text{or} \quad \left(\frac{\Delta\varepsilon}{90}\right) < \frac{\Delta\delta}{\delta} < \left(\frac{\Delta\varepsilon}{20}\right)$$

From this it is concluded that the cake thickness measurement is relatively insensitive to the cake dielectric constant measurement. This minimizes the effect of any error due to uncertainty in the dust cake bulk dielectric property that may arise due to changing test conditions.

## SENSITIVITY OF DEPOSIT THICKNESS DETERMINATION TO MEASUREMENT OF CAPACITANCE CHANGE

In order to determine the capacitance change resolution required to detect significant changes in dust deposit thickness an analysis similar to that just presented was performed. In this analysis the object was to determine the expected capacitance change due to a given dust deposit thickness change. Starting again with equation (5) the change in measured capacitance due to a change in deposit thickness can be determined from

$$\Delta\delta = \left(\frac{\partial\delta}{\partial(\Delta C)}\right) \Delta\,(\Delta C) \tag{11}$$

Where $\Delta C = (C - C_o)$ and $C_o$ is the cleaned, conditioned bag capacitance. If one lets

$$y\Delta C = 2\pi\varepsilon_o \ell \left(\frac{\Delta C}{CC_o}\right) \left(\frac{\varepsilon}{\varepsilon - 1}\right) \tag{12}$$

and if it is assumed that $\frac{\Delta C}{CC_o} \approx \frac{\Delta C}{C_o^2}$ since $C_o >> \Delta C$ then when the indicated operations are performed the following expression can be obtained:

$$\frac{\Delta\delta}{\delta} = \frac{y\; e^{y\Delta C}\Delta(\Delta C)}{(e^{y\Delta C} - 1)} \tag{13}$$

As before, when approximate values for the parameters are inserted in the exponent of equation (12) a small number is obtained

$$y\Delta C \approx 0.003\ \Delta C(pf)$$

Which justifies the approximation of the of the exponential term as

$$e^{y\Delta C} \approx 1 + y\Delta C \qquad (14)$$

This simplification leads to the final form

$$\left(\frac{\Delta\delta}{\delta}\right) = \left(\frac{\Delta(\Delta C)}{\Delta C}\right) \qquad (15)$$

In order to illustrate the implication of this result consider a typical case in which a 1% change in deposit is to be detected after a 2 pf change has occurred in the system. For this situation

$$\frac{\Delta\delta}{\delta} = \frac{(C_2 - C_o) - (C_1 - C_o)}{(C_2 - C_o)} = \frac{C_2 - C_1}{C_2 - C_o} = \frac{C_2 - C_1}{2} = .01$$

which means that a capacitance change of .02 pf must be detectable in a total reading of roughly 100-150 pf in order to resolve a 1% change in deposit thickness. This precision is easily attainable using a quality capacitance bridge and provides confidence that the technique is a viable method for the detection of very small changes in dust deposits on bag filters.

## EXPERIMENTAL VERIFICATION OF FCMD AMBIENT CONDITION TESTING

As a first step in experimental verification of this concept, the test unit shown schematically in Figure 3 was assembled. In this test apparatus a single woven ceramic cloth bag was supported on perforated metal mandrel which also served as the inner electrode of the capacitor system. The outer shell or filter vessel wall served as the outer electrode and was fitted at either end with grounded guard sections to eliminate end affects. Preweighed amounts of dust were entrained in a dry air flow that yielded a filter face velocity of 0.6 m/min. Capacitance measurements were made as a function of dust deposited on the bag filter. Figure 4 presents the results on a typical test run in which dust was deposited on the filter surface and then dislodged by pulse jet cleaning over 3 consecutive cycles. As can be observed from the figure the repeatability and sensitivity of the measurement provided encouragement to continue on to high temperature and pressure testing.

## HIGH TEMPERATURE AND PRESSURE APPLICATION OF THE FILTER CAKE MASS DETECTOR

Having experienced success in testing the transducer at ambient conditions, a decision was made to design, fabricate and test a high temperature and pressure version of the device in conjunction with on-going HTHP ceramic bag filter testing. It was also decided that the FCMD should be modified to allow for axial resolution of dust deposits by incorporating electrically isolated segments into the inner electrode/bag support

Dwg. 9364A13

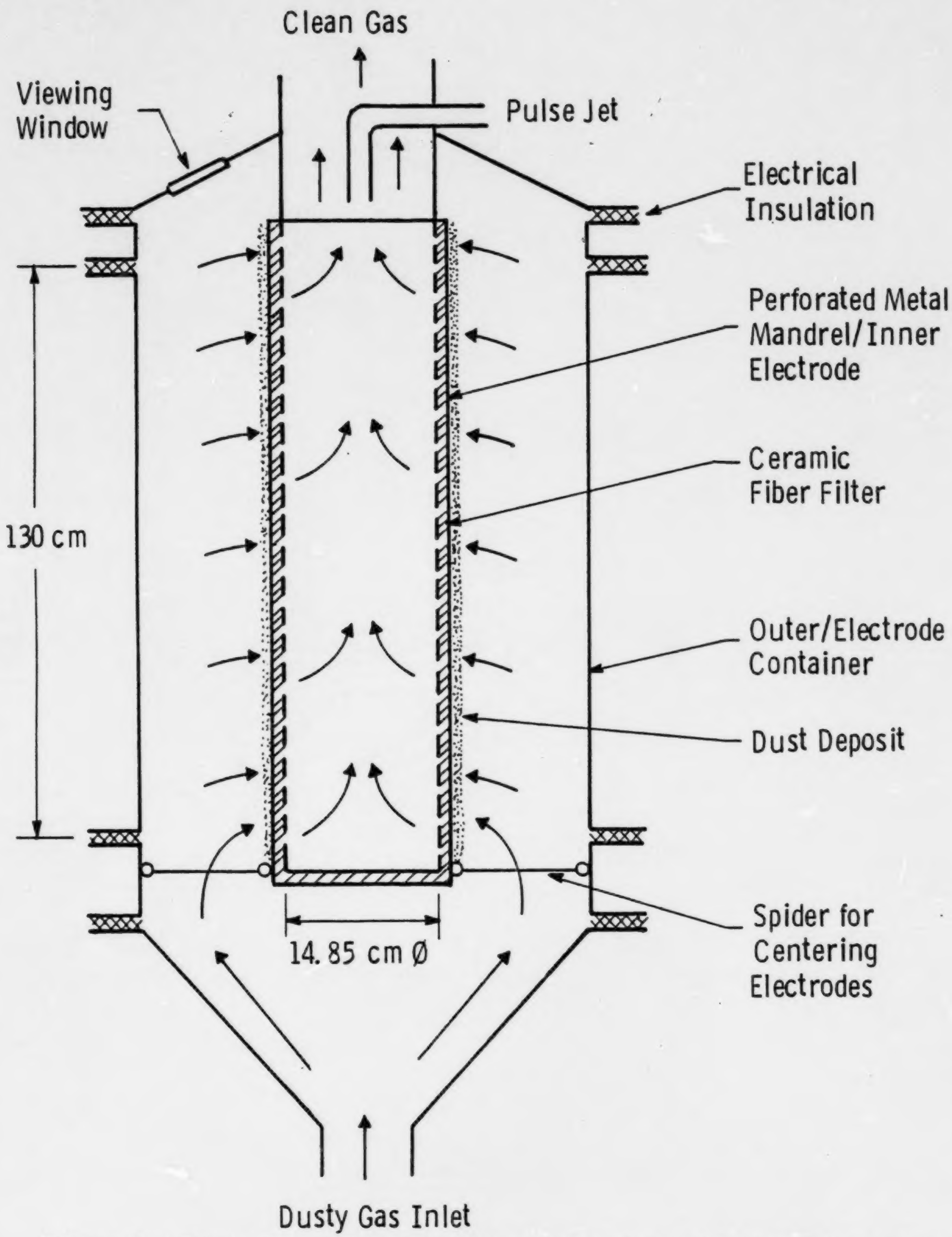
Clean Gas
Viewing Window
Pulse Jet
Electrical Insulation
Perforated Metal Mandrel/Inner Electrode
Ceramic Fiber Filter
130 cm
Outer/Electrode Container
Dust Deposit
Spider for Centering Electrodes
14.85 cm Ø
Dusty Gas Inlet

Figure 3. Fabric Filter Test Module Capacitive Filter Cake Determination

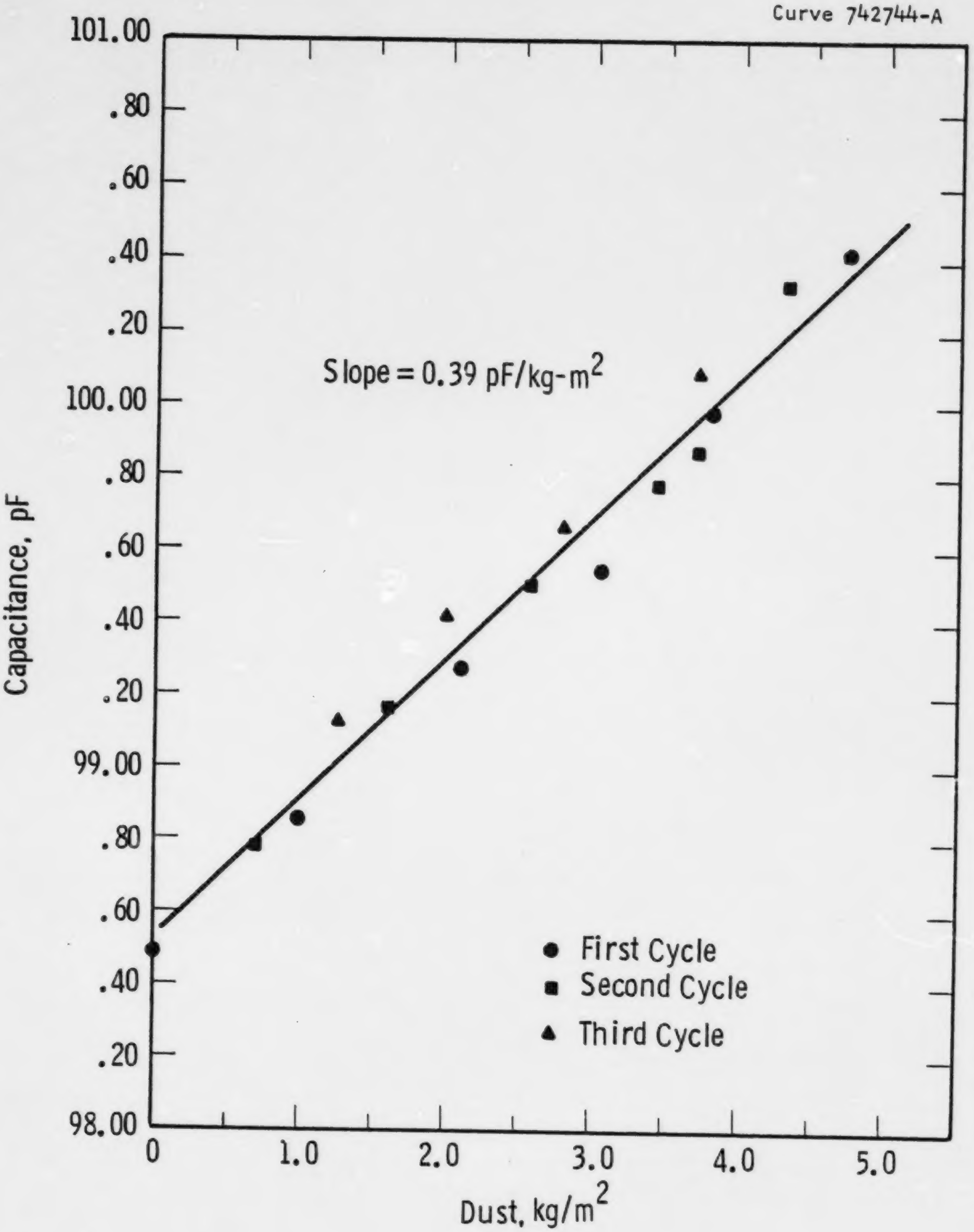

Figure 4. Measured Ash Capacitance of Conditioned Filter Bag Over Three Successive Cycles.

mandrel. The segmented electrode assembly consisting of four active sections was constructed and is shown in Figure 5. Each section of the electrode was physically and electrically isolated by sets of ceramic spacers placed between the individual electrode sections. To eliminate end effects, short grounded end sections were provided. The bottom guard was designed with a 3.8 cm (1.5 in) long centering pin for maintaining alignment between the inner and outer electrodes. The entire assembly was mounted in an existing HTHP filtration test loop capable of operation at 900°C and 15 atm.

Electrical interface of the capacitance bridge with the segmented electrode assembly required coaxial leads. These leads (high-temperature, coaxial heater wire) were brought out from the inner electrode assembly through the pressure containment vessel to switches that permitted sequential readings of the individual electrode segments on a capacitance bridge. Readings could be obtained for each individual segment or for combinations of electrode segments by appropriately positioning the switches. The bridge and switches were connected to a microprocessor unit for data acquisition, automatic switching, and display.

High temperature and pressure testing of the FCMD was carried out and a representative sample of the data obtained is presented here to demonstrate the usefulness of the device as on-line diagnostic tool and to illustrate the level of detailed information possible.

Figure 6 presents an example of FCMD data taken at high temperature and pressure. In this test a woven ceramic bag filter (3M's, ZS11 material) was operated at 500°C and at a pressure of 11 atm with a filtration velocity of 2 m/min. Figure 6 presents the first two filtration cycles that the bag experienced and plots both pressure drop and the capacitance of individual segments as a function of time. Notice that during the first cycle (the bag's initial exposure to dust) the pressure drop rises linearly with time. This reflects a uniform initial surface condition. Likewise the capacitance curve for each segment rises at a nearly constant, equal rate as would be expected. At a pressure drop across the bag of 3.75 kPa the dust feed was shut off and the system was allowed to equilibrate for several minutes. Then a cleaning pulse lasting about 0.2 seconds was administered from a 28 atm pulse reservoir. The subsequent pressure drop across the filter fell to a nearly clean reading of 0.125 kPa. Similarly, the capacitance measured for the bottom three segments was virtually returned to the initial state indicating nearly complete dust cake removal. The top segment, however, did not appear to be effectively cleaned, as the capacitance only fell about 6% from 43.75 pf to 43.62 pf. This response is consistent with previous pulse jet cleaning experience and is thought to occur because of a venturi effect due to the high velocity of the pulse jet at the mouth of the bag filter. In the upper region of the bag, where the pulse has not yet expanded to the mandrel walls there is actually an induced inward radial flow of gas resulting in little or no dust cake removal.

When dust feed to the system was resumed during the second cycle the pressure drop curve showed a relatively large initial slope which tended to diminish to a value equal to the slope of the initial pressure drop trace

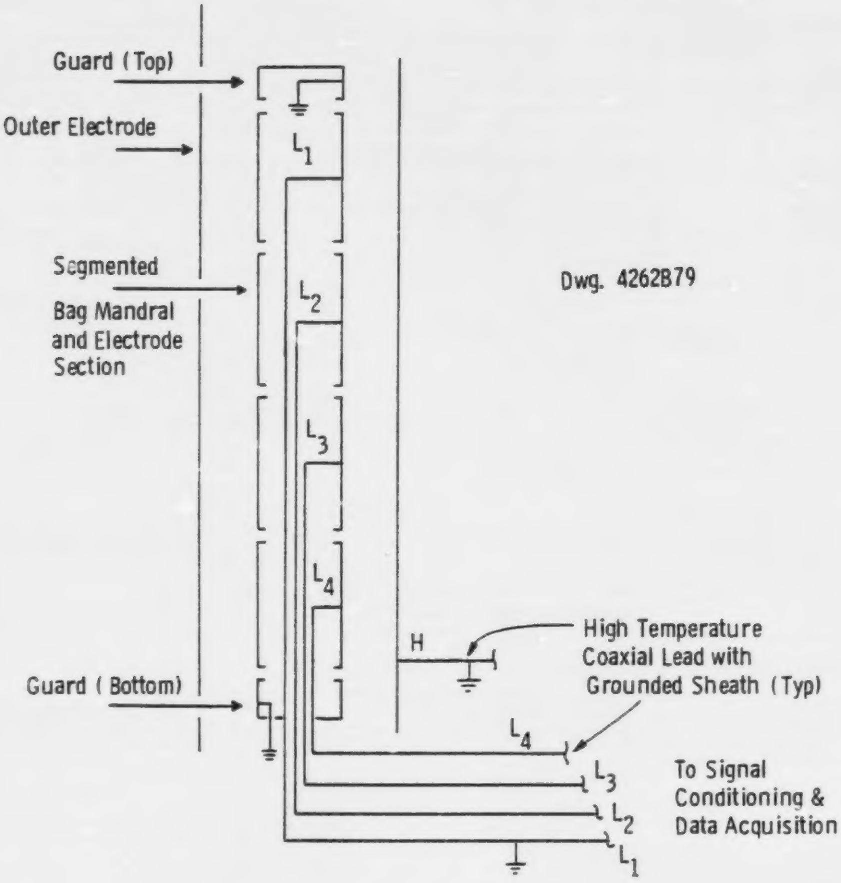
Guard (Top)
Outer Electrode
Segmented
Bag Mandral and Electrode Section
Guard (Bottom)
$L_1$
$L_2$
$L_3$
$L_4$
H
Dwg. 4262B79
High Temperature Coaxial Lead with Grounded Sheath (Typ)
$L_4$
$L_3$
$L_2$
$L_1$
To Signal Conditioning & Data Acquisition

Figure 5. Schematic of FCMD Electrical Connections

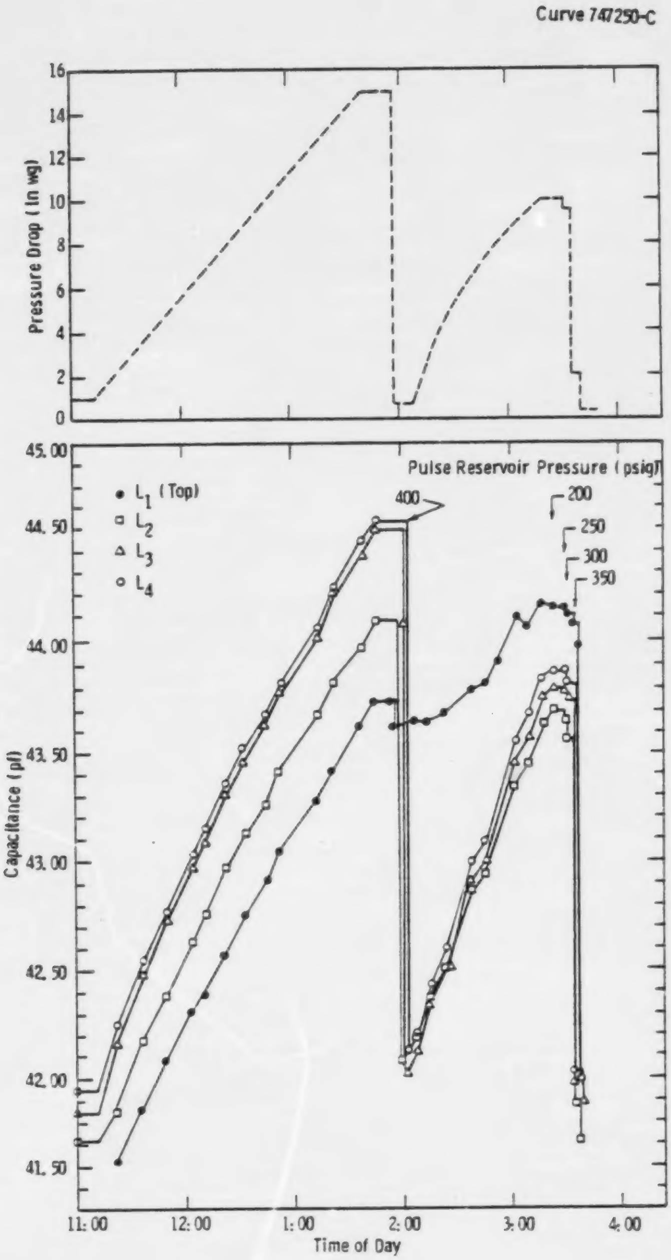

Figure 6. Capacitance FCMD Sections and Pressure Drop Vs Time for Test 4-12-83. T = 920°F. P = 150 psig.

and characteristic of uniform deposition over the entire bag surface. The capacitance curves for the lower three segments rose at relatively rapid and identical rates from their near clean state. The initial rate was about 1.5 times the rate observed in the first cycle. That was consistent with the capacitance based estimate of 80% effective dust cake removal. The capacitance trace for the upper segment was nearly flat during the initial part of the second cycle. This reflected the fact that virtually all of the flow was being accommodated by the lower 3/4 of the bag which had been effectively cleaned. For filters that require low face velocity for high efficiency this effect is important since it implies that the lower 3/4 of the bag was operating at a filter velocity roughly 30% higher than the nominal velocity. As dust cake accumulated over the lower part of the bag and the resistance became more comparable to the top section the flow began to distribute itself more uniformly. This could be inferred from the decreasing rate of rise in the pressure drop curve and the capacitance curves for the lower segments. Additionally the increase in slope of the upper segment's capacitance curve provided indication of increasing flow through this section.

Dust feed was again stopped when the filter pressure drop reached 2.5 kPa. This time the filter was pulsed cleaned with a series of increasing pulse reservoir pressures in an attempt to determine the minimum pulse pressure required to clean the bag. The first pulse of 14.5 atm yielded no observable change in either the pressure or capacitance levels. The second pulse (18 atm) resulted in a small decrease in pressure drop of about 0.125 kPa, but no significant change in capacitance. The third pulse was at a 21.5 atm level and resulted in a dramatic decrease in pressure drop from 2.4 kPa to 0.5 kPa. This pulse did not generate nearly as significant of a drop in capacitance with typically only about a 5% decrease in the capacitance observed. A fourth and final pulse at 24.8 atm yielded only a small additional decrease in pressure drop from about .5 kPa to about 0.1 kPa. This pulse did cause a major decrease in the capacitance reading for the lower three segments indicating that virtually all of the remaining 95% of the dust cake on these segments was removed. The upper segment, as before, was left essentially uncleaned.

Similar experiments have been carried out at operating temperatures up to 815°C and at pressures of 11 atm. The results have also been positive and have provided proof of operation in these extreme environments. In these tests the dielectric constant of the dust cake has been previously determined making capacitance measurements on a laboratory cell filled with the test dust, and tested at operating conditions. When used with the measured apparent density of the dust cake, the capacitance change data could easily be converted to average dust deposit thickness data through the use of equation (6).

## CONCLUSION

In conclusion, it can be said that the capacitance based filter cake mass detector has been shown to be a very useful instrument for the analysis of filter bag cleaning techniques, both at ambient and high temperature and pressure conditions. In many respects the use of such an instrument has been shown to give a much more detailed on-line picture of filter bag operation and dynamics than the traditional measurement of pressure drop. These insights have proved to be extraordinarily useful in the development of ceramic woven fabric filters for high temperature and pressure application.

# Session 3: ECONOMICS

John S. Lagarias, Chairman
Raymond-Kaiser Engineers
Oakland, CA

# ECONOMICS OF ELECTROSTATIC PRECIPITATORS AND FABRIC FILTERS

by: Victor H. Belba and Fay A. Horney
Stearns Catalytic Corporation
P.O. Box 5888
Denver, Colorado 80217

Robert C. Carr and Walter Piulle
Electric Power Research Institute
3412 Hillview Avenue
P.O. Box 10412
Palo Alto, California 94303

## ABSTRACT

This paper presents the relative economics of fabric filter (FF) and precipitator (ESP) systems for utility boilers firing fuel from five (5) major coal fields and meeting a range of particulate emission limitations. For example, to meet the current NSPS of 0.03 lb/MMBtu, ESPs and FFs were found to be economically equivalent for the more precipitable ash from high to medium sulfur eastern coals and North Dakota lignites. The FF is the economic choice for the low sulfur western coals investigated in this paper.

This paper also examines the cost benefits of optimizing FF and ESP designs. For example, the levelized costs of a conventional reverse gas FF can be reduced by increasing the air-to-cloth ratio above the more conventional design of 2.0 ft/min. Other technologies investigated are shake/deflate and sonic horn cleaning of FFs and gas conditioned ESPs. The sensitivity of a particulate collection system's cost estimate to such factors as air-to-cloth ratios, bag life and power consumption is demonstrated.

## INTRODUCTION

In June 1978, the Electric Power Research Institute (EPRI), published a report comparing the economics of fabric filters (FFs) and electrostatic precipitators (ESPs) for collecting fly ash from pulverized coal fired utility boilers(1). That study essentially predicted that FFs would be the economic choice over ESPs for emission limitations of less than the then current New Source Performance Standard (NSPS) of 0.1 lb/MMBtu.

Since the 1978 report, changes in the NSPS, fluctuations in ESP and FF pricing and improvements in FF and ESP technology have prompted a renewed study of FF and ESP economics. Despite the fact that the current NSPS is 0.03 lb/MMBtu, ESPs have continued to be successfully and economically applied to achieve NSPS and below. Since 1978, wide fluctuations in FF and ESP pricing have been observed as vendors have struggled to remain competitive in a changing economy(2). Since the original study, FFs have been applied, in general quite successfully, on over 10,000 MW of capacity. Advancements in FF and ESP technology have increased the number of options to consider and economically evaluate when specifying a particulate control system.

This current study has been performed for EPRI under Contract RP 1129-9 and was undertaken to investigate these changes and to update the work originally performed in 1978. This paper summarizes and previews the major conclusions reached by this current study.

## PREMISES

The following five U.S. coals were selected to study the range of the impact of coal and ash properties on the relative economics of ESPs and FFs: Appalachian medium sulfur, Utah Wasatch Plateau, East Central Illinois No. 6, North Dakota Lignite, and Wyoming Powder River Basin. In addition to the case studies for each coal, general comparisons of FFs and ESPs were made irrespective of the impact of coal and ash properties. These general comparisons are referred to as the base case.

The costs developed for this study are based on a new, 500 MW (net) unit which is located in Kenosha, Wisconsin. Note that site location, coal, unit size and whether the installation is at a new plant or a retrofit impact costs. Therefore, care should be taken in generalizing the results presented here. Also, specific design and operating parameters and economic conditions assumed for the FF and ESP affect the capital and operating costs. The parameters assumed follow.

### PRECIPITATOR DESIGN

Consistent with current utility trends, a cold-side, rigid frame ESP was selected as the basis against which the FF options were evaluated.

ESPs were sized using a precipitator performance model developed by Stearns Catalytic(3). Once the minimum size was determined using the model, a conservative design contingency of one additional field was added to allow for deterioration of performance between maintenance outages and to allow for off-design coal quality and system operation. The ranges of specific collection area (SCA) determined for each coal considered in this study are presented in Figure 1. Several ESP vendors were consulted to corroborate the sizing performed for this study. The sizing for each ash considered in this study falls within the ranges suggested by the vendors.

Table 1 indicates the conservative design parameters assumed in developing the ESP costs. Note that these are nominal and/or maximum values, and the actual parameters developed for ESPs sized for the five study coals vary according to coal-specific conditions. The following auxiliary equipment was included in the cost estimate for each ESP: support insulator heaters and heated purge-air system, ash fluidizing system, hopper level indicators and heaters, and insulation and lagging.

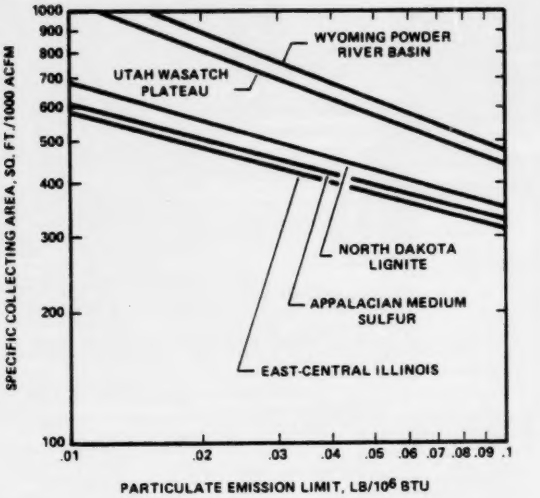

FIGURE 1. SPECIFIC COLLECTING AREA REQUIREMENTS OF ESP'S FOR FIVE CASE STUDY COALS

TABLE 1. ESP DESIGN PARAMETERS

| Design Parameter | Value |
|---|---|
| Maximum Face Velocity | 4.5 ft/sec |
| Maximum Plate Height | 42.65 ft |
| Minimum Aspect Ratio | 1.0 |
| Nominal Ft$^2$/T-R Set | 25,000 ft$^2$/T-R |

## FABRIC FILTER DESIGN

A conventional, reverse gas cleaned fabric filter with a gross air-to-cloth (A/C) ratio of 2.0 ft/min was considered to be the base case with which all economic comparisons were made. The conservative design parameters assumed in developing the FF costs are indicated in Table 2. These parameters represent nominal and/or maximum values and actual designs for each of the five case study coals vary slightly according to coal-specific conditions.

TABLE 2. FABRIC FILTER DESIGN PARAMETERS

| Design Parameter | Value |
|---|---|
| Bags per Compartment, Nominal | 360 |
| Bag Diameter, Nominal | 12 in |
| Maximum Bag Length | 32 ft |
| Rings per Bag | 7 |
| Bag Spacing (Center-Line to Center-Line) | 14 in |
| Reverse Gas A/C | 1.5 |
| Fabric | 10 oz/yd$^2$ fiberglass, 10% teflon finish |

The following auxiliary equipment was included in the cost estimate for each FF: ash fluidizing system, hopper heaters and level indicators, and insulation and lagging.

## ECONOMIC PREMISES

For most comparisons in this study, capital costs and levelized costs are presented. The levelized costs (mils/kwh) include escalation and interest during construction of the capital cost and escalated operating and maintenance costs.

The economic criteria for this study are based on EPRI's Economic Premises(4). The major premises are presented in Table 3.

TABLE 3. MAJOR ECONOMIC PREMISES

| Criterion | Value |
|---|---|
| Book Life | 30 years |
| Base Year | December 1982 $ |
| Labor Inflation Rate | 8.5 percent/year |
| Design Capacity Factor | 65 percent |
| Discount Rate | 12.5 percent/year |
| Operating Labor | $18.30/man-hour |

### Total Capital Required

The capital costs analyzed for this study represent the total cost for particulate control and include: the complete FF or ESP, including support steel and foundations; pressurized fly ash handling system complete through the ash silo; the additional cost of larger ID fans required to overcome the pressure drop across the FF or ESP; and, the additional ductwork required by the FF or ESP installation. These costs are based on vendor quotes obtained specifically for this study and from historical cost data in Stearns Catalytic's files. Also included are sales tax and direct and indirect construction costs.

The total capital required includes the cost for general facilities, and engineering and home office fees (one to three percent of the capital cost). A contingency, ranging from 0-25 percent, was added to the FF and ESP cost to account for uncertainty in maintaining compliance at the lower emission limit of 0.01 lb/MMBtu and/or the risk in applying the collector to a specific coal for which there was no previous experience.

The total capital requirement also includes a de-escalated allowance for funds used during construction (AFDC), and preproduction costs (start-up costs).

### Operation and Maintenance Costs

Fixed operation and maintenance costs for the particulate collection system include operating and maintenance labor, maintenance materials, filter bags and administrative and support labor. Variable costs are dependent upon the unit's capacity factor and include consumables such as power, chemicals, and ash disposal. These costs are based on estimates provided in EPRI's economic premises and on current FF and ESP field experience(5).

One of the major components of power cost for the FF or ESP is pressure drop across the collector. FF tubesheet (across the cloth) pressure drops for various cleaning methods and A/C ratios investigated in this study were assumed, based on data from pilot plants and field installations compiled by EPRI(6). The total flange-to-flange pressure drop includes an additional 2.0 in W.G. to account for losses through the inlet and outlet plenums. A 3.0 in. W.G., flange-to-flange pressure drop was assumed for the ESP, gas flow distribution devices and inlet and outlet nozzles.

In addition to these costs the FF also requires periodic bag replacement, assumed to be every three years (based on current bag life guarantees), and an unscheduled replacement of damaged bags (bag failure rate assumed to be 1% per year).

## CASE STUDIES

The five U.S. coals were selected to study the range of the impact of coal and ash properties on the relative economics of ESPs and FFs. A specific coal and ash mineral analysis was selected to represent each coal field; however, there are coals available in each of the five fields which would provide comparisons of ESPs and FFs that can be quite different than presented in this paper.

Figure 2 presents the total capital required ($/kW) for a conventional reverse gas FF and an ESP versus the particulate emission limit for each of the five case study coals. The levelized costs (mils/kWh) are presented in Figure 3.

Both figures suggest that the ESP and FF (A/C ratio of 2.0 ft/min) are competitive economically at NSPS (0.03 lb/MMBtu) for the more precipitable ashes, such as from high and medium sulfur eastern coals and typical North Dakota lignites. The FF is the economical choice for the difficult-to-precipitate ash from the low sulfur western coals (Powder River Basin and Wasatch Plateau) considered in this study. Although a higher A/C ratio (2.7 ft/min) shifts the economics slightly in favor of the FF, there still is no clear economic choice for the precipitable ashes at the NSPS. If emission levels lower than NSPS are required, the economic advantage shifts to the FF.

These plots of total capital requirement and levelized cost versus the particulate emission limit are not linear relationships below 0.03 lb/MMBtu. This is due to the contingency added to the capital cost of each collector at the lower emission limits.

## NOVEL DESIGNS

The Powder River Basin case study coal was assumed to compare novel FF and ESP designs. FFs with shake-and-deflate (S/D) cleaning, sonic horn assisted cleaning and a gas conditioned ESP were considered.

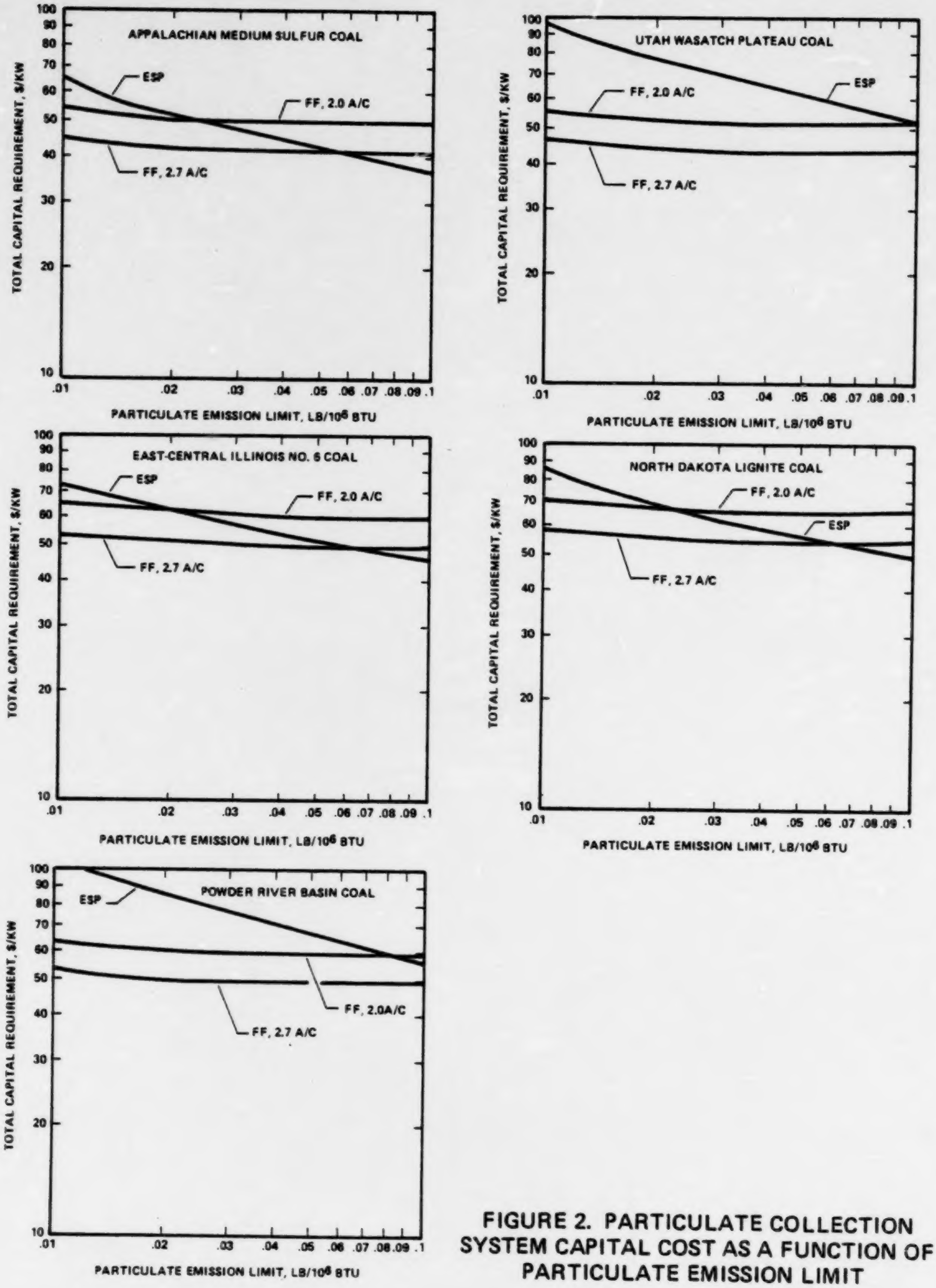

FIGURE 2. PARTICULATE COLLECTION SYSTEM CAPITAL COST AS A FUNCTION OF PARTICULATE EMISSION LIMIT

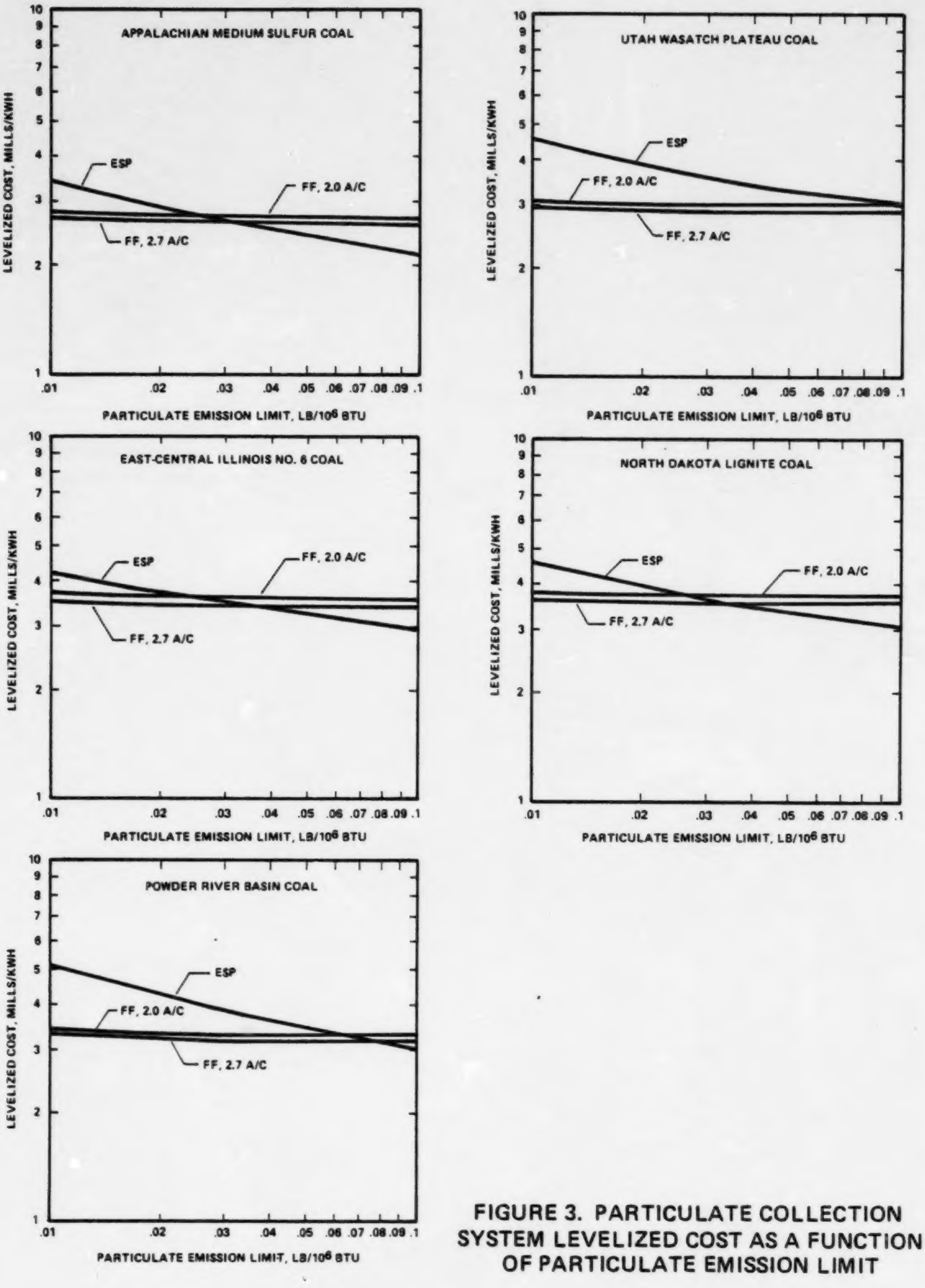

FIGURE 3. PARTICULATE COLLECTION SYSTEM LEVELIZED COST AS A FUNCTION OF PARTICULATE EMISSION LIMIT

## Shake-and-Deflate Cleaning

S/D cleaning allows a higher design A/C ratio compared to conventional reverse gas cleaning. Consequently considerable capital can be saved. Also, the use of S/D cleaning can result in lower average pressure drops. Full-scale and pilot FF data compiled by EPRI(6) suggests that, for a S/D FF at an A/C ratio of 2.7 ft/min the tube sheet pressure drop can be reduced to 3.8 in. from the 5.5 in. W.G. assumed in this study for a conventional reverse gas FF operating at an A/C ratio of 2.0.

The cost advantage of S/D cleaning is shown in Figure 4. A 15 percent levelized cost savings can be realized by using S/D cleaning at an A/C ratio of 3.0 rather than a conventional reverse gas FF with an A/C ratio of 2.0 ft/min.

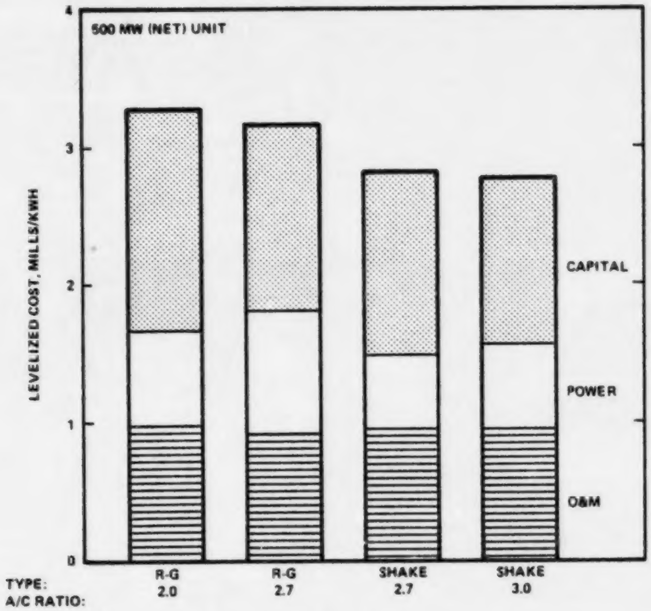

FIGURE 4. LEVELIZED FF COST - REVERSE GAS AND SHAKE-AND-DEFLATE CLEANING

A 3-year bag life was assumed for both reverse gas and S/D cleaning. There is insufficient data currently available to quantify bag life versus cleaning type; however, a reduced bag life of 2 years for the S/D option would increase the levelized cost by only 3 or 4 percent.

## Sonic Horn Cleaning

Pilot tests and field experience indicate that the use of sonic horn assisted cleaning can reduce the tubesheet pressure drop to 3 in. W.G. from the 5.5 in. W.G. assumed for the conventional reverse gas FF (A/C ratio of

2.0 ft/min) in this study (6) (7). Another advantage of sonic horn assisted cleaning is the ability to design to a higher A/C ratio, and thus trade off capital savings for increased power consumption at a higher pressure drop.

Figure 5 compares the levelized cost of FFs with and without sonic horn assistance. The results show a 10 percent cost decrease by using sonic horns for a FF with an A/C ratio of 2.7 rather than conventional reverse gas cleaning at an A/C ratio of 2.0 ft/min.

However, it is difficult to predict how effective sonic horns will be at reducing pressure drop. The effects of ash cake properties, sound power levels and frequencies, horn locations and quantity and the long term consequences of horn use have yet to be quantified (8).

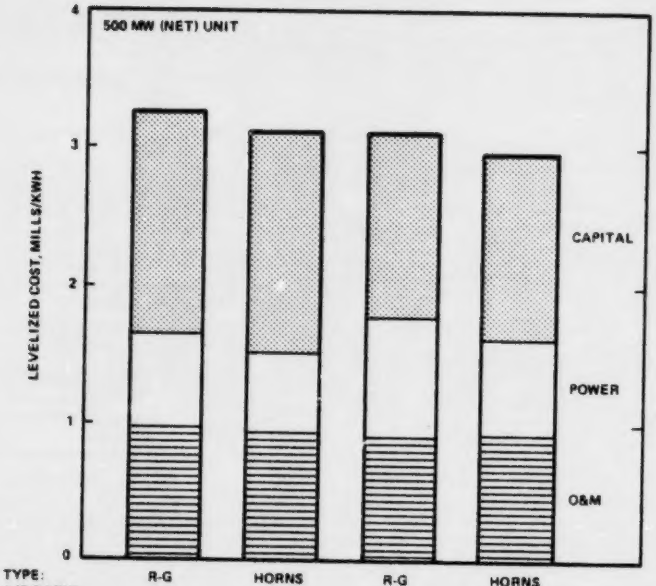

FIGURE 5. LEVELIZED FF COST - SONIC HORN CLEANING

## Gas Conditioned ESP

For the Powder River Basin coal considered in this study, sulfur trioxide gas conditioning reduced the required SCA sufficiently (by 240 $ft^2$/1000 ACFM) to make an ESP competitive with a conventional reverse gas FF at NSPS. The effects on capital and levelized costs of gas conditioning for the Powder River Basin coal are plotted in Figure 6. The figure indicates a 15 percent capital cost savings and a 10 percent levelized cost savings over a non-conditioned ESP sized to meet 0.03 lb/MMBtu.

However, it is difficult to predict how effective gas conditioning will be at reducing the required SCA. The ESP sizing for this study was based on data from an existing gas conditioned ESP collecting ash from a Powder River Basin coal which is very similar to the case study coal. Sizing a gas conditioned ESP would require a test burn of the proposed coal on a full-size ESP or extrapolating pilot test data from a unit burning the same coal.

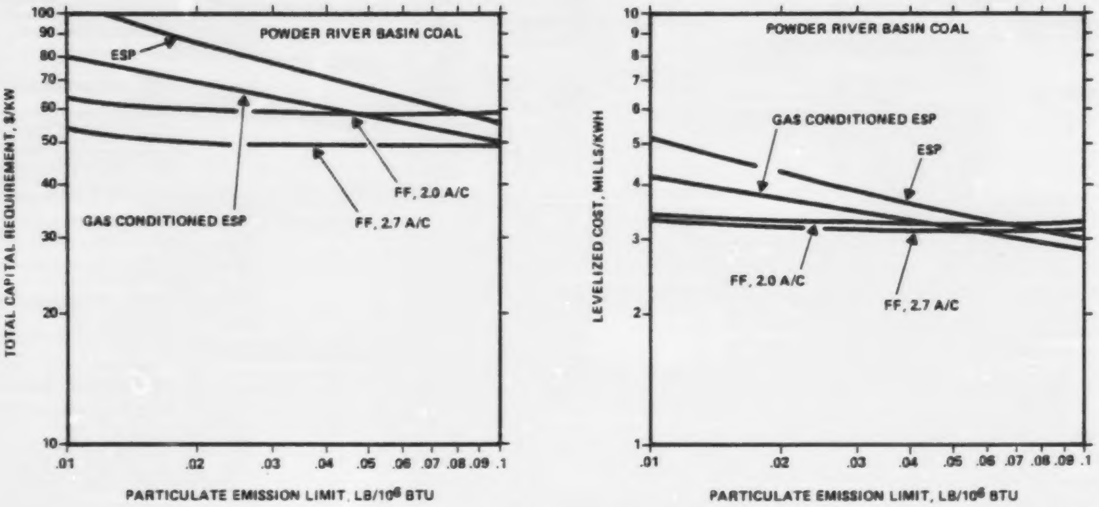

FIGURE 6. THE ECONOMICS OF GAS CONDITIONING FOR AN ESP

## BASE CASE

The base case comparisons of FF and ESP economics assumed typical flue gas conditions for a 500 MW unit (1.9 million ACFM). These comparisons were made irrespective of the impact of coal and ash properties on design and operating parameters, and were performed to provide general comparisons of FF and ESP economics and to optimize A/C ratio.

### GENERAL COMPARISONS AND OPTIMUM A/C RATIO

The capital and levelized costs for FFs and ESPs versus ESP size are shown in Figure 7. Figure 7 suggests that the capital and levelized costs of a conventional FF (A/C ratio of 2.0 ft/min) are approximately equal to an ESP with an SCA of about 450 $ft^2$/1000 ACFM. Therefore, Figure 7 suggests that a FF is the most economical option when design ESP sizes are above the breakdown point of 450 SCA.

Care should be taken in generalizing these conclusions to units of different sizes or even to different times. The FF and ESP marketplace is a very competitive and volatile one. Wide variations in FF and ESP pricing have been observed over the years, and in 1981, Reference 2 suggested a breakeven range of 600 SCA and higher. It is apparent that the relative economics of FFs and ESPs can shift considerably. The selection of one over the other is, therefore, not as predictable as suggested by the analysis presented here.

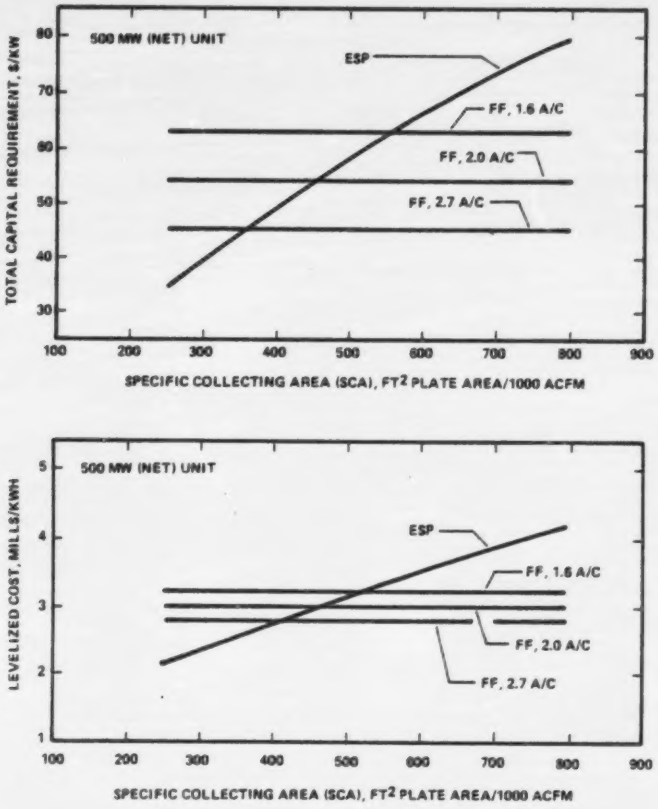

FIGURE 7. COMPARATIVE ECONOMICS OF FFs AND ESP (DEC., 1982 DOLLARS)

One of the goals in performing this study was to investigate and perhaps more accurately pinpoint the breakeven range. However, it was determined that a general economic analysis, such as this one, is no substitute for evaluating FF and ESP control options on a case-by-case basis. Anyone considering the purchase of a particulate control system should obtain bids for both ESPs and FFs.

Figure 7 also compares the economics of ESPs to FFs with A/C ratios of 1.6 and 2.7 in addition to the base of 2.0 ft/min. Increasing the A/C ratio to 2.7 ft/min decreases the ESP and FF breakeven point to about 425 SCA.

These changes in the relative economics of FFs and ESPs are due to the fact that an increase in A/C ratio results in a smaller FF size and, thus, reduced capital cost. The A/C ratio can be increased with miminal impact on the FF's collection efficiency. However, an increase in A/C ratio will result in increased pressure drop across the fabric, and thus, higher power consumption costs. The requirement for a larger ID fan will add slightly to the capital cost.

Figure 8 demonstrates these tradeoffs between FF capital and O&M costs. The minimum point of inflection in the total cost curve suggests that the "optimum" A/C ratio for a reverse gas FF is around 2.7 ft/min. A shorter plant life than the 30 years assumed here, e.g. a retrofit, could imply a different tradeoff between capital and O & M costs, and hence a different "optimum" A/C ratio.

Many assumptions were made in estimating this "optimum" A/C ratio of 2.7 ft/min. We would not recommend that a utility design reverse gas FFs to A/C ratios as high as 2.7 until such parameters as pressure drop can be predicted with greater certainty.

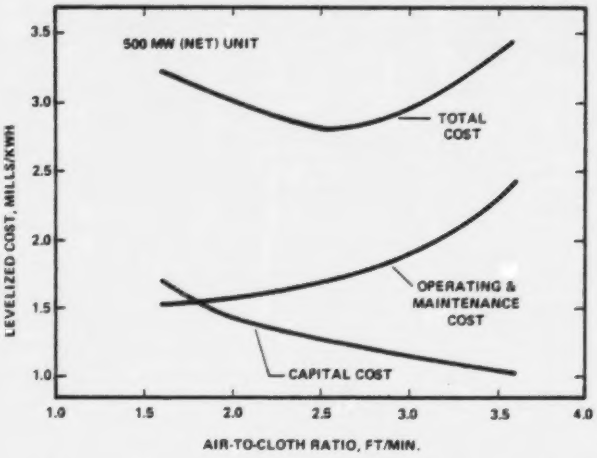

FIGURE 8. LEVELIZED FF COST AS A FUNCTION OF AIR-TO-CLOTH RATIO

## EFFECT OF BAG LIFE ON FABRIC FILTER COSTS

The 3-year bag replacement is the most costly maintenance item for the FF. Nevertheless, only a 3 percent levelized cost reduction results in assuming a three-year as opposed to a two-year bag life. The additional reduction by assuming a four- or five-year bag life is even smaller.

## SENSITIVITY OF FF COST TO PRESSURE DROP

It is difficult to predict with certainty the pressure drop at which a FF will operate. Therefore, a sensitivity analysis was performed to demonstrate the impact of pressure drop on the FF's levelized costs. Figure 9 presents these results for FFs with an A/C ratio of 2.0 ft/min. If a FF were to operate at a flange-to-flange pressure drop of 10 in. W.G. rather than the 7.5 in. assumed for the base case, a 6 percent increase in the levelized cost would result. Also, the ESP would be the economic choice for SCAs up to 550 ft$^2$/1,000 ACFM.

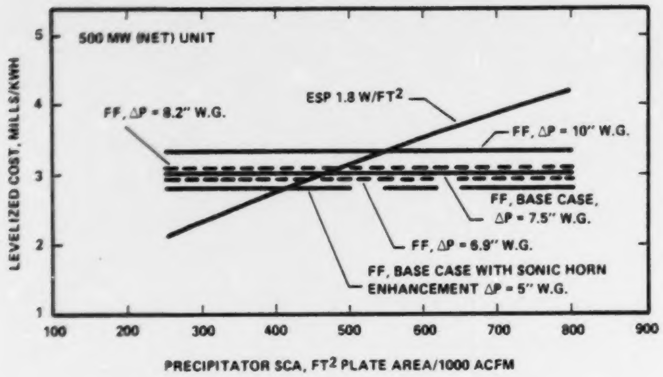

FIGURE 9. FF LEVELIZED COST SENSITIVITY TO PRESSURE DROP

If sonic horn assistance provided a flange-to-flange pressure drop reduction from the 7.5 in assumed for the base case to 5.0 in. a 6 percent levelized cost savings would result. The ESP would be an economic option only at SCAs of 400 $ft^2$/1,000 ACFM or less.

The flange-to-flange pressure drops assumed in this study are summarized in Table 4.

TABLE 4. FF PRESSURE DROPS

| | Flange-To-Flange Pressure Drop (in. W.G.)* | | | |
|---|---|---|---|---|
| FF Type | 1.6 A/C | 2.0 A/C | 2.7 A/C | 3.0 A/C |
| Reverse Gas | 6.3 | 7.5 | 9.8 | - |
| Sonic Horns | | | | |
| - Conservative | - | 6.0 | 7.5 | - |
| - Minimum | - | 5.0 | 6.8 | - |
| Shake-and-Deflate | - | - | 5.8 | 6.6 |

* Includes tube sheet and fabric pressure drop plus 2.0 inches due to inlet and outlet plenums and duct work.

## SENSITIVITY OF ESP COST TO T-R SET POWER CONSUMPTION

T-R set power consumption is by far the largest single O&M cost expenditure for the ESP. Unfortunately, it is very difficult to predict with certainty the amount of power required to energize an ESP. Therefore, a sensitivity analysis was performed to demonstrate the impact of T-R set power consumption on the precipitator's levelized costs.

Figure 10 demonstrates the impact of errors in predicting T-R set power on the ESP's levelized cost relative to a conventional reverse gas FF. The power density of 1.8 $W/ft^2$ is representative of a fairly precipitable ash and was selected for all of the base case analyses performed in this study. This power density is compared to densities of 2.7 and 0.9 W $ft^2$. It is felt that the power densities selected for this study are conservative. If the actual operating power densities do vary, they are likely to be lower than predicted, and by as much as 50%.

Figure 10 suggests that if the operating power density is at 0.9 rather than the predicted 1.8 $W/ft^2$, the economic breakeven point for the FF is increased from an SCA of about 460 to about 540 $ft^2$/1,000 ACFM. Halving the power estimate results in a reduction of levelized cost by about 10 percent for ESPs in this size range.

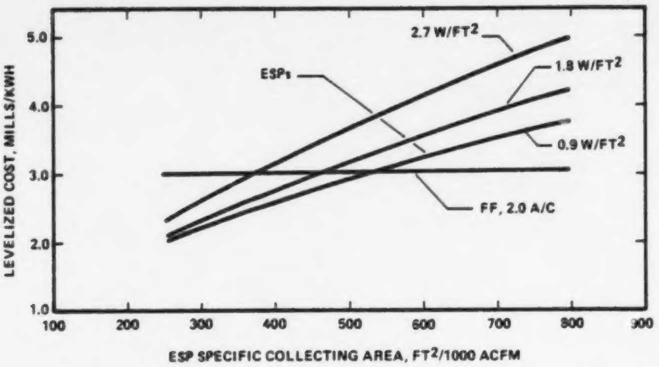

FIGURE 10. ESP COST SENSITIVITY TO T-R SET AC POWER

## Estimating T-R Set Power Consumption

The T-R set power consumption was assumed to vary according to the ESP outlet ash loading. The power was estimated for each case based on a curve of "Outlet Residual Loading versus Useful Specific Corona Power," as presented in Figure 11(9). This curve was adapted from work originally published by Dr. H.J. White(10).

Once the "useful" corona (DC) power for a precipitator has been estimated, the value must be adjusted to account for non-useful power which is consumed, and to account for other losses in the AC to DC conversion.

The primary non-useful power inputs to a precipitator are consumed in sparking and arcing within the ESP, and in back corona. Actual corona power for this study was assumed to equal two times the useful corona power values based on Figure 11. This multiplier of 2 was based upon comparing the useful corona power curves of Figure 11 with "actual" corona power values determined from the literature(8) and from data in Stearns Catalytic's files.

It is not a trivial matter to get from DC power estimates to actual AC power consumption. Little work has been done and published with respect to correlating AC power consumption to DC readings taken from T-R set control cabinets. Measuring power consumed, even ahead of the ESP substation transformers, is difficult with electro-mechanical watt-hour meters due to the non-sinusoidal waveforms generated by the T-R set controls and transformer.

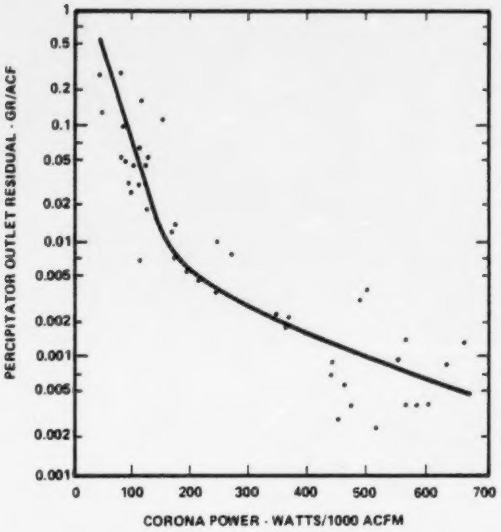

FIGURE 11. PRECIPITATOR OUTLET FLY ASH CONCENTRATION VERSUS SPECIFIC CORONA POWER

We conservatively estimated AC power consumption of the ESPs by multiplying actual corona power (DC) values by 2 to account for the power consumed and/or lost in energizing the ESPs. This number was based on field experience.

The losses in the AC to DC conversion involve the T-R set, control package, linear reactor, and T-R set form factor. T-R set form factor is the ratio of the effective peak voltage output to the average voltage output of the T-R set. The form factor has been said to be a measure of quality control in manufacturing the T-R set. Some of the other three losses listed above may also be accounted for by the form factor.

The following formula has been suggested to determine actual AC power from T-R set readings:

Actual AC Power = (DC Power) x (Form Factor) x (Power Factor)

Discussions with some vendors have revealed that the lowest form factor practically available for T-R sets is about 1.4. The form factor can range up to 3 or higher. This possible variation in form factor of over 2 times implies considerable uncertainty in predicting actual AC power consumption. Power factor has been measured to range from 0.45 to 0.9 for ESPs. This range in power factor of 2 times and the uncertainties in measuring power factors for non-sinusoidal wave forms also adds to the uncertainty in predicting actual AC power consumption.

Figure 12 is a plot of collection efficiency versus specific corona power. This figure demonstrates the uncertainty in predicting T-R set power consumption. The shaded portion on Figure 12 encloses the area bounded by the range of data points which represent "actual" corona power values. The data points not enclosed within the shaded area are "useful" corona power values.

Figure 12, for example, suggests that a collection efficiency of 99.9 percent could require an actual corona power of from 350 to over 1500 watts/1000 ACFM (off the scale). For the base case, 500 MW unit, these corona power requirements convert to AC power ranging from 2.6 to 11.4 MW. For the higher power levels above 600 watts/ACFM the shaded band becomes nearly horizontal. This implies that for very small changes in collection efficiency, very large changes in corona power would be required.

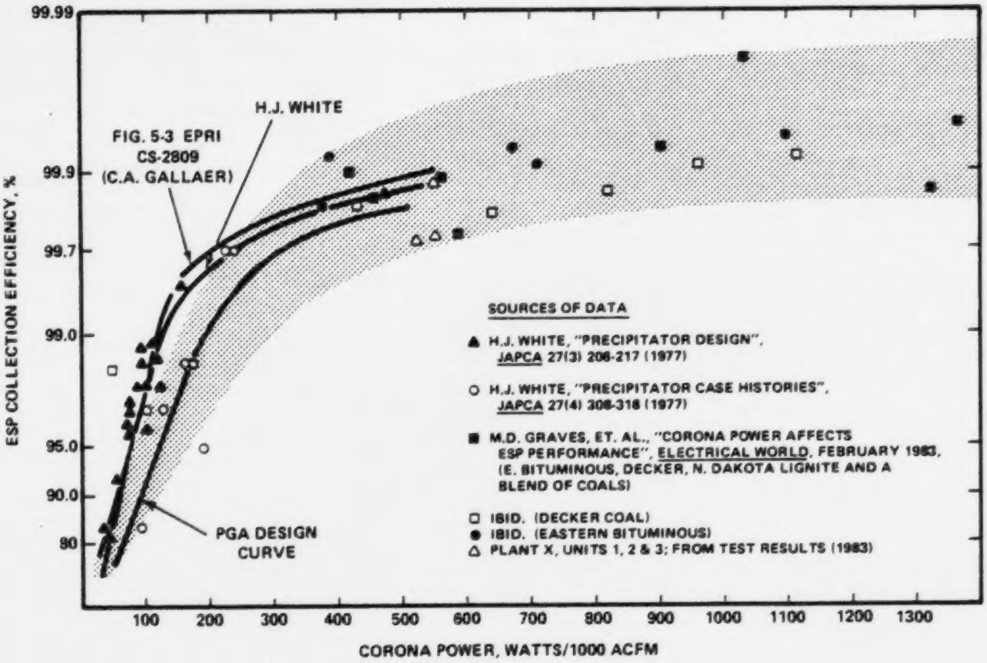

FIGURE 12. RANGE OF ESP COLLECTION EFFICIENCIES VERSUS SPECIFIC CORONA POWER

An independent contractor was consulted to estimate T-R set power consumption figures, so as to check the values used in this study. Table 5 is a comparison of SCA and AC power consumption as determined by Stearns Catalytic (SC) and the independent contractor, Peter Gelfand Associates (PGA). The table shows relatively good agreement between SC's and PGA's SCA requirements. Good agreement also exists between the differing power consumption figures on three of the five case study coals.

TABLE 5. DESIGN COMPARISON

| | SCA* | | AC POWER* | | | |
|---|---|---|---|---|---|---|
| | $Ft^2$/100 ACFM | | Watts**/1000 ACFM | | Watts**/$ft^2$ | |
| Coal | PGA | SC | PGA | SC | PGA | SC |
| App. Med% S | 444 | 452 | 517 | 851 | 1.17 | 1.88 |
| Utah Wasatch | 650 | 702 | 750 | 856 | 1.07 | 1.22 |
| E. Central Illinois | 409 | 434 | 833 | 850 | 2.03 | 1.96 |
| ND Lignite | 436 | 496 | 833 | 853 | 1.91 | 1.72 |
| PRB | 707 | 753 | 825 | 858 | 1.17 | 1.14 |

*@ 0.03 lb/MMBtu
**Reported by Peter Gelfand Associates as KVA.

The largest variations between SC's and PGA's power consumption estimates show up for the Appalachian and the Wasatch coals. It was determined that the variations of 39% and 12%, respectively, were due to the different methodologies used by SC and PGA. SC based its estimates on a curve of outlet loading (grains/acf) versus useful specific corona power; whereas, PGA based its estimates on a curve of collection efficiency versus specific corona power (see Figure 12) and checked the results by comparison with values from a data base of performance data for similar coals.

It is felt that the maximum variation between SC's and PGA's results of 39% is reasonable for the degree of accuracy currently achievable in estimating T-R set power consumption. Also, note that P. Gelfand Associates reported their values as KVA. Considering the uncertainties involved, we feel that these values are a reasonable representation of the power generated and paid for by the utility in energizing an ESP.

## NOTICE

The work described in this paper was not funded by the U.S. Environmental Protection Agency and therefore the contents do not necessarily reflect the views of the Agency and no official endorsement should be inferred.

## REFERENCES

1. Campbell K.S., et.al., Economic Evaluation of Fabric Filtration Versus Electrostatic Precipitation for Ultrahigh Particulate Collection Efficiency. Stearns-Roger, Inc., EPRI FP-775. June 1978.

2. V.H. Belba, F.A. Horney, "The Future of Electrostatic Precipitation for the Collection of Fly-Ash from Pulverized Coal-Fired Steam Generators," Coal Technology 1981, Volume 3, (Proceedings of the Fourth International Coal Utilization Exhibition and Conference, Houston, Texas; November 1981).

3. F.A. Horney, V.H. Belba, "An Empirical Model of Cold-Side Precipitator Performance Based Upon Coal and Ash Chemistry." IEEE Transactions on Industry Applications. October 1982.

4. 1983 EPRI Economic Premises for Electric Power Generating Plants; Complete Plant Utility Financing. Issue Date: December 15, 1982.

5. ESP, Fabric Filter, and Fly Ash Removal System Reliability. Draft Report, EPRI, RP 1401-1.

6. Carr, R.C. Performance Evaluation of Reverse Gas Baghouses on Coal-Fired Utility Boilers. Second Conference on Fabric Filter Technology for Coal-Fired Power Plants, Denver, CO. March 22-24, 1983.

7. Cushing, K.M., et.al., "A Study of Sonic Cleaning for Enhanced Baghouse Performance," Proceedings: Second Conference on Fabric Filter Technology for Coal-Fired Power Plant, EPRI CS-3257, November 1983.

8. Carr, R.C. and Smith W.B., "Fabric Filter Technology for Utility Coal-Fired Power Plants, Part V: Development and Evaluation of Bag Cleaning Methods in Utility Baghouses, Journal of the Air Pollution Control Association, Volume 34, No. 5, May 1984.

9. Gallaer, C.A. "Electrostatic Precipitator Reference Manual" EPRI CS-2809, January 1983.

10. White, H.J. Electrostatic Precipitation of Fly Ash, APCA Reprint Series, Air Pollution Control Association, Pittsburgh, PA, 1977.

# ESTIMATING THE BENEFITS OF SO3 GAS CONDITIONING ON THE PERFORMANCE OF UTILITY PRECIPITATORS WHEN BURNING U.S. COALS

by: Peter Gelfand P.E.
P. Gelfand Associates
Trumbull, Connecticut 06611

## ABSTRACT

SO3 gas conditioning is frequently considered as a means of upgrading the performance of existing esps and for some new installations to reduce overall equipment size and cost. This paper considers the potential benefits SO3 may have on existing utility esps burning coals from the major coal producing regions of the U.S.

Criteria are developed for identifying SO3 candidate installations, and using the matts-ohnfeldt precipitation model, relevant exponents, migration velocities and enhancement factors attainable with SO3 conditioning are estimated. The results are then compared to existing installations.

## DISCUSSION

### SO3 GAS CONDITIONING

Briefly, Gas Conditioning is the process by which small quantities of SO3 gas are added to the main gas stream to improve the collection of high resistivity ashes (10-11 to 10-14 ohm-cm). This avoids the detrimental effects of high resistivity dusts by eliminating premature electrical breakdown of the dust layer or the formation of back corona, either of which can significantly reduce precipitator performance. The SO3 acts on the collected dust by reducing the surface resistivity of individual ash particles to levels where the precipitation process can easily be maintained. Normally, the resistivity of the ash must be reduced to within the range of 10-8 to 10-10 ohm-cm. Lower values are not desirable because they may produce poorer overall performance due to increased dust reentrainment losses.

Chemically, the influence of SO3 is to reduce the surface resistivity of the ash by combining to form sulfates. This reaction is very sensitive to the temperature and moisture content of the gas, as well as the PH of the ash. The amount of SO3 needed will vary as a function of the ash chemistry, the gas conditions, and the specific surface area of the ash to be treated. It is important to note that if the gas temperature is low and the moisture content of gas is high, achieving the concentrations of SO3 necessary to condition may be prohibited by the acid dew point temperature of the gas.

The concentrations of SO3 injected into the gas stream up-stream of the precipitator normally exceed the amount necessary to condition the ash layer. This is due to losses and practical gas distribution problems encountered in the injection process. Typical values of SO3 system designs are in the range of 20-50 ppm v/v injected.

For the most part ashes produced by the combustion of U.S. coal are amenable to conditioning with SO3, provided the gas temperature is less than 320 degrees F. At temperatures above 320 degrees, the effectiveness of SO3 reaction with the ash layer is greatly reduced. The SO3 tends to pass through the precipitator without acting on the ash, only later to appear as troublesome sulfuric acid droplets as the temperature cools. Occasionally, some ashes that are acidic may not be responsive to SO3 conditioning. It is always beneficial to review the ash mineral analysis of any candidate ash proposed to predict the electrical resistivity with and without SO3 at the specific operating conditions. In some cases a laboratory test of the ash's electrical properties in the presence of SO3 may also be warranted.

Full advantage of gas conditioning may not be gained without having power equipment large enough to apply the additional energy levels the reduced ash resistivity now permits (>40 ma/1000 ft2 of collecting surface).

## CRITERIA

Identifying installations that are suitable for SO3 gas conditioning. Criteria for these installations:

BOILER - all types and designs

GAS TEMPERATURE - cold side installations <450 degrees F. Most effective SO3 temp <320 degrees F. Gas must be able to carry increased SO3 concentration.

ELECTROSTATIC PRECIPITATORS - all dry type designs: weighted wire, and rigid mast and frames.

## ESP MINIMUM SIZE - 125 SCA

Three factors determine the smallest precipitator (SCA) to be considered in this paper. Firstly, the precipitator candidate should be large enough to be sufficiently benefitted by SO3 conditioning so as to achieve a minimum emission level of .1 lbs/mmbtus, that is, collect at efficiencies greater than about 97%. Secondly, that the ESPs face velocity is below 6ft/sec., since at higher velocities the dust reentrainment losses can be so great as to suppress much of the benefit of SO3 injection. Thirdly, the majority of the existing ESPs have gas passage duct spacings of 9 -12 inches. These considerations result in a minimum SCA of 125 ft2/1000ft/min., with corresponding gas treatment lenghts of approximately 16.875 - 22.5 ft., depending on duct spacing.

## FUEL - ALL U.S. COALS

The benefits to be derived by SO3 gas conditioning will vary as a function of the specific application. From a fuel stand point those factors in the coal or ash that effect ash resistivity will be significant. For example, the quantity of sulfur content naturally found in coal will be important in determining the base line resistivity and therefore the unconditioned precipitator performance.

Because of the great variations in the properties of coal found in the U.S. and resultant differences in ash characteristics, precipitator performance and therefore size can range widely. In this paper, precipitators are grouped by the generic coal type burned corresponding to the eight major coal producing regions in the USA. This will narrow the differences in the performance and permit establishing an appropriate SO3 enhancement level for each coal. The coal types are:

A: APPALACHIAN LOW SULFUR
B: APPALACHIAN MEDIUM SULFUR
C: EAST CENTRAL ILLINOIS
D: UTAH WASATCH PLATEAU
E: WYOMING SUBBITUMINOUS
F: POWDER RIVER BASIN
G: NORTH DAKOTA LIGNITE
H: TEXAS LIGNITE

The analysis of typical fuels from each of these regions is shown in Table 1.

## PRECIPITATOR PERFORMANCE MODEL

We used the Matts-Ohnfeldt equation (1) to estimate ESP performance:

$$n=1-\exp-(a/v*w)k$$

## Table 1. Coal and Ash Analysis

ULTIMATE COAL ANALYSIS:

| | CARBON | HYDROGEN | OXYGEN | NITROGEN | SULFUR | WATER | ASH | BTU/LB |
|---|---|---|---|---|---|---|---|---|
| APPALACHIAN MED. SULFUR | 69.7 | 4.9 | 8.1 | 1.3 | 2.0 | 6.0 | 8.0 | 12,700 |
| APPALACHIAN LOW SULFUR | 65.0 | 4.6 | 6.4 | 1.2 | 0.8 | 8.0 | 14.0 | 12,700 |
| EAST CENTRAL ILLINOIS | 57.5 | 3.7 | 5.8 | 0.9 | 4.0 | 12.0 | 16.1 | 10,100 |
| UTAH WASATCH PLATEAU | 64.21 | 4.6 | 10.98 | 1.16 | 0.58 | 7.54 | 10.98 | 11,240 |
| WYOMING SUBBITUMINOUS | 58.32 | 3.9 | 12.9 | 0.8 | 0.56 | 11.8 | 11.72 | 10,090 |
| POWDER RIVER BASIN | 47.85 | 3.4 | 10.82 | 0.62 | 0.48 | 30.41 | 6.42 | 8,020 |
| NORTH DAKOTA LIGNITE | 39.71 | 2.7 | 11.4 | 0.6 | 0.68 | 37.11 | 7.8 | 6,580 |
| TEXAS LIGNITE | 39.50 | 2.7 | 9.91 | 0.8 | 1.08 | 31.00 | 15.0 | 6,720 |

ASH ANALYSIS:

| | $Li_2O$ | $Na_2O$ | $K_2O$ | MgO | CaO | $Fe_2O_3$ | $Al_2O_3$ | $SiO_2$ | $TiO_2$ | $P_2O_5$ | $SO_3$ |
|---|---|---|---|---|---|---|---|---|---|---|---|
| APPALACHIAN MED. SULFUR | .01 | 0.5 | 1.5 | 0.8 | 3.4 | 17.2 | 27.7 | 46.2 | 1.0 | 0.6 | 1.1 |
| APPALACHIAN LOW SULFUR | .04 | 0.19 | 2.7 | 0.85 | 0.56 | 4.1 | 32.2 | 56.4 | 2.3 | 0.15 | 0.18 |
| EAST CENTRAL ILLINOIS | .01 | 0.6 | 1.9 | 1.0 | 7.0 | 20.0 | 18.0 | 45.0 | 1.0 | 0.2 | 3.5 |
| UTAH WASATCH PLATEAU | .01 | 1.48 | 1.11 | 2.4 | 10.7 | 4.5 | 17.3 | 53.5 | 0.7 | 0.27 | 1.0 |
| WYOMING SUBBITUMINOUS | .01 | 0.32 | 1.31 | 2.4 | 12.0 | 6.4 | 17.3 | 52.6 | 0.7 | 0.4 | 1.0 |
| POWDER RIVER BASIN | .01 | 1.3 | 0.4 | 4.7 | 22.8 | 4.6 | 15.3 | 31.6 | 1.1 | 0.8 | 2.0 |
| NORTH DAKOTA LIGNITE | .01 | 6.3 | 0.6 | 7.1 | 25.0 | 13.4 | 10.8 | 31.5 | 0.2 | 0.1 | 4.6 |
| TEXAS LIGNITE | 0.0 | 0.75 | 1.25 | 1.4 | 2.8 | 8.8 | 22.8 | 57.1 | 1.1 | 0.08 | 3.23 |

where:
n= efficiency
a= collecting plate area
v= gas volume flow rate
w= dust migration velocity
k= exponent

In general,collection efficiency is determined by the electrical properties of the ash, gas conditions, particle size distribution, the quantity of gas to be cleaned, and the dimensions of the precipitator. The use of the Matts-Ohnfeldt model allows the isolation of these factors into the specific terms of the equation. The electrical properties of the ash, resistivity, and gas conditions are reflected in the value of the dust migration velocity, w, the relative size of collector by the ratio of collecting plate surface area to gas flow volume by a/v, and the effect of the particle size distribution of the dust by the value of the exponent k. The specific values of w and k to apply are determined by a combination of empirical methods (test data) and analytical procedures.

For this paper the values of w were determined using our proprietary model empirically developed from test data on gas conditioned preciptators. For example, Figure 1, plots the test data and the relationship between SCA and COLLECTION EFFICIENCY for SO3 gas conditioning on pulverized coal. The k value is 0.5 and w equals 50 cm./sec.

Since the particle size distribution at the inlet of the ESP varies as a function of the boiler design, the fuel and of course the presence of any up stream dust collector it is necessary to determine an exponent value k for each situation. These k-values are determined independently of the migration velocity and precipitator size from the measurements of the particle size distribution for each case by using a computer numerical integration procedure (2).

K-VALUES

| BOILER TYPE: | K |
|---|---|
| PULVERIZED (wall,face fired) | 0.50 |
| (cornered-fired) | 0.53 |
| CYCLONE | 0.68 |
| STOKER | 0.42 |

In the event that a mechanical dust collector preceded the precipitator, the particle size distribution may be finer than that emitted by the boiler:
MECHANICAL COLLECTORS --------------------------------K= 0.588

Some coals burn to produce a finer particle size distribution. This has been attributed to high moisture content and/or the presence of high levels of alkaline (3).

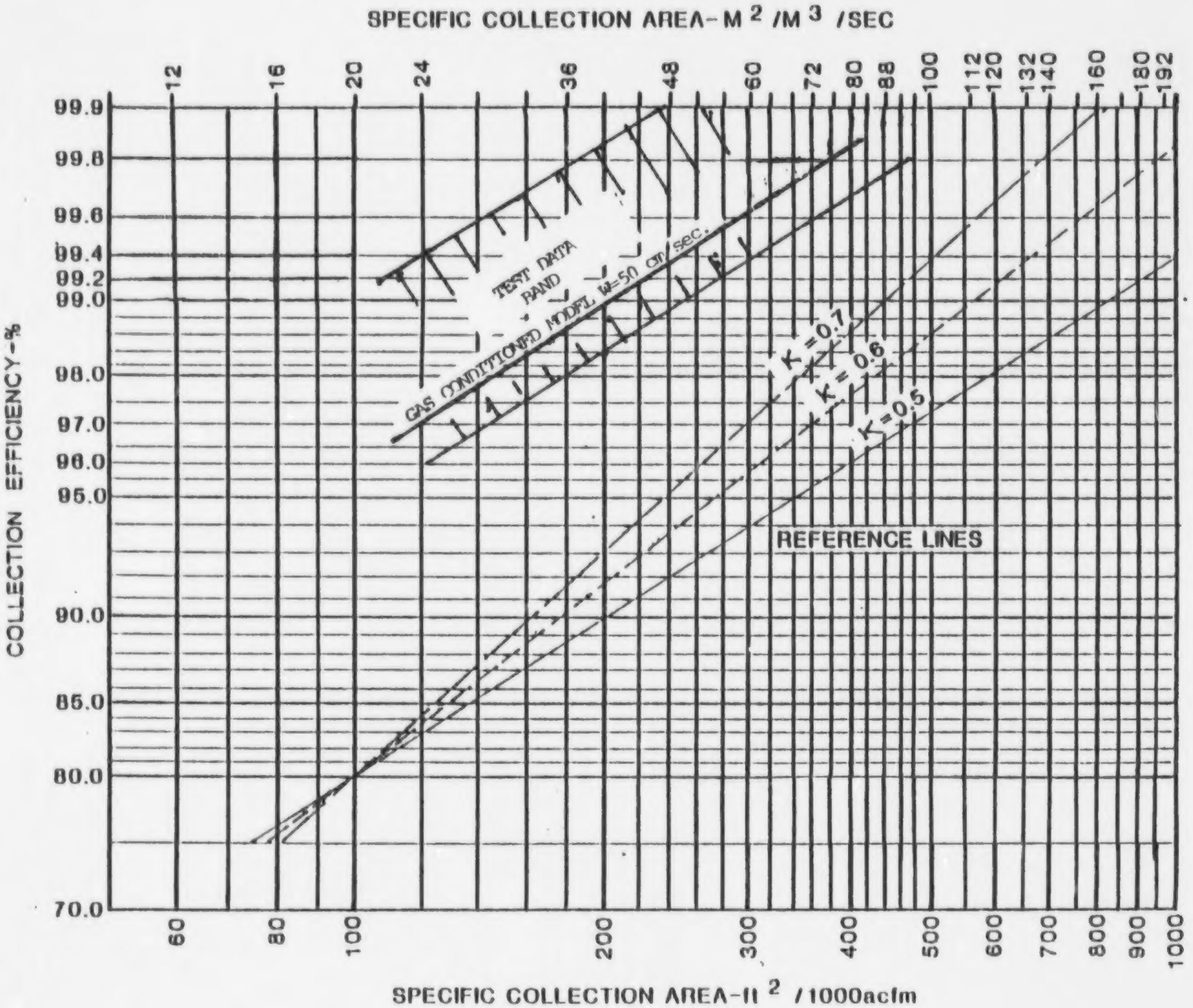

Figure 1. Pulverized Coal - $SO_3$ Test Data

### FUELS INFLUENCE

NORTH DAKOTA LIGNITE ----------------------------------K= 0.513
TEXAS LIGNITE ----------------------------------------K= 0.60
POWDER RIVER BASIN -----------------------------------K= 0.54
UTAH WASATCH PLATEAU ---------------------------------K= 0.54

We used the largest value for K (finest particle distribution) to determine SO3 enhancement since this is a conservative approach. This has been done in the following tables:

SO3 ENHANCED -W/K VALUES:

### PULVERIZED (WALL/FACE FIRED)

| COAL | W-VALUE (CM/SEC.) | K-VALUE |
|---|---|---|
| A: APPALACHIAN LOW SULFUR | 50.0 | .50 |
| B: APPALACHIAN MEDIUM SULFUR | 50.0 | .50 |
| C: EAST CENTRAL ILLINOIS | 50.0 | .50 |
| D: UTAH WASATCH PLATEAU | 27.28 | .54 |
| E: WYOMING SUBBITUMINOUS | 50.0 | .50 |
| F: POWDER RIVER BASIN | 27.28 | .54 |
| G: NORTH DAKOTA LIGNITE | 48.15 | .513 |
| H: TEXAS LIGNITE | 25.46 | .60 |

### PULVERIZED (CORNER FIRED)

| COAL | W-VALUE (CM/SEC.) | K-VALUE |
|---|---|---|
| A: APPALACHIAN LOW SULFUR | 32.43 | .53 |
| B: APPALACHIAN MEDIUM SULFUR | 32.43 | .53 |
| C: EAST CENTRAL ILLINOIS | 32.43 | .53 |
| D: UTAH WASATCH PLATEAU | 27.28 | .54 |
| E: WYOMING SUBBITUMINOUS | 32.43 | .53 |
| F: POWDER RIVER BASIN | 27.28 | .54 |
| G: NORTH DAKOTA LIGNITE | 32.43 | .53 |
| H: TEXAS LIGNITE | 25.46 | .60 |

### CYCLONE BOILER

ALL COALS -------------- W= 15.26 CM/SEC. -------------K= 0.68

### ESP FOLLOWS MECHANICAL COLLECTOR
### (e.g. STOKER WITH CARBON REINJECTION)

ALL COALS EXCEPT
TEXAS LIGNITE ----------- W= 28.20 CM/SEC. -------------K= 0.588

TEXAS LIGNITE ----------- W= 25.46 CM/SEC. -------------K= 0.600

### STOKER BOILER (GENERALIZED CASE)

ALL COALS --------------- W= 90.0 CM/SEC. --------------K= 0.42

With some specific coals the naturally occurring sulfur content and favorable minerals in the fly ash may make SO3 gas conditioning unwarranted.

This could be especially true for Dakota Lignites and some of the higher sulfur Appalachian Coals.

## ESTIMATE OF ENHANCEMENT MULTIPLYING VALUES WITH SO3 CONDITIONING

To aid in estimating the level of benefit SO3 conditioning produces for these coals and to help serve as a reference, we have developed specific precipitator size estimates based on a typical coal and mineral ash analysis for each region (see Table 1 analysis).

From the precipitator size a reference was determined for each case, then this value is divided into the w estimate with SO3 injection to calculate an enhancement multiplier. Since these enhancement multipliers are ratios they are independent of particle size distribution, therefore it is only necessary to show the pulverized (wall/face fired) case.

As we pointed out earlier, some specific coals have adequate sulfur and favorable ash minerals to make SO3 conditioning unwarranted. This was the case for the typical coal and ash analysis used to select the precipitator for the East Central Illinois coal. The enhancement multiplier was when stated as dependent on sulfur/ash analysis.

PULVERIZED (WALL/FACE FIRED)

| COAL | W-VALUE (CM/SEC.) SO3 | /REFERENCE | ENHANCEMENT MULTIPLIER |
|---|---|---|---|
| A:APPALACHIAN LOW SULFUR | 50.0 | /28.35 | 1.76 |
| B:APPALACHIAN MEDIUM SULFUR | 50.0 | /38.38 | 1.30 |
| C:EAST CENTRAL ILLINOIS | 50.0 | /57.13 | DEPENDS ON SULF/ASH |
| D:UTAH WASATCH PLATEAU | 27.28 | /22.92 | 1.19 |
| E:WYOMING SUBBITUMINOUS | 50.0 | /26.97 | 1.88 |
| F:POWDER RIVER BASIN | 27.28 | /19.77 | 1.38 |
| G:NORTH DAKOTA LIGNITE | 48.15 | /44.42 | 1.08 |
| H:TEXAS LIGNITE | 25.46 | /18.30 | 1.39 |

The performance migration velocity for a gas condition esp has been estimated for various coals and fuels and boiler designs. A user contemplating the use of a gas conditioner can match his existing esp to the criteria and estimate the magnitude of the migration velocity with SO3 conditioning and the performance he can reasonably expect.

EXAMPLES:

CASE 1 Medium Resistivity Eastern Fuel
Efficiency with SO3 = 98.15%
precipitator follows mechanical collector
SCA = 185, K = .588
calculated W = 28.9 cm/sec.
estimated W = 28.2 cm/sec.

CASE 2 High Resistivity Western Fuel
Efficiency with SO3 = 99.7%
SCA 320, K = .50

CASE 2 (CONT)
calculated $W = 53.6$ cm/sec.
estimated $W = 50.0$ cm/sec.

Often wide variations are reported for values of w and k. The SO3 estimated values for w and k selected here will normally fall conservatively below the actual values observed in the field. In the event that lower values are found, this could be symptomatic of some process or equipment problems.

## CONCLUSION

- * Criteria are developed to sort out the most likely candidates for SO3 conditioning.
- * Generalized enhancement factors are developed for the most common types of combustion and fuels.
- * The use of the estimated migration velocity and k values developed permits the benefits of the SO3 gas conditioning for a specific esp to be predicted.

The work described in this paper was not funded by the U.S. Environmental Protection Agency and therefore the contents do not necessarily reflect the views of the Agency and no official endoresment should be inferred.

## REFERENCES

(1) S. Matts and P. Ohnfeldt, "Efficient Gas Cleaning with S.F. Electrostatic Precipitators".

(2) P.L. Feldman, "Effects of Particle Size Distribution on the Performance of Electrostatic precipitators".

(3) Robert S. Dahlin, "Prediction of Mass Loading and Particle Size Distribution for use in a Precipitator Sizing Procedure".

# MICROCOMPUTER MODELS FOR PARTICULATE CONTROL

by: A. S. Viner and D. S. Ensor
Research Triangle Institute
P. O. Box 12194
Research Triangle Park, North Carolina 27709

L. E. Sparks
Industrial Environmental Research Laboratory
U. S. Environmental Protection Agency
Research Triangle Park, North Carolina 27711

## ABSTRACT

The phenomenal growth of the microcomputer industry has made it possible for almost anyone in industry to have a relatively fast and easy-to-use computer at their disposal. Unfortunately, the specialized software needs of the air pollution community have not been met. In an attempt to address this need, the Research Triangle Institute, under contract to the U. S. Environmental Protection Agency, has developed a set of programs especially for air pollution related problems. In this paper we will describe microcomputer models of electrostatic precipitator performance, an implementation of the GCA/EPA baghouse model, an in-stack opacity prediction program, and a plume opacity model. The theoretical models for each program are briefly described, followed by a description of their utility to the air pollution community. Plans for making the programs widely available are also discussed.

This paper has been reviewed in accordance with the U. S. Environmental Protection Agency's peer and administrative review policies and approved for presentation and publication.

## INTRODUCTION

Microcomputers are beginning to appear in the offices and laboratories of nearly every engineer and scientist. The tasks of data acquisition and analysis, data management, and word processing are now routine operations. One of the areas in which microcomputers have not been heavily employed is that of modeling, such tasks being relegated to minicomputers or mainframes. This is largely due to the limited memory capacity and speed of microprocessors; however, the strong points of microcomputers are their small size and manageability. These aspects can be (and are) well exploited in making easy-to-use programs. This same potential has been recognized in producing simplified models for air pollution control research.

The strength of desk-top computers is that they are so easy to use. There is no need to worry about passwords or IDs, computer accounts, modems and phone lines, or unexpected computer outages. A program can be run by simply turning on the power and inserting a diskette in a drive. It is this simplicity that drove us to develop sophisticated software for these small machines. It is recognized that the limitations of microcomputers make them inadequate for modeling complex physical situations. However, most models can be simplified so as to require less memory and to run faster. If the original model is a good one, then the simplified version will give a reasonable picture of the "big model" results. The reason for writing a simplified model is to provide a fast and easy means (via microcomputer) to test different designs and operating strategies before going on to running a more complex model. In this way, a microcomputer does not eliminate the need for a mainframe or minicomputer but serves to complement and make more efficient use of it. An hour spent using a simple model on a microcomputer can point the way for future, more detailed work on a large computer and save the researcher many hours (or days) of valuable time.

Under contract to the U.S. Environmental Protection Agency, the Research Triangle Institute has developed programs for modeling electrostatic precipitator performance under a variety of conditions, predicting stack opacity, and predicting the opacity of detached plumes. In addition, we have modified the GCA/EPA baghouse model to run on a microcomputer. In this paper we will briefly describe what each model program does, how the model works, and how we have used it in our research programs. Afterwards there will be a discussion of plans for making these programs generally available.

## CONTROL DEVICE MODELS

The control device models to be described here are for electrostatic precipitators (ESPs) and fabric filters (baghouses). Models (and programs) exist for other devices such as venturi scrubbers and spray dryers and are described in the literature.(1,2) The ESP model is employed in two separate programs which are complementary. The first program is called the ESP sectional model, and the second is the ESP dynamic model. These programs will be described below, along with the baghouse program.

### ESP SECTIONAL MODEL

This model calculates the steady-state emissions from each section of an ESP as well as the stack opacity. The program can estimate the effect of nonidealities in ESP operation and design such as gas sneakage, rapping reentrainment, electrical failures, and maldistribution of gas velocities. The program is designed to simulate three different modes of ESP operation. The first mode uses the Deutsch-Anderson collection process with losses due to sneakage and rapping included. Abnormal modes of operation include either section failures or velocity maldistribution. By comparing the normal operation with the abnormal operation cases, a user can gauge the effect of each problem in a fairly qualitative manner.

The program uses the Deutsch-Anderson model for calculating particle penetrations. The particle size distribution is characterized by the mass median diameter of the dust. The particle migration velocity in each section is based only on this particle size, thus saving a large amount of computational effort. This is a crude approximation; however, it greatly cuts down on the program run time. Also, the MMD is adjusted from one section to the next to account for the effects of particle collection. For the purposes of keeping the programming effort manageable, the ESP is assumed to be rapped continuously.

The effects of sneakage are simulated by specifying a fraction of the gas flow that passes through the hoppers or busbar region of the ESP, thus bypassing the particle collection region. Similarly, the rapping reentrainment is specified as a fraction of the dust mass on the plates that reenters the gas stream during rapping. Both of these fractions can be entered by the user, and the rapping reentrainment factor is allowed to vary from one section to the next.

The real value of this program lies in its ability to simulate the effects of section failures and velocity maldistribution in an ESP. (Section failures are generally due to failure of the electrical components in a section; e.g., broken wires.) The program user is allowed to enter a fraction corresponding to the amount of area that is removed from service (effectively reducing the SCA in a portion of the precipitator). The model then calculates the emissions based on the adjusted SCA. The collection efficiency of an ESP can also be affected in a subtle way by velocity maldistributions. When there is a range of velocities across an ESP, the localized SCA will vary according to the local velocity. Hence, particles will be subject to the different collection efficiencies based on the local velocity. For lack of experimental data, velocity is assumed to follow a normal distribution, the parameters of which can be specified by the program user.

The strength of this program is that it provides insight into the relative importance of various nonidealities of ESP design and operation. The section failure model allows a quick look at the relative significance of a section failure in guidance for more detailed modeling. The velocity maldistribution model allows the user to understand the relative importance of correcting gas flow problems and the relative improvement that might be expected. The weakness of the program is that it is not as accurate as a mainframe model, but it is much more convenient and easy to use.

## ESP DYNAMIC MODEL

This program presents a real-time simulation of a precipitator. The program includes the effects of sneakage and rapping reentrainment while showing the effects of the rapping schedule on instantaneous and average opacities and emissions. The program provides a screen display that simulates a strip chart recorder, showing the emission and opacity histories.

This program is like the ESP sectional model in that it uses a simple (Deutsch-Anderson) model of the particle collection process and accounts for losses due to sneakage and rapping reentrainment. Particle collection is calculated based on the mass median diameter of the dust distribution. As with the sectional model, this diameter is recalculated at the inlet of each section to account for the change in the size distribution due to particle collection in the previous section. Unlike the sectional model, this program allows the dust load to vary randomly in the same way that a boiler would fluctuate. Also, this program calculates the instantaneous values of penetration and opacity, taking into account the effects of section rapping. The rapping schedule can be specified by the user as part of the program input. The degree of dust load fluctuation can also be specified in the program input. Sneakage and rapping reentrainment also can be selected.

The dynamic display model is designed to give a quick look at the relative significance of rapping on outlet emissions and opacity. Specifically, the effects of different rapping schedules and rapping strategies can be evaluated quickly and concisely. Also, this program can be used as a training tool to show the effects of various ESP design factors such as SCA, number of electrical sections, sneakage, and rapping reentrainment. This program is ideally suited for a microcomputer because it uses a simple model and relies heavily on user interaction. Graphic screen displays and easy program control via the keyboard make this program a useful learning tool.

### GCA/EPA BAGHOUSE MODEL

This program is a comprehensive model of fabric filter (baghouse) performance developed by GCA Corporation under contract to the U.S. Environmental Protection Agency. The program predicts instantaneous and cycle-average emissions and tube-sheet pressure drops based on user-specified design and operating parameters. Because of an empiricism in the model, it is limited to modeling baghouses using glass fiber fabrics.

The model considers each bag in a compartment as a number of different flow paths, each with a different dust load. These areas represent parallel flow resistances that can be added to give the overall flow resistance for the compartment. The flow resistances for each compartment are then summed to give the flow resistance (hence pressure drop) for the entire baghouse. The flow resistance for each individual area is due to the presence of the dust cake. This resistance is calculated from Darcy's law. Dust penetration is calculated with an empirical formula developed by GCA from laboratory data. The complete method is described in the reports by Dennis, et al.(3,4)

This program is a microcomputer version of a mainframe model. While the program input steps have been modified, the computations are the same as the mainframe model and are, therefore, much slower than the mainframe version. Neither of the programs predicts the opacity of the stack gas. The advantage of this program is that it is easier to use than the mainframe version and can be used for modeling some small cases.

## OPACITY MODELS

There are two opacity prediction models to be described: the in-stack opacity model and the plume opacity model. The in-stack opacity model predicts the opacity that would be measured by a transmissometer in a stack. The plume opacity model predicts the opacity of a plume of stack gases after it leaves the stack and travels downstream. Both of these models are described below.

### IN-STACK OPACITY MODEL

The in-stack opacity model performs a rigorous calculation of the in-stack opacity based on the particle size distribution. The results of this program are more accurate than the approximate results provided by the ESP models.

This program provides a number of options for calculating the particle light extinction efficiency factors, depending on the desired degree of accuracy. The full Mie theory is the most rigorous method of calculating the extinction coefficients, but it is very slow. The Deirmendjian approximation is available in the program to speed up the calculations while giving results usually within ± 4% of the Mie theory results. Other approximations are also available, depending on the desired degree of accuracy.

Once the extinction coefficients have been calculated for the range of particle sizes, the Romberg method is used to integrate the efficiency factors over the particle size range to yield the opacity. The details of the Romberg integration, along with a complete discussion of the Mie theory and the various approximations to it, are given by Cowen, et al.(5)

The program is useful for evaluating the stack opacity for control devices, given the gas conditions. The program assumes that the particle size distribution is log-normal so that the user must enter the mass median diameter and geometric standard deviation of the distribution. The full Mie theory gives the most accurate results, but it is quite slow on the microcomputer. In most cases the Deirmendjian approximation (or one of the variations on it) will give satisfactory results. In general, the quality of the predicted results will be limited only by the quality of the available particulate data.

## PLUME OPACITY

The plume opacity model is designed to predict the opacity of a plume of stack gas as it travels from the stack exit downstream and mixes with the atmosphere. Oftentimes a plume of smoke can have a higher opacity downstream of the stack than was measured in the stack. It is believed that the homogeneous and heterogeneous condensation of water vapor and/or sulfuric acid in the plume increases the number of light scattering particles in the plume, thereby increasing the opacity.

This model takes into account the conservation of mass, momentum, and energy in a "fundamental principles" approach to the problem of the condensing plume. The plume gas is diluted and cooled by mixing with the ambient air, fostering particle generation. The rate of mixing between the plume and ambient air is described by an empirical equation. The program uses the Runge-Kutta method to solve the simultaneous differential equations for plume position, gas concentrations, and particle concentrations as a function of time. Particle extinction coefficients are calculated for a number of particle sizes. These coefficients are then integrated over the entire size range at one wavelength and refractive index to generate the plume opacity at each time. A thorough description of the modeling equations is given by Damle, et al.(6)

This program is useful for predicting the presence of a condensing plume based on the stack gas and ambient conditions. The program implementation of the model is relatively fast and, thus, it has not been run on a mainframe computer. Also, because of the lack of experimental data, the model has not been thoroughly validated; however, it is believed that the fundamental nature of the modeling equations ensures that at least relative effects can be predicted accurately.

## FUTURE WORK

It is not enough that a program be based on a sound model. For a program to be useful, it must also be convenient and fairly easy to use. A user should not have to consult a reference manual every time he/she wants to run a test case. Towards this end, a great amount of effort has been invested in the development and documentation of the programs described above. All of the programs use a menu format for program execution, and data entry and default values are supplied for all entries. Input parameters can be stored in disk files as well as listed on a line printer. The program printouts are formated for maximum clarity, using simple graphing techniques where appropriate. A report that describes all of these programs in more detail, with complete user instructions and program listings, is now in preparation.

It is felt that these programs offer important capabilities to everyone interested in particulate control problems--from researchers, to industrial users, to regulators. Unfortunately, it appears that the programs as they are now available (for TRS-80 computers) are not in the most widely accepted format. In an attempt to remedy this situation, a task has begun to develop an integrated package of pollution control programs that will run on MS-DOS computers. This package will incorporate all of the programs discussed above in an integrated fashion so that input data can be shared by all programs and so that the output from a control device program can be directly read into one of the opacity programs. Further, the package will have a well defined file structure so that as future models become available they can be added to the package.

It is clear to even the most casual observer that microcomputers are becoming standard tools just as pocket calculators did a decade ago. The air pollution community suffers from a lack of convenient and useful software. It is hoped that these programs will be a first step in meeting those needs.

## REFERENCES

1. Yung, S., Calvert, S., and Barbarika, H. F. Venturi scrubber performance model. EPA-600/2-77-172 (NTIS PB271515), U. S. Environmental Protection Agency, Research Triangle Park, North Carolina, 1977.

2. Damle, A. S., and Sparks, L. E. Modeling of $SO_2$ removal in a spray dryer flue gas desulfurization system. Paper presented at the Fifth Symposium on the Transfer and Utilization of Particulate Control Technology, Kansas City, Missouri. August 27-30, 1984.

3. Dennis, R., et al. Filtration model for coal fly ash with glass fabrics. EPA-600/7-77-084 (NTIS PB276489), U. S. Environmental Protection Agency, Research Triangle Park, North Carolina, 1977.

4. Dennis, R., and Klemm, H. A. Fabric filter model format change, Vol. I, Detailed technical report. EPA-600/7-79-043a (NTIS PB293551), U. S. Environmental Protection Agency, Research Triangle Park, North Carolina, 1979.

5. Cowen, S. J., Ensor, D. S., and Sparks, L. E. TRS-80 in-stack opacity computer programs user and programmer manual. Report prepared under Cooperative Agreement No. R-806718010 for U. S. Environmental Protection Agency, Research Triangle Park, North Carolina, 1984.

6. Damle, A. S., Ensor, D. S., and Sparks, L. E. Prediction of the opacity of detached plumes formed by condensation of vapors. Atmospheric Environment. 18(2): 435-444, 1984.

# THE IMPACT OF PROPOSED ACID RAIN LEGISLATION ON POWER PLANT PARTICULATE CONTROL EQUIPMENT

by: William H. Cole
Gibbs & Hill, Inc.
New York, N.Y. 10001

## ABSTRACT

It is possible that some form of acid rain legislation will be enacted in the near future, although the initial phase may be limited to an accelerated research and development program. If sulfur dioxide control measures are required for selected plants not so equipped, the impact on particulate control equipment could range from the use of coal washing, limestone injection into the boiler, a switch to low sulfur coal, or the use of flue gas scrubber systems. The applicability of these alternatives is examined for several levels of legislation, with approximate costs for a 500 Mw unit. These levels range from a 40 percent reduction in present emission, to the most stringent requirement of the New Source Performance Standards. The effects on the performance of particulate control equipment are examined, with cost estimates for remedial measures where required.

## INTRODUCTION

Proposed acid rain legislation will most likely have a significant effect on particulate air quality control systems installed at existing power plants targeted for a decrease in sulfur dioxide ($SO_2$) emission. This is evident from the fact that the large majority of these plants are equipped with electrostatic precipitators (ESP's) rather than baghouses, which were not used for the utility power plant application until the 1970's.

Based on an extensive literature review, the preponderance of evidence indicates that a significant source of the acid rain problem in the northeast and middle Atlantic states originates from the midwest utilities that generally burn a high sulfur coal. However, it appears that any legislation may be delayed in favor of an accelerated research program to better define the problem. Possibly more responsible for a delay would be the time required to formulate an implementation program that would be politically acceptable to the special interest groups that include the midwest utilities and coal industry. Since legislation would most likely require compliance on the basis of current emission, a delay could be beneficial. It would provide time to implement presently available and cost effective methods for substantially reducing $SO_2$ emission, in order to avoid any "hit list" of targeted plants that might be mandated to install very costly systems such as wet scrubber flue gas desulfurization (FGD).

Most publicity has been given to the legislation proposed by the Waxman/Sikorsky Bill (H.R. 3400). This would target the 50 utility plants with the highest $SO_2$ emission in tons/yr. based on 1980 statistics. The required compliance would be in accordance with the New Source Performance Standards (NSPS), which require a removal efficiency of up to 90 percent. A statistical review of the published data confirmed that the worst offenders are the larger generating plants with an average generating capacity of approximately 1700 Mw. The analysis further indicated that an average 83 percent $SO_2$ removal would be required for compliance with this legislation. At the present time, wet scrubbers are the only commercially acceptable system that can reliably achieve efficiency levels in the 80 to 90 percent range on high sulfur coal appplications. Assuming an average capital cost of $225/Kw for a retrofit FGD, the cost for a typical plant would be $383 million. A 1983 study for the Edison Electric Institute indicated that the cost of implementing the Waxman/Sikorsky Bill over a period from 1985 to 2008 would be $222 billion including capital and operating costs.

It is difficult to conceive of legislation with requirements as stringent as the Waxman/Sikorsky Bill becoming a reality. Aside from the cost, a major objection is the fact that the targeted plants are at least 10 years old, and were not designed to accommodate the very large FGD systems that would be required for a typical 1700 Mw plant.

Considering the above factors, the content of this paper is based on the following conclusions:

(1) Methods of achieveing compliance with legislation when it occurs will be site specific based on such factors as plant design site constraints, and cost effectiveness. No single equipment system or process will be suitable for all plants, and hence there will be no single fixed level of compliance.

(2) There are presently alternatives other than FGD systems that can provide a substantial decrease in $SO_2$ emission. These should be evaluated on their own merits without comparison to an arbitrary guideline of $SO_2$ removal up to the 90 percent level.

## BASIC SYSTEM DESIGN PARAMETERS

The statistical review of the plants with highest $SO_2$ emission indicated an average generating unit size of approximately 500 Mw. Other parameters including typical high sulfur coal characteristics are provided in Table 1.

TABLE 1. BASIC SYSTEM DESIGN PARAMETERS

| | |
|---|---|
| Unit Size | 500 Mw |
| Gas Flow Rate | 1,800,000 ACFM |
| Gas Temperature | 300 F |
| Heat Input | 5,140 MMBtu/hr |
| Coal Firing Rate | 475,000 lbs/hr |
| ESP Inlet Loading | 3.45 GR/ACF |
| Ash Emission | 0.08 lbs/MMBtu |
| ESP Efficiency | 99.20 percent |
| Coal Characteristics: | |
| Sulfur Content | 3.30 percent |
| Ash Content | 14.0 percent |
| Heating Value | 10,825 Btu/lb |

## ALTERNATIVES FOR $SO_2$ REMOVAL

There are four basic alternatives for reducing $SO_2$ emission currently being evaluated by Government agencies such as EPRI and the EPA, and by the utilities, equipment suppliers, and others involved in power plant air quality control. These include coal cleaning, limestone injection into a multi-stage burner (LIMB), flue gas desulfurization using scrubbers, and coal switching. The advantages and limitations of each including cost estimates are dicussed in the following sections.

The cost estimates for each alternative are all derived from the same base of assumed operating and cost parameters to permit direct comparison. These parameters are summarized in Table 2.

TABLE 2. OPERATING AND COST PARAMETERS

| | |
|---|---|
| Remaining Plant Life | 25 Yrs. |
| Operating Hours/Yr. | 8000 |
| Avg. Load Factor | 70 Percent |
| Capacity Factor | 63 Percent |
| Capacity Charge(1) | \$700/KW |
| Fixed Charges on Investment | 17 Percent |
| Incremental Energy Charge | \$0.020/KWH |
| Limestone Stoichiometry (FGD) | 1.10 |
| Ca/S Stoichiometry (LIMB) | 2.25 |
| Limestone Reagent Cost | \$14/Ton |
| Sludge Disposal(2) | \$12/cu. yd. |

(1) Prorated from \$1000/Kw for a 35 yr. plant life

(2) Assumes disposal by truck 5 miles from plant site

Of importance in Table 2 is the assumed capacity factor of 63 percent which is the approximate statistical average for generating units of 500-750 Mw. This factor reflects the impact of fixed investment charges on annual cost parameters that are a function of load (e.g. mills/KWH, \$/Ton of $SO_2$ removal). The fixed charge component of annual cost is independent of load, whereas the KWH's and tons/yr $SO_2$ removal are decreased in proportion to capacity factor. This results in high ratios for the above parameters at low load. However, this is realistic since it incorporates the effect of investment cost when comparing alternatives. Parameters such as reagent stoichiometry are based on discussions with those investigating a particular alternative in detail. Limestone cost is the average of \$8 to \$20/ton price quotations depending on transportation charges.

## COAL CLEANING

Coal cleaning is accomplished by physical separation methods, and is used at various levels of cleaning by many utilities that burn a high sulfur/high ash coal. The primary purpose to date has been for economic reasons. A major study has been reported by TVA on 60 generating units during the period from 1962 to 1980.(1) This study examined coal quality vs. boiler performance and overall plant operation. The result was a model which indicated a savings from \$1.50 to \$2.00 per ton of coal. The savings results from higher boiler efficiency, fewer forced outages, reduced maintenance costs, and lower cost of coal transportation, ash handling, and disposal. Although typical sulfur removal from midwest coals is 30 to 40 percent at a low level of cleaning, this alternative could have applicability as an acceptable solution for reducing $SO_2$, particularly if used in conjunction with other alternatives such as limestone injection into the boiler, or with dry scrubbers which do not operate as effectively on high sulfur coal.

The literature occasionally states that a disadvantage of coal cleaning is the adverse effect on the ESP's. However, this is a superficial disavantage. Although in most cases the ESP efficiency will show a small decrease as a result of the lower sulfur content, the important parameter which is outlet emission will generally show a dramatic improvement because of the reduced ash content. With respect to efficiency per se, the decrease will generally be small. For a high sulfur coal, the residual sulfur after cleaning may provide essentially the same performance. In the case of a low sulfur coal (which is less frequently cleaned), the sulfur removal by cleaning is less effective, and this in turn minimizes the effect on efficiency. These effects are illustrated by the examples in Table 3, which also includes typical cost parameters for low level coal cleaning.

---

(1) TVA quantities value of burning physically cleaned coal on plant operating, maintenance, FGD costs; Electric Light & Power, December, 1983.

TABLE 3. EFFECT OF COAL CLEANING ON $SO_2$ AND ASH EMISSION

| | Raw Coal | Cleaned Coal | Raw Coal | Cleaned Coal |
|---|---|---|---|---|
| Sulfur Content (%) | 3.3 | 2.3 | 2.0 | 1.6 |
| Ash Content (%) | 14.0 | 7.0 | 14.0 | 7.0 |
| Heating Value (Btu/lb) | 10,825 | 12,000 | 10,825 | 12,000 |
| ESP Efficiency (%) | 99.20 | 99.11 | 99.20 | 99.08 |
| Ash Emission (lbs/MMBtu) | 0.083 | 0.042 | 0.083 | 0.043 |
| $SO_2$ Emission (lbs/MMBtu) | 6.10 | 3.83 | 3.70 | 2.67 |
| Percent Decrease in $SO_2$ | | 37.2 | | 27.8 |
| Incremental Price ($/ton) | | 10 | | 10 |
| Incremental Price (w/credits)* | | 6 | | 6 |
| $ Per Ton $SO_2$ Removal | | 221 | | 487 |
| Incremental Cost (Mills/KWH* | | 2.6 | | 2.6 |

*Includes $4.00/ton credits for improved boiler and plant operation

It will be noted in Table 3, that in the case of the higher 3.3 percent sulfur coal with 30 percent of the sulfur removed by cleaning, the $SO_2$ and ash emission decreased by 37 and 50 percent respectively. However, for the medium 2.0 percent sulfur coal with ony 20 percent removal by cleaning, the decrease in $SO_2$ is only 28 percent while the decrease in ash emission is essentially the same as for the higher sulfur coal.

The cost data in Table 3 are based on a previous study by Gibbs & Hill which indicated an incremental cost of $7.00/ton for coal cleaning which falls in the range of published data. However, most utilities purchase the clean coal from a fuel supplier at an average of $3.00/ton above cost for an estimated purchase price of $10.00/ton.

## LIMESTONE INJECTION INTO THE BOILER

This alternative involves the injection of finely ground limestone into the boiler using a multi-stage burner (LIMB). The limestone ($CaCO_3$) is flash calcined to lime (CaO), which reacts with the $SO_2$ and any $SO_3$ in the flue gas to form calcium sulfate ($CaSO_4$). An extensive amount of work on the LIMB concept is being pursued by the boiler manufacturers, and full scale field evaluation is planned by the EPA on a 200 Mw boiler, and in a joint venture of B&W with Research-Cottrell Inc. on a 600 Mw unit at the Homer City Plant of Pennsylvania Electric Co. Hence, the process is in the development stage with possible commercialization at least 4 to 5 years in the future. On this basis, the alternative is difficult to assess from both a technical and economic viewpoint. However, the process appears to have some merit for the retrofit application if used in conjunction with auxiliary equipment or other alternatives depending on the decrease in $SO_2$ required by legislation. It appears to be compatible with various system designs to achieve several discrete $SO_2$ removal efficiencies of 50, 70 and 85 percent. These optional systems utilizing LIMB are as follows:

## LIMB With A Baghouse Replacing An Existing ESP

Limestone injection into the boiler can reportedly result in 50 percent $SO_2$ removal, although at a high stoichiometric ratio of Ca/S in the range of 2.25 to 2.50. The high stoichiometry and relatively low 50 percent removal of $SO_2$ results in chemical compounds that substantially increase the particulate loading to the existing precipitator. This is evident from the reaction products and operating parameters summarized in Table 4 for the assumed 500 Mw unit design parameters in Table 1.

TABLE 4. LIMB OPERATING PARAMETERS

| | | |
|---|---|---|
| Ca/S Stoichiometry | 2.25 | |
| $SO_2$ Removal | 50 Percent | |
| Limestone Requirements ($CaCO_3$) | 162,400 Tons/Yr. | |
| Inlet Particulate to ESP: | Lbs/hr | Gr/acf |
| Fly Ash | 37,226 | 3.45 |
| CaO | 11,998 | 1.11 |
| $CaSO_4$ | 23,316 | 2.16 |
| Inerts | 2,030 | 0.19 |
| Total: | 74,570 | 6.91 |
| Unreacted CaO | 56 Percent | |
| Est. ESP Emission (100% Load)* | 4.0 Lbs/MMBtu | |

*Assumes an estimated ESP efficiency of 80 percent

A review of Table 4 indicates that the effect of the assumed Ca/S stoichiometry of 2.25 (which is somewhat optimistic) is reflected in a high limestone requirement of 162,400 tons/yr at a 63 percent capacity factor, and 11,998 lbs/hr (47,992 tons/yr) of unreacted calcined lime. It is also noted that the products of the chemical reactions doubles the inlet grain loading to the ESP from 3.45 to 6.91 Gr/acf. An ESP can generally tolerate this increase in particulate loading with only a moderate effect on efficiency due to dust space charge and some increase in re-entrainment. However, even if the ESP efficiency remained unchanged, the emission in lbs/MMBtu would double and place the unit out of compliance.

In the case of LIMB, the added particulate loading is comprised of lime and calcium sulfate which should have a disastrous effect on the ESP performance due to electrical resistivity. Experience with precipitators used for the gypsum (calcium sulfate) application has shown poor performance without a flue gas moisture content in the range of 15 percent by volume. It is also noted that for the LIMB application, there will be insignificant $SO_3$

in the flue gas to provide conditioning of the fly ash by the formation of sulfuric acid, since the small amount of $SO_3$ (e.g. 35 to 40 ppm) will readily react with the CaO to form additional $CaSO_4$. In addition to resistivity, the CaO poses a problem because of the fine particle size distribution. In order to achieve 50 percent removal of $SO_2$, the limestone reagent must be finely ground to provide maximum specific surface area to the CaO produced in order to enhance the reaction with the $SO_2$. The particle size distribution has variously been reported as 100 percent finer than 50 microns, or 50 percent less than 11 microns.(1) Based on resistivity and particle size distribution of the limestone reagent products, it is estimated that the ESP efficiency will decrease from 99.20 percent to the 80 percent level, with a resulting emission of approximately 4.0 lbs/MMBtu. This estimate is clearly a rough approximation, since it is impossible to estimate ESP efficiency with any accuracy in the presence of back corona which is anticipated.

The expectation of a major deterioration in the ESP performance was not noted in the literature review. Reference (1) allowed $5.00/kw for additional soot blowers and ESP upgrading. Even if the high concentration of $CaSO_4$ and CaO in the flue gas (3.44 gr/acf) did not affect the operating characteristics of the precipitator, the entire amount, or $2,500,000 for a 500 Mw unit would be required for the 30 percent additional collecting plate area to maintain a constant emission because of the factor of 2 increase in the particulate loading. From the above considerations, it is concluded that a baghouse would be required to replace an existing ESP at an estimated installed cost of $20 million.

## Combined Coal Cleaning With LIMB

Coal cleaning used in conjunction with LIMB should provide an attrative option for a retrofit installation, if legislation does not require more than a 70 percent decrease in $SO_2$ emission. This is the approximate level expected with this alternative as a result of the combined effects of a 30 percent decrease in sulfur content from cleaning, a 10 percent lower coal rate due to the higher heating value, and 50 percent removal of the remaining $SO_2$ from the limestone injection into the boiler. An additional benefit is the reduced particulate loading to the existing ESP. This results from a 50 percent decrease in ash content from the coal cleaning, and the reduced limestone requirement due to the lower sulfur content. The combined effect is a decrease in particulate inlet loading to the approximate level without the limestone injection. The net effect would be a particulate emission of 0.088 lbs/MMBtu, provided the ESP efficiency can be maintained at the 99.20 percent level. This might be achieved by the use of a sulfur burner flue gas conditioning system utilizing $SO_3$ injection at a sufficiently high concentration. It would appear necessary to inject sufficient $SO_3$ to form a molecular layer of calcium sulfate on the surface of the unreacted lime particulate, and also provide second stage conditioning to provide the sulfuric acid for conditioning the calcium sulfate. The amount of $SO_3$ would depend to a large extent on the specific surface area of the CaO particle size distribution. Based on the equivalent of two stage conditioning and high specific surface area of CaO and $CaSO_4$, it is estimated that 80 to 100 ppmv of $SO_3$ would be required as compared to the conventional 20 to 40 ppmv typically used to condition fly ash.

---

(1) Barsin, J.A. Options for reducing $NO_x$ and $SO_2$ emission during combustion. In: Proceedings of the acid rain conference, Washington, D.C., March 26, 1984.

Gas conditioning will be field tested on the LIMB application in early 1985. If successful, it would be a preferrable alternative to the use of a baghouse for particulate removal. In addition to being less costly, it would utilize the existing ESP with minimal outage time, and avoid any problem with the substantially greater space required by a baghouse. On this basis, it is included in the alternate LIMB system cost summary provided in Table 5. The gas conditioning equipment and operating characteristics are discussed in a subsequent section of the paper.

TABLE 5. ALTERNATE LIMB SYSTEM COST ESTIMATES (in 000'S)

| Investment Costs: | LIMB With A Baghouse | Coal Cleaning Plus LIMB w/Baghouse | Coal Cleaning Plus LIMB w/Conditioning |
|---|---|---|---|
| Modifications to Boiler | $ 7,500 | $ 7,500 | $ 7,500 |
| Limestone Handling/Preparation | 10,000 | 10,000 | 10,000 |
| Baghouse | 20,000 | 20,000 | - |
| Gas Conditioning System | - | - | 4,850 |
| Capacity Charge | 1,358 | 1,358 | 687 |
| Total: | $38,858 | $38,858 | $23,037 |
| **Annual Costs:** | | | |
| Fixed Charges | $ 6,606 | $ 6,606 | $ 3,916 |
| Coal Cleaning* | - | 7,200 | 7,200 |
| Limestone | 2,275 | 2,275 | 2,275 |
| Incremental Energy | 310 | 310 | 320 |
| Sulfur | - | - | 256 |
| Steam | - | - | 22 |
| Maintenance | 600 | 600 | 220 |
| Total: | $ 9,791 | $16,991 | $14,209 |
| Percent Decrease in $SO_2$ | 50 | 69 | 69 |
| $/Ton Decrease in $SO_2$ | 223 | 282 | 236 |

*Based on purchased coal at $10/ton less $4/ton credits.

The costs in Table 5 for coal cleaning plus limestone injection into the boiler are attractive based on $/ton decrease in $SO_2$ in the event legislation would require a removal efficiency at the 70 percent level. It is also noted that the limestone handling and preparation costs assume raw limestone storage and preparation on the plant site. However, it is most likely that space constraints and other factors will dictate the purchase of pulverized limestone for silo storage and direct feed to the boiler. This should increase the cost to the plant depending on market price, but should not significantly affect the results for comparison with other alternatives.

## Combined LIMB And Dry Scrubber System

This alternative appears to be attractive as compared to a wet scrubber FGD system for 85 percent $SO_2$ removal which is the typical requirement to meet the New Source Performance Standards. The use of the dry scrubber (i.e. spray dryer) has generally been limited to lower sulfur coal (e.g. less than 2 percent sulfur), and utilizes a lime reagent in order to achieve removal efficiencies up to the 85 percent level. The compatibility with the LIMB system is evident based on the following considerations.

(1) Assuming 50 percent removal of $SO_2$ by LIMB, the $SO_2$ inlet concentration to the dry scrubber would be equivalent to that resulting from a 1.65 percent sulfur coal. A dry scrubber removal efficiency of 70 percent would provide a total system removal of 85 percent typically required by NSPS. The relatively low design efficiency of the spray dryer would reduce equipment size and result in an estimated savings of $10 million in installed equipment cost as compared to a wet scrubber FGD system using a limestone reagent. This combined with an estimated lower energy capacity charge of $5.7 million nearly offsets the capital investment cost of $17.5 million for the LIMB system.

(2) The lime reagent requirement for a $CaO/SO_2$ stoichiometry of 1.10 in the spray dryer would be 29,600 tons/yr. However, there is 48,000 tons/yr of unreacted lime in the flue gas from the LIMB process, and about 62 percent recovery of this lime in the existing ESP would satisfy the requirement for the slurry feed to the spray dryer. Since the final particulate cleanup would be accomplished by a baghouse or ESP following the spray dryer, an existing ESP following the air heater could operate at the 70 to 75 percent efficiency level to reclaim the unreacted lime, despite poor electrical operating characteristics due to particulate resistivity. This was discussed in a previous section on ESP performance in conjunction with limestone injection into the boiler.

It is evident from the above factors, that the LIMB system used in conjunction with a dry scrubber results in a synergistic effect on overall system annual cost. The savings in lime reagent cost, incremental energy, maintenance, and sludge disposal is estimated at $5.0 million/yr. This should result in a $60-70 per ton decrease in the cost of $SO_2$ removal.

## Wet Scrubber FGD

At the present time, the wet scrubber FGD system is essentially the only commercially available alternative for $SO_2$ removal at efficiency levels up to 90 percent on high sulfur coal applications. However, the process requires close supervision and control by trained personnel, high maintenance cost, marginal availability by electric utility standards, and cannot be considered cost effective. These factors are illustrated by the following typical cost parameters:

(1) The investment cost for a retrofit system is typically 25 percent of the total plant cost in present day dollars (i.e. a new plant).

(2) Energy requirements for a limestone reagent system are 4 to 5 percent of the plant gross generating capacity.

(3) The average staff budget is about 25 percent of that for the total plant, and the FGD system will constitute 10 to 40 percent of the annual plant operating cost.(1)

(4) The cost of $SO_2$ removal at the 85 percent efficiency level is in the range of $400-500 per ton.

(5) Stabilized sludge for the base case considered in this study (i.e. 500 Mw unit with 63 percent capacity factor burning a 3.3 percent sulfur coal), would result in 250-300 acre feet of landfill per year.

Although the wet FGD system is not cost effective for retrofit units wi a relatively short remaining plant life, it should continue to be the only acceptable alternative in the foreseeable future if legislation requires the NSPS for $SO_2$ emission. It must be acknowledged that the technology and system availability has been improved during the past five years by material of construction and control of the process chemistry. It should also be not that the high energy and maintenance cost, and the less than desirable syste availability pertain primarily to a limestone system which is most commonly used for new generating units because of reagent cost. However, at least in the early years of FGD installations, a lime reagent was selected for 75 percent of retrofit applications. The use of lime should be particularly attractive for retrofit systems installed as a result of acid rain legislation, since the worst offenders are located in the Ohio Valley region (e.g. 10 in Ohio), where the evaluated cost of lime is highly competitive. A lime system has a number of advantages which include about 53 percent of the reagent requirements as compared to limestone, less reagent storage and handling, and about 50 percent of the incremental energy cost. Based on a technical evaluation, the use of a magnesium buffered lime (e.g. about 4-5 percent magnesium) can justify some cost premium since it minimizes scaling and plugging due to greater solubility of the calcium sulfite and sulfate products of the scrubbing process. These factors are acknowledged to be the primary cause of most scrubber maintenance.

Although the retrofit of a wet scrubber FGD system has no impact on particulate control equipment, cost estimates have been summarized in Table 6 to serve as a base cost for comparison with other alternatives.

---

(1) Tearney, J., Froelich, D., Graves, G. $SO_2$ control by nonregenerable wet FGD systems. Proceedings of the Acid Rain Conference, Washington, D.C., March 26, 1984.

TABLE 6. COST ESTIMATE FOR WET LIMESTONE FGD SYSTEM

| | | |
|---|---|---|
| **Investment Costs** | | |
| FGD System Installed @ $225/kw | | $112,500,000 |
| Capacity Charge(1) | | 9,120,000 |
| | Total | $121,620,000 |
| **Annual Costs** | | |
| Fixed Charges on Investment | | $ 20,675,000 |
| Limestone Reagent | | 1,890,000 |
| Incremental Energy (16,000 kw) | | 2,560,000 |
| Maintenance | | 2,000,000 |
| Stabilized Ash/Sludge Disposal(2) | | 4,810,000 |
| | Total | $ 31,935,000 |
| $/Ton of Coal | | $ 24.00 |
| Mills/KWH | | 11.40 |
| $/Ton $SO_2$ Removal | | 428.00 |

(1)Prorated for 20 yrs. remaining plant life from 35 yrs. @ $1000/kw

(2)Assumes disposal by truck 5 miles from the plant site

## Coal Switching

The alternative that is most cost effective for a significant reduction in $SO_2$ emission at the present time, is the change to a medium-low sulfur coal defined here as a sulfur content in the range of 1.10 to 1.40 percent. This has been given due consideration in some of the literature, but was not considered promising because of the following a priori assumptions and limitations.

(1) It was assumed that this switch would be to a low sulfur eastern coal (e.g. 0.7 percent) or to a western coal (e.g. 0.5 percent). Both of these coals would result in a decrease in $SO_2$ emission of about 80 percent as compared to the 3.3 percent midwest coal in Table 1.

(2) Low sulfur Central Appalachia coal is in relatively short supply with a typical price premium of $17-20 per ton.

(3) The cost of low sulfur western coal would be acceptable to some regions of the midwest with the lowest transportation cost. However, most midwest plants were designed for bituminous coal, and use of the sub-bituminous western coal creates the potential for slagging and fouling of the boiler.

(4) The political pressure to protect the midwest coal industry which employs 50,000 workers in the mining and coal related industries would be insurmountable.

As noted in the introduction, it is most probable that methods used to implement any legislation will of necessity be site specific in many cases. In addition, it is important to note that a decrease in $SO_2$ emission of 80-90 percent is an arbitrary guideline that was only one of a number of proposals for legislation. It was not endorsed by the regulatory agencies, and would most certainly have been subject to compromise in order to accommodate site constraints, and perhaps the cost of implementation.

The switch to a relatively low sulfur coal indicates that a decrease in $SO_2$ emission in excess of 60 percent can be achieved in an expeditious and economical manner, with minimal effect on plant operation. The specific case for evaluation utilizes a 1.30 percent sulfur coal which is well within the range of that which is in abundant supply from Central Appalachia. The salient factor in such a fuel change is the differential in delivered price to a midwest plant as compared to the high sulfur midwest coal, and this will depend to a large extent on plant location and transportation cost. However, 17 of the 50 plants with the highest $SO_2$ emission based on 1980 statistics are located in Ohio, Kentucky and West Virginia. Based on recently published data and inquiries to coal suppliers and utilities, a plant in Ohio can obtain a 1.3 percent sulfur coal from eastern Kentucky or West Virginia at a plus cost differential of $4.85/ton as compared to the 3.3 percent midwest coal. This cost differential includes an adjustment for the higher heating value.

It is of interest to evaluate the reduction in $SO_2$ emission by the switch to a 1.3 percent sulfur coal based on relatively firm costs, as opposed to estimates and ranges in the published data which are reflected in the generality of the conclusions. The change to a higher quality coal should require negligible, if any, cost for boiler modification. Hence, the capital investment would be limited to maintaining the original ESP performance with the low sulfur coal. This is economically and reliably accomplished by the use of a sulfur burner type flue gas conditioning system. The experience with more than 125 installations of this equipment to date indicates that it meets all of the criteria for automation, reliability, and availability required by the electric utility application. In addition, the equipment requires little space, and would comprise a liquid sulfur storage tank, a metering pump skid, and a single sulfur burner/$SO_3$ converter skid. The storage tank can be remotely located, and each of the two equipment skids would measure approximately 9 x 17 ft. Of salient importance is the control system and level of automation. The steam jacketed sulfur storage tank and piping to the burner skid maintains a liquid sulfur temperature to the burner skid in the range of 250-300 F. At startup, a push button activates the electric ambient air heaters to raise the temperature of the vanadium pentoxide catalyst bed to the required process temperature of 800 F. This requires approximately 4 hours from a cold start, at which time a secod push button activates the sulfur flow to the burner/converter skid at a feed rate controlled by the metering pump. The rate is adjusted following installation of the system to provide an optimum feed of sulfur trioxide in ppm by volume to the ESP inlet probes. Thereafter, the rate is automatically regulated by a boiler signal to maintain a constant ppm of $SO_3$ injection to the flue gas over the entire range of boiler load. It is also noted that the operating cost is not very sensitive to boiler load, since the conversion of $SO_2$ to $SO_3$ is an exothermic reaction which generates heat required by the catalyst bed. Hence, at higher feed rates, the sulfur cost is approximately offset by the reduced auxiliary heat required from the electric heaters.

The gas conditioning system operating and cost parameters are summarized in Table 7.

TABLE 7. SULFUR BURNER FLUE GAS CONDITIONING SYSTEM OPERATING AND COST PARAMETERS

| | |
|---|---|
| Coal Sulfur Content | 1.30 Percent |
| Ash Content | 14.0 Percent |
| Heating Value | 11,460 Btu/lb |
| $SO_3$ Injection Rate | 13 ppm by vol. |
| System Design | 25 ppm by vol. |
| Liquid Sulfur Requirement | 266 Tons/yr |
| ESP Efficiency | 99.20 Percent |
| Liquid Sulfur Cost (Delivered) | $125.00/Ton |
| Steam Cost (45 psig-sat.) | $0.003/lb |
| Coal Differential (1.3 vs. 3.3% Sulfur) | $4.85/Ton |
| Decrease in $SO_2$ Emission | 63 Percent |

A critical parameter is the expected $SO_3$ injection rate, although the system is generally designed to provide twice the expected value to accommodate the optimum rate determined during startup. This is based on the maximum ESP performance as indicated by stack opacity. The expected rate in this case is the additional $SO_3$ concentration added to the flue gas that would be obtained with a 2.5 vs. a 1.3 percent sulfur coal. The 2.5 percent level is selected as the base since this sulfur content typically provides optimum ESP performance.

The cost of coal switching based on the cost of the conditioning system and the incremental cost increase of $4.85/ton for the 1.3 vs. the originial 3.3 percent sulfur coal (adjusted for heating value) is summarized in Table 8.

TABLE 8. COST OF COAL SWITCHING

| Gas Conditioning System | | |
|---|---|---|
| Investment Costs | | |
| Installed Equipment (Incl. Engr'g) | | $2,100,000 |
| Capacity Charge | | 138,000 |
| | Total | $2,238,000 |

Annual Costs

| | |
|---|---|
| Fixed Charges | $ 380,500 |
| Incremental Energy | 32,200 |
| Liquid Sulfur | 33,300 |
| Steam | 6,000 |
| Maintenance | 10,000 |
| Annual Cost of Gas Conditioning | $ 462,000 |
| Annual Cost of Coal Switching | $6,091,000 |
| Total Annual Cost | $6,553,000 |
| $/Ton of Coal for Gas Conditioning | $0.368 |
| Mills/KWH (Coal Change & Conditioning) | 2.3 |
| % Decrease In $SO_2$ Emission | 63 |
| $/Ton Decrease in $SO_2$ Emission | 119 |

A review of Table 8 clearly indicates that switching to a medium-low sulfur coal, plus the addition of a gas conditioning system to maintain the ESP design efficiency is the most cost effective alternative that results in a substantial decrease in $SO_2$ emission. The 63 percent decrease may well satisfy any legislation, particularly for the large midwest plants with 20 years or less remaining plant life.

## SUMMARY

The various alternatives considered for reducing $SO_2$ emission cover a range from 37 to 85 percent. However, in order to evaluate the cost effectiveness of each alternative, the percent decrease must be evaluated on the basis of cost parameters such as initial investment, and annual cost per ton of $SO_2$ removal and cost per KWHR. A summary of these costs is provided in Table 9.

TABLE 9. COST SUMMARY

| | % $SO_2$ Removal | Investment Cost ($/Kw)(2) | Annual Cost (Mills/KWH) | $/Ton $SO_2$ Removal |
|---|---|---|---|---|
| Coal Cleaning (1) | 37 | - | 2.6 | 221 |
| LIMB Systems: | | | | |
| w/o Baghouse (3) | 50 | 36 | 2.0 | 131 |
| w Baghouse | 50 | 78 | 3.5 | 223 |
| Cleaning w/Baghouse | 69 | 78 | 6.1 | 282 |
| Cleaning w/Conditioning | 69 | | 5.1 | 236 |

| | | | | |
|---|---|---|---|---|
| Coal Switching with Gas Conditioning | 63 | 450 | 2.3 | 119 |
| Wet Scrubber FGD | 85 | 243 | 11.4 | 428 |
| LIMB w/Dry Scrubber FGD | 85 | 247 | 9.7 | 363 |

(1)Based on purchased coal at $10/ton less $4/ton credits

(2)Includes capacity charge

(3)This alternate not feasible because of high particulate emission.

## CONCLUSIONS

The following conclusions are indicated as a result of the study.

(1) Despite the publicity given to several proposals for acid rain control, it is concluded that any legislation for a decrease in $SO_2$ emission will not mandate compliance with the New Source Performance Standards. These standards require the use of wet scrubber FGD systems with high sulfur coal to provide removal efficienies in the range of 80-90 percent. The average generating capacity of the 50 plants with the highest $SO_2$ emission in tons/yr based on 1980 statistics is approximately 1700 Mw. This would result in an investment cost of $413 million at $225/kw plus capacity charge. It is further concluded that control measures in many cases will of necessity be site specific based on a number of factors including plant design, space constraints, and cost effectiveness.

(2) There are a number of alternatives that could provide a substantial decrease in $SO_2$ emission including limestone injection into the boiler (LIMB) or coal switching. Limestone injection could reduce the emission by approximately 50, 70, or 85 percent, depending on the extent of the system. Used alone with a baghouse, or possibly flue gas conditioning with an existing ESP should result in 50 percent $SO_2$ removal. This alternative combined with coal cleaning would provide approximately 70 percent removal. In the event that 85 percent removal is required in some cases, LIMB used in conjunction with a dry scrubber appears to offer a number of advantages as compared to wet FGD, including space requirements and cost. However, it is important to note that limestone injection is still in the development stage, and use of the process as a viable and cost effective alternative for $SO_2$ removal will depend on the results of at least two full scale demonstration units by EPA and Babcock & Wilcox in the near future.

(3) Switching to a relatively low sulfur eastern coal in conjunction with a sulfur burner flue gas conditioning system will provide a substantial decrease in $SO_2$ emission in the range of 60 to 65 percent. It is by far the most cost effective alternative, with an annual cost including fixed charges on investment of 2.3 mills/KWHR. In addition, it should require minimal, if any, modification to the boiler, and minimum outage time for installation of the $SO_3$ conditioning system injection probes in the ESP inlet ductwork. This alternative is also not limited by space constraints because of the compact

size of the skid mounted equipment, which can be installed above grade if necessary.

(4) It is most probable that the effect of $SO_2$ legislation would be directed at those plants with the highest emission in ton/yr. As noted previously, a delay in legislation could be advantageous in providing time for those plants to implement a sufficiently effective means of reducing emission in order to avoid any "hit list" associated with the legislation. Noting that in a few years these plants will be at least 12 to 15 years old, a cost effective alternative would entail minimum initial investment and reasonable annual operating cost. Coal switching with flue gas conditioning is clearly compatible with these objectives based on an investment cost of $0.368/ton of coal including capacity charge, and the total annual cost of 2.3 mills/KWHR. It would appear prudent for a utility to give consideration to this option at the present time. This would pre-empt any legislative constraints against coal switching on a large scale in order to provide acceptable protection to the midwest coal industry.

The work described in this paper was not funded by the U.S. Environmental Protection Agency, and therefore the contents do not necessarily reflect the views of the Agency, and no official endorsement should be inferred.

## REFERENCES

1. TVA quantifies value of burning physically cleaned coal on plant operatin maintenance, FGD costs. In: Electric Light & Power, December 1983.

2. Barsin, J.A. Options for reducing $NO_x$ and $SO_2$ emissions during combustion. In: Proceedings of the acid rain conference, Washington, D.C., March 26-28, 1984.

3. Tearney, J., Froelich, D., Graves, G. $SO_2$ control by nonregenerable wet FGD systems. In: Proceedings of the acid rain conference, Washington, D.C., March 26-28, 1984.

## Session 4: NOVEL CONCEPTS

Dale L. Harmon, Chairman
U.S. Environmental Protection Agency
Air and Energy Engineering Research Laboratory
Research Triangle Park, NC

# PARTICLE CHARGING WITH AN ELECTRON BEAM PRECHARGER*

by: J. S. Clements, A. Mizuno**, and R. H. Davis
Physics Department, The Florida State University
Tallahassee, Florida 32306

**On leave from Toyohashi University of Technology, Japan

## ABSTRACT

The charging performance of both high and low energy electron beam prechargers has been evaluated for the bi-electrode and tri-electrode geometries. The effects of electron beam energy, beam current, electric field strength, current density, and exposure time on charging efficiency were investigated by measuring the charge acquired by large conducting spheres and 1 and 3 μm diameter PSL particles. The performance of the high energy precharger was unsatisfactory because the energetic scattered electrons created positive ions in the negative charging region which degraded the charging performance.

In the low energy electron beam precharger measurements, the beam energy was adjusted so that the ionization zone (bipolar region of ionized air) was smaller than the electrode spacing. This avoids spurious ionization by scattered electrons and establishes a monopolar charging region due to the separation of the bipolar ions by the electric field. Particle charges greater than 5 times the theoretical ionic charging value were observed using the low energy bi-electrode precharger. The increased charge may be caused by space-charge enhancement of the electric field and/or free electron charging.

## INTRODUCTION

The use of electron beam ionization in electrostatic precipitator (1,2) geometries for pulverized coal combustion emission control has been investigated in a continuing series of studies (3-5). The various electron beam ionization regimes present in a precipitator-like parallel electrode system have been measured and analyzed (4,5). Initial experiments using electron beam ionization in electrostatic precipitator geometries yielded measured ion current densities more than 500 times greater than those generally obtained in a conventional corona-wire electrostatic precipitator (1-5).

When an electron beam passes through air it ionizes the air molecules forming a plasma of positive and negative ions. These ions can be separated from the plasma and collected by applying an electric field as shown in Figure 1. The initial experiments showed that the positive and negative ions could be effectively separated even when a large electron beam current was used. This separation of the bipolar ions is essential to the operation of an electron beam precharger because a copious supply of exclusively monopolar ions is required for efficient particle charging.

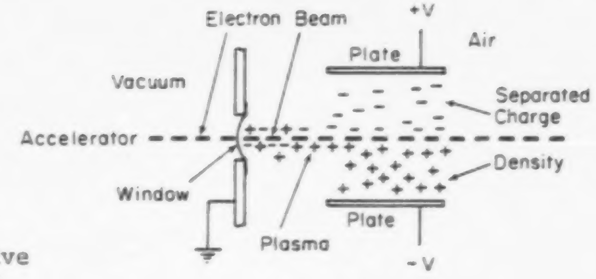

Figure 1. Formation of ions by electron beam irradiation of air molecules. Ions of opposite charge are separated by an applied electric field.

Successful electron beam precharger development must meet several objectives, the most important being increased charge on the particles. For small particles (< 0.2 μm diameter) diffusion charging dominates, and for a given charging time the amount of charge deposited on the particle depends on the ion current density (1,2). For large particles (> 0.5 μm diameter) field charging dominates, and the electric field strength determines the saturation charge of the particles (1,2). The rate of field charging depends on the ion current density. The very large ion current densities in the electron beam precharger are expected to increase the amount of charge received by the small particles due to diffusion charging, and also decrease the time necessary for field charging of large particles. The large ion current densities can also cause space charge enhancement of the electric field, which will increase the saturation charge of the larger particles.

In addition to enhancing the ionic charging mechanisms, the electron beam precharger may advantageously utilize free electron charging of particles. There is evidence that free electron charging occurs at high temperatures (> 300°C) due to the increased thermal energy of the electrons (6,7). An electron beam in air produces a swarm of scattered electrons with a continuous energy distribution decreasing from the initial beam energy. For a particle of given size and electric charge, a certain fraction of these electrons will have sufficient energy to overcome the Coulomb repulsion of the charged particle and attach to the particle, thereby raising the charge above the limit possible with ionic charging alone.

An electron beam precharger test facility has been constructed to evaluate the particle charging performance of an electron beam precharger for two-stage (charging, collection) electrostatic precipitation of high resistivity fly ash (8). In this paper the results of preliminary measurements of the performance of electron beam prechargers are reported. These experiments were done outside of the electron beam precharger test facility using a large portable frame with various configurations of electrodes. This allowed different precharger designs and configurations to be tested and changed quickly and easily. A Mark II precharger with a design based on these results is currently being constructed in the test facility for a comprehensive experimental evaluation.

## HIGH ENERGY ELECTRON BEAM PRECHARGERS

The 3 MeV Van de Graaff accelerator at Florida State University was used to generate a high energy electron beam which was brought out into air from vacuum through a 0.005 in. (0.13 mm) thick aluminum foil window. The electron beam energy is variable between 1 and 3 MeV but for these experiments a 1 MeV beam was used. The beam current was varied by controlling it at the accelerator cathode source and by mechanically restricting the amount of beam leaving the foil window with baffles.

### IONIZATION ZONE BOUNDARY

It is important to accurately measure the extent of the electron beam ionization zone in air. Inside this region, the electron beam ionization produces copious numbers of ion pairs (positive and negative) which neutralize any charge on a particle if no means of charge separation (i.e. an electric field) is provided. The drop shot method (see Figure 2a) was used to determine the extent of the ionization zone. Conductive spheres (shots) were dropped through a corona charger (Figure 2a) so that they received a constant amount of negative charge. The corona charger consists of a negative

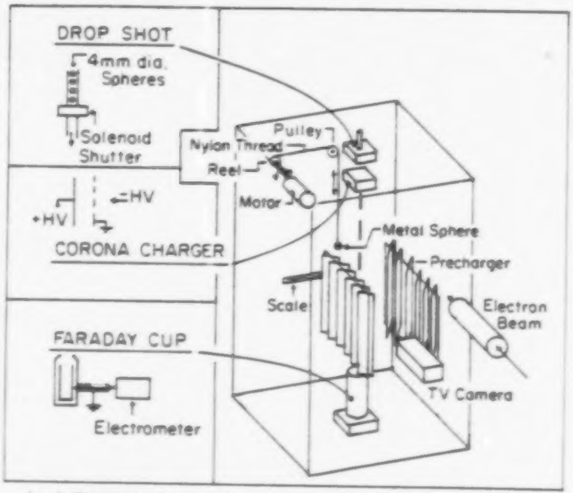
DROP SHOT
4mm dia. Spheres
Solenoid Shutter
+HV
−HV
CORONA CHARGER
FARADAY CUP
Electrometer
Nylon Thread
Pulley
Reel
Motor
Metal Sphere
Precharger
Scale
Electron Beam
TV Camera

(a.) Frame (Drop Shot and Suspended Sphere)

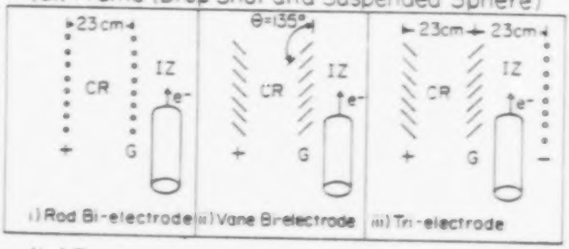
23cm
CR
IZ
e⁻
+
G
θ=135°
23cm
23cm
−
i) Rod Bi-electrode
ii) Vane Bi-electrode
iii) Tri-electrode

(b.) Precharger Configurations

Figure 2. Portable electron beam precharger test system.
a) Schematic of the portable test system showing the drop shot and suspended sphere methods of charge determination.
b) Various rod and vane electrode configurations of the high energy electron beam precharger. (CR = charging region, IZ = Ionization zone, G = ground electrode, + = anode electrode, - = cathode

corona point, a grounded grid electrode, and a positive plate electrode. The shot was dropped through the region between the grid and plate electrodes where it was charged using a uniform electric field. The shot then fell through the test region into a Faraday cup, where the amount of charge remaining on the shot was measured using an electrometer.

The extent of the ionization zone is very large for 1 MeV electrons because the electron range in air is ~ 4 meters (9). At a distance of 1.7 meters perpendicular to the beam axis, the positive ions (created by the beam) completely discharged the shot at 0.5 $\mu$A beam current, and at 0.1 $\mu$A only 50% of the shot charge remained. The effect was due to positive ions formed by energetic scattered electrons since in a separate experiment x-rays produced by a 1 $\mu$A electron beam had no effect on the shot charge. These measurements indicate that using a high energy electron beam produces a large ionization zone which discharges particles if no electric field is applied. Therefore, the ionization zone must be confined to the precharger volume to prevent the particles from being discharged after they exit the precharger.

## CONFINEMENT OF THE IONIZATION ZONE

In order to confine the ionization zone to a 1 $ft^3$ ($0.03m^3$) precharger volume, various orientations of vane-type electrodes were used to block the scattered electrons. The vane-electrodes consisted of 2'(60 cm) high x 2" (5 cm) wide x 1/8" (3 mm) thick rectangular aluminum plates arranged in a vertical rack geometry (see Figure 2). When the vanes were set perpendicular to the beam axis ($\theta = 90°$) they had no effect in preventing the penetration of scattered electrons (the remaining charge was the same as in the case without the vane electrodes). When the vanes were set at $\theta = 135°$, they decreased the discharging. At a beam current of 0.05 $\mu$A the remaining charge, ($Q_R$), was $Q_R = 80\%$ at $\theta = 135°$ and $Q_R = 35\%$ at $\theta = 90°$. For a beam current of 0.1 $\mu$A, $Q_R = 55\%$ at $\theta = 135°$ and $Q_R = 10\%$ at $\theta = 90°$. It was not possible to completely confine the ionization zone using vane electrodes without also blocking the air flow through the electrodes.

## CHARGING PERFORMANCE OF THE HIGH ENERGY ELECTRON PRECHARGERS

The charging performance of the high energy electron beam precharger was evaluated for both the bi-electrode and tri-electrode configurations. The saturation charge of a 5 mm diameter conducting sphere was determined by suspending the sphere by a nylon thread at various locations in the precharger volume as shown in Figure 2a. The saturation charge acquired by the conducting sphere is calculated by measuring the deflection of the sphere due to the electric field at the point of observation and using:

$$q = mgx/\ell E \tag{1}$$

where

$q$ = saturation charge of the sphere
$m$ = mass of the sphere

$g$ = acceleration due to gravity
$\ell$ = length of nylon thread
$x$ = measured deflection of the sphere
$E$ = electric field strength

The particle charging rates were obtained using the drop shot method with the corona charger removed. The shot is charged as it passes through the precharger volume, with the total charge received by the shot dependent on the charging rate and the exposure time.

The precharger configurations tested are shown in Fig. 2b where the anode electrodes are labeled with a "+", the cathode electrodes with a "-", and the ground electrodes with a "G". The charging regions are labeled with a "CR" and the regions of intense ionization are labeled with an "IZ". In actual operation the particle-laden gas flow would be from right to left for all three configurations.

## Bi-Electrode Precharger (Rod Type)

In the rod bi-electrode configuration (see Figure 2b(i)) two racks of 1/4 in. (6 mm) diameter rods are placed downstream from the electron beam. In the region between the rod electrodes, the applied electric field separates the positive and negative ions and the particle receives a negative charge when it passes into the region containing negative ions near the anode.

Using the suspended sphere method the saturation charge was measured at various positions inside the rod-electrode precharger volume. The values were much lower than those predicted by Pauthenier's field charging theory (1,2). This was due to the presence of positive ions (produced by scattered electrons) in the precharger volume which reduced the negative saturation charge. The final charge on the particle is predominantly determined by the ratio of the negative and positive ion densities last experienced by the charged particle before it exits to an ion-free region (10). For example, if the objective is to charge a particle negatively, the maximum charge which the particle will retain is reduced by 20% below the theoretical monopolar saturation charge if 1% of the ion population is positive with the rest negative.

In the rod bi-electrode precharger the ionization zone extends into the entire inter-electrode region (because the electron beam scatters in all directions), therefore a complete separation of the positive and negative ions is not possible since positive ions are created near the anode by the scattered electrons. The electric field does not completely separate the ions but produces a concentration gradient of positive ions between the electrodes. Downstream from the anode in the region where there is no electric field the ions are not separated and particles in a gas stream would be discharged after exiting the precharger.

### Bi-Electrode Precharger (Vane Type)

The rod electrodes were replaced by vane electrodes (as shown in Figure 2b(ii)) to reduce the number of scattered electrons reaching the region near the anode. A vane electrode was used for the anode to further shield the volume downstream from the anode from scattered electrons. The measured saturation charge for the vane-type precharger agreed with Pauthenier's field charging theory and was higher than that in the rod-type precharger because the vane electrodes prevented most of the scattered electrons from entering the charging volume. However, the drop shot experiments showed that the charging rate was low (the vanes reduced the negative ion current density).

### Tri-electrode Precharger (Vane Type)

In order to increase the flow of negative ions through the grounded vane electrode a third electrode was added to the precharger (see Figure 2b(iii)). The electric field supplied by the third electrode extracts the negative ions out of the ionization region and into the charging region. The saturation charge was measured in the charging region of the tri-electrode precharger and it also agreed with field charging theory. The drop shot measurements taken in the charging region indicated that the charging rate was higher than that for the bi-electrode vaned precharger. However, this charging rate was lower than optimum because the vanes still blocked many of the negative ions extracted from the ionization zone.

The results of the high energy electron beam precharger experiments indicate that using vane electrodes to confine the ionization zone (scattered electrons) is not satisfactory because the vanes do not stop all the scattered electrons, the vanes block some of the negative ion charging current, and they restrict the air flow through the precharger. Since it is very difficult to confine the ionization zone formed by a high energy electron beam, the precharger volume should be larger than the ionization zone volume.

## LOW ENERGY ELECTRON BEAM PRECHARGERS

A direct and effective method of achieving a well controlled ionization zone localized in a prescribed volume of precharger is to simply choose a beam energy such that the ionization zone is smaller than the precharger volume. The volume of the ionization zone depends on the range of the electron beam in air, which decreases with decreasing electron beam energy. Therefore a low energy (< 100 keV) electron beam was used to provide a well defined ionization zone commensurate in size with the precharger module of the electron beam precharger test system.

The low energy electron accelerator was designed and constructed as shown in Figure 3. The accelerator consists of a hot filament cathode and accelerating electrodes which are all contained within a 2" (5 cm) diameter PVC tube that is under high vacuum. Negative high voltage was applied to the filament, and a resistor chain was used to divide the voltage so that the accelerating electrodes were maintained at successively lower voltages with the final electrode being at ground potential. In operation, electrons are emitted by the hot filament and are accelerated by the high voltage to the final electrode where they pass through a 0.001 in. (25 μm) thick aluminum foil window into the air. The energy of the electron beam can be set between 0 and 100 keV and the current can be varied between 0 and 10 μA (measured on the foil window at the end of the accelerator). The electron beam energy and current decrease when the beam passes through the foil window.

Tri-electrode and bi-electrode prechargers which were constructed outside the test system for the first experiments with the low energy electron beam are shown in Figures 4 and 5. In both prechargers the low energy electron beam passes

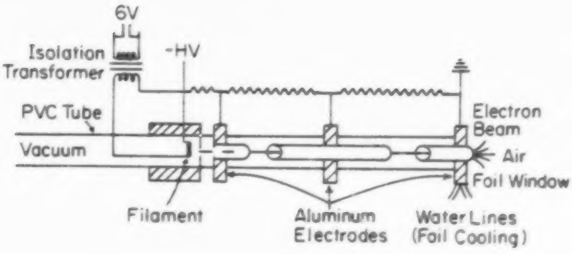
6V
Isolation Transformer
-HV
PVC Tube
Vacuum
Electron Beam
Air
Foil Window
Filament
Aluminum Electrodes
Water Lines (Foil Cooling)

Figure 3. Low energy electron accelerator .

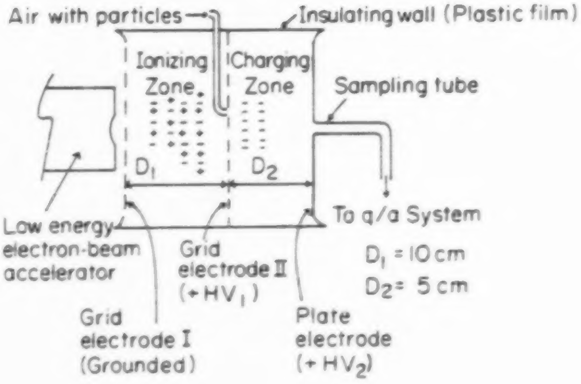
Air with particles
Insulating wall (Plastic film)
Ionizing Zone
Charging Zone
Sampling tube
$D_1$
$D_2$
To q/a System
Low energy electron-beam accelerator
Grid electrode II (+HV$_1$)
Grid electrode I (Grounded)
Plate electrode (+HV$_2$)
$D_1$ = 10 cm
$D_2$ = 5 cm

Figure 4. Schematic diagram of the tri-electrode low energy electron beam precharger.

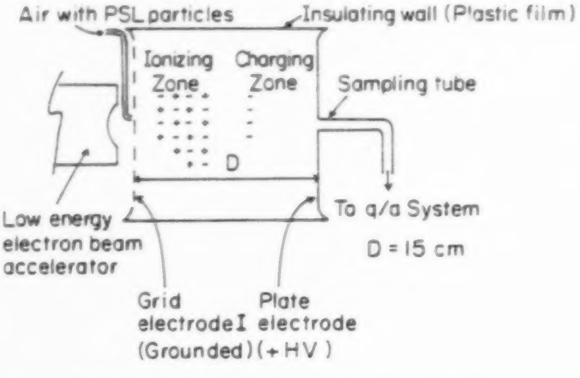
Air with PSL particles
Insulating wall (Plastic film)
Ionizing Zone
Charging Zone
Sampling tube
D
To q/a System
Low energy electron beam accelerator
D = 15 cm
Grid electrode I (Grounded)
Plate electrode (+HV)

Figure 5. Schematic diagram of the bi-electrode low energy electron beam precharger.

through the grounded grid electrode I (which is placed 0.5 cm from the foil window) and produces the ionization zone inside the precharger electrode assembly. Negative ions and free electrons are extracted from the ionization zone by an applied electric field. In the tri-electrode precharger a high voltage grid electrode II was used to provide an extraction electric field. The charging electric field is determined by the voltage difference between the grid electrode II and the plate electrode.

The charging performance of the low-energy bi-electrode and tri-electrode prechargers was studied using the suspended sphere method and also by measuring the charge acquired by 1.1 μm or 3.0 μm diameter PSL particles (uniform spheres of polystyrene latex). The aerosol was generated from a solution of ethanol and PSL which was atomized using a FLAG (Fluidized Aerosol Generator). Dry air (less than 8% relative humidity) or nitrogen gas was used at room temperature (22°C) for the resuspension of the PSL particles. This test gas was injected into the precharger volume which was sealed with plastic film. The particles were sampled from the charging region with a sampling tube located at the center of the plate electrode. The particle charges were measured using the charge-to-radius (q/a) measuring device (11). The accuracy of the q/a device was verified by comparing the measured charge of 1.1 μm diameter PSL particles which were charged by the corona charger (see Figure 2a) using a known electric field strength and current density to the charge predicted by field charging theory. The size of the PSL particles was verified by measuring their free fall velocity in the q/a device. In the following precharger experiments, the q/a of ~ 30 particles was measured, averaged, and plotted for each condition with the standard deviations indicated by bars on the data plots.

## IONIZATION ZONE BOUNDARY

When an electron beam passes through air it loses energy and intensity due to collisions with air molecules. The decrease of the electron beam intensity (current) with penetration distance in air was measured using a probe electrode. The beam energy was 90 keV and the beam current was 10 μA (measured on the foil window). The aluminum probe electrode consists of a 2" (5 cm) diameter and 3/8" (1 cm) thick measuring electrode surrounded by a grounded guard electrode. The electron beam current intercepted by the probe was read using an ammeter connected between the measuring electrode and ground. The probe current vs. probe distance from the foil window is shown in Figure 6. The beam current decreases rapidly with increasing distance. This measurement indicates that the beam penetration range is about 10 cm.

The drop shot method was also used to determine the beam penetration range (extent of the ionization zone) by measuring the discharging of a negatively charged sphere dropped at various distances in front of the accelerator. When the sphere was dropped 50 cm from the accelerator foil window all the charge remained, but as the distance from the accelerator was decreased the remaining charge decreased, with no charge remaining when the sphere was dropped 10 cm from the accelerator. The partial discharging of the sphere in the region between 10 and 50 cm from the accelerator window indicated that in the absence of an electric field the positive ions were diffusing out of the ionization zone and discharging the sphere. Therefore a different method was used to verify that the ionization zone extended 10 cm from the accelerator window at 90 keV beam energy.

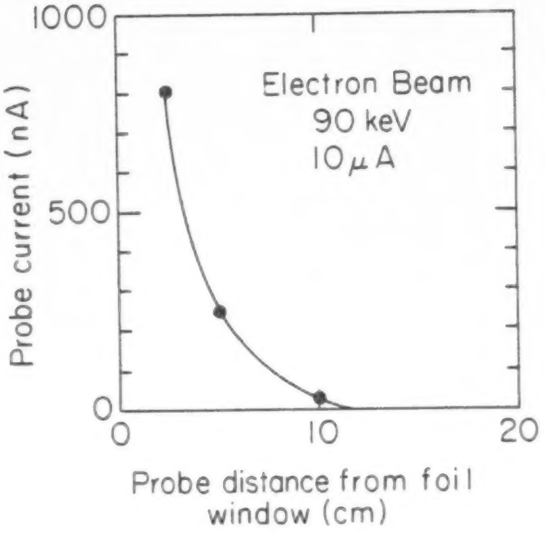

Figure 6. Decrease of the low energy electron beam intensity (current) in air.

The ionization zone was experimentally determined by using the tri-electrode precharger geometry shown in Figure 4. Both grid electrodes were grounded and dc +10 kV (+$HV_2$) was applied to the plate electrode. The PSL particles suspended in dry air were injected between the grid and plate electrodes and their charge was monitored continuously. The electron beam current was 10 μA (measured on the foil window). The accelerator voltage (beam energy) was raised gradually until charged PSL particles were observed. This charging onset indicates that the range of the ionization zone produced by the electron beam reached the position of grid electrode II (10.5 cm from the foil window) so that negative ions were extracted into the charging zone by the electric field and the particles were charged. The PSL particles were charged when the beam energy exceeded 90 keV, which is in agreement with the penetration range of 10 cm for a 90 keV beam obtained with the beam probe measurement. This beam energy also agrees with the value predicted by theory for a penetration range of 10.5 cm in air (9).

## CHARGING PERFORMANCE OF THE LOW ENERGY ELECTRON BEAM PRECHARGERS

### Tri-Electrode Precharger

The particle charging efficiency of the tri-electrode low energy electron beam precharger (see Figure 4) was measured. In this precharger, a 10 μA electron beam with an energy of 80 keV is used so that the ionization zone is contained between grid electrodes I and II (separation $D_1$ = 10 cm) where an extraction electric field of 1.0 kV/cm is applied. The negative ions (and possibly free electrons) are extracted into the 5 cm wide charging region between grid electrode II and the anode plate. The suspended sphere method was used to obtain the saturation charge for a

10 mm (3/8") diameter conducting sphere suspended in the center of the charging region with electric field strengths of 1 to 8 kV/cm. The measured values agreed with those predicted by ionic field charging theory. When the extraction electric field strength was increased to 4 kV/cm the measured values of charge were slightly higher than the theoretical values.

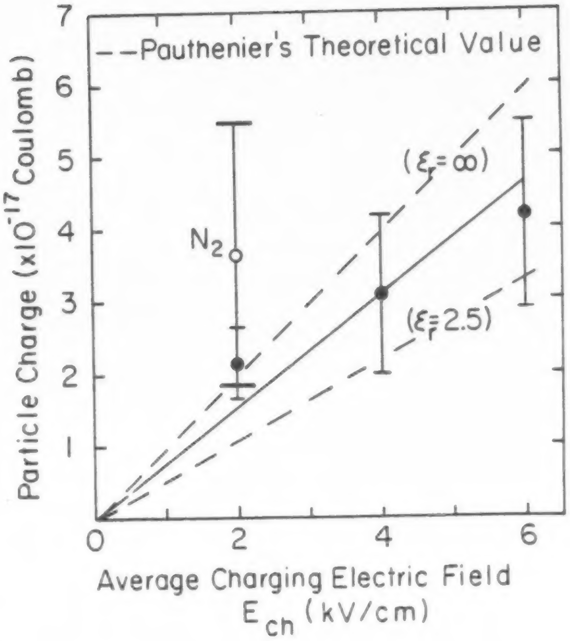

Figure 7. Average particle charge vs. average electric field strength for 1.1 μm diameter PSL particles in the tri-electrode low energy electron beam precharger. The dotted lines are Pauthenier's theoretical ionic field charging values for the saturation charge of 1.1 μm diameter particles with relative dielectric constants of $\varepsilon_r = 2.5$ and $\varepsilon_r = \infty$.

The charging performance of the low energy tri-electrode precharger was also determined by measuring the charge acquired by 1.1 μm diameter PSL particles. The test gas (dry air or pure nitrogen) containing the PSL particles was injected through a nozzle located at grid electrode II. The average residence time of the PSL particles in the charging zone was 7 sec. This was much longer than the charging time constant of several milliseconds. When dry air is used, the number of free electrons extracted at 1 kV/cm from the ionization zone to the charging zone is negligible because electrons attach to electronegative oxygen molecules and become negative ions. In pure nitrogen, however, free electrons can be extracted into the charging zone.

In Figure 7 the average measured charge of the PSL particles is plotted against the charging electric field strength $E_{ch}$. At each charging electric field value the current density in the charging zone was $\{E_{ch}(\mathrm{kV/cm}), J(\mathrm{mA/m^2})\}$ = (1, 0.5), (2,1), (3, 1.5), and (4, 2.5). The extraction electric field strength was 1 kV/cm. The measured charge of the 1.1 μm diameter PSL particles in air was proportional to the charging electric field $E_{ch}$ for $E_{ch}$ = 2.0 to 6.0 kV/cm. In Figure 7 Pauthenier's theoretical saturation charge for a 1.1 μm diameter spherical particle is indicated by dotted lines (1,2). The upper line is for conductive particles having a relative dielectric constant $\varepsilon_r = \infty$, and the lower line for PSL particles with $\varepsilon_r = 2.5$.

The measured charge was higher than the theoretical value for PSL particles but was lower than the theoretical value for conducting ($\varepsilon_r = \infty$) particles. The reason for this increased charge will be discussed later. The proportionality of the charge vs. charging electric field strength indicates that the charge of 1.1 μm diameter PSL particles is mainly determined by Pauthenier's field charging mechanism and that the effect of ion diffusion charging (1,2) is relatively small for these experimental conditions.

The measured charge of PSL particles suspended in nitrogen is also shown in Figure 7. The charge measured at $E_{ch}$ = 2.0 kV/cm was more than 1.5 times larger than that of PSL particles in air. The charge measurement at higher $E_{ch}$ could not be made because the PSL particles were collected inside the precharger so that no particles could be introduced into the q/a measuring device. This result suggests that the charge of PSL particles in nitrogen was much higher than that in air.

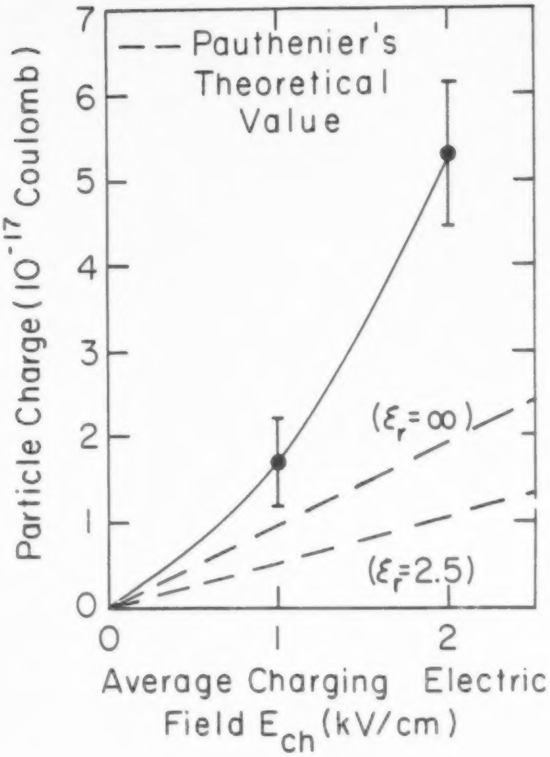

Figure 8. Particle charging in the bi-electrode low energy electron beam precharger (D = 25 cm) using 1.1 μm PSL particles. The dotted lines are theoretical field charging values for the saturation charge of 1.1 μm diameter particles with $\varepsilon_r$ = 2.5 and $\varepsilon_r = \infty$.

## Bi-Electrode Precharger

The charging performance of the bi-electrode precharger was investigated. Positive dc high voltage was applied to the plate electrode and electrode separations of 15 and 25 cm were used. The energy of the electron beam was 90 keV and the beam current was 10 μA (measured on the foil window). This beam produces an ionization zone which extends approximately 10 cm from grid electrode I (which was placed 0.5 cm from the foil window). The charging region is between the ionization zone and the anode plate. The suspended sphere method was used to obtain the saturation charge of a 10 mm diameter conducting sphere suspended in the charging region of the bi-electrode precharger with a 15 cm electrode separation. For average electric field strengths between 2 and 4 kV/cm, the measured deflection of the suspended sphere (see Eq. 1) was approximately four times larger than that predicted by field charging theory. In the bi-electrode precharger, a large enhancement of the charging electric field is expected because of the presence of the ionization zone. However, space charge enhancement of the electric field was not considered in this comparison, i.e., the average electric field strength (voltage difference divided by electrode separation) was used in Eq. 1 and in the field charging theory.

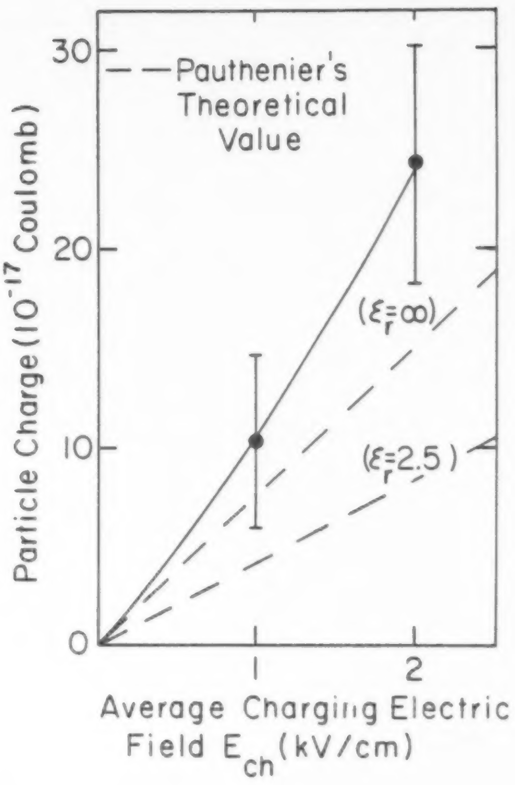

Figure 9. Particle charging in the bi-electrode low energy electron beam precharger (D = 25 cm) using 3.0 µm diameter particles. The dotted lines are the theoretical saturation charge values for 3.0 µm diameter particles with $\varepsilon_r = 2.5$ and $\varepsilon_r = \infty$.

The charging performance of the low energy electron beam bi-electrode precharger was determined by measuring the charge acquired by 1.1 µm and 3.0 µm PSL particles. Dry air was used for the resuspension of PSL particles with the nozzle for particle injection placed at grid electrode I. The average residence time of the PSL particles in the entire precharger volume was 35 sec. Since the particles are not charged in the ionization zone, the actual charging time is the residence time in the charging region which is estimated to be 21 sec. The average measured charge is plotted vs. average charging electric field strength for 1.1 µm diameter PSL particles in Figure 8 and for the 3.0 µm diameter PSL particles in Figure 9. Pauthenier's theoretical values for $\varepsilon_r = \infty$ and $\varepsilon_r = 2.5$ are plotted in these figures. At each average charging electric field value the current density $\{E_{ch}(kV/cm), J(mA/m^2)\}$ was: E = 1,J = 0.6 and E = 2,J = 2.5. Using the bi-electrode precharger the PSL particles acquired a very high charge. The measured charge of the 1.1 µm diameter PSL particles was 5 times larger than the theoretical value for PSL particles ($\varepsilon_r = 2.5$) at $E_{ch} = 2.0$ kV/cm. The charge measurement at higher values of $E_{ch}$ was attempted, but the PSL particles were completely collected inside the precharger volume so that no particles could be sampled. This result suggests that the PSL particles had a very high level of charge.

## DISCUSSION

Since PSL particles are atomized from a liquid suspension they may have a residue on their surface which hinders evaporation of the liquid (12) and results in a slightly conductive layer on the particle surface. This layer allows a more uniform surface potential distribution (13) and increases the effective relative dielectric constant of the particle to a value between $\varepsilon_r = 2.5$ and $\varepsilon_r = \infty$ (a good conductor has a very uniform surface potential and $\varepsilon_r = \infty$). Therefore the value of the saturation charge from field charging should be between Pauthenier's theoretical values for $\varepsilon_r = 2.5$ and $\varepsilon_r = \infty$.

In the bi-electrode precharger the suspended sphere and the PSL particles received a charge which is much higher than that possible with normal ion charging. The increased charge may be partly caused by the space charge enhancement of the charging electric field. This occurs because the ionization zone (conductive bi-polar plasma) reduces the effective electrode spacing. Charging electric field enhancement also occurs due to the finite drift velocity of the space charge in the monopolar region.

Free electron diffusion charging may also produce an increase in particle charge in the bi-electrode precharger. This may occur when the particles are in the region near the end of the ionization zone. This region contains a large number of free electrons which have not lost sufficient energy to become attached to $O_2$ molecules and form negative ions.

The comparison of the PSL particle charges in the bi-electrode precharger (Figures 8 and 9) shows that the increase in charge of 3.0 μm diameter particles was substantial, but that the increase for 1.1 μm diameter particles was even greater. At $E_{ch} = 2.0$ kV/cm the charge acquired by the 3.0 μm diameter particles is 3 times higher than Pauthenier's theoretical value for 3 μm particles while the charge of 1.1 μm diameter PSL particles is 5 times larger than the theoretical value for 1.1 μm particles. This suggests an increase in diffusion charging efficiency with decreasing particle size. Free electrons may be involved in this diffusion charging in addition to ions. As shown in the results of the tri-electrode precharger operated at a similar level of $E_{ch}$ and J as the bi-electrode precharger, the effect of ion diffusion charging for 1.1 μm diameter particles is relatively small. The theoretical charge acquired by a 1.1 μm diameter particle by ion diffusion charging (1,2) is $2 \times 10^{-17}$C when the current density is 2.5 $mA/m^2$ and the residence time is 21 sec. This calculated ion diffusion charge is smaller than the measured value of particle charge. These considerations suggest free electron diffusion charging contributes to the increase in charge in the bi-electrode precharger.

In the tri-electrode precharger, the measured charge of the suspended sphere and the 1.1 μm diameter PSL particles in air is not as high as the bi-electrode precharger values. Using the tri-electrode configuration greatly reduces the space charge enhancement of the charging electric field, and at $E_{ext}$ = 1 kV/cm the percentage of free electrons in the charging region is also lower than in the bi-electrode precharger because the charging region is farther from the end of the ionization zone. The measured charge agrees with Pauthenier's theoretical field charging values and is proportional to the charging electric field. These results suggest that the particle charge in the tri-electrode precharger is mainly determined by the field charging mechanism, and that the effect of diffusion charging due to ions as well as electrons is small. However, ion diffusion charging may slightly increase the particle charge at lower electric field strengths where field charging is less effective.

Using nitrogen gas in the tri-electrode precharger results in a higher value of PSL particle charge. In this case the percentage of free electrons in the charging region increases because electrons do not attach to nitrogen molecules. The charge of the conductive sphere suspended in the tri-electrode precharger in air was slightly higher than the theoretical ionic field charging value when the extraction electric field ($E_{ext}$) was increased from 1 kV/cm to 4 kV/cm. This also suggests that free electron charging is occurring because electrons are less likely to attached to $O_2$ molecules at higher electric field strengths. However, the particle charge should not be significantly effected by the presence of free electrons if field charging determines the saturation charge. This suggests that free electron diffusion charging may cause the increased particle charge.

## CONCLUSION

The results of these measurements of the performance of the high and low energy electron beam prechargers are summarized as follows:

1) When a high energy (~ 1 MeV) electron beam passes through air the electrons are scattered and produce a large (> 2m) ionization zone (region of bipolar charge) which discharges particles if no electric field is applied to separate the ions.

2) The performance of the vane-electrode high energy electron beam precharger was unsatisfactory because the vanes were not completely effective in confining the scattered electrons. These energetic scattered electrons created positive ions in the negative charging region which degraded the charging performance. Therefore the precharger volume should be larger than the ionization zone volume.

3) A low energy electron beam (80-90 keV) produces a small, well defined, and easily controlled ionization zone inside the precharger volume. This eliminates the degradation of the charging performance and the discharging of particles outside the precharger by spurious ionization due to scattered electrons.

4) The tri-electrode low energy electron beam precharger uses a uniform and controllable charging field to achieve slightly higher than theoretical charge values for suspended spheres and for 1.1 μm diameter PSL particles in air. When the PSL particles are suspended in nitrogen gas (non-electronegative gas), the charge becomes 1.5 times higher than that in air. This suggests a significant contribution of free electron diffusion charging.

5) The bi-electrode low energy electron beam precharger charges suspended spheres and 1.1 and 3.0 μm diameter PSL particles to a much higher value than that predicted by ionic charging theory. The increased charge may be caused by space charge enhancement of the electric field and by free electron diffusion charging.

6) Taken together, these results indicate that a low energy electron beam precharger with a bi-electrode geometry is extremely effective in charging 1.1 and 3.0 μm diameter particles. The next step is to install the low energy electron beam precharger in the precharger test facility (8) and evaluate its charging performance using polydisperse aerosols with medium and high particle concentrations.

## REFERENCES

1. H.J. White. Industrial Electrostatic Precipitation. Addison-Wesley, Reading, Massachusetts, 1963.

2. S. Oglesby and G.B. Nichols. Electrostatic Precipitation. Marcel Kedder, Inc., New York, 1978.

3. R.H. Davis and W.C. Finney. Ionization by Electron Beams for Use in Electrostatic Precipitators. Energy Research 2, 1978, pp. 19-27.

4. W.C. Finney, L.C. Thanh, J.S. Clements, and R.H. Davis. Primary and Secondary Ionization in an Electron Beam Precipitator System. In: Proc. of the Third Symposium on the Transfer and Utilization of Particular Control Technology, sponsored by U.S. EPA, Orlando, Florida, March 1981.

5. J.S. Clements, W.C. Finney, O. Tokunaga, and R.H. Davis. Stable Secondary Ionization in a Test Geometry for Electron Beam Precipitators. In: Conf. Record of the IAS-IEEE Annual Meeting, Philadelphia, PA, October 1981, pp. 1136-1141.

6. C.C. Shale. New Concept of Electron Detachment for Air in Negative Corona at High Temperature. Circular 8353, U.S. Bureau of Mines, 1967.

7. J.S. McDonald, M.H. Anderson, R.B. Mosely, and L.E. Sparks. Charge Measurements on Individual Particles Exiting Laboratory Precipitators. In: Proc. of the Second Symposium on the Transfer and Utilization of Particulate Control Technology, Volume II, Electrostatic Precipitators, EPA-600/9-80-0396, 1980, p. 93-113.

8. J.S. Clements, W.C. Finney, and R.H. Davis. An Electron Beam Precharger Test Facility for Two-Stage Electrostatic Precipitation of Coal Fly Ash. In: Proceedings of ASME Industrial Pollution Control Symposium, Houston, TX, Feb. 1983, pp. 159-164.

9. M.J. Berger and S.M. Seltzer. Tables of Energy Losses and Ranges of Electrons and Positrons. NASA SP 3012, 1964, p. 124.

10. S. Masuda. Resistivity and Back Corona. In: Proc. First International Conference on Electrostatic Precipitation, sponsored by EPRI, AGCI, and APCA, Monterey, CA, October 1981, pp. 360-362.

11. A. Mizuno and M. Otsuka. Development of a Charge-to-Radius Measuring Apparatus for Sub-micron Particles--Preliminary Study. In: Conf. Record of IAS-IEEE Annual Meeting, San Francisco, California, October 1982, p. 1111.

12. O. Raabe. The Dilution of Monodisperse Suspensions for Aerosolization. American Industrial Hygiene Association Journal, 29, 1968, pp. 439-443.

13. S. Masuda, M. Washizu, A. Mizuno, and K. Akutsu. Boxer Charger-A Novel Charging Device for High Resistivity Powders. In: Conf. Record of IAS-IEEE Annual Meeting, Toronto, Canada, October 1978, p. 16.

*Supported by U.S. DOE Contract No. DE-AC22-83PC60266

The work described in this paper was not funded by the U.S. EPA and therefore the contents do not necessarily reflect the views of the Agency and no official endorsement should be inferred.

# CHARGING OF PARTICULATES BY EVAPORATING CHARGED WATER DROPLETS

by: G.S.P. Castle*, I.I. Inculet*, and R. Littlewood**
*The University of Western Ontario, London, Ontario
Faculty of Engineering Science
**Stelco Incorporated
Hamilton, Ontario

## ABSTRACT

The paper describes experiments which show the feasibility of charging aerosols by injecting fast evaporating charged water droplets. The charged water droplets having charge to mass ratios in excess of 50 microcoulomb per gram are produced by combined ultrasonic atomization and conduction charging. Laboratory tests show the effectiveness of charging in a modified two stage electrostatic precipitator system. Potential applications of the new system are presented.

# INTRODUCTION

Depending upon the application of interest there are many physical processes available for producing electric charges on particles. For example, fracturing of the material, contact electrification, spraying of liquids, thermionic emission and ionic bombardment are all methods which can be used in certain circumstances. However, in applications such as electrostatic precipitation where the intent is to maximize the collection of particles, experience has shown that the preferred method involves bringing the particles into contact with a copious supply of unipolar air ions. These ions, normally produced in a corona (1) or similar type of discharge (see for example the "boxer" charger (2)), charge the particle through the combined effects of field directed ionic bombardment and random diffusion impact.

Although charging by corona is normally the most effective way to maximize the particle charge there are certain constraints with the process, namely;

(a) the geometrical requirements of corona and the high mobility of the air ions restrict the effective charging zone to relatively small lateral dimensions i.e.: tens of centimeters maximum,

(b) the charge adhering to the particles corresponds to a very small fraction of the total ion charge and thus the process is inefficient and wasteful of electric power,

(c) although the corona discharge itself is inherently safe (3), the high electric fields required may lead to sparkover which presents explosion hazards in certain environments,

(d) in collection of high resistivity dust the continuous passage of corona current leads to back ionization and resultant reduction in the net charge,

(e) the corona discharge produces ozone a byproduct which is particularly undesirable in air cleaning precipitators.

None of these constraints implies that corona charging is unacceptable but it does establish some boundaries where other charging methods should be considered. Examples exist when it is desirable to;

(a) charge large volumes of particles from a local source,

(b) maximize the efficiency of ion utilization in charging,

(c) minimize the danger of explosion,

(d) charge and collect high resistivity dust,

(e) eliminate the generation of ozone.

In a previous study (4) it was demonstrated that it is possible, under proper conditions, to inject charge into a cloud of particles using charged water droplets as a carrier and subsequently transfer much of this charge onto the particles present in the volume. In this process very small pure water droplets are initially charged by either conduction or induction charging. The droplets then act as a charge transfer medium and as they move through space undergo the combined effects of evaporation and droplet disruption caused by the Rayleigh instability. This ultimately leads to the liberation of highly mobile ions (5) which will quickly adhere to clusters of molecules and particle surfaces thus producing charging analogous to the diffusion charging component of the corona discharge.

In the case where the water is impure, i.e.: has dissolved salts or contains other solid materials, this leads to a net charge on the residue following evaporation.

It is important to realize that this process differs considerably from other forms of charged droplet scrubbers (6) or agglomerators (7) in that the spray must be designed to allow full evaporation of the water.

The laboratory tests described previously (4) showed the feasibility of this being applied to fugitive dust emissions in large enclosed structures such as foundries etc. A larger scale injection system with a charged droplet throw of approximately 10 m at a water flow rate of 5 kg/hour and a charge to mass ratio of over 8 microcoulomb/gram has been constructed and is currently awaiting field testing (8).

However, the process also suggests several other possible applications, namely in specialized purpose two stage precipitators and in spray humidification systems.

The remainder of this paper describes experiments that have been carried out to demonstrate the feasibility in these two applications.

## EXPERIMENTAL

### CHARGED WATER ATOMIZER

In the previous study, air jet atomization was used with combined conduction-induction charging. This atomizer worked well but had very limited output and required voltages as high as 12 kV for optimum performance. In this work ultrasonic atomization was used and a commercial nozzle (SONIMIST$^{TM}$ Model 600-1) was modified to allow conduction charging. This was accomplished by replacing the original metallic liquid stem and holder assembly (see Figure 1) with an identical unit made from Delrin, an electrical insulator. The metallic main body was grounded and the liquid feed was isolated from ground using a plastic syringe and tubing.

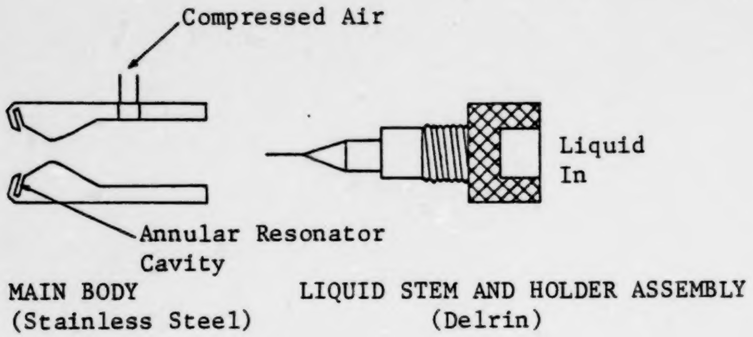
Compressed Air
Liquid In
Annular Resonator Cavity
MAIN BODY (Stainless Steel)
LIQUID STEM AND HOLDER ASSEMBLY (Delrin)

Figure 1. Exploded Crossectional View of the Ultrasonic Nozzle

The plunger of the syringe was modified by adding a conductive core which made contact with the water. This was connected to a regulated D.C. voltage source (0 - 1.2 kV, Keithley 240A). In normal operation the voltage was set at 1.2 kV, the water feed rate at 2.2 mℓ/min and the ultrasonic nozzle was activated with compressed air at 200 kPa (30 psi). Under these conditions 95% of the water droplets produced are in the size range 0.1 - 1.0 μm diameter (9).

The effective charge to mass ratio for the particles was determined using the arrangement shown in Figure 2. The measured current and mass flow rate are related as:

$$\text{charge/mass}\left(\frac{C}{kg}\right) = \frac{\text{current (A)}}{\text{mass flow rate (kg/s)}}$$

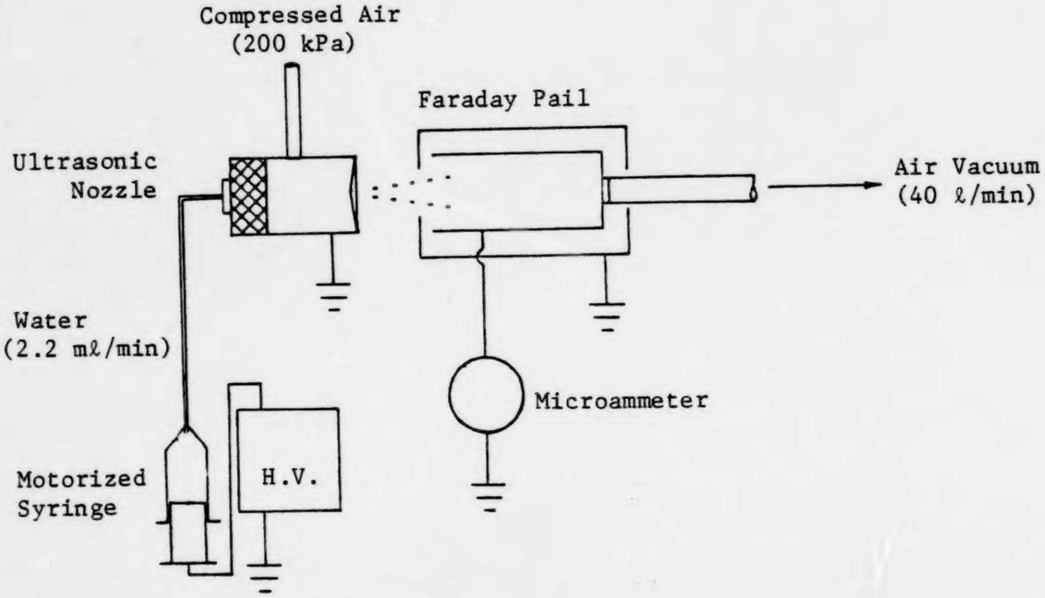
Compressed Air
(200 kPa)
Faraday Pail
Ultrasonic Nozzle
Air Vacuum
(40 ℓ/min)
Water
(2.2 mℓ/min)
Microammeter
Motorized Syringe
H.V.

Figure 2. Experimental Arrangement for Determining Charge to Mass Ratio

The resulting values of charge to mass ratio as a function of voltage are shown in Figure 3.

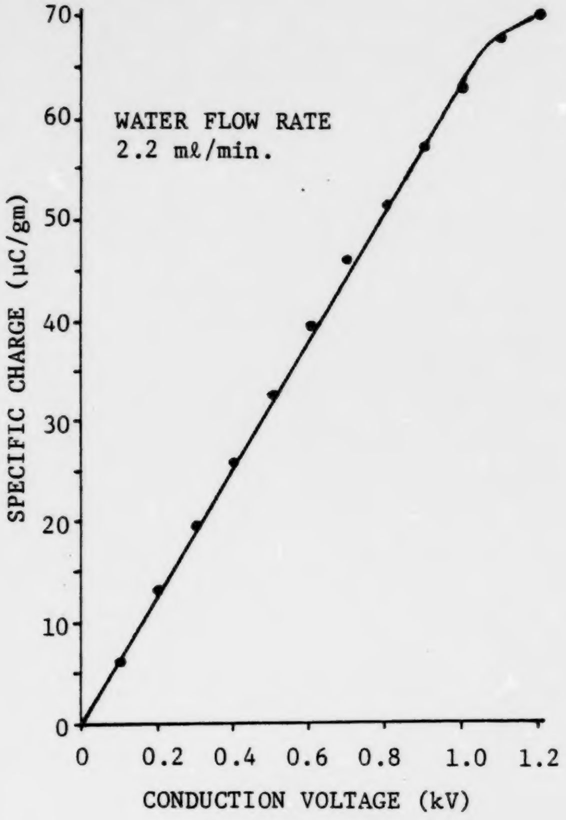

Figure 3. Charge to Mass Ratio For Water With Conduction Charging in Ultrasonic Nozzle

PARTICLE GENERATOR

Methylene blue particles were used as the test aerosol. For the precipitator testing these were generated using a spinning disk aerosol generator (Environmental Research Corp. Model 8320). The disk was fed from a motorized syringe at a rate of 2.2 mℓ/min with a liquid solution consisting of 75% ethanol and 25% distilled water containing 1% by weight of methylene blue and 0.5% by weight uranine. By previous testing (10) it was known that this produced particles approximately 5 μm mass mean diameter and containing the fluorescent tracer in direct proportion to the mass of methylene blue.

TEST DUCT

Experiments were carried out in a test duct 36 cm high consisting of a blower, mixing chamber, main duct, conventional two-stage precipitator and exhaust fan. (See Figure 4.) Each section was electrically isolated from

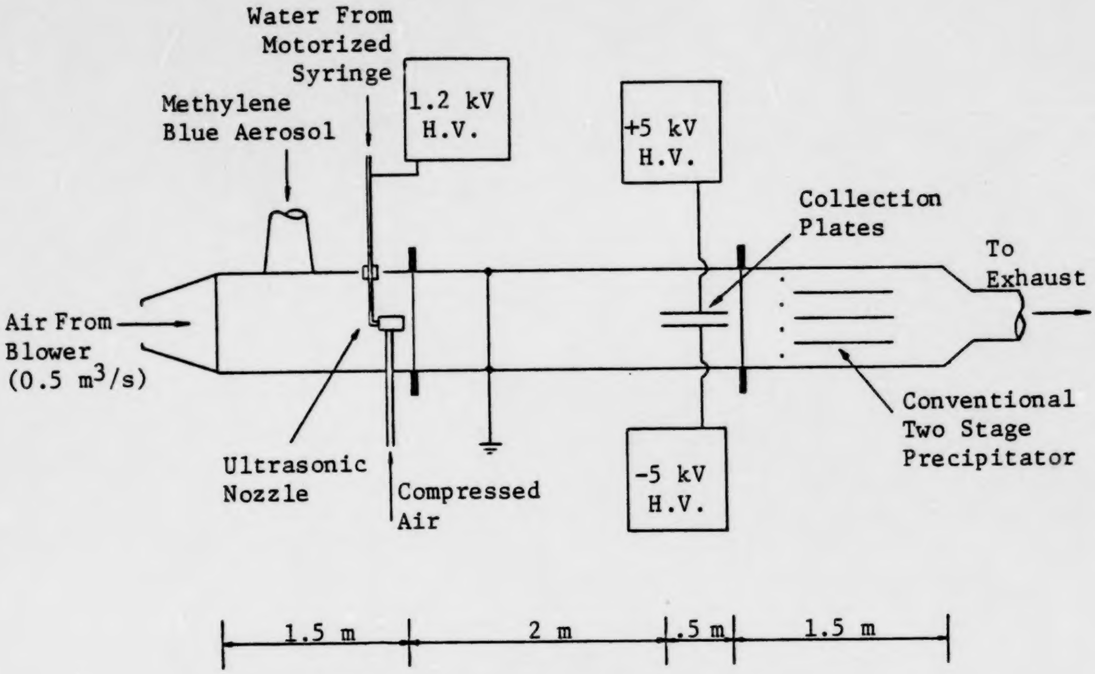
Water From Motorized Syringe
Methylene Blue Aerosol
1.2 kV H.V.
+5 kV H.V.
Collection Plates
To Exhaust
Air From Blower (0.5 m³/s)
Ultrasonic Nozzle
Compressed Air
-5 kV H.V.
Conventional Two Stage Precipitator
1.5 m
2 m
.5 m
1.5 m

Figure 4. Test Duct Arrangement

the adjoining section and connected to ground via a microammeter. The mixing chamber was made of plexiglass and had an inlet port fed from the particle generator. Downstream from this point, the ultrasonic nozzle was mounted and oriented upstream to give maximum mixing with the main air flow. Particle collection was measured in the main duct using a pair of collection plates 30 cm high by 30 cm long separated by a spacing of 2 cm. (This sampled approximately 10% of the duct crossection.) The collection plates were maintained at a potential difference of 10 kV thus creating a static collection field of 5 kV/cm. Each collection plate was subdivided lengthwise into four separate removable sampling sections 30 cm high by 7.5 cm wide. These sections were covered with aluminum foil to allow sampling of the particle collection along the length of the duct. The commercial two stage precipitator was used for comparative testing.

## ANALYSIS

The quantity of methylene blue collected in the experiments was determined by fluorometric analysis. Following each test the aluminum foil was removed from each section of the collection plates and carefully washed in a fixed volume of ethanol. This solution was then analysed in a fluorometer (Turner model 100) for the concentration of uranine which could then be related to the quantity of methylene blue using a calibration curve established beforehand.

A similar procedure using isokinetic sampling and millipore filter paper was used to establish collection efficiency in the two stage precipitator.

## TESTING AND RESULTS

### TWO STAGE ELECTROSTATIC PRECIPITATOR

The first set of experiments was intended to determine the effectiveness of using the charged water atomizer as a charging mechanism instead of the corona charging normally used in the precipitator.

In these tests the methylene blue was injected as described previously and four separate conditions were maintained for the ultrasonic atomizer namely:

Test 1 ≡ atomizer off

Test 2 ≡ atomizer on, 0 kV

Test 3 ≡ atomizer on, + 1.2 kV

Test 4 ≡ atomizer on, - 1.2 kV

The amount of methylene blue collected on the test plates was measured for each of these conditions and is shown graphically in Figure 5. (Each result is based upon five sets of experiments and are consistent to within a standard deviation of 15%.) Table 1 below shows the total mass deposition on the collection plates.

TABLE 1 - MASS DEPOSITION ON COLLECTION PLATES, TEST 1 - 4

| | Total Mass of Positive Particles Collected (μg) | Total Mass of Negative Particles Collected (μg) | Total Mass Collected (μg) |
|---|---|---|---|
| Test 1 | 138 | 270 | 408 |
| Test 2 | 75 | 183 | 258 |
| Test 3 | 430 | 42 | 472 |
| Test 4 | 36 | 445 | 481 |

Further tests were carried out using isokinetic sampling before and after the two stage electrostatic precipitator. Test conditions 1 - 4 above were followed with the second stage field of the precipitator activated (i.e. no corona in the first stage). Finally a test was carried out with the water atomizer turned off and the two stage precipitator fully activated. (Test 5) Although the results of these tests were more inconsistent (i.e. the standard deviations on the input measurements were often as high as 50%), no significant particle leakage was measured past the precipitator plates under test conditions 1, 3, 4, and 5, (i.e. approximately 100% collection) whereas under test condition 2 it was estimated that the collection efficiency was approximately 80%.

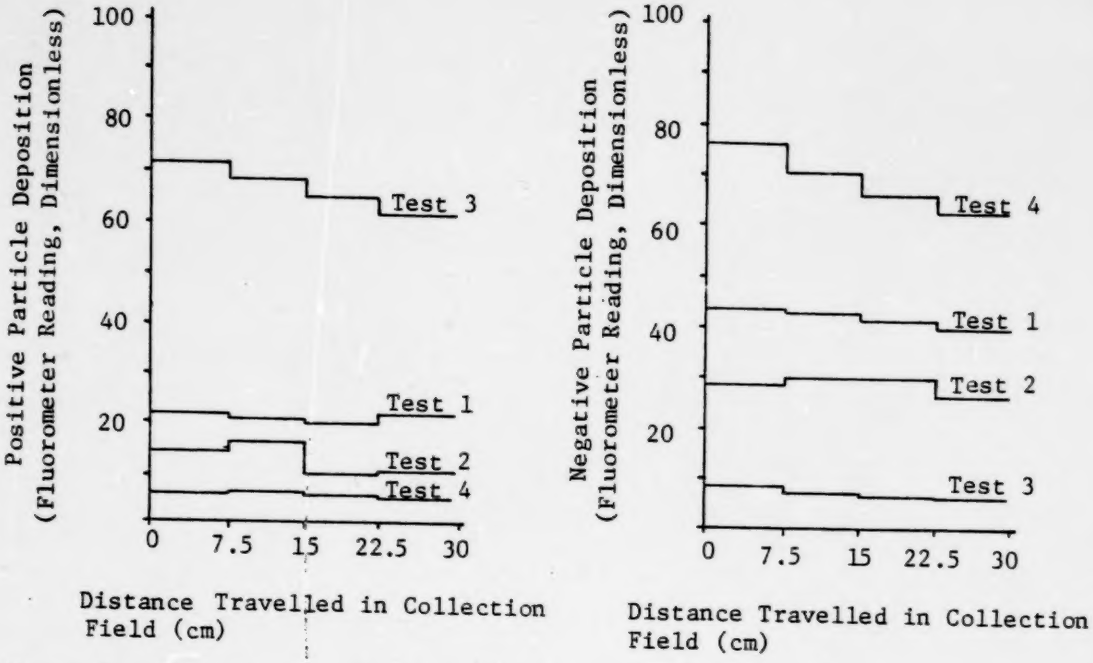

Figure 5. Particle Deposition on Collection Plates for Two Stage Precipitation Test

## SIMULATED SPRAY HUMIDIFIER

Experiments were also carried out in an attempt to show the effectiveness of this process of charging in a situation involving spray humidification. In this case the methylene blue was used to simulate the chemical residue resulting from spraying "hard" water. For this test the spinning disk atomizer was disconnected and the methylene blue solution was sprayed at a rate of 2.2 mℓ/min from the ultrasonic nozzle.

The quantity of methylene blue collected on the sample plates was determined under the following conditions of voltage applied to the atomizer:

Test A ≡ 0 kV

Test B ≡ + 1.2 kV

Test C ≡ - 1.2 kV

The results of these experiments are shown in Fig. 6.

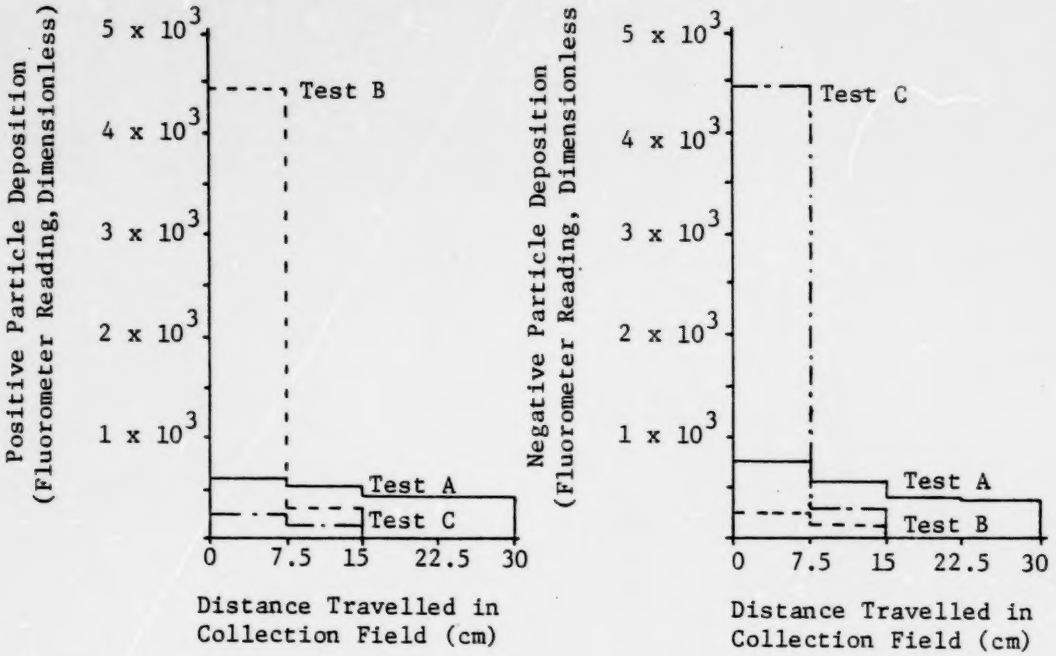

Figure 6. Particle Deposition on Collection Plates for Spray Humidification Tests

## OBSERVATIONS AND DISCUSSION

### TWO STAGE ELECTROSTATIC PRECIPITATOR

Referring to Figure 5 and each test condition in turn, Test 1 shows that significant collection of the methylene blue occurred even in the absence of any intentional charging. This demonstrates that charging takes place as a result of the spinning disk atomization with a bias of approximately 2/1 in favour of negative particles. (This phenomenon could be normally eliminated in the generator through the use of a bi-polar neutralizer energized with a radioactive source.) In fact the test using the second stage of the electrostatic precipitator activated showed approximately 100% collection indicating that all the particles were charged (albeit some positive and some negative.) Thus in interpreting the significance of the subsequent tests it is important to realize that there is this initial distribution of charges and that it is the effective charge transfer that needs to be considered.

Test 2 was intended to show any reduction in the aerosol due to the scrubbing effect of the uncharged spray. The amount of methylene blue collected on each electrode was reduced by approximately 35% in one case, 45% in the other. However, because of the presence of the initial charges it was impossible to determine if this was the result of a reduction in the quantity of aerosol by scrubbing or some charge neutralization due to the bi-polar charge generated by the water spray itself. In fact, evidence pointing to the latter effect was found in the precipitator test which showed that only about 80% of the total methylene blue was collected. Presumably the remaining 20% was uncharged (i.e. neutralized by the water spray).

In any case, the results of Test 2 were assumed to be the base level for determining the effectiveness of charge transfer from the electrified sprays. The results of Test 3 and 4 (positive and negative sprays respectively) are summarized from the data of Table 1 in ratio form in Table 2 below.

TABLE 2 - RATIO OF CHARGED PARTICLES COLLECTED

| Test 3 | Test 4 |
|---|---|
| Positive Charged Spray | Negative Charged Spray |
| $\frac{\text{Positive: Test 3}}{\text{Positive: Test 2}} = 5.7$ | $\frac{\text{Negative: Test 4}}{\text{Negative: Test 2}} = 2.4$ |
| $\frac{\text{Positive: Test 3}}{\text{Negative: Test 3}} = 10.2$ | $\frac{\text{Negative: Test 4}}{\text{Positive: Test 4}} = 12.4$ |
| $\frac{\text{Negative: Test 3}}{\text{Negative: Test 2}} = 0.23$ | $\frac{\text{Positive: Test 4}}{\text{Positive: Test 2}} = 0.48$ |
| 91% of particles collected were +ve | 93% of particles collected were -ve |

Looking at the results of Test 3 it can be seen that the addition of the positive charged spray caused an increase of about 5.7 times in the amount of positive particles and a reduction to about 0.23 in the number of negative particles collected. Expressed in another way, looking at the ratio of positive particles to negative particles this increased to 10.2 (from an initial value of only 0.41) a net change of effective charge of almost 25 times. Clearly, significant charge transfer occurred from the evaporating water spray to the methylene blue particles. The fact that the methylene blue was initially charged probably partially accounts for the fact that some particles of opposite sign remained in the aerosol. (In Test 3 approximately 91% of the particles collected were positively charged.) However, another factor was probably due to the fact that although the ultrasonic nozzle was positioned to give the maximum mixing effect with the aerosol stream it was impossible to arrange it to give uniform distribution across the duct. It is believed that if two atomizers were used the distribution of particle charge could be biased even further to the polarity of the spray. A similar pattern is shown from the results of Test 4.

## SIMULATED SPRAY HUMIDIFIER

The results of this test given in Figure 6 show the very rapid and complete collection of the methylene blue as the particles pass through the collection plates. In each case i.e. for Test B and Test C almost all of the charged spray residue is collected in the first segment indicating a relatively high level of charging. This may be compared with the smaller but more uniform quantity of particles collected on both the positive and negative plates as a result of bipolar charging from the unbiased sprayer as shown by the results of Test A.

It was also observed for Test B and C that a significant proportion of the aerosol deposited on the walls of the duct prior to the collection zone. This was observed physically and also by measuring the component of current flowing from the duct walls to ground. This confirms the important role that space charge deposition fields can play in unipolar charged sprays (4). No significant deposition of this sort was observed in Test A.

## CONCLUSIONS

The results of these experiments show that evaporating charged water sprays can provide unipolar charge transfer to aerosols and that significant charge will remain on the chemical residue of a charged water spray.

The unipolar charge transfer from the evaporating water spray can be used to provide charging for particles to allow subsequent capture in a static electric field. When used instead of corona charging it may offer advantages in that it requires negligible electric power, produces no ozone and provides no explosion hazard. Optimization of the number and positioning of the spray nozzles must be carefully considered. The process does add water vapour to the gas stream but this quantity may be adjusted and may in fact be an advantage in certain air cleaning applications. If used in a spray humidification process significant advantage comes from charging the spray in that it allows very efficient collection of any chemical residue.

## ACKNOWLEDGEMENTS

The authors acknowledge with thanks the ongoing interest and support of Stelco Inc. and the BILD Corporation of the Ontario Government. Special thanks are extended to R. Richardson and R.J. Nowak for carrying out several of the tests.

The work described in this paper was not funded by the U.S. Environmental Protection Agency and therefore the contents do not necessarily reflect the views of the Agency and no official endorsement should be inferred.

# REFERENCES

1. White, H.J. Industrial Electrostatic Precipitation, Addison-Wesley, 1963, pp. 74-150.

2. Masuda, S. and Washizu, W. Ionic Charging of a Very High Resistivity Spherical Particle. J. of Electrostatics, 6, 1979, pp. 57-67.

3. Barreto, E., Reynolds, S.I. and Jurenka, H. Ignition of Hydrocarbons and the Thermalization of Electrical Discharges, J. Appl. Phys., Vol 45, #8, 1974, pp. 3317-3327.

4. Castle, G.S.P., Inculet, I.I. and Littlewood, R. Ionic Space Charges Generated by Evaporating Charged Liquid Sprays. Inst. Phys. Conf. Ser. No. 66, 1983, pp. 59-64.

5. Iribarne, J.V. and Thompson, B.A. On the Evaporating of Small Ions from Charged Droplets. Joun. Chem. Phys., Vol. 64 #6, 1976, pp. 2287-2294.

6. Melcher, J.R., Sachar, K.S. and Warren, E.P. Overview of Electrostatic Devices for Control of Submicrometer Particles. Proc. IEEE, Vol. 65 #12, 1977, pp. 1659-1669.

7. Hoenig, S.A. Fugitive and Fine Particle Control Using Electrostatically Charged Fog. Conf. Rec. IAS-IEEE Annual Meeting, Toronto, 1978, pp. 1-15.

8. Nowak, R.J. The Interaction of a Charged Aerosol with Airborne Particles. E.S. 400 Project Report, Faculty of Engineering Science, The University of Western Ontario, 1984.

9. Output Characteristics of the SONIMIST™ Ultrasonic Spray Nozzle Model 600-1. Data Sheet HS-DS-101, July 1983. Heat Systems Ultrasonics Inc., Farmingdale, New Jersey.

10. Behie, S.W. Aerosol Capture, Jet Dispersion and Pressure Drop Studies of a Large and Small Venturi Scrubber. M.E.Sc. Thesis, Faculty of Engineering Science, The University of Western Ontario, 1974, pp. 213-216.

# ROLE OF ELECTROSTATIC FORCES IN HIGH VELOCITY PARTICLE COLLECTION DEVICES

by: H.C. Wang[1], J.J. Stukel[1,2], K.H. Leong[1], P.K. Hopke[1,3]

[1]Department of Civil Engineering

[2]Department of Mechanical Engineering

[3]Institute for Environmental Studies

University of Illinois at Urbana-Champaign
Urbana, Illinois 61801

## ABSTRACT

For high velocity particle collection devices, charge enhancement has not yielded the desired increases in collection efficiency. In order to better understand the tradeoffs between the impaction and Coulombic forces for the collection of fine particles, a series of experiments were run in which the collection efficiency of an accelerating cloud of charged drops was measured at various positions downstream of the drop inlet. Results are presented as a function of the Stokes number, Coulombic parameter and the particle-droplet relative velocities. The equations of particle and droplet motion were solved using a computer. Theoretical results are presented for overall collection efficiencies as a function of Stokes number, Coulombic parameter and downstream distance and are compared to experiment.

## INTRODUCTION

Inertial impaction has been a popular method to remove particulate matter from anthropogenic emissions and has contributed to the significant reduction of the total particulate mass in ambient air since the establishment of the National Ambient Air Quality Standards in 1971. Among the high velocity particle collection devices, venturi scrubbers are perhaps the most widely used devices because of their flexibility, simplicity, and efficiency (1,2). However, the high water usage rate and energy consumption in venturi scrubbers increase the operating cost significantly. Hence, methods to reduce the operating cost and to increase the efficiency of an existing venturi scrubber are of interest.

One of the methods proposed to improve the performance of high velocity collection devices is to utilize electrostatic forces to enhance the collection efficiency due to inertial forces. In order to better understand the tradeoffs between the inertial and Coulombic forces for particle collection, experiments were performed to obtain the collection results of an accelerating droplet at various positions downstream of the droplet inlet. The experimental results were compared with theoretical predictions and the problems associated with the limited improvement upon charge enhancement were discussed.

## EXPERIMENTAL DESIGN

The schematic design of the experimental system is shown in Figure 1. A 4-inch stainless-steel pipe of length 2.10 m supported vertically by a channel-steel structure was used as the wind tunnel with the flow induced by a blower at the bottom. An absolute filter was installed at the top of this system to remove any airborne particles from the intake air. The flow velocity was measured by a flow measuring system consisting of a pitot tube, a monometer, a thermometer, and a humidity analyzer. Monodisperse aerosol of uniform charge was generated and introduced into the wind tunnel immediately after the filter. The particle charge and the particle mass flux in the wind tunnel were measured by an aerosol characterization system. Water droplets of uniform size and charge were injected into the wind tunnel to collect particles. Those droplets in the central region of the pipe were collected and counted by this system. The amount of particle mass collected by this system was analytically determined and was used to deduce the integrated particle mass collected by a single droplet.

The total particle mass collected by a droplet was measured at five downstream ports. The corresponding distances from water inlet were 15cm, 30cm, 60cm, 90cm, and 120cm for these five ports, respectively.

The major components of this experimental design were the aerosol generation and charging device and droplet collection system.

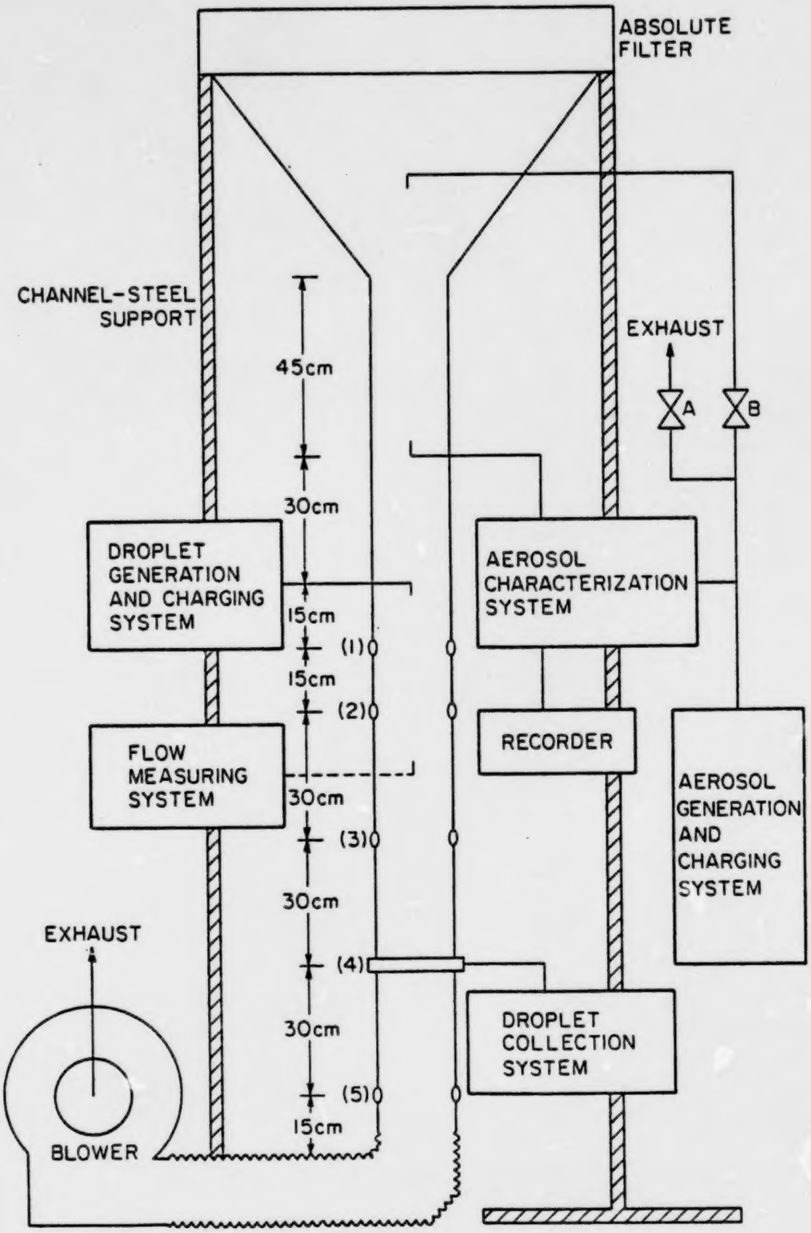
ABSOLUTE FILTER
CHANNEL-STEEL SUPPORT
45cm
30cm
15cm
15cm
30cm
30cm
30cm
15cm
(1)
(2)
(3)
(4)
(5)
EXHAUST
A
B
DROPLET GENERATION AND CHARGING SYSTEM
FLOW MEASURING SYSTEM
AEROSOL CHARACTERIZATION SYSTEM
RECORDER
AEROSOL GENERATION AND CHARGING SYSTEM
DROPLET COLLECTION SYSTEM
EXHAUST
BLOWER

Figure 1. The Schematic Design of the Experimental System for Accelerating Droplets

Monodisperse charged particles of controllable size and charge were required for this experiment. A vibrating orifice aerosol generator (3), modified for induction aerosol charging (4), was used to obtain an aerosol of uniform charge and size.

Additional modifications to the standard Berglund and Liu system (3) included replacing the syringe pump by a flowmeter (Gilmont 10) and a solution reservoir driven by a nitrogen pressure feed at 35 psi. The major advantages for this configuration are longer operation time with on-line monitoring and better and more accurate flow control.

Since water droplets were used as the collectors, particles of high solubility were required. For the convenience of analytical detection, highly specific and sensitive material was desirable. Uranine (sodium fluorexcien), a commonly used tracer, was chosen to meet these requirements. The drying process of liquid droplets generated by the vibrating orifice aerosol generator is critical to insure the aerosol quality. The drying rate should be high enough to evaporate all the solvent before introduction into the wind tunnel. However, too high a drying rate may result in non-spherical particles. Since uranine is hygroscopic and may not be dry if dissolved in water, a 50:50 mixture of water and 100% ethanol was used as solvent and gave satisfactory results.

The particle charge and mass concentration in the wind tunnel needed to be determined and was the main function of the aerosol characterization system. Ideally, these two variables could be obtained by simultaneously taking charge measurements and filter samples from the wind tunnel. It was impractical, however, to install a filter holder in a 4-inch pipe because of the significant disturbance to the flow. Also, the particle concentration was too low to obtain a filter sample within a reasonable time interval. Therefore, the measurements of particle charge were made before the aerosol entered the wind tunnel where the particle concentration was 2 orders of magnitude higher than in the wind tunnel. This concentrated aerosol stream was divided into two equal streams. The flow in each stream was controlled by flowmeters. One stream went directly to a membrane filter where the total mass of the particles collected was measured. The other stream went to an aerosol electrometer (TSI 3068) equipped with a modified straight inlet where the total charge during the same sampling period of the filter was measured. Thus, the charge-to-mass ratio of particles was obtained. Because the particle diameter, and thus the particle mass, was specified for the vibrating orifice aerosol generator, the particle charge was obtained.

With the assumption of a constant charge-to-mass ratio, the particle concentration in the wind tunnel can be determined by making charge measurements. This method, although indirect, does have some advantages that the integrated filter sample technique does not have. It is continuous, sensitive, accurate and provides on-line monitoring which gives aerosol quality information for each experimental run. The aerosol was sampled using an isokinetic sampling probe, filtered in a Faraday cage, and electrically discharged through an electrometer (TSI 3000). The measured current was monitoring by means of a recorder (Houston Instrument B5217-5).

Droplet formation was achieved by forcing deionized water through a stainless-steel needle of 0.1905mm ID by a constant pressure feed to the plexiglass reservoir containing deionized water. The needle was bended 90 degrees and the needle tip was located at the center of the wind tunnel. The water droplets formed at the tip were continuously dislodged by the air flowing by the needle tip. With a constant water feed rate and a constant air velocity at the center of the wind tunnel, droplets of uniform size were produced. The droplet charge was obtained by contact changing. A high voltage source was electrically connected to the stainless-steel needle to provide high voltage and the voltage was well controlled by means of a digital multimeter. The needle was covered by a ceramic tubing (1.6mm OD) for insulation purpose. The droplet size was determined microscopically by collecting the droplets in a dish filled with castor oil and examining under a microscope.

A droplet collection system was used to collect droplets, to measure droplet charge, and to count the number of droplets collected. The schematic design is shown in Figure 2. The droplet collection device was made of three separable pieces; the metal boat, the collecting rod, and the stainless-steel cover. The separable design was necessary because this device was used at five different ports and the metal boat had to be taken out for analytical measurements after each experimental run. The metal boat seated in a stainless-steel trough was used to collect the droplets passing through the slot of 1cm x 0.31cm on the stainless-steel cover. This boat was electrically connected to an electrometer by means of a spring-loaded connector. The charge carried by the droplets was discharged through the electrometer and the pulse was counted by a pulse counter. Thus, the total charge and the total number of droplets collected in the boat were directly determined. In addition, the uniformity of droplet charge was checked using an oscilloscope. Nearly identical pulse heights indicated that each droplet carried the same charge. To avoid the electrical noise induced by the charged droplets and/or particles in the surrounding of this device, all the electrical passage was covered with teflon insulation and shielded by a grounded outer layer. Since only the particles collected by droplets during transit were of interest, it was necessary to prevent extraneous particles from entering the droplet collection device. Based on the fact that the droplet size is about 2 order of magnitude greater than the particle size, this can be accomplished by directing a flow through the slot in the opposite direction of the flow velocity in the wind tunnel. The particles having smaller stopping distance can not penetrate into this device. On the other hand, the droplets having greater inertia are not affected by the upward flow and fall into the boat. Good alignment of the slot was insured by a flange to hold the collecting rod in right position and by a screw to fix the slot at the center of the wind tunnel.

## THEORY

Particle collection by a fixed sphere has been extensively discussed in the literature (5-9), with the assumption of a constant relative velocity between the particles and the collector. These literature results are not applicable for a charge-enhancement venturi scrubber, where the droplets are accelerating during the collision process. Recently, Wang et al. (10)

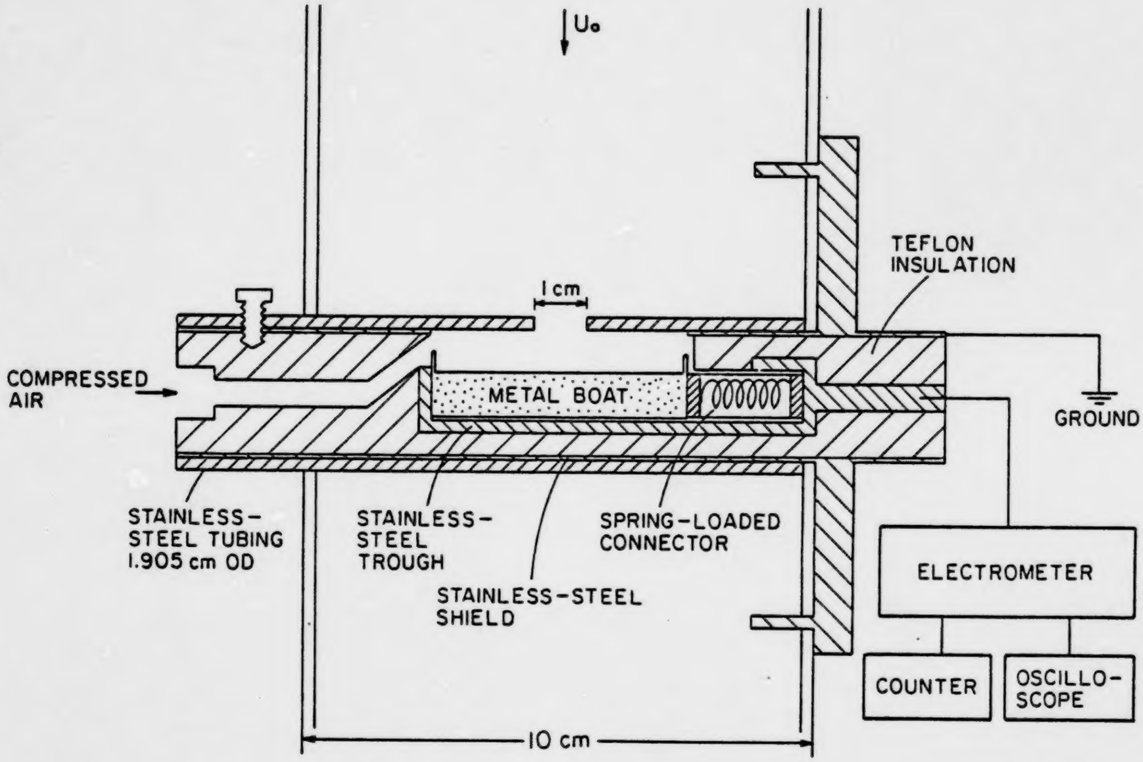

U₀
1 cm
TEFLON INSULATION
COMPRESSED AIR
METAL BOAT
GROUND
STAINLESS-STEEL TUBING 1.905 cm OD
STAINLESS-STEEL TROUGH
SPRING-LOADED CONNECTOR
STAINLESS-STEEL SHIELD
ELECTROMETER
COUNTER
OSCILLO-SCOPE
10 cm

Figure 2. Droplet Collection System

proposed an accelerating collector model to predict the collision efficiency of an accelerating droplet as a function of its travel distance. Because the equations of droplet motion are incorporated in the model, the Stokes number (St) and Coulombic parameter (Kc), that characterize respectively the inertial force and Coulombic force in the collision process, can be redefined at any downstream point of interest and the corresponding efficiency is obtained by numerical integration or empirical fitting (10). To obtain the efficiency curve of an accelerating droplet as a function of its travel distance, ten points were selected for efficiency calculation. Starting at the injection point, this model automatically chose the other nine points at equal spacing and ended at a user input distance, corresponding to the physical length of scrubbers under consideration. The efficiency thus calculated is the instantaneous efficiency at the calculation point.

However, it is not feasible to measure the instantaneous collection efficiency of an accelerating droplet at a desired point. Instead, the measurable variable is the total particle mass collected by this accelerating droplet after injection, in other words, the integrated particle collection. To be able to compare theory with experiment, integration of the theoretical efficiency curve over the travel distance is necessary. Considering a droplet of radius $R_c$ introduced into the wind tunnel with flow velocity $U_o$ and aerosol mass concentration $C_m$, the total mass collected by this droplet over downstream distance Z is

$$M = \int_0^Z C_m \pi R_c^2 E \, (U_o - V_c)/U_o \, dZ' \tag{1}$$

where $V_c$ is the droplet velocity and E is the droplet collision efficiency. With the following non-dimensionalized parameter,

$$Z^* = \frac{Z}{U_o \tau \Psi} \tag{2}$$

$$V_c^* = \frac{V_c}{U_o} \tag{3}$$

where $\tau$ and $\Psi$ are the droplet relaxation time based on Stokes law and the non-Stokesian correction factor (11), and assuming that the droplet size and the particle mass concentration remain constant for a distance Z, the above equation can be rearranged and gives

$$\frac{M}{C_m \pi R_c^2 U_o \tau \Psi} = \int_0^{Z^*} E(1-V_c^*) \, dZ^{*\prime} \tag{4}$$

where the left hand side term is the dimensionless particle mass collected by this droplet and can be experimentally determined while the integral on the right hand side can be calculated using the theoretical model proposed by Wang et al. (10).

# RESULTS AND DISCUSSIONS

The condition chosen for this study were as follows:

Particle radius ($R_p$) = 1.973±2.0% μm
Particle charge ($Q_p$) = $4.135\text{x}10^{-16}$±4.3% C
Droplet radius ($R_c$) = 207±3.5% μm
Droplet charge ($Q_c$) = $2.64\text{x}10^{-11}$±6.0% C
Flow velocity ($U_o$) = 16.10±6.3% m/s

In order to compare experiment with theory, the measured results have to be reduced to dimensionless form (Equation 4). Therefore,

$$M^* = \frac{M_T/n}{C_m \pi R_c^2 U_o \tau \Psi}$$

where $M_T$ is the total mass collected in the boat located at a distance Z from droplet inlet and n is the total number of droplet counted by the pulse counter. For $R_c$=207 m and $U_o$ =16.10m/s, $\tau$=0.5219sec and $\Psi$=0.1932. The particle mass concentration ($C_m$) was continuously monitored by the aerosol characterization system.

The theoretical and experimental results are plotted as a function of downstream distance Z* in Figure 3. Although the most unbiased way to present the experimental results was to show all the data obtained, it was difficult here because at least 12 experimental data were taken from each port. The 95% confidence interval, defined as

$$\left| I_{95\%} - \text{Mean} \right| \leq \frac{2\text{STD}}{\sqrt{N}}$$

where STD and N are the standard deviation and the number of samples, was used to present the experimental results. Also, the upper and lower limits of experimental results are shown in Figure 3.

For high velocity particle collection devices such as venturi scrubbers, charge enhancement has not yielded the desired improvement in particle removal efficiency. To identify the cause, the accelerating collector model (10) was used to analyze this problem. For the convenience of discussions, a typical industrial example was taken with the following physical parameters:

$U_o$=50 m/s
$R_p$=1 μm
$R_c$=100 μm
$Q_p$=$7.48\text{x}10^{16}$ C
$Q_c$=$6.687\text{x}10^{-12}$ C

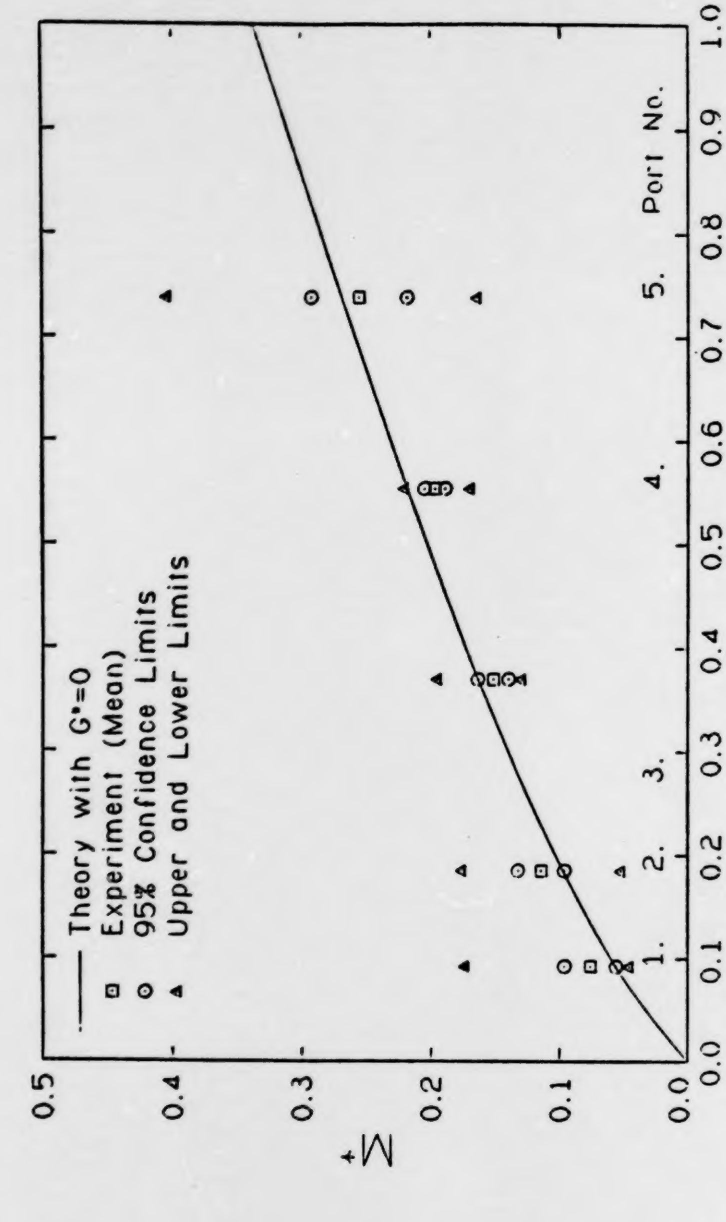

Figure 3. M* as a Function of Z* with Corrected Aerosol Charge-to-mass Ratio

where $Q_p$ was the sum of field and diffusion charging under industrial conditions and $Q_c$ was 1/3 of the Rayleight limit. In a conventional venturi scrubber, the single droplet collision efficiency (target efficiency) can be well represented by an empirical equation given by Calvert (12) as

$$E = \left(\frac{St}{St + 0.35}\right)^2 \qquad (11)$$

for St>0.2. Also, the critical Stokes number below which the impaction efficiency vanishes was 1/12 for potential flow (13). With charge enhancement, the efficiency was calculated using the accelerating collector model. Figure 4 shows the differences in collision efficiency between a conventional venturi scrubber and a charged droplet scrubber (CDS). Significantly higher efficiency for a CDS indicated the promise of charged enhancement to improve the performance of a conventional venturi scrubber. The fact that the efficiency of a CDS increases with downstream distance is somewhat misleading in determining the optimum scrubber length. For example, an infinite scrubber length would be required if the above argument were correct. As a matter of fact, the increase of single droplet collision efficiency does not necessarily imply a larger amount of particles being collected. According to the definition of collision efficiency, a smaller number of particles being swept out by a droplet also results in the increase of the single droplet collision efficiency. Therefore, a better indicator is the dimensionless total particle mass collected by the droplet.

The dimensionless particle mass collected by a single droplet was calculated and shown in Figure 5 for both cases. In a conventional scrubber, the total collected mass levels off at approximately Z*=2.1, which corresponds to 2m for the assumed physical parameters. It is not surprising that venturi scrubbers of 1m physical length (Z*=1 approximately) are commonly used for cost effectiveness. However, the total collected mass does not significantly increase upon charge enhancement until large values of Z* is achieved. If a venturi scrubber of 1m physical length is modified to a CDS while maintaining the same length and operating conditions, only limited increase in total collected mass (46%) will occur. On the other hand, more than one order of total mass (1272% increase) will be collected if the dimensionless collection length (Z*) is 5. Therefore, to obtain the desired increase in efficiency with charge enhancement, large values of Z* must be used. From Equation 2 there are three ways to increase Z*:

(1) increase the physical length of the scrubber,
(2) decrease the flow velocity,
(3) decrease the droplet size.

The first alternative is subjected to the limitations of capital cost and site availability and can not apply to an existing unit. The other two alternatives can be achieved by adjusting the operating conditions. However, decreasing the flow velocity results in an increase of droplet size because of the nature of atomization technique used in venturi scrubbers. Following the Nukiyama and Tanasawa correlation given by Calvert (12) as

$$D_c = \frac{16400}{U_o} + 1.45\,(Q')^{1.5}$$

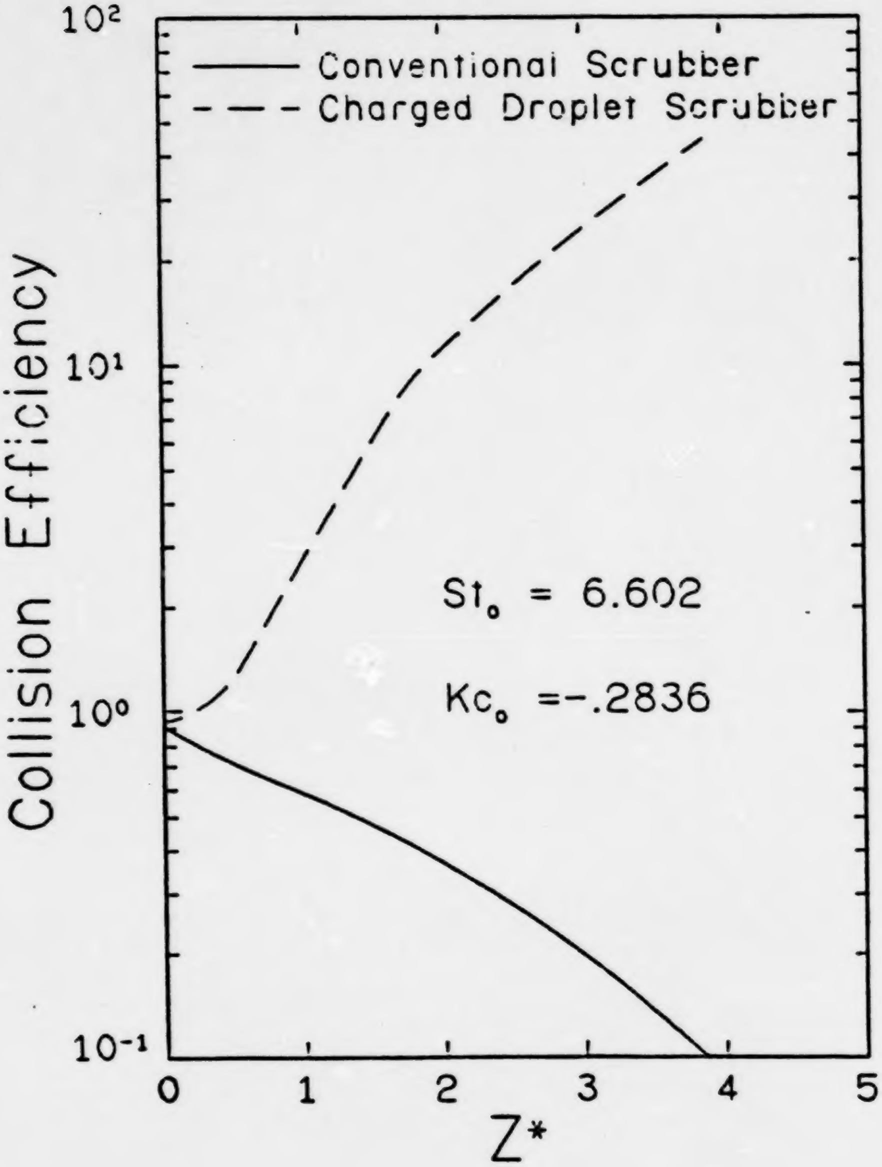

Figure 4. The Comparison of E Between a Conventional Scrubber and a CDS

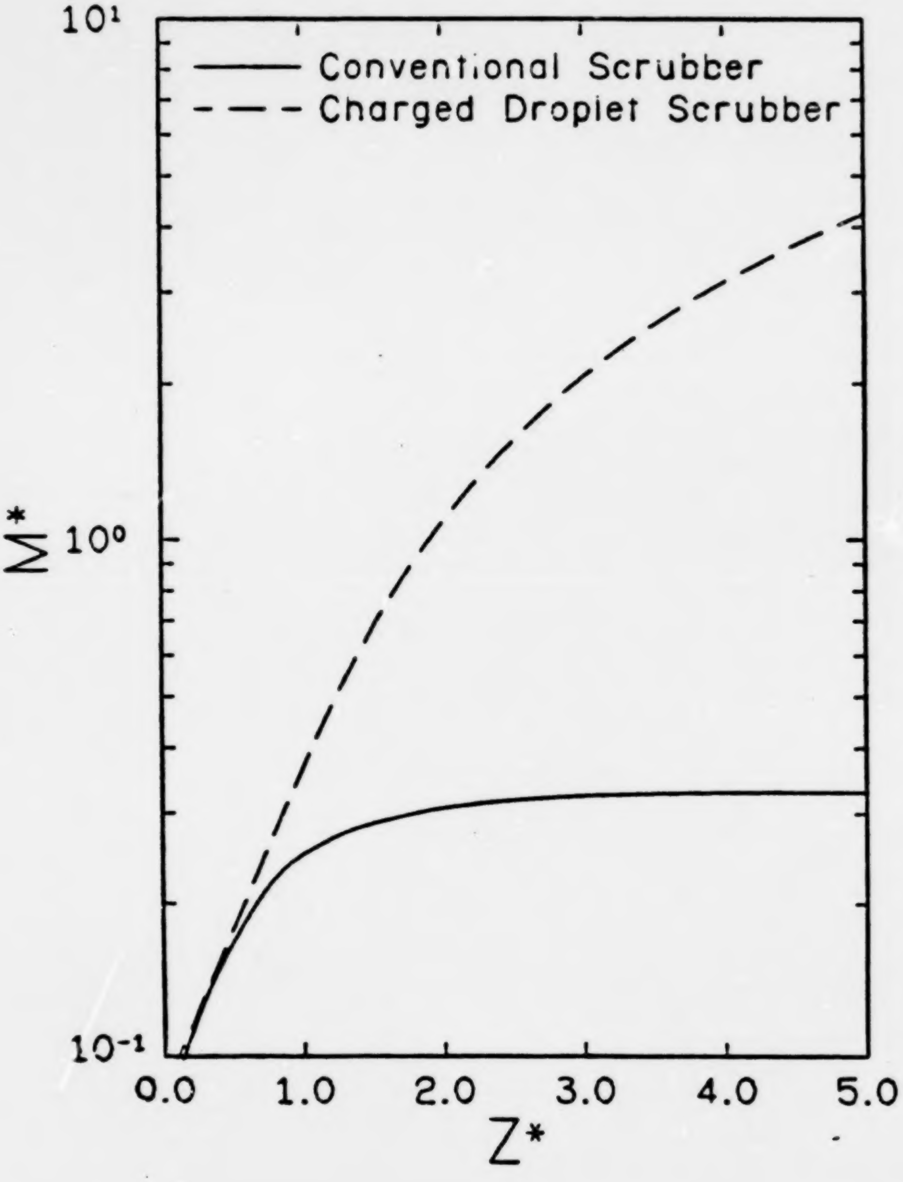

Figure 5. The Comparison of M* Collected Between a Conventional Scrubber and a CDS

the droplet size ($D_c$) which is not an independent variable any longer can be calculated with known flow velocity ($U_o$) and ratio of liquid-to-air flow rate (Q'). An analysis of the effect of $U_o$ and Q' on Z* reveals that large values of Z* are realized when a high velocity and low liquid-to-air ratio are used. Since the number of droplets must be large enough to insure no holes in the cross-section of scrubbers, the lowest liquid-to-air ratio is fixed. Although high velocity is desired in terms of increasing Z*, the increase of flow velocity leads to lower single droplet efficiency, and thus smaller particle mass being collected. The trade-off is difficult to quantify because the total particle mass collected by a droplet is a complicated function of flow velocity and highly depends on operating conditions. It requires an advanced optimization technique to obtain an optimum design and/or operation, and will be a good topic for future studies.

# REFERENCES

1. Bethea, R.M. Air Pollution Control Technology, McGraw-Hill Book Company, New York, 1978.

2. Calvert, S., Yung, S.C., Barbarika, H., and Patterson, R.G. Evaluation of four novel fine particulate collection devices. EPA-600/2-78-062, U.S. Environmental Protection Agency, Research Triangle Park, North Carolina, 1978.

3. Berglund, R.N. and Liu, B.Y.H. Generation of monodisperse aerosol standards. Environmental Science & Technology, 7:147, 1973.

4. Reischl, G., John, W., and Devor, W. Uniform electrical charging of monodisperse aerosol. Journal of Aerosol Science, 8:55, 1977.

5. George, H.F. and Poehlein, G.W. Capture of aerosol particles by spherical collectors. Environmental Science & Technology, 8:46, 1974.

6. Nielsen, K.A. and Hill, J.C. Capture of particles on spheres by inertial and electrical forces. Industrial Engineering Chemical Fundamentals, 15:157, 1976.

7. Beizaie, M. and Tien, C. Particle deposition on a single spherical collector. Canadian. Journal of Chemical Engineering, 58:12, 1980.

8. Wang, H.C., Stukel, J.J., Leong, K.H. and Hopke, P.K. Particle deposition on spheres by inertial and electrostatic forces-theory. Submitted to Aerosol Science & Technology, 1984.

9. Wang, H.C., Stukel, J.J., Leong, K.H. and Hopke, P.K. Particle deposition on spheres by inertial and electrostatic forces-experiment. Submitted to Aerosol Science & Technology, 1984.

10. Wang, H.C., Stukel, J.J., Leong, K.H. and Hopke, P.K. Charged particle collection by an oppositely-charged accelerating droplet. Submitted to Journal of Aerosol Science, 1984.

11. Israel, R. and Rosner, D.E. Use of generalized Stokes number to determine the aerodynamic capture efficiency of non-Stokesian particles from a compressible gas flow. Aerosol Science & Technology, 2:45, 1983.

12. Calvert, S. Venturi and other atomizing scrubber's efficiency and pressure drop. Journal of American Chemical Engineering, 16:392, 1970.

13. Friedlander, S.K. Smoke, dust, and haze. Fundaments of aerosol behavior. Wiley-Interscience, New York, 1977.

# HOT-GAS FABRIC FILTRATION 500° F - 1500° F

## NO UTOPIA BUT REALITY

by: Lutz Bergmann, President
Filter Media Consulting, Inc.
LaGrange, Georgia 30240

## INTRODUCTION

Not fully recognized is the feasibility of cleaning and controlling particulates at temperatures above 500° F. The availability of filter media that can withstand very high temperatures (between 500° F - 2000° F) has opened completely new technical possibilities to design filter systems and to control particulates.

Energy is the major driving force to acceptance of the potential market for hot-gas filtration. Since high temperature of processing of materials directly effects the cost structure of manufacturing, there are many advantages of hot-gas fabric filtration.

The electricity cost in 1950 represented 18% of total manufacturing cost, which raised in 1980 to 32%. It is expected in the year 2000 to represent 45%, the single largest cost factor, larger than wages and raw materials.

A common procedure is to cool gases so they can be treated in conventional fabric filters below 500° F. On the other hand, hot gases can be filtered with a maximum of energy by direct heat exchanging or by using them for preheating of process materials. Cooling and heat exchange equipment is prone to corrosion. Working under hot-gas conditions, however, reduces chances to run through the acid dew point and damage equipment or possibly destroy filter materials. There has been an increasing search for possibilities to recover heat from loaded hot industrial gases in a simpler manner. Other advantages of hot-gas filtration can be summarized as follows:

1. Heat Recovery
2. Corrosion Free Environment
3. Dry Product Recovery vs. Wet Scrubber
4. Equipment and Maintenance Savings
5. Re-use and Recirculation of Clean Hot Inplant Air or Gas

Heat recovery is not the only benefit from operating at elevated temperatures. There are other industrial applications which offer technical and economical advantages, such as listed in Table 1.

TABLE 1. HOT GAS FILTRATION POTENTIAL

| | APPLICATION | OBJECTIVES | TEMPERATURE RANGE |
|---|---|---|---|
| 1. | SHALE OIL RETORT VAPOR | VAPOR PHASE PARTICULATE REMOVAL | 800°-1200° F |
| 2. | PFBC | TURBINE BLADE PROTECTION | @1500° F |
| 3. | WOOD/PEAT GASIFIERS | PARTICULATE REMOVAL | 1200°-1600° F |
| 4. | CATALYTIC CRACKING | PRODUCT RECOVER, "EXPANDER" PROTECTION | PROPRIETORY |
| 5. | SILICONE PROCESSING | SILICA DUST REMOVAL IN CHLOROSILANE GAS | PROPRIETORY |
| 6. | IRON AND STEEL INDUSTRY | WASTE HEAT RECOVERY | 1000°-1500° F |
| 7. | GOLD REFINING | OXIDIZING (ARSENICUMOXIDE) $SO_2$ $SO_3$ | @600° F |
| 8. | CEMENT (CLINKER COOLER) | OXIDIZING | 500°-1000° F |
| 9. | CHEMICAL INDUSTRY | CALCINATION-REDUCING | 600°-700° F |
| 10. | CARBON ELECTRODE MFG. | REDUCING | @800° F |
| 11. | GLASS INDUSTRY | FURNACE-OXIDIZING<br>(CL: 0.4%)<br>(LEAD SULPHATE & OXIDES 100% BELOW 1 MICRON) | @1000° F |
| 12. | INCINERATION | PARTICULATE AND GAS REMOVAL/ DRY INJECTION COMBINATION | 300°-800° F |
| 13. | CLAY INDUSTRY | DRY PRODUCT RECOVERY | 500°-700° F |
| 14. | GASIFIER | CONTROL OF "DIRTY" FUEL ON GAS TURBINES | 1800°-2000° F |
| 15. | POLYPHOSPHATE PRODUCTION | DRY PRODUCT RECOVERY | 700°-900° F |
| 16. | CERAMIC INDUSTRY | CONTROL FLUORINE EMISSIONS FROM KILNS | 600°-1000° F |

(Table 1 continued)

| | APPLICATION | OBJECTIVES | TEMPERATURE RANGE |
|---|---|---|---|
| 17. | SECONDARY ZINC | REPLACING WET SCRUBBER AT ENERGY SAVINGS | $400^{\circ}$-$600^{\circ}$ F |
| 18. | PETROLEUM REFINING | CATALYSTS FILTRATION | $1400^{\circ}$ F |
| 19. | TITANIUM DIOXIDE | CONTROL CHLORINE GAS UNDER HYDROFLUORIC ACID CONDITIONS | $600^{\circ}$ F |
| 20. | COKE CALCINER PROCESS | PARTICULATE CONTROL & CONTROL OF HYDROCARBONS | $2500^{\circ}$-$2800^{\circ}$ F |
| 21. | FRACTIONAL CONDENSATION PROCESS | SEPARATING PRODUCTS LIKE $Sb_2O_3$ - $AS_2O_3$ | $500^{\circ}$-$850^{\circ}$ F |

## AREAS OF CONCERN

There are, however, areas of concern with regards to the acceptance of hot-gas filtration which can be summarized in the following:

1. Little understanding of the underlying high temperature processes, lack of common language between OEM, fiber and fabric manufacturer, and end-user of filtration equipment.
2. Education of engineering, design and plant operating people.
3. Need for pilot installations to prove the feasibility and suitability of such systems.
4. Economic model to show why entire system has to be judged against initial investment of the filter itself and possibly expensive media.
5. Proof of the advantages towards energy savings, heat recovery, reduction of corrosion potential and others like maintenance cost.
6. Super clear definition of the subject as compared to others similar technolgies.

## PRACTICAL EXAMPLE OF HOT-GAS FABRIC FILTER INSTALLATIONS

It is important, however, to realize that actually a number of hot-gas installations are already on-stream or will start up shortly. These are relatively small systems and have to be considered pilot, respective prototype installations. Here is a list of such application under construction or in existence:

1. Polyphosphate Production - extensive pilot evaluations were conducted at two German industrial plants in the chemical process industry to replace existing wet scrubbers. The solution was a baghouse, operating at a temperature between 680° F - 734° F. This is an outside collecting system, at an A/C Ratio 6: 1. The cleaning

pressure is based on 4 - 6 bar with a cleaning interval of approximately one minute. The dust inlet loading was described with .45 gr/cu.ft., with fluor content of the gas with approximately 30 mg/Ncbm; chloride content of approximately 35 mg/Ncbm, and particulates finer than 20 microns.

The filter material chosen for this 12,500 acfm unit was sintered stainless steel material. Energy savings in this particular case were substantial, and amounted on an operating basis of 7,920 hours to $256,000 per year. This was based on a fuel price of $.024 per Kwh.

2. Clinker Cooler in Cement Industry - a small unit handling between 4,500 - 8,700 acfm was installed in Belgium, next to a clinker cooler and an existing electrostatic precipitator. These trials were initiated in 1980 at a temperature range of 250° C - 350° C, with a maximum of 450° C (665° F - 935° F). The installation was supplied by ETS. NEU, a French original equipment manufacturer which supplied a pulse-jet filter. There were a total of 24 filter bags representing 360 sq.ft. of cloth area. The dust inlet loading was approximately 44 gr/cu.ft.; the outlet emission .008 - .02 gr/cu.ft., though very efficient.

   This demonstration unit was run at times up to 18: 1 A/C Ratio, at regular times at 10: 1. The unit was later removed from this location but the feasibility of a hot-gas fabric filter for this application was demonstrated quite successfully.

3. Synthetic Fuel Industry - For an existing oil shale process, a hot-gas fabric filter installation represents approximately 400 sq.ft., with a total of 40 filter bags, manufactured from ceramic fiber, Nextel$^{R}$ 312. This is a proprietary process so that the owner of the installation as well as the manufacturers involved, are not willing to share any information. The installation is expected to be on-stream or going to be on-stream during 1984. This is a significant breakthrough based on an expected filter media life of approximately one year.

4. Waste Incinerator - There is a pilot installation currently erected behind a waste incinerator for a temperature range of 500° F - 600° F. The total installation will handle approximately 18,750 acfm, with a total filter area of 1,500 sq.ft. This unit is designed at an A/C Ratio 12: 1. This is sensational considering conventional units run at 6 - maximum 8: 1. The material for this installation is going to be sintered stainless steel metal. It is a proprietary system in which also due to dry injection, HC 1 removal is accomplished. This unit is expected to start up late 1984, respective January, 1985.

5. Pressurized Fluidized Bed Combustion - At a University in Germany, an installation with a total filter area of 4,730 sq.ft. is currently erected and expected to go on-stream early in 1985. This is a four compartment pulse-jet outside collecting system

with on-line, off-line, and reverse air cleaning options. The hardware is supplied by RESEARCH COTTRELL. The installation is expected to work at 315° C (650° F). The filter material chosen for this installation is a sintered Inconel$^R$ stainless steel metal filter bag, temperature resistant upt o 1000° F.

6. Wood Gasifier - Start up date is expected September - October, 1984, for a relatively small slip stream unit, handling a total air flow of 200 acfm. The application is a wood gasification plant for temperatures between 1450° F - maximum 1600° F. Dust is collected, like fly ash, with 50% finer than 10 - 15 micron. Dust inlet loading is expected to be 4.5 gr/cu.ft. The system is pressurized and expected to work at 250 p.s.i. As filter medium, a porous metal in for of candles is expected to be used. This installation is located in Canada.

These are just a few examples of existing units, respective installations, which will go on-stream later in 1984. There are other examples of hot-gas filter media applications where energy savings are the major driving force. One such installation is a zinc secondary smelting operation in Germany, handling a total air flow of 25,000 acfm, at temperatures of approximately 340° F.

The energy requirements for the current wet scrubber was based on 200 kW/hr. Since the fabric filter was installed, energy requirements dropped to roughly 20 kW/hr. This represented a savings for 8,760 hr/yr. operation of approximately $95,000/yr. Other advantages are: no costly deposit of wet scrubber sludge and recycling of valuable dry products, which allowed a payback for the initial investment.

Hot-gas cleaning of a 1200 MW gasifier combined cycle power plant has been evaluated. G. P. Reed has reported about design parameters and made a comparison to cold gas cleaning, capital cost, equipment and operating expenses resulting in a very attractive payback period of 1 - 24 months, depending on design.

Power plant output and cycle efficiency could be approximately 10% higher as compared to conventional cold gas cleaning; a side stream system has been operated at 950° C (1745° F) for 200 hours; however, the longer lasting test to substantiate the 8,000 - 16,000 hr. must be undertaken, therefore, a test rig is under construction for the investigation of extended exposure performance.

(Reference: "HOT-GAS CLEANING IMPROVES THE ECONOMICS OF ELECTRICITY FROM COAL"

Presented at THE FILTRATION SOCIETIES FILTEX CONFERENCE 9/83)

The recovery of precious metals like gold ore contains arsenic (AS) which forms trioxide ($AS_{03}$) which suplimates at 315° C (595° F). Mineral fiber and metal fiber felts have performed in pulse-jet filters in order to allow the gaseous $AS_2O_3$ to condensate to powder. This fractional condensation process can be seen from Figures 1 and 2.

SOURCE: BEKAERT STEEL WIRE CORP.

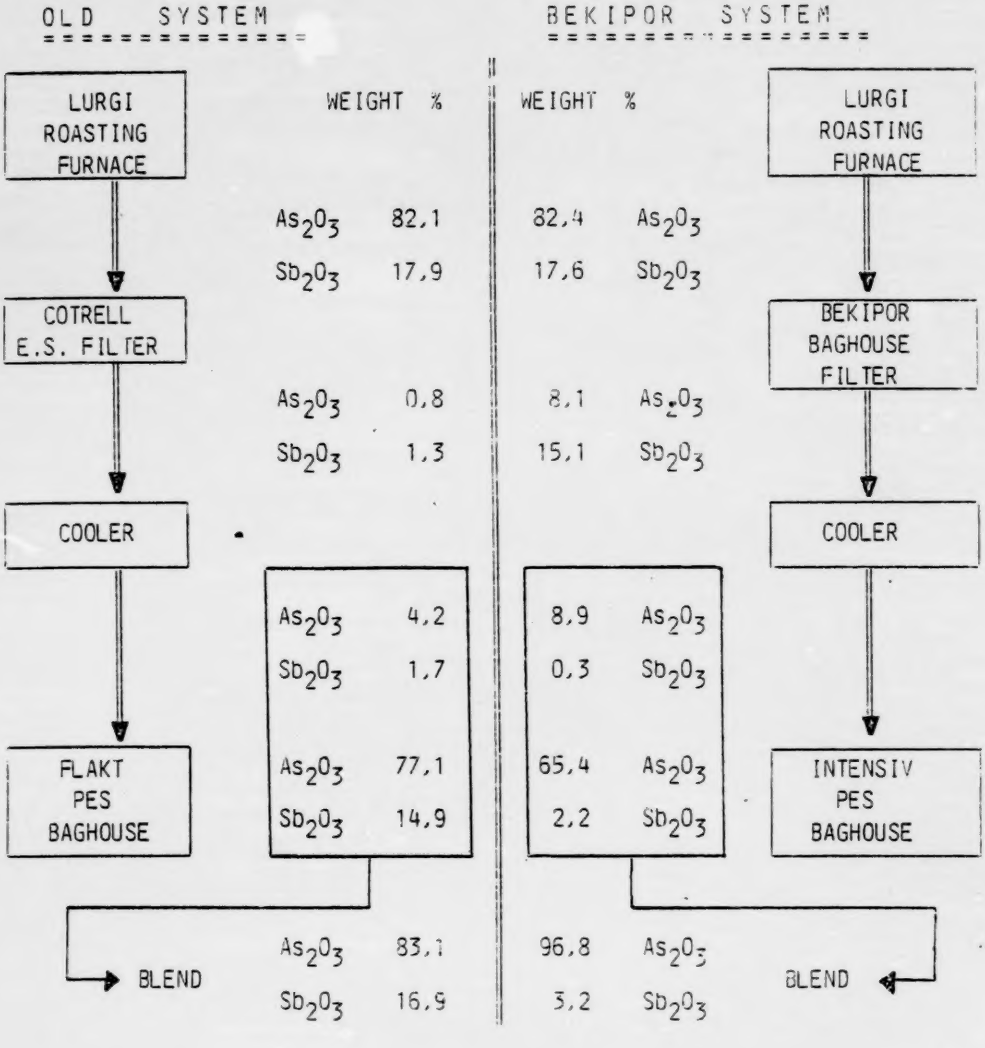
OLD SYSTEM
BEKIPOR SYSTEM
LURGI ROASTING FURNACE
WEIGHT %
WEIGHT %
LURGI ROASTING FURNACE
As2O3 82,1
Sb2O3 17,9
82,4 As2O3
17,6 Sb2O3
COTRELL E.S. FILTER
BEKIPOR BAGHOUSE FILTER
As2O3 0,8
Sb2O3 1,3
8,1 As2O3
15,1 Sb2O3
COOLER
COOLER
As2O3 4,2
Sb2O3 1,7
8,9 As2O3
0,3 Sb2O3
FLAKT PES BAGHOUSE
As2O3 77,1
Sb2O3 14,9
65,4 As2O3
2,2 Sb2O3
INTENSIV PES BAGHOUSE
BLEND
As2O3 83,1
Sb2O3 16,9
96,8 As2O3
3,2 Sb2O3
BLEND

Figure 1. Fractional Condensation Process As - Sb Oxides - Efficiencies Old System Compared to Bekipor Filtration System

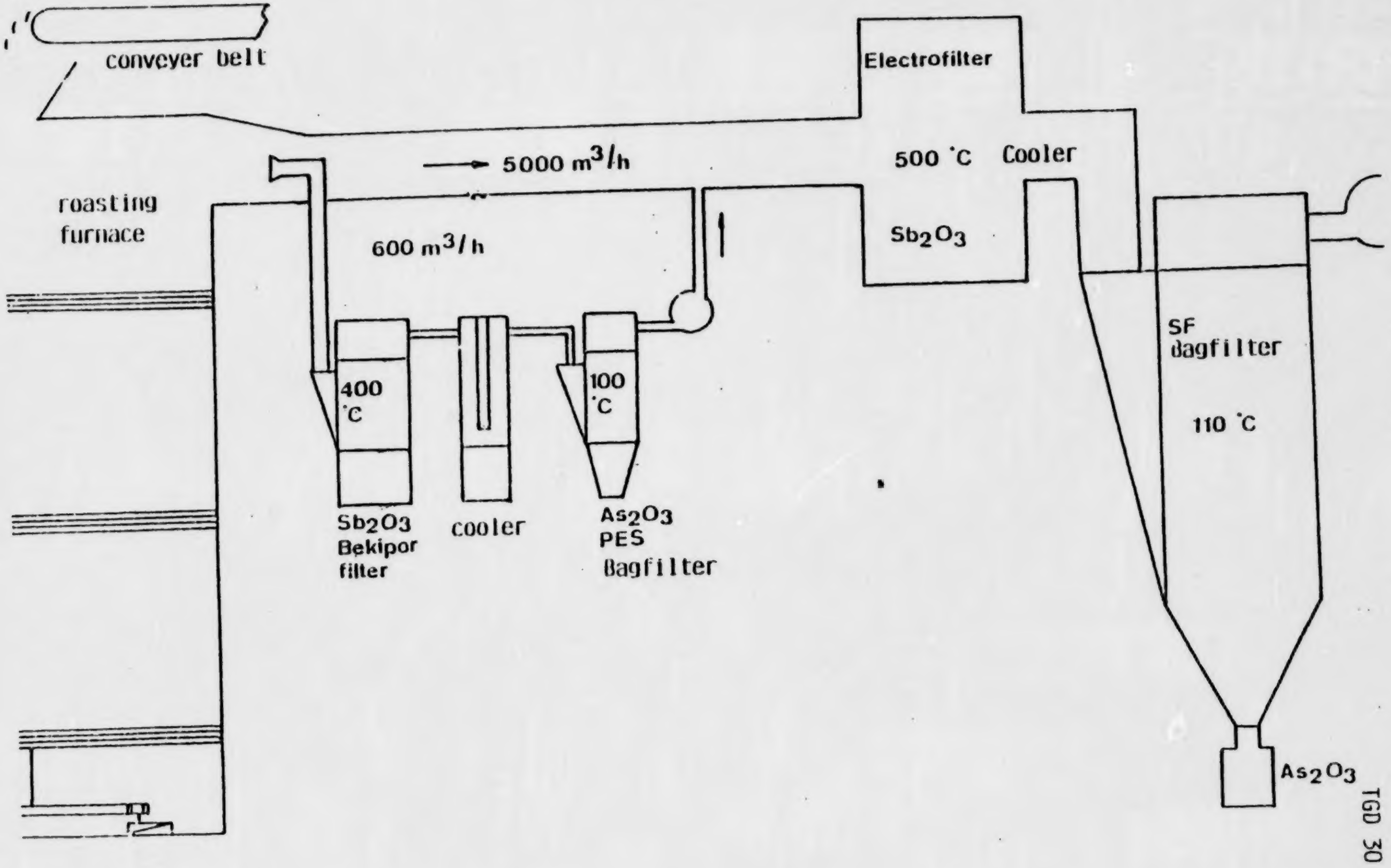
conveyer belt
roasting furnace
→ 5000 $m^3/h$
600 $m^3/h$
400 °C
$Sb_2O_3$ Bekipor filter
cooler
100 °C
$As_2O_3$ PES Bagfilter
Electrofilter
500 °C
$Sb_2O_3$
Cooler
SF dagfilter
110 °C
$As_2O_3$
TGD 30

Figure 2. Fractioned Condensation of $Sb_2O_3$ en $As_2O_3$

## FILTER MEDIA

As filter media, mainly two major fibers are being used depending on the application, and most importantly, the temperature range. In more detail, the following information is addressing stainless steel fibers. Temperature resistant up to 1000° F.

Stainless steel fibers range in diameters between 4 - 22 micron. The available alloys are stainless steel 316 L, and heat resistant steel Inconel^R 601. The different kinds of stainless steel fiber media are:

- BEKIPOR^TM woven fabrics.
- Stainless steel needled felts obtained by applying a stainless steel scrim and stainless steel fibers needled on both sides.
- Stainless steel three-dimensional structure of randomly laid fibers, sintered together into a porous plate and later shaped into filter bags.

Stainless steel filter media offer the following technical advantages:

- It can be used in temperatures up to 1000° F, even in oxidizing atmospheres and in the presence of $SO_2$.
- Because of their fine fibers, one obtains high efficiency and greater gas velocities under normal differential pressure.
- They behave as normal textile media with very great efficiency.
- They can be cleaned in conventional fabric filter systems mainly in pulse-jet compressed air filters.
- They withstand pyrophoric reaction of the filter cake.

These characteristics offer a number of potential applications in different industries.

Nextel^R 312 is a woven ceramic fiber material manufactured by the 3M COMPANY in St. Paul, Minnensota. 3M has entertained an extensive evaluation program and at this time, developed a seamless tubular filter bag, which has been tested under different conditions. (See Table 2.)

## TABLE 2

| | TEST A | TEST B |
|---|---|---|
| Dust Type | 25.5 um mass median diameter PFBC flyash | 8.3 um mass median diameter PFBC flyash |
| Dust Loading | 6.2 to 8.0 gr/ACF | 3.7 to 5.4 gr/ACF |
| Operating Temperatures | 800° F | 800° F |
| Filter Face Velocity | 3.0 to 3.7 ft.min. | 3.3 to 3.7 ft/min. |
| Differential Pressure Across Filter: | | |
| Before Cleaning | 5 in. $H_2O$ | 5 in. $H_2O$ |
| After Cleaning | 1.7 in. $H_2O$ | 1.7 in. $H_2O$ |
| Overall Mass Collection efficiency, percent | 98.7(a) to 99.8 | 98.9(a) to 99.8 |
| Cleaning Pressure | 80 psig | 80 psig |
| Cleaning Frequency at 3.7 ft./min. | 2 hours | 1 hour |
| Total Test Time | 102 hours | 115 hours |

(a) Post Cleaning

TEST C

Dust - Recirculated PFBC Flyash
Temperature - 1650° F
Pressure - 11 atmospheres
Efficiency - 99+%
Time - 100 hours

TEST D

Coal fired hot-gas generator
Temperature - 1800° F
Efficiency - 99+%
Time - 100 hours

TEST E

Pilot coal gasifier
Temperature - 950° F
Efficiency -
Time - 400 hours - test continuing

SOURCE: 3M COMPANY
St. Paul, MN

Long term exposure (1200+ hours) of Nextel$^R$ filter bags to temperatures of 1000° F confirm that the fiber and fabric remain flexible and strong under conditions without a lubricant such as is needed on glass. It has been postulated that this is because the ceramic fiber is harder than glass and does not scratch from contact with other fibers.

Another interesting finding is that it is extremely important that the surface temperature of the bag be kept below the ash fusion temperature of the filter cake. If the fusion temperture is reached, the ash melts and wets the fabric. Upon subsequent cooling, the ash hardens and causes failure of the fabric when it is flexed. It acts like a drop of shellac on your shirt. Typical ash fusion temperatures for pressurized fluidized bed combustion flyash are 2200° F - 2300° F.

Additional information on ceramic fiber media will be made available as time goes by. There is growing interest in a number of different applications where this fabric will represent great potential for temperatures above 1000° F.

## CONCLUSION

Is hot gas filtration an unknown quantity anymore? Sure not - although most of the experience is limited to relatively small existing or planned units, and much more research is needed to establish a hot-gas fabric filtration history. The potential, however, is great, and there is an increasing interest on behalf of a number of different industries to employ this technology for the benefit of mankind.

The work described in this paper was not funded by the U. S. Environmental Protection Agency and therefore the contents do not necessarily reflect the views of the Agency and no official endorsement should be inferred.

# THE PREDICTION OF PLUME OPACITY FROM STATIONARY SOURCES

by: David S. Ensor, Ashok S. Damle, and Philip A. Lawless
Research Triangle Institute
Research Triangle Park, NC 27709

and Leslie E. Sparks
U.S. Environmental Protection Agency
Industrial Environmental Research Laboratory
Research Triangle Park, NC 27711

## ABSTRACT

The visual appearance of stack emissions (or plume opacity) is an effective regulatory tool. Therefore, it is important to provide ways of designing control equipment to meet plume opacity as well as mass emission limitations. Two general problems are of interest: opacity resulting from primary emissions of solid particles and opacity resulting from particles due to condensing materials. The key variable in both cases is the particle size distribution. For dry particles, the particle size distribution is shaped by the industrial process and the control device. Condensing plumes result from the nucleation of vaporous material onto primary particulate matter. The resulting plume opacity depends on the primary particle size distribution and the time/temperature history of the flue gas.

## INTRODUCTION

### OBJECTIVE

The objective of this research is the development of techniques to improve accuracy of prediction of plume opacity from stationary sources. Often opacity may be estimated during the design of particulate emissions control equipment to provide assurance of meeting opacity regulations. In addition, the understanding of the physical basis of opacity is essential to the definition of problems in existing equipment.

### SCOPE

The scope of this paper is to evaluate the mechanisms leading to expected behavior for electrostatic precipitators, baghouses, and scrubbers. In addition, recent research predicting the opacity of detached plumes is summarized. Detached plumes develop in situations where the emission contains condensing vapors that form visible aerosol upon contact with the atmosphere.

## OPACITY

### DEFINITION

The opacity of a smoke plume is defined by:

$$Op(\%) = 100(1-I/I_o) \tag{1}$$

where

$Op$ = the plume opacity

$I$ = the light intensity entering the plume

$I_o$ = the light intensity leaving the plume

$I/I_o$ = the light transmittance.

The light transmittance is related to the flue gas properties by:

$$I/I_o = \exp(-b_{ext}\ L) \tag{2}$$

where

$b_{ext}$ = the extinction coefficient

$L$ = the pathlength.

MASS EXTINCTION COEFFICIENT

The parameter of interest is the mass concentration of the emission. Therefore, some algebraic manipulations must be made to introduce mass concentration into Equation (2). This is accomplished by:

$$I/I_o = \exp[-(b_{ext}/M)\ M\ L]\ . \tag{3}$$

Let

$$S_m = b_{ext}/M \tag{4}$$

then

$$I/I_o = \exp\ (-S_m\ M\ L) \tag{5}$$

where

$M$ = the mass concentration under actual conditions

$S_m$ = the mass extinction coefficient.

The use of the mass extinction coefficient is useful when the opacity is being estimated from the mass concentration and particle size distribution (1). In earlier work reported by Ensor and Pilat (2), the reciprocal of $S_m$, called "K," was used as a calibration coefficient for relating opacity monitors to mass concentration.

## PARTICLE SIZE DISTRIBUTION

The mass extinction coefficient is a function of the particle size distribution, particle refractive index, and particle density. The mass extinction coefficient is computed by:

$$S_m = \frac{\pi \, Q(x,m) \, r^2 \, n(r) \, dr}{\rho \, \pi \, 4/3 \, r^3 \, n(r) \, dr} \qquad (6)$$

where

$Q$ = the light extinction factor

$x$ = the size parameter $2 \pi r/\lambda$

$\lambda$ = the wavelength of light

$n(r)$ = the particle size distribution by number, the number of particles of radius r between r and r + dr

$\rho$ = the particle density.

Often the particle size distribution is reported by mass such as that measured by a cascade impactor. In these cases the mass distribution, w(r), must be converted to number distribution. One way to accomplish this is incremental calculation with:

$$n(r) = w(r)/(\rho \, 4/3 \, \pi \, r^3) \qquad (7)$$

This equation is simply the division of the incremental mass by the mass per size increment to obtain the number per size increment or number size distribution. Detailed information on these calculations is provided by Cowen et al. (3).

## OPTICAL PROPERTIES OF THE EMISSION

The mass extinction coefficient of the emission depends on the particle size distribution and refractive index of the material. The refractive index is a complex number. The real part is the ratio of the speed of light in vacuum to the speed of light in the media, and the imaginary part describes the light absorption or the conversion of light to heat. In a recent study by Cowen et al. (3), the refractive indexes of 24 different coals were measured. The real part of the fly ash refractive index ranged from 1.535 to 1.61, and the imaginary part ranged from 0.0005 to 0.029, depending on the carbon content. However, the importance of the refractive index depends on the particle size distribution, as shown in Figures 1 and 2 for the special case of the log-normal particle size distribution. The absorption part of the refractive index is very important in the submicron particle range. The mass extinction coefficient is insensitive to refractive index for particles larger than 2 µm. For application to the control of fly ash, the mass extinction coefficient is not sensitive to the refractive index because the particle distributions are usually above 4 µm in

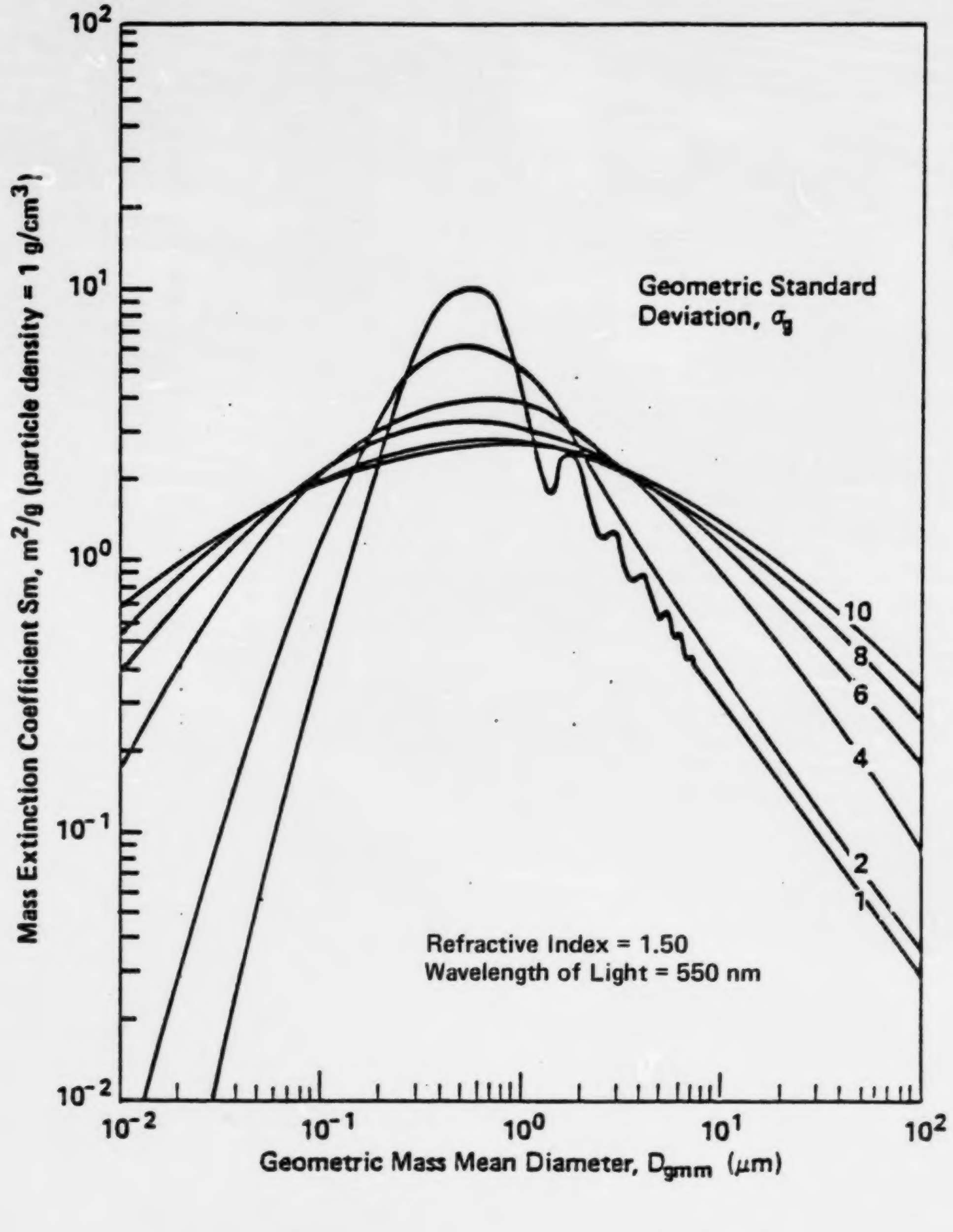

Figure 1. Mass extinction coefficient as a function of particle size distribution for a nonabsorbing aerosol.

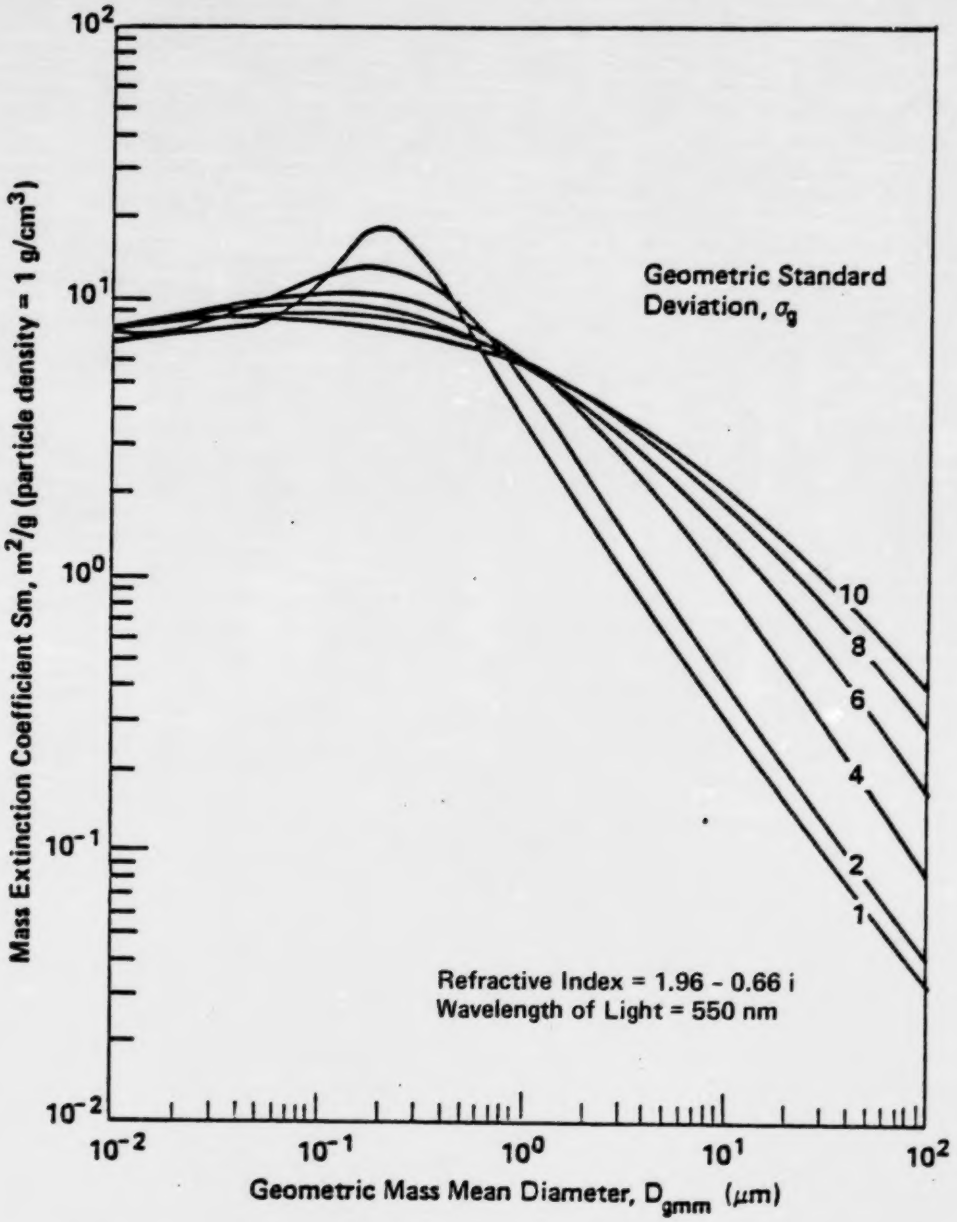

Figure 2. Mass extinction coefficient as a function of particle size distribution for an absorbing aerosol.

diameter. One possible exception to this generalization is submicron carbon particles or soot formed by boiler upsets. As shown in Figure 2, submicron carbon particles have a very high mass extinction coefficient.

The opacity and mass concentration relationships are affected by mechanisms in the control equipment that may change the particle size distributions of the emissions. The particle size distributions emitted downstream of a control device include features introduced by the control device. For example, in a coal-fired boiler, the combustion of pulverized coal produces a bimodal distribution with one mode at about 0.1 μm and the other mode at above 4 μm, depending on the ash content of the coal as summarized by Damle et al. (4) and McElroy et al. (5). The control device then modifies the particle size distribution according to its characteristics. The characterictics of the control device will depend on both the collection and entrainment processes.

## ELECTROSTATIC PRECIPITATION

### MATHEMATICAL MODEL

Predictive electrostatic precipitation computer models are available for design and research. The model used in this study is described by Lawless et al. (6) and is based in part on the Southern Research Institute (SoRI) model described by McDonald (7) and Mosley et al. (8). The important mechanisms included in the model are:

- Collection
- Sneakage
- Rapping reentrainment.

The rapping particle size distribution reported by Gooch and Marchant (9) was used in the model calculations.

### PARAMETRIC STUDY

The parametric study was conducted by varying the key inputs: particle size distribution, rapping losses, and specific collection area. The input parameters are summarized in Table 1. The objective is to evaluate these parameters over the extremes and midpoint values.

### RESULTS

The results are summarized in a series of figures and tables. The basic question is the sensitivity of the mass extinction coefficient to the rapping entrainment and particle size distribution. The computer runs are summarized in Table 2. As shown in Figure 3, the mass extinction coefficient was computed as a function of cumulative specific collection area (SCA). This illustrates how the particle size distribution changes through the precipitator and subsequent modification of the mass extinction coefficient. As shown in the figure, the rapping reentrainment mechanism is even more

## TABLE 1. SUMMARY INPUT PARAMETERS

| | | | |
|---|---|---|---|
| Wire-to-plate spacing, m | 0.127 | | |
| Wire radius, m | $2.54 \times 10^{-10}$ | | |
| Area per section, $m^2$ | 1,477 | | |
| Sections | 6 | | |
| Gas flow rate, $m^3/s$ | 1.17 | | |
| Total specific collection area $m^2/m^3/s$ ($ft^2/ft^3/min$) | 78.3 (398) | | |
| Temperature, °C | 1.60 | | |
| Pressure, atm | 1.0 | | |
| Length of section, m | 8 | | |
| Resistivity, ohm-cm | $2 \times 10^{10}$ | | |
| Applied voltage, kV (depending on section and operating conditions) | up to 55 | | |
| Current density, $A/m^2$ (depending on section and operating conditions) | up to $4 \times 10^{-4}$ | | |
| Sneakage/section, % | 3 | | |
| Rapping reentrainment, % | 0, 10, 20 | | |
| Σ (standard deviation of gas velocity) | 0.25 | | |
| | Case 1 | Case 2 | Case 3 |
| Geometric mass mean diameter, μm | 4 | 20 | 50 |
| Geometric standard deviation | 3 | 4 | 5 |
| Mass concentration at inlet actual conditions | 2.29 | 2.29 | 2.24 |
| Submicron particle mode | 1% by mass at 0.1 μm diameter (5) | | |
| Refractive index | 1.57 - 0.007i (10) | | |
| Particle density, $g/cm^3$ | 2.27 (10) | | |

## TABLE 2. SUMMARY OF ELECTROSTATIC PRECIPITATOR SIMULATIONS

| Section | Rapping reentrainment % | 4 μm Diameter |  | 20 μm Diameter |  | 50 μm Diameter |  |
|---|---|---|---|---|---|---|---|
|  |  | Mass, g/m$^3$ | Sm, m$^2$/g | Mass, g/m$^3$ | Sm, m$^2$/g | Mass, g/m$^3$ | Sm, m$^2$/g |
| Inlet |  | 2.29 | 0.474 | 2.29 | 0.111 | 2.29 | 0.0399 |
| 1 | 0 | 1.28 | 0.621 | 0.0841 | 0.687 | 0.0276 | 0.537 |
|  | 10 | 1.38 | 0.590 | 0.203 | 0.392 | 0.0821 | 0.296 |
|  | 20 | 1.49 | 0.568 | 0.322 | 0.322 | 0.137 | 0.246 |
| 2 | 0 | 0.260 | 1.194 | 0.0103 | 1.345 | 0.00319 | 1.145 |
|  | 10 | 0.382 | 0.8987 | 0.0334 | 0.559 | 0.0127 | 0.434 |
|  | 20 | 0.523 | 0.731 | 0.0795 | 0.349 | 0.0328 | 0.281 |
| 3 | 0 | 0.0314 | 2.127 | 0.00222 | 1.74 | 0.000781 | 1.462 |
|  | 10 | 0.0789 | 1.198 | 0.00608 | 0.784 | 0.00229 | 0.656 |
|  | 20 | 0.146 | 0.7797 | 0.0196 | 0.383 | 0.00801 | 0.327 |
| 4 | 0 | 0.00615 | 2.771 | 0.000652 | 1.974 | 0.000232 | 1.665 |
|  | 10 | 0.0161 | 1.463 | 0.00134 | 1.115 | 0.000494 | 0.938 |
|  | 20 | 0.0387 | 0.784 | 0.00496 | 0.463 | 0.00201 | 0.395 |
| 5 | 0 | 0.00182 | 3.093 | 0.000209 | 2.185 | 0.0000716 | 1.881 |
|  | 10 | 0.00391 | 1.872 | 0.000353 | 1.445 | 0.000125 | 1.233 |
|  | 20 | 0.0105 | 0.903 | 0.00130 | 0.573 | 0.000519 | 0.485 |
| 6 | 0 | 0.000598 | 3.295 | 0.0000686 | 2.383 | 0.0000221 | 2.119 |
|  | 10 | 0.00111 | 2.251 | 0.000105 | 1.718 | 0.0000352 | 1.498 |
|  | 20 | 0.00298 | 1.070 | 0.000355 | 0.7093 | 0.000138 | 0.599 |

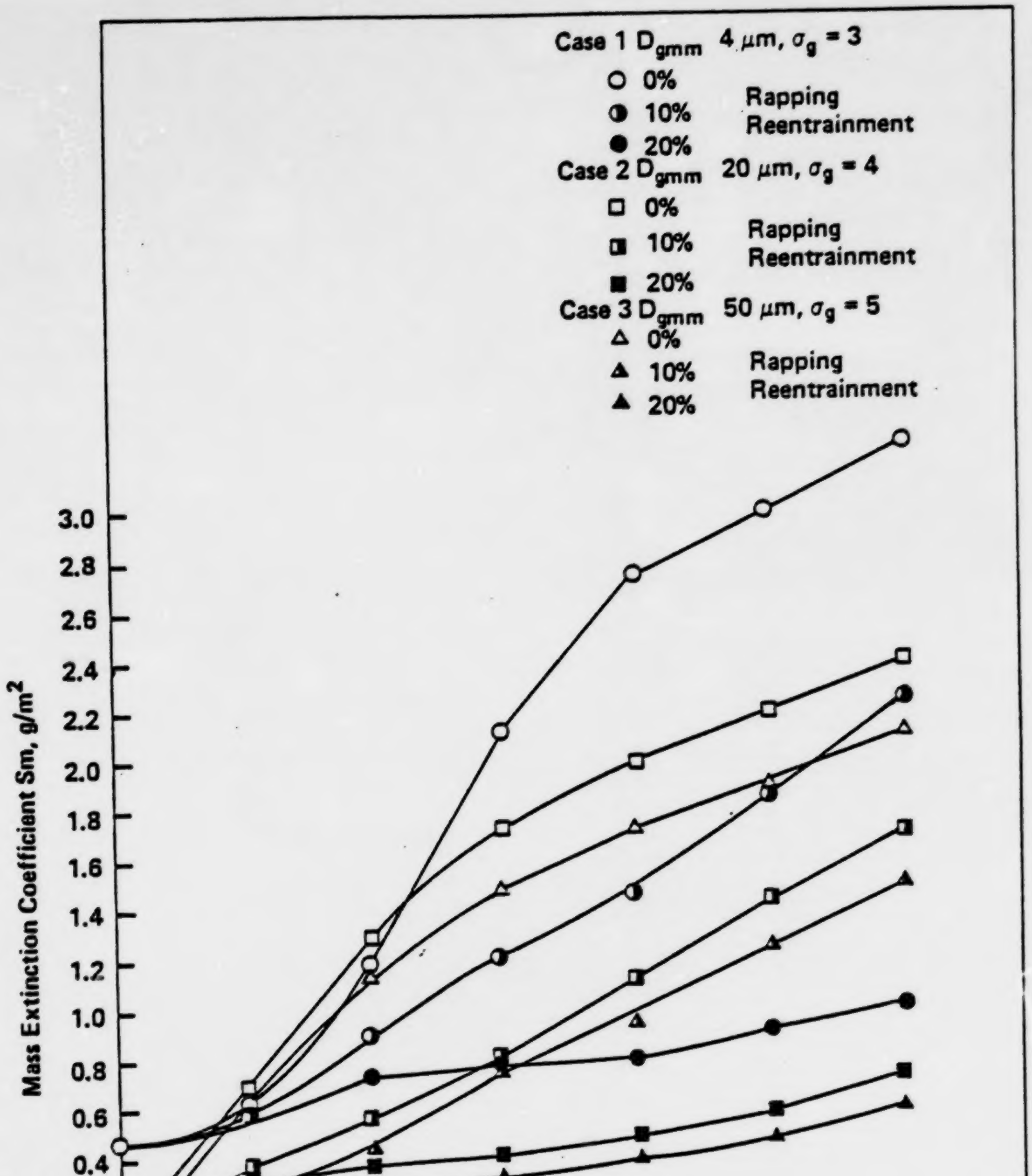

Figure 3. Mass extinction coefficient as a function of SCA.

important to the mass extinction coefficient than the inlet particle size distribution.

In Figure 4, the mass extinction coefficient is shown as a function of mass concentration. The implication is that the mass extinction coefficient depends on the efficiency of the precipitator. As reported by Ensor et al. (11), the data from transmissometer measurements during mass source tests have similar trends of increasing mass extinction coefficient with decreasing mass concentration. In Figure 5, the light transmittance for these cases is reported as a function of mass concentration with rapping reentrainment as a parameter. Two points should be made:

1. The rapping reentrainment is an important factor in mass correlation studies; therefore, effort should be made during field tests to report other data documentating precipitator operating modes.

2. The opacity mass concentration data should be nonlinear because of the changing mass extinction coefficient. This fact is not taken in account in most mass correlation studies.

## FABRIC FILTRATION

### MECHANISMS IN FABRIC FILTRATION

In recent years, fabric filtration has become an accepted control option for utility boilers. There has been limited work in the development of a predictive computer model by Dennis and Klemm (12) and more recent efforts have been summarized by Ensor et al. (13). In most installations, opacity is not a limitation because of the inherently high efficiency of fabric filtration.

Dennis and Klemm (12) concluded that, because most of the penetration of the ash was through pinholes in the fabric, the emissions leaving the baghouse should have the same size distribution as the inlet. However, Ensor et al. (14) determined that a baghouse has a particle-size-dependent penetration. Ensor postulated two mechanisms to explain measurements at the Kramer station: straight-through penetration of the particles and seepage of collected material through the fabric. Ensor et al. (14) also reported that, just after cleaning a compartment, the emission particle concentration was increased followed by a decay back to the precleaning concentration. This cleaning puff was estimated to contribute as much as 80 percent of the emissions. Smith et al. (15) reported and measured the size distribution of the burst of submicron particles following cleaning.

The mechanisms for particle penetration through the ash deposit and fabric are as follows. When the fabric is cleaned, cracks or other passageways develop through the filter cake. After cleaning, the particles pass through the cracks and supporting fabric. The classical collection processes of impaction, interception, and diffusion are effective in removing large and small particles. The penetration is a maximum of particles in the 0.1 to 1.0 µm size range. As the cracks and other passages fill, this penetra-

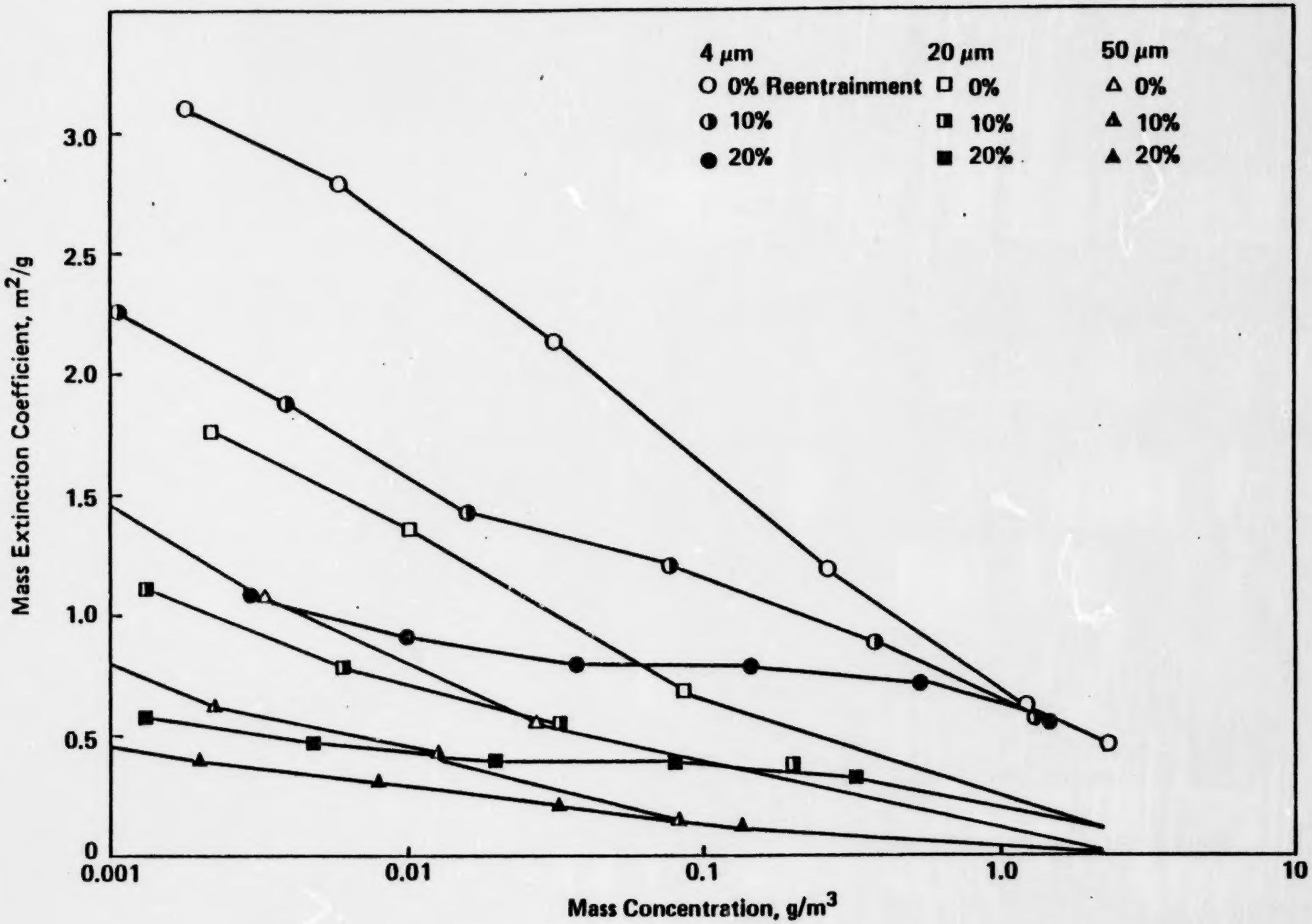

Figure 4. Mass extinction coefficient as a function of outlet concentration.

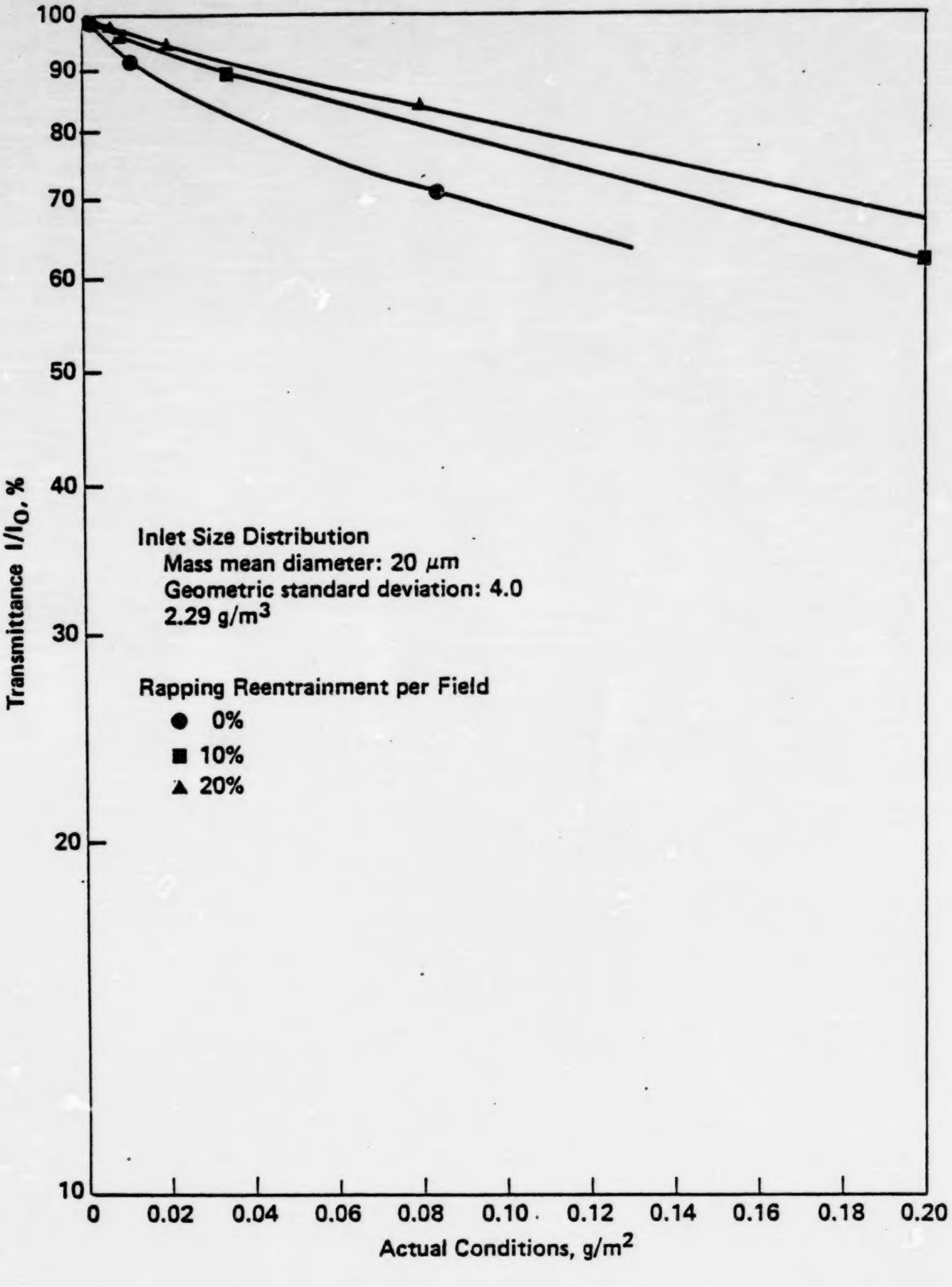

Figure 5. Opacity-mass as a function of rapping reentrainments.

tion mechanism gradually ends. The seepage emissions (14) are in the greater than 2 μm range. Bag leaks will cause outlet emissions to be similar to the inlet size distribution with minor change. As an approximation, the seepage emissions will be considered to be similar to the inlet size distribution.

Therefore visible emissions from a fabric filter would result from two sources: breaks in the fabric (resulting in an emission of the unchanged inlet emissions) and cleaning of associated emissions.

## PUFF VERSUS SEEPAGE

The mass extinction coefficient was estimated using the puff distribution data reported by Smith et al. (15). The seepage or leak emissions were estimated using the mass extinction coefficient for our model inlet size distribution. The results are summarized in Table 3. The mass extinction coefficient for baghouses is expected to be much smaller than that for other processes. Excessive emissions are quite likely the result of gross bag leaks and tears.

TABLE 3. FABRIC FILTER OPACITY SUMMARY

| Source | $D_{gmm}$ μm | $\sigma_g$ | Sm $m^2/g$ |
|---|---|---|---|
| Cleaning puff | 1.5 | 2.0 | 1.49 |
| Inlet | 20 | 4.0 | 0.216 |
| Composite<br>(70% cleaning emission) | | | 1.11 |

## SCRUBBERS

## MATHEMATICAL MODEL

Wet scrubbers designed only for particle removal have not been built for utility boiler applications in the last few years. However, low-pressure-drop $SO_2$ absorbers preceded by electrostatic precipitators are currently being installed. Thus, it is worthwhile to consider the effect of scrubbers on plume opacity although enforcement activity is limited because of the difficulty of measuring opacity in emissions with large quantities of water vapor.

The design model developed by Calvert et al. (16) and Yung et al. (17) has proven to be very predictive in the design of scrubbers. The principal mechanism in a gas-atomized scrubber is the internal impaction of particles by water droplets.

The penetration of particles through a venturi scrubber is given by:

$$Pt(d_d) = \exp\left[\frac{2\ Q_L\ u_G\ \rho_L\ d_d\ F(K,f)}{55\ Q_G\ \mu_G}\right] \tag{8}$$

where

$Q_L$ = the liquid volume flow

$u_G$ = gas velocity in the throat

$\rho_L$ = the liquid density

$d_d$ = the droplet diameter

$f$ = the empirical factor, 0.5

$Q_G$ = the gas volume flow

$\mu_G$ = gas viscosity

$F(k,f)$ = defined by equation 10

and

$$K = u_G\ C\ \rho_p\ d_p{}^2/(9\ \mu_G\ d_d) \tag{9}$$

where

$C$ = the Cunningham slip correction factor

$\rho_p$ = the particle density

$d_p$ = the particle diameter

$d_d$ = the droplet diameter

and

$$F(K,f)=K^{-1}\ [-(Kf+0.7) + 1.4\ \ln(Kf+0.7/0.7) + 0.49/(Kf+0.7)]\ . \tag{10}$$

For water, the droplet diameter can be estimated by (18):

$$d_d = 50/u_G + 91.8\ (Q_L/Q_G)^{1.5}\ . \tag{11}$$

These equations were evaluated with a personal computer (Radio Shack TRS-80 Model I) version of a calculator program described by Cowen et al. (3). The particle-size-dependent penetrations are integrated over the particle size distribution to obtain an overall penetration. The outlet particle size distribution is used in a program described by Cowen et al. (10) to obtain the opacity of the emission.

The simulation conditions are summarized in Table 4. The only independent variable was the pressure drop through the scrubber.

### RELATING OPACITY TO COLLECTION MECHANISMS

The opacity from the internal collection mechanisms follows a predictable pattern. The results from the simulation are shown in Table 5. As the pressure drop increases, smaller and smaller particles are captured. This is shown in Figure 6. The changes in the mass extinction coefficient as a function of outlet mass concentration are shown in Figure 7. The mass extinction coefficent is a nonlinear function of the outlet mass concentration with a definite minimum. This minimum results when the scrubber efficiency has increased to the point where the particles with efficient light extinction efficiency are being removed (see Figure 1). The opacity mass concentration curve is not straight as shown in Figure 8. If an electrostatic precipitator precedes a wet scrubber, the maximum light extinction particle size range is expected to be even more pronounced. The rapping emissions from the electrostatic precipitator are easily removed in a low pressure drop scrubber resulting in an emission with a high mass extinction coefficient, as pointed out by Sparks et al. (19). An aerosol from the condensation of sulfuric acid may be formed by quenching sulfur trioxide in a scrubber. This aerosol is submicron and in the optically active region. Therefore very high pressure drops would be required to effect a reduction in the mass extinction coefficient.

## DETACHED PLUMES

### PROBLEM DEFINITION

Detached plumes have presented a problem in efforts to regulate air pollution sources. Volatile material within the stack condenses to form a visible plume upon dilution/cooling in the atmosphere. Transmissometers installed in the stack may indicate an acceptable opacity level while the opacity in the plume may be quite high and unacceptable. The mathematical description of detached visible plumes is very complex and has been solved only recently by Damle et al. (20). A limitation in this research has been the lack of complete data sets taken under the conditions of detached plume formation to provide a test of the complete model. However, it should be pointed out that the components of the model such as liquid/vapor equilibria, nucleation, coagulation, and light scattering have been individually tested many times. The mathematical model agrees qualitatively with the limited existing data and is summarized here.

### MATHEMATICAL APPROACH

The mathematical model consists of setting up mass, momentum, and energy balances. The differental equations are described by Damle et al. (20), and the original paper should be reviewed for more information.

### TABLE 4. INPUT PARAMETERS USED IN SCRUBBER SIMULATION

| | |
|---|---|
| Gas velocity in throat, m/s | 6.5 |
| Gas temperature, °C | 65 |
| Gas viscosity, poise | $1.8 \times 10^{-4}$ |
| Liquid-to-gas flow rate ratio | $9 \times 10^{-4}$ |
| Liquid density, $g/cm^3$ | 1 |
| Particle density, $g/cm^3$ | 2.4 |
| Particle concentration, $g/m^3$ | 10 |
| Geometric mass mean diameter, μm | 20 |
| Geometric standard deviation | 4 |

### TABLE 5. SIMULATION OF PLUME OPACITY EXPECTED FOR VARIOUS VENTURI SCRUBBER PRESSURE DROPS

| Pressure drop cm $H_2O$ | Penetration (fractional) | Efficiency % | Concentration $g/m^3$ | Geometric mean diameter, μm | Geometric mean standard deviation | Sm, $m^2/g$ | Opacity % | $I/I_o$ (fractional) |
|---|---|---|---|---|---|---|---|---|
| 0 | 1 | 0 | 10 | 20 | 4 | 0.216 | -- | -- |
| 0.3 | 0.139 | 86.1 | 1.39 | 1.2 | 2.23 | 1.44 | 99.99 | 0.000045 |
| 7.6 | 0.01678 | 98.3 | 0.1678 | 0.56 | 2.17 | 2.35 | 86.0 | 0.14 |
| 19.47 | 0.00736 | 99.26 | 0.0736 | 0.420 | 2.4 | 2.16 | 54.9 | 0.451 |
| 30.42 | 0.00471 | 99.53 | 0.0471 | 0.357 | 2.65 | 1.92 | 36.3 | 0.637 |
| 95.22 | 0.00114 | 99.89 | 0.0114 | 0.192 | 3.83 | 1.23 | 6.78 | 0.932 |

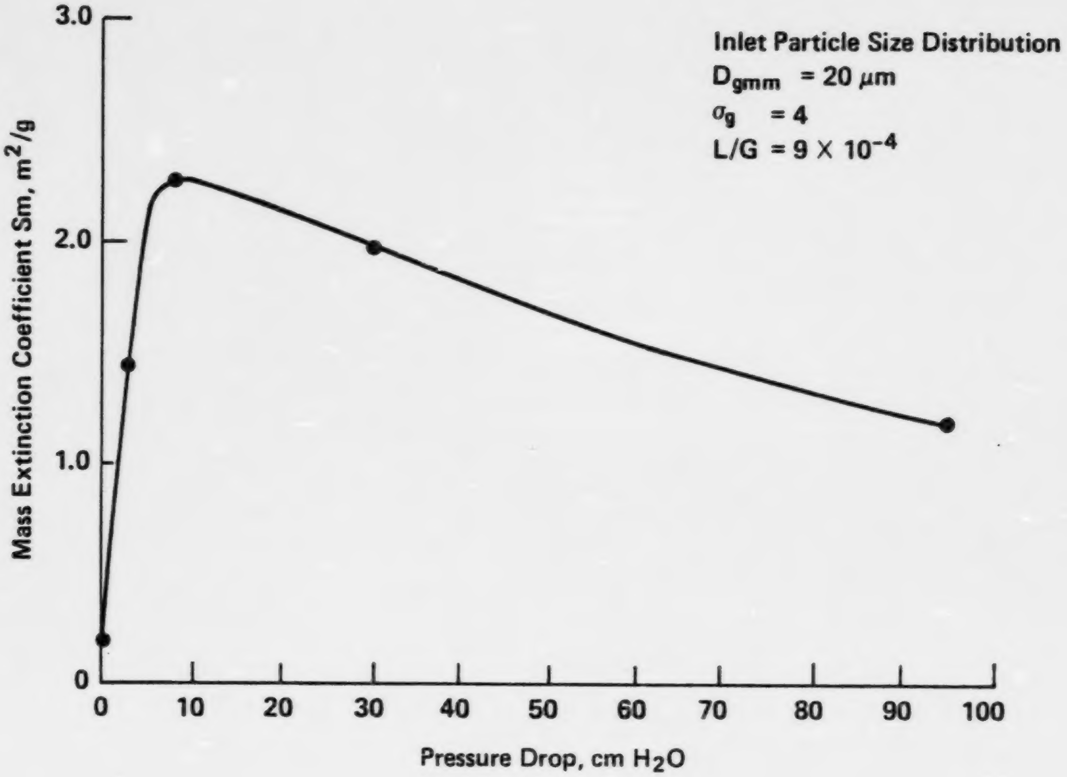

Figure 6. Mass extinction coefficient as a function of scrubber pressure drop.

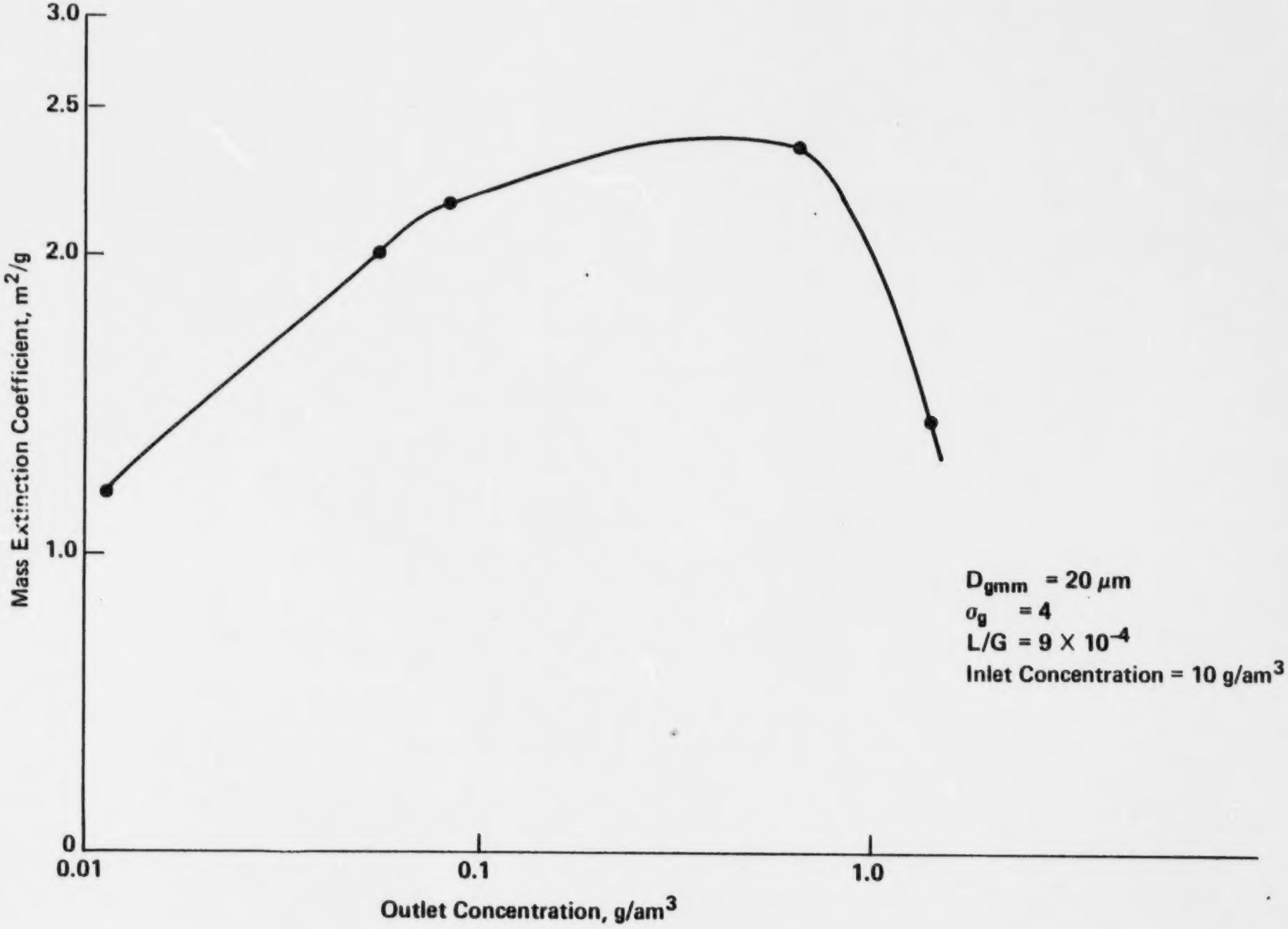

Figure 7. Mass extinction coefficient as a function of outlet concentration.

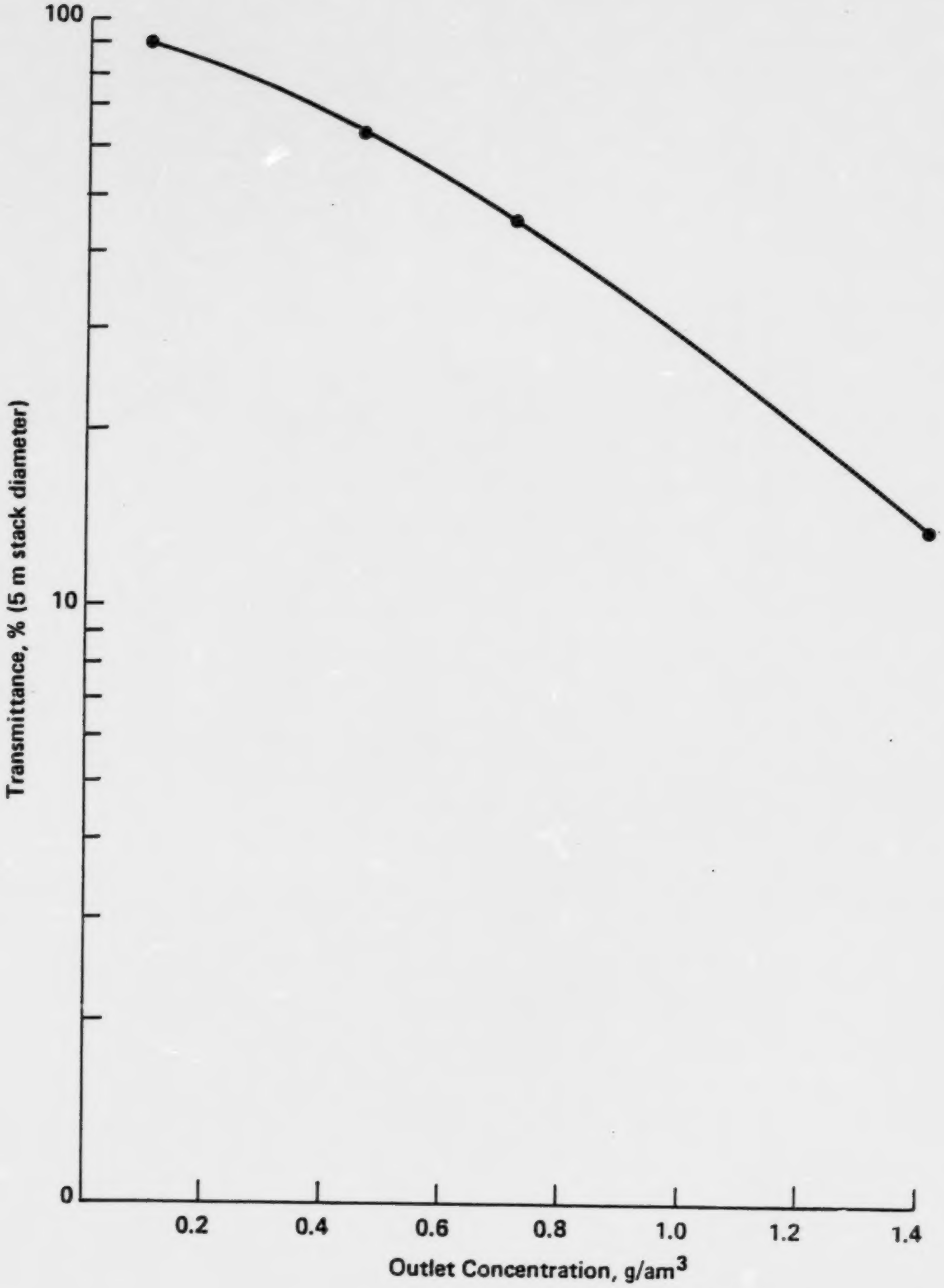

Figure 8. Transmittance/mass concentration relationship for venturi scrubber.

### RESULTS

Some representative results are shown in Table 6. It was found in the simulation that sulfuric acid concentration is the primary variable in affecting the downwind opacity. The concentration of primary submicron particles may have some importance because of their role in the heterogeneous nucleation mechanism. The absence of submicron particles causes homogeneous nucleation, which delays nucleation because of the high supersaturations required. During this delay the plume may be diluted by mixing, lowering the observed opacity. In some cases, downwind opacity due to condensing material may be lowered by controlling primary submicron particles.

## SUMMARY AND CONCLUSIONS

### OPACITY PREDICTION APPROACH

Opacity prediction is based on examining each part of the process and identifying the mechanisms that change the particle size distribution. The most critical part of the process affecting plume opacity is the control device. Plume opacity can be estimated using computer programs written for personal computers. The use of the mass extinction coefficient allows the comparison of various sources and processes.

### SUMMARY OF MECHANISMS

#### Conventional Control Devices

The various mechanisms affecting the mass extinction coefficient are summarized in Table 7. The influence of the control equipment can be great, depending on its operation. This suggests that the control device should be investigated first in opacity troubleshooting.

#### Detached Plumes

The current work in the prediction of detached plumes due to the condensation of sulfuric acid was summarized. The exterior plume is directly related to the concentration of sulfuric acid.

### RESEARCH DIRECTION

The research in plume opacity is directed in two areas. The prediction models are being adapted to microcomputers as described by Viner et al. (21), and these should be available in an integrated format in the future. The second area needing work is the taking of field data comparing predicted opacity with the models.

## ACKNOWLEDGMENTS

This research was conducted as part of U.S. Environmental Protection Agency Cooperative Agreement CR808936-01-0.

TABLE 6. CALCULATION OF EXPECTED PEAK PLUME OPACITY FROM CONDENSING SULFURIC ACID

| $H_2SO_4$ concentration ppm | Peak opacity % |
|---|---|
| 0 | 11.5 |
| 4 | 20 |
| 10 | 35 |
| 20 | 52 |
| 40 | 70 |

Conditions:

| | |
|---|---|
| Small particle mode | |
| Geometric mass mean diameter, μm | 0.15 |
| Geometric standard deviation | 1.3 |
| Concentration, number/$cm^3$ | $1 \times 10^6$ |
| Large particle mode | |
| Geometric mass mean diameter, μm | 2.0 |
| Geometric standard deviation | 1.8 |
| Concentration, number/$cm^3$ | $6 \times 10^3$ |
| Stack diameter, m | 4 |
| Stack temperature, °C | 200 |
| Stack moisture, % by volume | 5 |
| Particulate concentration, mg/$m^3$ | 100 |
| Stack exit velocity, m/s | 20 |
| Ambient temperature, °C | 20 |
| Wind velocity, m/s | 5 |

TABLE 7. COMPARISON OF CONTROL DEVICE MECHANISMS

| Control device | Mechanism | Effect on Sm |
|---|---|---|
| Electrostatic precipitator | Collection | Increases |
| | Rapping | Reduces |
| | Sneakage | Reduces |
| Scrubber | Collection | Increases then decreases |
| Baghouse | Collection | Not a major change |
| | Cleaning puff | Increases |

## REFERENCES

1. Ensor, D. S., Lawless, P. A., and Cowen, S. J. Modeling smoke plume opacity from particulate control equipment. Third Symposium on the Transfer and Utilization of Particulate Control Technology, Vol. IV, EPA-600/9-82-005d (NTIS PB83-149617). U.S. Environmental Protection Agency, Research Triangle Park, NC, July 1982.

2. Ensor, D. S., and Pilat, M. J. Calculation of smoke plume opacity from particulate air pollutant properties. JAPCA. 21:496-501, 1971.

3. Cowen, S. J., Ensor, D. S., and Sparks, L. E. TI-59 programmable calculator programs for in-stack opacity, venturi scrubbers, and electrostatic precipitators. EPA-600/8-80-024 (NTIS PB80193147). U.S. Environmental Protection Agency, May 1980.

4. Damle, A. S., Ensor, D. S., and Ranade, M. B. Coal combustion aerosol formation mechanisms--a review. Aerosol Sci. Technology. 1:119-133, 1982.

5. McElroy, M. W., Carr, R. C., Ensor, D. S., and Markowski, G. R. Size distribution of fine particles from coal combustion. Science. 215:13-19, 1982.

6. Lawless, P. A., Dunn, J. W., and Sparks, L. E. A computer model for ESP performance. Third Symposium on the Transfer and Utilization of Particulate Control Technology, Vol. II, EPA-600/9-82-005b (NTIS PB83-149591). U.S. Environmental Protection Agency, Research Triangle Park, NC, July 1982.

7. McDonald, J. R. A mathematical model of electrostatic precipitation (revision 1): Vol. I. Modeling and programming. EPA-600/7-78-111a (NTIS PB284614). U.S. Environmental Protection Agency, June 1978.

8. Mosley, R. B., Anderson, M. H., and McDonald, J. R. A mathematical model of electrostatic precipitation (revision 2). EPA-600/7-80-034 (NTIS PB80-190994). U.S. Environmental Protection Agency, February 1980.

9. Gooch, J. P., and Marchant, G. H. Electrostatic precipitator rapping reentrainment and computer model studies. Electric Power Research Institute Report No. EPRI FP-792, 1978.

10. Cowen, S. J., Ensor, D. S., and Sparks, L. E. TRS-80 in-stack opacity computer programs user and programmer manual. EPA draft report, 1984.

11. Ensor, D. S., Lawless, P. A., and Sparks, L. E. Interpretation of data from electrostatic precipitator field tests. Fourth Symposium on the Transfer and Utilization of Particulate Control Technology, Houston, Texas. October 1982.

12. Dennis, R., and Klemm, H. A. A model for coal fly ash filtration. JAPCA, 29:230-234, 1979.

13. Ensor, D. S., VanOsdell, D. W., Viner, A. S., and Hovis, L. S. Modeling baghouse performance. Fifth Symposium on the Transfer and Utilization of Particulate Control Technology, Kansas City, Missouri. August 1984.

14. Ensor, D. S., Cowen, S. J., Shendrikar, A., Markowski, G., Woffinden, G., Pearson, R., and Scheck, R. Kramer Station fabric filter evaluation. EPRI Report No. CS-1669, 1981.

15. Smith, W. B., Cushing, K. M., and Carr, R. C. Measurement procedures and supporting research for fabric filters. Proceedings, First Conference on Fabric Filter Technology for Coal-Fired Power Plants. CS-2238, pp. 3-89 to 3-111, February 1982.

16. Calvert, S., Goldshmid, J., Leith, D., and Mehta, D. Scrubber handbook. EPA-R2-72-118a (NTIS PB 213016). U.S. Environmental Protection Agency, August 1972.

17. Yung, S. C., Calvert, S., and Barbarika, H. F. Venturi scrubber performance model. EPA-600/2-77-172 (NTIS PB 271515). U.S. Environmental Protection Agency, August 1977.

18. Sparks, L. E. SR-52 programmable calculator programs for venturi scrubbers and electrostatic precipitators. EPA-600/7-78-026 (NTIS PB 277672). U.S. Environmental Protection Agency, March 1978.

19. Sparks, L. E., Ramsey, G. H., and Daniel, B. E. In-stack plume opacity from electrostatic precipitator scrubber systems. Second Symposium on the Transfer and Utilization of Particulate Control Technology, Vol. IV. EPA-600/9-80-039d (NTIS PB81-122228). U.S. Environmental Protection Agency, September 1980.

20. Damle, A. S., Ensor, D. S., and Sparks, L. E. Prediction of the opacity of detached plumes formed by condensation of vapors. Atmos. Environment. 18:435-444, 1984.

21. Viner, A. S., Ensor, D. S., and Sparks, L. E. Microcomputer models for particulate control. Fifth Symposium on the Transfer and Utilization of Particulate Control Technology, Kansas City, Missouri. August 1984.

# APPENDIX: Attendees

# Transfer & Utilization of Particulate Control Tech.

08/27/84-08/30/84
Hyatt Regency Hotel

## List of Attendees

Peter J. Aa
Product Mgr.
Research-Cottrell, Inc.
P.O. Box 1500
Somerville, NJ 08876
201/685-4000

David W. Ablin
Sales Engineer
FMC Corp. Air Quality Control
1501 Woodfield Road
Schaumburg, IL 60195
312/843-1700

Larry Adair
Director Production Engr.
KC Board of Public Utilities
700 Minnesota Ave.
Kansas City, KS 66101
913-281-8366

Rui F. Afonso
Senior Staff Engineer
Dynatech R/D Co.
99 Erie Street
Cambridge, MA 02139
617/868-8050

Anthony J. Ahern
Section Mgr.
American Electric Power
One Riverside
Columbus, OH 43216
614/223-3260

Carl-Eric Akerlund
Chief Engr.
Flakt AB
351 87
Vaxjo, Sweden
0470-87403

Terry L. Albrecht
n/a
Farmland Ind., Inc.
P.O. Box 570
Coffeyville, KS 67337
316/251-4000

Charles A. Altin
Project Mgr.
Ebasco Services, Inc.
145 Technology Park
Norcross, GA 30092
404/662-2347

Ralph F. Altman
Project Mgr.
Electric Power Research Inst.
516 Franklin Bldg.
Chattanooga, TN 37411
615/899-0072

Ron Anderson
Project Engineer
Cominco, Inc.
Trail, B.C. B1R 4L8
N/A
604/364-4658

Karl-Hugo Andersson
Chief Engr.
Flakt Industri AB
351 87
Vasjo, Sweden
0470-87550

Richard A. Aquino
Regional Sales Manager
Belco Pollution Control Corp.
119 Littleton Road
Parsippany, NJ 07054
201/263-8900

Yasuo Arai
Project Mgr.
Electric Power Research Inst.
3412 Hillview Ave.
Palo Alto, CA 94303
415/855-2278

Bill Armiger
N/A
EPSCO
325 Mountain View Rd.
Skillman, NJ 08558
609/466-3488

James A. Armstrong
Senior Research Engineer
Denver Research Institute
P.O. Box 10127
Denver, CO 80210
303/871-2810

Franklin A. Ayer
Consultant
Research Triangle Institute
P.O. Box 12194
Research Triangle Park, NC
919 541-6260 OR 6992

Michael Babb
Sales & Serv. Engr.
Martin Marietta Basic Prod.
Executive Plaza II
Hunt Valley, MD.
301/667-0200

Robert A. Babb
Supervisor, Mech. Design
TVA
400 Summit Hill
Knoxville, TN 37902
615/632-2617

S. M. Babish
Regional Manager
Air Clean Damper Co.
P.O. Box 188
Grandview, MO 64030
816/941-2655

Steve Babiuch
Sr. Applications Engr.
Standard Havens Inc.
8800 East 63rd St.
Kansas City, MO 64133
816/737-0400

Armand A. Balasco
Engineering Consultant
Arthur D. Little, Inc.
Acorn Park
Cambridge, MA 02140
617/864-5770

Joseph A. Barabas
Project Engineer, R&D
Fuller Co.
P.O. Box 204
Bethlehem, PA 18001
215/266-5038

William E. Barkovitz
N/A
Consultant
1021 Harrison
Lincoln Park, MI 48146
313/381-8005

Richard Barnes
Res. Chemist
Burlington Glass Fabric
110 Andrews St.
Greensboro, NC 27406
919/379-2867

C. B. Barranger
Mgr.Fabric Filters
Flakt, Inc.
Environmental Systems Div.
P.O. Box 87
KNOXVILLE, TN 37901

Kenneth S. Basden
Senior Lecturer
Un. of New South Wales
Kensington NSW 2033
Australia
AUS.02-663-0351

D. S. Batchelor
Special Projects Mgr.
Kerr-McGee Chemical Corp.
Kerr-McGee Center, MT-1503
Oklahoma City, OK 73125
405/270-3371

Pat Bauer
Service Supv.
General Electric
10550 Barkley
Overland Park, KS 66212
913/967-6307

Walter A. Baxter
Director, Engineering
Environmental Elements
P.O. Box 1318
Baltimore, MD 21203
301/368-7046

David S. Beachler
Manager
RTI Office for ETS
111 Edenburg Rd.
Raleigh, NC 27608

Daniel C. Beal
Business Repv.-Environmental Syst.
General Electric Co.
2015 Spring Road
Oak Brook, IL 60521
312-986-3021

Kevin F. Bean
Electrical Engr.
City Water Light & Power
3100 Stevenson Dr.
Springfield, IL 62757
217/786-4034

Robert J. Beaton
Plant Superintendent
Nebraska Public Power District
P.O. Box 306
Bellevue, NE 68005-0306
402-291-1500

Clifford H. Beck
Consultant
Power Design Services, Inc.
2155 Scotch Pine
Northbrook, IL 60062
312/833-5710

Andrew Becker
Mgr. Tech. Div.
ENELCO
7249 National Dr.
Hanover, MD 21076
301/796-8622

R. Bectaghon
Sales Mgr.
Wheelabrator Sinto Do Brazil
CAIXA Postal 4584
01D00 Sao Paulo, Brazill
412/288-7416

Robert C. Bedick
Project Manager
U.S. Dept. of Energy
880 Collins Ferry Road
Morgantown, WV 26505
304/291-0795

Victor H. Belba
Staff Engr.
Stearns Catalytic Corp.
P.O. Box 5888
Denver, CO 80217
303/758-2878

Steve Bellmore
Reg. Sales Mgr.
W.W. Criswell Co.
800 Industrial Hwy.
Riverton, NJ 08077
609/829-6300

Lawrence J. Bennett
V.P.- General Mgr.
Filters For Industry
1340 E. Eighth St.
Tempe, AZ 85281
602/968-6447

Lutz Bergmann
President
Filter Media Consulting, Inc.
P.O. Box 2189
La Grange, GA 30241
404-822-3108

Sharad Bhatia
Environmental Engineer
Kansas Power & Light
P.O. Box 889
Topeka, KS 66601
913/296-6567

Roy E. Bickelhaupt
President
Bickelhaupt Assoc., Inc.
P.O. Box 3532
Carbondale, IL 62901
618/529-5296

Brian Bierman
Electronic Tech.
Neundorfer, Inc.
4590 Hamann
Cleveland, OH 44094
216/942-8990

Ray Bieser
Electrical Maintenance Engr.
Missouri Public Serv. Co.
P.O. Box 408
Sibley, MO 64088
816/249-6196

Barbara J. Billman
Grad. Research Asst.
North Carolina State Univ.
Marine, Earth, & Atmos. Sci. Dept.
Raleigh, NC 27695-8208
919/541-2811

H. R. Black
Engineer
Texas Air Control Board
6330 Hwy. 290 E
Austin, TX 78731
512/451-5711 X240

Gary M. Blythe
Sr. Chemical Engr.
Radian Corp.
P.O. Box 9948
Houston, TX 78766
512/454-4797

Ronald Blythe
Envirochemical Supv.
Southwestern Public Serv. Co.
P.O. Box 1261
Amarillo, TX 79170
806/381-6217

Jim Boak
Product Specialist
Nalco Chemical Co.
2901 Butterfield
Oakbrook, FL 60521
312/887-7500

Vaughn V. Boley
Engr.
Ohio Edison Co.
Box 176
Stratton, OH 43961
614/537-1546 X-353

John E. Bollinger
Electrical Engr.
Babcock & Wilcox
20 S. Van Buren
Barberton, OH 44203
216/860-6234

William Borowy
Staff Engr.
VEPCO
OJRP P.O. Box 26666
Richmond, VA 23261
804/771-4896

Paul W. Bowden
Technical Manager
Albany International
P.O. Box 417
Gosford N.S.W. 2250 Australia
043-282222

C. F.P. Bowen
President
NELS Constulting Services, Inc.
P.O. Box 2367, St. B
St. Catharines, Ontario
CANADA L2M 7M7

Russell H. Boyd, Jr.
Supervising Engr.
Envirosphere Co.
145 Technology Park
Norcross, GA 30076
404/449-6639

Howard A. Boyer
Mgr. New Bus. Dev.
Allied Corp.
P.O. Box 1087R
Morristown, NJ 07960
N/A

Keith M. Bradburn
n/a
Flakt
Crosspark Plaza
Knoxville, TN 37921
N/A

Willis P. Bradford
Manager Special Projects
AMAX Environmental Serv., Inc.
1707 Cole Blvd.
Colden, CO 80401
303-231-0678

Rick Brandt
Mgr. Precipitator Prod. & Tech. Div
BHA Co.
8800 E. 63rd. St.
Kansas City, MO 64133
816/356-8400

Thomas E. Britcher
Sales Mgr. S.W. Region
Environmental Elements
3700 Koppers St.
Baltimore, MD 21203
301/368-7290

Theodore G. Brna
Mgr., Dry FGD Program
U.S. EPA
1 ERL MD 61
Research Triangle Park, NC 29711
919/541-2683

Steve Brown
Assoc. Engr. Fuel Additives
Martin Marietta
1445 S. Rolling Rd.
Baltimore, MD 21227
301/247-0770 X-414

Joe Brumfield
Research Chemist
U.S. Navy
Code G51
Dahlgren, VA 22448
703/663-8621

Bill Brunker
Environmental Mgr.
Owens-Corning Fiberglas
300 Sunshine Rd.
Kansas City, KS 66115
913-281-9485

Dean E. Budrow
Sr. Technician
Environmental Consultant
2501 W. Behrend Ste. 7
Phoenix, AZ 85027
602/582-5155

Winston Budrow
President
Environmental Consultant Co.
2501 W. Behrend Ste. 7
Phoenix, AZ 85027
602/582-5155

Richard Bundy
Mgr. Air Pollution Control
Standard Havens Inc.
8800 East 63rd St.
Kansas City, MO 64133
816/737-0400

George F. Burnett
Sr. Mechanical Engr.
Burns & McDonnell Engr.
4800 E. 63rd. St.
Kansas City, MO 64052
816/333-4375

Timothy T. Burnett
Mgr. Filtration & Aerospace
J.P. Stevens & Co., Inc.
P.O. Box 208
Greenville, SC 29602
803/239-4828

John C. Buschmann
Process Engr. Mgr.
Flakt, Inc.
9111 Cross Park Drive
Knoxville, TN 37923
615/693-7550

Vann Bush
Research Physicist
Southern Research Inst.
P.O. Box 55305
Birmingham, AL 35255-5305
205/323-6592

Jean Bustard
Assoc. Physicist
Southern Research Inst.
P.O. Box 10155
Denver, CO 80210
303/922-9765

Robert B. Candelaria
Env. Engr.
Salt River Project
P.O. Box W
Page, AZ 86040
602/645-8811

Robert C. Carr
Program Manager
Electric Power Research Inst.
3412 Hillview Avenue
Palo Alto, CA 94303
415-855-2422

Tim Carr
Director
C. P. Environmental, Inc.
15 W. 700 Frontage Rd.
Hinsdale, IL 60521
312-985-4800

Joseph C. Carvitti
Speaker
PEDCO Environmental, Inc.
11499 Chester Rd.
Cincinnati, OH 45246
513/782-4700

Peter Castle
Prof. of Electrical Engr.
University of Western Ontario
London, Ontario
Canada N6A 5B9
519/679-3333

Gary Cerantola
Administrator
Alberta Power Ltd.
10035 105 St.
Edmonton, Alberta
CANADA T5J 2V6

Richard L. Chambers
Supervisory Engr.
Southwestern Public Serv. Co.
P.O. Box 1261
Amarillo, TX 79170
806/378-2121

Ramsay Chang
Sr. Staff Engr.
Acurex Corp., Energy & Envirn. Div.
P.O. Box 7555.
Mountain View, CA 94039
415/964-3200

Edward L. Chapman
Western Regional Mgr.
FMC Corp.
1501 Woodfield Rd.,Ste. 300 E.
Schaumburg, IL 60195
312/843-1700

Yang-Jen Chen
Sr. Research Engr.
Joy Industrial Equipment Co.
P.O. Box 2744, Terminal Annex
Los Angeles, CA 90015
213/240-2300

W. A. Cheney
Vice President
United Air Specialists, Inc.
4440 Creek Rd.
Cincinnati, OH 45242
513/891-0400

Ta-Kuan Chiang
Senior Engineer
G.E. Environmental Serv., Inc.
n/a
Lebanon, PA 17042
717/274-7000

David F. Ciliberti
Engr.
Westinghouse Electric Corp.
1310 Beulah Rd.
Pittsburgh, PA 15235
412/256-2256

Leo Cirotski
Supt. Process Engr.
Kerr-McGee Chemical Corp.
Main St., P.O. Box 367
Trona, CA 93562
619/372-4311

Wayne Clark
V. P. & Gen. Mgr.
Lucidyne, Inc.
4235 Ponderosa Ave.
San Diego, CA 92123
619-571-7032

Sid Clements
Research Scientist
Department of Physics
The Florida State Univ.
Tallahassee, FL 32306
904/644-6246

E. L. Coe, Jr.
Technical Director
WAHLCO, INC.
3600 W. Segerstrom Ave.
Santa Ana, CA 92704
714-979-7300

William H. Cole
Consulting Engr.
Gibbs & Hill, Inc.
11 Penn Plaza
New York, NY 10001
212/760-5706

Quincy D. Corey
Assoc. Engr.
Duke Power Co.
P.O. Box 33189
Charlotte, NC 28242
704/373-7245

Cheryl E. Cortright
Senior Engineer
Salt River Project
1521 Project Drive
Tempe, AZ 85281
602-236-5183

John R. Cotter
Air Pollution Control Engr.
Kansas City Dept. of Health
619 Ann Ave.
Kansas City, KS 66101
919/321-4803

Chatten J. Cowherd
Head, Air Quality Assess. Sec.
Midwest Research Inst.
425 Volker Blvd.
Kansas City, MO 64110
816/735-7600

Fred Cox
General Sales Mgr.
Menardi Southern
P.O. Box 240
Augusta, GA 30913
404/724-8241

David W. Coy
Sr. Engr.
Research Triangle Inst.
P.O. Box 12194
Research Triangle Park, NC 27709
919/541-6940

Kevin Craft
Assoc. Engr.
Baltimore Gas & Electric
P.O. Box 1475
Baltimore, MD 21203
301/234-7637

Brent Craven
Utilities Manager
Farmland Industries, Inc.
P.O. Box 570
Coffeyville, KS 67337
316/251-8015

Philip B. Crommelin, Jr.
Consultant In ESP
N/A
Box 38
Stanton, NJ 08885
201/236-23244

Robert R. Crynack
Mgr. EP RID
Wheelabrator APC
5100 Casteel Dr.
Coraopolis, PA 15108
412/787-9710

Ed Cullinan
Sales
Midwest Power Corp.
3960 Industrial Ave.
Rolling Meadows, IL 60008
312/870-2400

John D. Cunic
Senior Staff Engineer
Exxon Research & Engineering Co.
P.O. Box 101
Florham Park, NJ 07932
201-765-6471

Richard Cunningham
Tech. Asst.
Eastman Kodak Co.
Utilities Div., Bldg 31
Rochester, NY 14650
716/477-4207

Kenneth M. Cushing
Head, Fabric Filter Research Sec.
Southern Research Inst.
P.O. Box 55305
Birmingham, AL 35255-5305
205/323-6592

Richard R. D'Auteuil
Dir. Environmental Affairs
Buckeye Power, Inc.
P.O. Box 29149
Columbus, OH 43229
614/846-5757

Robert S. Dahlin
Research Chemical Engr.
Southern Research Inst.
P.O. Box 55305
Birmingham, AL 35255-5305
205/323-6592

Ashok S. Damle
Research Engineer
Research Triangle Inst.
P.O. Box 12194
Research Triangle Park, NC 27709
919/541-5829

E. A. Danko
Research Engr.
So. California Edison Co.
P.O. Box 800
Rosemead, CA 91770
818/572-2780

John R. Darrow
Associate
W. L. Gore & Associates
101 Lewisville Rd.
Elkton, MD 21921
301-392-3300

Jane H. Davidson
Grad. Research Assist.
Duke University
Department of Engineering
Durham, NC 27706
919/684-2832

Wayne T. Davis
Assoc. Prof. of Civil Engr.
The University of Tennessee
220 Perkins Hall
Knoxville, TN 37996-2010
615/974-7728

Mark Dershowitz
Marketing Representative
Shell Mining Co.
P.O. Box 2906
Houston, TX 77252
713/870-2835

Robert Desantis
Mngr., National Accounts
PPG Industries, Inc.
322 Park Ave.
Scotch Plains, NJ 07076
201/322-7320

Edward B. Dismukes
Sr. Research Advisor
Southern Research Inst.
P.O. Box 55305
Birmingham, AL
205/323-6592

R. P. Donovan
Physicist
Research Triangle Inst.
P.O. Box 12194
Research Triangle Park, NC 27709
919-541-6826

Martin P. Downey, Jr.
District Marketing Manager
Pullman Power Products
P.O. Box 2
Houston, TX 77001
713-672-2491

Delmar J. Doyle
Manager International
Wheelabrator Frye
600 Grant Street
Pittsburgh, PA 15219
412-288-7416

Ed Drdla
Special Projects Engineer
Omaham Public Power District
1623 Harney St.
Omaha, NE 68102
402/536-4487

Carter Dreves
Dir. Marketing Communications
Wheelbrator Air Pollution Control
600 Grant St.
Pittsburgh, PA 15219
412/288-7325

Gerald W. Driggers
Par. R&D Mgr.
Combustion Engineering
31 Inverness Ct.
Birmingham, AL 35243
205/967-9L00

Rod Dubinsky
Service Engr.
Bischoff Environmental Systems
135 Cumberland Rd.
Pittsburgh, PA 15237
412/364-8860

Michael Duncan
Project Enginner
Air Pollution Tech., Inc.
5191 Santa Fe Street
San Diego, CA 92109
619-272-0050

Dewayne E. Durst
Tech. Advisor
U.S. EPA
324 E. 11th St.
Kansas City, MO 64106
816/374-3791

James L. DuBard
Sr. Physicist
Southern Research Inst.
2000 Ninth Ave. So.
Birmingham, AL 35255
205/323-6592

Fitzroy A. Dyer
Project Manager
Church & Dwight Co., Inc.
20 Kingsbridge Road
Piscataway, NJ 08854
201-885-1220

Richard T. Egan
Mgr. Market Development
Munters Corp.
P.O. Box 6428
Ft. Myers, FL 33904
813/936-1555

Brooke Eldredge
Conferences & Travel Coordinator
Electric Power Research Inst.
3412 Hillview Ave.
Palo Alto, CA 94303
415/855-7919

David Elkins
Manager, Unit 3
Dayton Power & Light
Box 468
Aberdeen, OH 45101
513/795-2672

Monte R. Elmore
Research Engr.
Battelle Northwest
Battelle Blvd.
Richland, WA 99352
509/375-2311

Robert D. Emerson
Plant Engineer
Sunflower Electric Coop
P.O. Box 430
Holcomb, KA 67851
316/277-2590

Heinz L. Engelbrecht
Director R/D
Wheelabrator-Frye, Inc.
5100 Castell Dr.
Coraopolis, PA 15108
412-787-9710

David S. Ensor
Mgr. Aerosol Tech. Prog.
Reseach Triangle Inst.
P.O. Box 12194
Research Triangle Park, NC 27709
919/541-6735

Paul S. Farber
Consultant
P. Farber & Assoc.
7619 Virginia Ct.
Willowbrook, IL 60514
312/920-8227

Greg Faulkner
Research Physicist
Southern Research Inst.
P.O. Box 55305
Birmingham, AL 35255-5305
205/323-6592

James Fehr
Mechanical Engineer
Nebraska Public Power Dist.
P.O. Box 499
Columbus, NE 68601
402-563-5394

Paul Feldman
Manager, Physical Process Dev.
Research-Cottrell
P.O. Box 1500
Somerville, NJ 08876
201-685-4880

Larry G. Felix
Prog. Mgr. for Fabric Filter Eval.
Southern Research Inst.
P.O. Box 55305
Birmingham, AL 35255
205/323-6592

Stephen W. Felix
Sales Engineer
Huyck Felt
Washington Street
Rensselaer, NY 12144
518-445-2754

Alan Ferguson
Systems Engineer
Black & Veatch
1500 Meadowlake Parkway
Kansas City, MO 64114
913/967-2190

James J. Ferrigan
Regional Sales Manager
WAHLCO, INC.
P.O. Box 3141
Princeton, NJ 08540
201-238-7300

Donald H. Fiedler
Mgr., Market Development
Phillips Fibers Corp.
I-85 & Ridge Rd., Box 66
Greenville, SC 29602
803/242-6600 EXT.219

Ervin Fields
Project Engr.
Carolina Power & Light
P.O. Box 1551 3A3
Raleigh, NC 27602
919/836-7397

Wright C. Finney
Associate in Research
Dept. of Physics
Florida State Un.
Tallahassee, FL 32306
904/644-2878

Richard A. Fitch
President
Lucidyne, Inc.
4235 Ponderosa Ave.
San Diego, CA 92123
619/571-7032

Harold R. Fletcher
Air Pollution Control Equip. Engr.
Detroit Edison Company
2000 Second Ave.
Detroit, MI 48226
313-897-1315

Peter E. Frankenburg
Research Associate
Du Pont
Chestnut Run
Wilmington, DE 19898
302-999-4858

William F. Frazier
Staff Engr.
VEPCO
P.O. Box 26666
Richmond, VA 23261
804/775-5285

Norman W. Frisch
President
N.W. Frisch Assoc., Inc.
P.O. Box 582
Kingston, NJ 08528
609/924-1144

M. Frischenmeyer
Sales Mgr.
National Filter Media
8895 Deerfield
Olive, MS 38654
601/895-4660

Jim Fulton
Plant Engr., Operations
Baltimore Gas & Electric
P.O. Box 1475
Baltimore, MD 21203
301/234-7624

Peter W. Funnell
Mgr. Environmental Systems
Flakt Australia Ltd.
P.o. Box 42
St. Leonards NSW Australia 2065
(2) 439-8000

Pamela Gadd
President
Sonic Engineering, Inc.
P.O. Box 8358
Coral Springs, FL 33075
305-753-7281

Joseph L. Gaines
Senior Staff Engineer
Rust International Corp.
1130 So. 22nd St.
Birmingham, AL 35205
205/254-4517

Charles A. Gallaer
Consultant
Self Employed
1801 Tyburn Ln.
Pittsburgh, PA 15241
412/221-1762

Duane Galloway
Director, Env. Engr.
City Utilities
301 E. Central
Springfield, MO 65802
417/831-8501

Mark A. Garner
Environmental Technician
Granite City Steel
20th & State Sts.
Granite City, IL 62040
618-451-4023

Gary Gawreluk
Product Manager
Research-Cottrell
Box 1500
Sommerville, NJ 08876
201/685-4288

Peter Gelfand
President
P. Gelfand Assoc.
56 Friar Lane
Trumbull, CT 06611
203/377-4464

Michael Gervasi
Speaker
Philadelphia Electric Co.
R.D. 3, Box 12
Phoenixville, PA 19460
215/933-8995

Darlene R. Gilbert
Sales Operations Mgr.
W.W. Criswell
800 Industrial Hwy.
Riverton, NJ 08077
609/829-6300

Dan Giovanni
Consultant
Electric Power Technologies
Box 990
Antioch, CA 94509
415/757-8008

Robert J. Gleason
Director R & D
Research-Cottrell, Inc.
P.O. Box 1500
Somerville, NJ 08876
201-685-4884

Peter K. Goldbrunner
Proj. Mgr.
Burns & Roe
800 Kinderkamack Rd.
Oradell, NJ 07649
201/265-2000 X-2703

John P. Gooch
Head, Control Device Reseach Div.
Southern Research Inst.
P.O. Box 55305
Birmingham, AL 35255-5305
205/323-6592, X-2446

Dennis Greashaber
Assistant Supt.-Results
Missouri Public Serv. Co.
P.O. Box 408
Sibley, MO 64088
816/249-6196

Bob Green
Mgr. APC
Apptech
2 Kent St.
Belmore, 2192 NSW Australia
412/288-7416

Jack H. Greene
Administrative Officer
U.S. EPA-IERL
MD-61
Research Triangle Park, NC 27711
919/541-2903

Gary P. Greiner
Exec. Vice President
ETS, Inc.
3140 Chaparral Dr., S.W., C-103
Roanoke, VA 24018-4394
703/774-8999

James Gross
Pollution Control Spec.
Regional Air Pollution Control
451 W. 3rd. St.
Dayton, OH 45422
513/225-4435

Theron Grubb
Technical Director
W.W. Criswell Co./Signal
800 Industrial Hwy.
Riverton, NJ 08077
609/829-6300

John T. Guffre
Regional Sales Manager
WAHLCO, INC.
5775-E Peachtree Dunwoody Rd.
Atlanta, GA 30342
404-255-8300

John M. Gustke
N/A
Black & Veatch Eng.-Architects
P.O. Box 8405
Kansas City, MO 64114
913/967-2000

Joseph Hahn
International Sales Mgr.
Dresser Industries, Inc.
601 Jefferson
Houston, TX 77002
713/750-2092

H. J. Hall
President
H.J. Hall Assoc., Inc.
1250 State Rd.
Princeton, NJ 08540
609/924-1933

Jim Hall
Sales manager
Envirocare
100 Galli Dr.
Navato, CA 94947
415/883-3594

Ole H. Hansson
Vice Executive, Sales Indus. Equip.
F.L. Smidth & Co. A/S
77 Vigorslev Alle DK-2500
Copenhagen, Denmark
(01) 30 11 66

Douglas E. Hardesty
Air Quality Engr. Specialist
Air Quality Bureau
450 W. State-5th Floor
Boise, ID 83720
208-334-5360

John Harman
Regional Mgr.
Martin Marietta Basic Prod.
Executive Plaza II
Hunt Valley, MD 21030
301/667-0200

Dale L. Harmon
Chemical Engineer
U.S. EPA-IERL
MD-61
Research Triangle Park, NC 27711
919/541-2429

Mike Hasenkamp
Electrical Engineer
Nebraska Public Power Dist.
P.O. Box 499
Columbus, NE 68601
402-563-5394

Victoria Hathaway-Sarver
Pollution Control Spec.
Regional Air Pollution Contl. Agy.
451 W. 3rd. St.
Dayton, OH 45422
513/225-4435

Dennis W. Haverlah
Air Quality Supv.
L. C. R. A.
P. O. Box 220
Austin, TX 78613
512/473-3215

J. T. Headley
Division VP
Midwesco
1126 E. Driftwood Dr.
Tempe, AZ 85283
602/894-1165

H. Heer
Mgr. Gas Cleaning Div.
Rothemuehle
P.O. Box 5140
Olpeiwenden, West Germany 5963
02762-611314

Willard G. Henkel
Marketing Strategy Mgr.
Du Pont Co.
Textile Fibers Dept.Centre Rd. Bldg
Wilmington, DE 19898
302/999-3096

Robert A. Herrick
Dir., Envirn. Engr. & Tech.
Owens Corning Fiberglass
Fiberglass Tower
Toledo, OH 43659
419/248-7126

T. R. Hewitt
Environmental Design Manager
CRS Sirrine, Inc.
P.O. Box 12748
Research Triangle Park, NC 27709
919/541-2081

David J. Hickey
President
Boiler Equipment Serv. Co.
2310 Perimeter Park
Atlanta, GA 30341
404/452-8811

John J. Hiers
Product Dev. Mgr.
Lydall, Inc. Westex Div.
P.O. Box 109
Hamptonville, NC 27020
919/468-8522

John W. Hilborn
Engineer
Ohio Edison Company
76 South Main St.
Akron, OH 44308
216-384-5768

Wanda Hooks
Prod. Chemist
Southwestern Public Serv. Co.
P.O. Box 1261
Amarillo, TX 79170
806/381-6246

Richard G. Hooper
Project Manager
Electric Power Research Inst.
P.O. Box 10577
Denver, CO 80210
303/936-7281

Charles B. Hotchkiss
Marketing Manager
Menardi-Southern Corp.
1201 Francisco St.
Torrance, CA 90502
213-321-8910

Louis S. Hovis
Chemical Engineer
U.S. EPA
MD-61
Research Triangle Park, NC 27711
919/541-3374

Tom Hoyne
Sr. Business Rep.
General Electric Co.
9350 Flair Dr.
El Monte, CA 91731
818-572-5207

Albert Hudson
Consulting Engr.
Environmental Management Assocs.
7201 Wellington Drive
Knoxville, TN 37919
615/588-0330

John A. Hudspeth
Engineer
Southwestern Public Serv.
P.O. Box 1261
Amarillo, TX 79170
806/965-2194

Martin Hughes
Associate Professor
VA Polytechnic Inst. & University
Dept. of Civil Engineering
Blacksburg, VA 24061
703/961-6635

Bill Ingesson
Mgr. Precipitator Tech.
Flakt Industri AB
351 87
Vaxjo, Sweden
0470-87000

Clyde Ingraham
Dir. of Technical Serv.
Westmoreland Coal Co.
2500 Fidelity Bldg.
Philadelphia, PA 19109
215-545-2500

Lee Ivey
Sales Representative
Burlington Glass
14567 Croton Road
Centerburg, OH 43011
614/363-1415

Steve Jaasund
Industrial Sales Mgr.
Dresser Industries, Inc.
601 Jefferson
Houston, TX 77002
713/750-2092

Sam Jacobson
Western Regional Mgr.
Munters Corp.
1205 Sixth St.
Ft. Myers, FL 33907
813/936-1555

Lawson F. Jenkins
Maintenance Engr.
Duke Power Co.
P.O. Box 33189, 400 Tryon St.
Charlotte, NC 28242
704/373-7541

Robert M. Jensen
Engineering Specialist
Bechtel Power Corp.
50 Beale St.
San Francisco, CA 94119
415/768-2842

H. F. Johnson
Mgr., Research & Development
James Howden Australia PTY Ltd.
North Sydney, 2060, P.O. Box 84
North Sydney, Australia
929-4566

Michael E. Johnson
Associate
W. L. Gore & Associates, Inc.
P.O. Box 1010
Elkton, MD 21921
301-392-3200

Robert Johnson
Regional Sales Manager
Belco Pollution Control
119 Littleton Road
Parsippany, NJ 07054
201/263-8900

Robert E. Jonelis
President
Midwest Power Corp.
3960 Industrial Avenue
RollingMeadows, IL 60008
312/870-2400

Allen Jorgensen
Area Sales Mgr.
Dresser Industries, Inc.
601 Jefferson
Houston, TX 77002
713/750-2092

Marie Kalinowski
Scientist
Owens-Corning Fiberglas
Rt. 16
Granville, OH 43023
614/587-7620

Gregory A. Kallio
Graduate Student
Washington State University
Dept. of Mechanical Engineering
Pullman, WA 99164-2920
509/335-1027

Tom Kalman
Air Quality Engr.
Ohio EPA
361 East Broad St.
Columbus, OH 43215
614/462-6283

Joe Kaminski
Engineering Technician
TECO
P.O. Box 111
Tampa, FL 33601
813/247-2629

Bill Kamm
Results Engineer
KC Board of Public Utilities
700 Minnesota Ave.
Kansas City, KS 66101
913-281-8366

Edward R. Kashdan
Environmental Engineer
Research Triangle Inst.
P.O. Box 12194
Research Triangle Park, NC 27709
919/541-6749

Don Kawecki
Field Service Engineer
Foster Wheeler Energy Corp.
110 S. Orange Ave.
Livingston, NJ 07039
402/873-9116

William Kemner
Assistant Dir. Engr.
PEDCO Env.
11499 Chester Road
Cincinnati, OH 45246
513/782-4700

Henry Kemp
Principal Engineer
Baltimore Gas & Electric Co.
P.O. Box 1475
Baltimore, MD 21203
301/787-5332

Mark Kercheval
Dev. Engr.
ENELCO
7249 National Dr.
Hanover, MD 21076
301/796-8622

Jim Kessling
Sr. Engr.
Houston Lighting & Power
12301 Kurland St.
Houston, TX 77034
713/481-7921

Carl R. King
Project Engineer
Cleveland Electric Ill.
55 Public Sq.
Cleveland, OH 44101
216-622-9800 X3262

John A. Knapik
Manager, Engineering
Neundorfer Engineered Equipment
4590 Hamann Pkwy.
Willoughby, OH 44094
216/942-8990

Phillip W. Kobett
Supv. Design Engr.
Nevada Power Co.
P.O. Box 230
Las Vegas, NV 89151
702/367-5671

Thomas E. Kobett
Vice President
AMCA Eng. & Constructors
P.O. Box 1281
Houston, TX 77251-1281
713/497-6200

John Kolbe
Service Engr.
Martin Marietta Basic Prod.
Executive Plaza II
Hunt Valley, MD 21030
301/667-0200

Wayne R. Kozacka
Chief Mechanical Engineer
WAHLCO, INC.
3600 W. Segerstrom Ave.
Santa Ana, CA 92704
714-979-7300

Henry V. Krigmont
Applications Engr.
Joy Industrial Equipment Co.
4565 Colorado Blvd.
Los Angeles, CA 90015
213/240-2300

Peter M. Kutemeyer
General Mgr.
Bischoff Environmental Systems
135 Cumberland Rd.
Pittsburgh, PA 15237
412/364-8860

John S. Lagarias
Director, Environmental Quality
Raymond-Kaiser Engineers
F. Box 23210
Oakland, CA 94623
415/271-5207

George E. Lamb
Principal Scientist
Textile Research Inst.
P.O. Box 625
Princeton, NJ 08542
609/924-3150

Carl Landham
Arapahoe Facility Ops. Mgr.
Southern Research Inst.
P.O. Box 10155
Denver, CO 80210
303/922-9764

Joseph B. Landwehr
Air Quality Design Section Chief
Burns & McDonnell Eng.-Architects
4800 E. 63rd St.
Kansas City, MO 64141
816/333-4375

Ellen Lanum
Conferences & Travel Supv.
Electric Power Research Inst.
3412 Hillview Ave.
Palo Alto, CA 94303
415/855-2193

Rick Lassahn
Principal Engineer
Baltimore Gas & Electric
P.O. Box 1475
Baltimore, MD 21203
301/7887-5377

Kenneth W. Lau
Marketing Prog. Mgr.
E.I. du Pont de Nemours & Co.
PPD Dept.-Rm.D11084, 1007 Market St
Wilmington, DE 19898
302/774-9460

Preben Lausen
Chief Engr.
F.L. Smidth & Co. A/S
Vigerslev Alle 77, DK 2500
Copenhagen-Valby, Denmark
(01) 30 11 66

Lloyd L. Lavely, Jr.
Regional Mgr.
Research Cottrell
6701 W. 64th St., Ste. 212
Shawnee Mission, KS 66202
913/432-8288

Philip A. Lawless
Research Physicist
Research Triangle Inst.
P.O. Box 12194
Research Triangle Park, NC 27709
919/541-6782

Bob Lawrence
President
KPN International Inc.
19 Pebble Road
Newtown, CT 06470
203/426-3639

David Lehman
Techinical Support Superintendent
Public Service Co. of Oklahoma
P.O. Box 220
Oologah, OK 74053
918/443-2322

Carl V. Leunig
Dir. of Engineering
Albany International
P.O. Box 1109
Albany, NY 12201
518/447-6562

Daniel A. Lisiecki
Asst. V.P. Air Pollution Contl Dept
F.L. Smidth & Co.
300 Knickerbocker Rd.
Cresskill, NJ 07626
201/871-3300

Jack D. Lokey, Jr.
Environmental Engr.
TVA
n/a
Muscle Shoals, AL 35660
205/386-2033

David Lombardi
Mgr. Prod. Applications
Martin Marietta Basic Prod.
Executive Plaza II
Hunt Valley, MD 21030
301/667-0200

Thomas A. Lott
Engineer
Pacific Gas & Electric Co.
3400 Crow Canyon Rd.
San Ramon, CA 94583
415-820-2000

Wayne C. Love
Project Engineer
Florida Power Corp.
3201 34th St. So.
St. Petersburg, FL 33733
813-866-4755

Jim Lund
Sales Manager
BHA
8800 E. 63rd St.
Kansas City, MO 64133
816/356-8400

Sharon Luongo
Conferences & Travel Coordinator
Electric Power Research Inst.
3412 Hillview Ave.
Palo Alto, CA 94303
415/855-2010

Gary Maier
Project Manager
Florida Power & Light Co.
P.O. Box 14000
Juno Beach, FL 33408
305/863-3608

Bert Marker
Staff Engineer
NY State Electric & Gas
4500 Vestal Parkway
Binghamton, NY 13902
607-729-2551

Thom Martin
Mgr, Engr. System Sales
BHA
8800 E.63rd St.
Kansas City, MO 64133
816-356-8400

Veronica Martinez
Chemical Engineer
Franklin Associates
8340 Mission
Prairie Village, KS 66202
913/649-2225

Robert Marzoli
Division V.P. of Sales
Midwesco, Inc.
P.O. Box 2075
Winchester, VA 22601
703-667-8500X252

Senichi Masuda
Professor
Un. of Tokyo, Dept. of E. E.
7-3-1, Hongo, Bunkyo-ku
Tokyo, Japan 113
812-2111, EXT. 6653

LaRoy Mathews
Research Specialist
Southern Co. Services
P.O. Box 2625
Birmingham, AL 35202
205/877-7614

James D. Mathis
Mech. Engr.
Lower Colorado River Authority
P.O. Box 220
Austin, TX 78767
512/473-3546

Paul Mattes
Electrical Maint. Foreman
Northern Indiana Public Serv.
Rt. 1, Box 320
Wheatfield, IN 46392
219/956-5124

Gernot Mayer-Schwinning
Sr. Manager
Lurgi GmbH
Gwinnerstrasse 27/33, d-6000
Frankfurt am Main 60, West Germany
0 69 4011-262

Gary E. McArthur
Permits Engr.
Texas Air Quality Board
6330 Hwy. 290 East
Austin, TX 78723
512/451-5711

William J. McCabe
Design Engr. II
Duke Power Co.
522 S. Chruch
Charlotte, NC 28242
704/373-8764

James McCauley
Lead Engr.
Public Serv. Electric & Gas
80 Park Plaza
Newark, NJ 07101
201/430-7360

Les McEvoy
Chief Technical Engr.
Dresser Industries, Inc.
601 Jefferson
Houston, TX 77002
713/750-2092

John McGovern
Member Services Mgr.
Air Pollution Control Assoc.
P.O. Box 2861
Pittsburgh, PA 15230
412/621-1090

Marilyn McIlvaine
Editor
McIvaine Co.
2970 Maria Ave.
Northbrook, IL 60062
312/272-0010

Robert McIlvaine
President
McIlvaine Co.
2970 Maria Ave.
Northbrook, IL 60062
312/272-0010

John D. McKenna
President
ETS, Inc.
3140 Chaparral Dr., S.W., C-103
Roanoke, VA 24018
703/774-8999

B. G. McKinney
Regional Mgr.
Electric Power Research Inst.
516 Franklin Bldg.
Chattanooga, TN 37411
615/899-0072

B. R. McLaughlin
Supervising Process Engr..
United Engineers & Constr. Inc.
23 Inverness Way East
Englewood, CO 80112
303-790-7310

Kenneth J. McLean
Reader
University of Wollongong
P.O. Box 1144
Wollongong N.S.W. 2500, Australia
(042) 297311

Richard D. McRanie
Mngr., Part. Control & Combustion
Southern Services, Inc.
P.O. Box 2625
Birmingham, AL 35207
202/870-6332

John Meinders
Senior Mechanical Engr.
KC Board of Public Utilities
700 Minnesota Ave.
Kansas City, KS 66101
913-281-8366

Randy L. Merritt
Research Physicist
Southern Research Inst.
P.O. Box 55305
Birmingham, AL 35255-5305
205/323-6592

Sheldon Meyers
Deputy Asst. Admin.
U.S. EPA
401 M. St., S.W.
Washington, DC 20460
202/382-7400

H. I. Milde
Division Manager
Ion Physics Co.
F. C. Box 416
Burlington, MA 01803
617/272-2800

Michael J. Miller
Technical Specialist
Electric Power Rersearch Inst.
P.O. Box 10412
Palo Alto, CA 94303
415/855-2461

Richard K. Miller
Mechnical Engr.
Dayton Power & Light Co.
P.O. Box 1247 Courthouse Plaza S.W.
Dayton, OH 45401
513/224-5974

Stanley J. Miller
Research Sup., Particulate Char.
University of ND Energy Res. Ctr.
P.O. Box 8213 University Sta.
Grand Forks, ND 58202
701/777-5210

Glenn Mitchell
Sales & Serv. Engr.
Martin Marietta Basic Prod.
Executive Plaza II
Hunt Valley, MD 21030
301/667-0200

Gus T. Monahu
Consulting Engineer
Ash Systems Engineering
160 Bond St.
Elk Grove, IL 60007
312/437-5224

Barry Morris
N/A
Textile Research Inst.
P.O. Box 625
Princeton, NJ 08542
609/924-3150

Dana S. Morris
Environ. Engr.
Ks. Dept. of Health & Environ.
Forbes Field
Topeka, KS 66620
913/862-9360 X-273

Mike Morris
N/A
General Electric
P.O. Box 2044
Overland Park, KS 66201
913/967-6272

Ronald B. Mosley
Mgr. Tech. Services
Crestmont Associates, Inc.
235 Main St., Suite 202
Trussville, AL 35173
205/655-7801

Robert B. Moyer
Manager, Fabric Filters
Research-Cottrell, Inc.
P.O. Box 1500
Somerville, NJ 08876
201/685-4000

Leonard W. Muscelli
Sr. Marketing Specialist
Dupont Co.
Centre Rd. Bldg.
Wilmington, DE 19898
302/999-4607

John Mycock
Vice President
ETS, Inc.
3140 Chaparral
Roanoke, VA 24016
703/774-8999

Mike Nelson
Sr. Engr.
Southern Services Co.
P.O. Box 2625
Birmingham, AL 35202
205/870-6518

Franz Neulinger
Lurgi Gmbh
Gervinusstrasse 17/19,D-6000
Frankfurt am Main 1
West Germany
0 69 157-3792

Grady B. Nichols
Director, Res. & Envir. Science
Southern Research Inst.
2000 9th Ave., S.
Birmingham, AL 35255

Joseph Niemeyer
Systems Engineer
Lucidyne, Inc. Ave.
4235 Ponderosa Ave.
San Diego, CA 92123
619-571-7032

Gary M. Nishioka
N/A
Owens Corning Fiberglas
Rt. 16, Technical Center
Granville, OH 43023
614/587-7612

Leslie M. Noland
Regional Mgr.
Martin Marietta Basic Prod.
Executive Plaza II
Hunt Valley, MD 21030
301/667-0200

John P. O'Connor
Senior Engineer
Public Serv. Electric & Gas
P.O. Box 570
Newark, NJ 07101
201/430-8240

David O'Hara
Research Assistant
Florida State Un.
FSU Physics Dept.
Tallahassee, FL 32306
904/644-2867

Allan Oestmann
Environmental Coordinator
Kiewit Mining & Engineering
1000 Kiewit Plaza
Omaha, NE 68131
402/342-2052

Gene Ogilvie
V.P., Division Mgr.
Midwesco, Inc.
P.O. Box 2075
Winchester, VA 22601
703-667-8500X253

Sabert Oglesby, Jr.
President
Southern Research Institute
P.O. Box 55305
Birmingham, AL 35255
205-323-6592

Sidney R. Orem
N/A
Industrial Gas Cleaning Inst.
700 N. Fairfax St., Ste. 304
Alexandria, VA 22314
703/836-0480

Herman R. Osmers
President
Chemical Engr. & Policy Analyses
1835 St. Paul St., Suite 105
Rochester, NY 14621
716-544-9277

Ronald G. Ostendorf
Sr. Engr.
Proctor & Gamble Co.
7162 Reading Rd.
Cincinnati, OH 45222
513/763-4457

John E. Paul
n/a
Paul & McDonald Assoc., Inc.
P.O. Box 360626
Birmingham, AL 35236-0626
205/988-8L92

Randy Peltier
Tech. Director
United Air Specialists
4440 Creedk Rd.
Cincinnati, OH 45242
513/891-0400

Rowan P. Perkins
Sr. Consultant
E.I. Dupont De Nemours
Engineering Dept., L-3364
Wilmington, DE 19898
302/366-2603

John Perry
Supervisory Design Engineer
Southwestern Public Service Co.
P.O. Box 1261
Amarillo, TX 79170
806/378-2121

Jim Petrie
Director
C. P. Environmental, Inc.
15 W. 700 Frontage Rd.
Hinsdale, IL 60521
312-985-4800

Leo Pflug
Mgr. Particulate Start-up
Research-Cottrell, Inc.
P. O. Box 1500
Somerville, NJ 08876
201-685-4297

B. D. Pfoutz
V. P. & Division Mgr.
Belco Pollution Control Corp.
119 Littleton Rd.
Parsippany, NJ 07054
201-263-8900

N. D. Phillips
Sr. Project Engr.-A.P.C.
Fuller Co.
2040 Avenue C
Bethlehem, PA 18001
215-264-6850

Walter E. Piulle
Project Manager
Electric Power Research Inst.
P.O. Box 10412
Palo Alto, CA 94303
415/855-2470

Norman Plaks
Chief, Particulate Tech. Branch
U.S. EPA-IERL
MD-61
Research Triangle Park, NC 27711
919/541-3084

Everett L. Plyler
Dir., Utilities & Ind. Power Div.
U.S. EPA-IERL
MD-61
Research Triangle Park, NC 27711
919/541-2918

Jack Podhorski
Regional Sales Manager
Joy Manufacturing Co.
P.O. Box 2744 Terminal Annex
Los Angeles, CA 90051
818/240-2300

Duane H. Pontius
Head, Applied Science Section
Southern Research Inst.
P.O. Box 55305
Birmingham, AL 35255-5305
205/323-6592

Kjell Porle
Mgr. Air Pollution Tech.
Flakt Industri AB
351 87
Vaxjo, Sweden
0470-87415

Bill Poundstone
Coal Consultant
BHA Company
8800 E. 63rd
Kansas City, MO 64133
N/A

Jon P. Power
Sr. Emissions Control Engr.
Central & Southwest Servs. Inc.
2121 Sna Jacinto St.
Dallas, TX 75266-0164
214/754-1371

Charles A. Prebay
Prod. Line Mgr.
K.V.B., Inc.
18006 SkyPark Blvd.
Irvine, CA 92714
714/250-6200

George T. Preston
Dept. Dir., Env. Control Sys.
Electric Power Research Inst.
P.O. Box 10412
Palo Alto, CA 94303
415/855-2000

Keith Price
Market Mgr.
Burlington Glass Fabrics Co.
1345 Ave. of Americas
New York, NY 10105
212/621-1109

Frank T. Princiotta
Director
U.S. EPA
IERL-RTP MD-60
Research Triangle Park, NC 27711
919/541-2821

Bobby E. Pyle
Research Physicist
Southern Reseach Inst.
P.O. Box 55305
Birmingham, AL 35255-5305
205/323-2547

Tim Quarles
Mechanical Engineer
Navy Energy & Envir.
Code 111 C
Port Hueneme, CA 93043
805/982-5292

Todd Quattlebaum
Proposal Administrator
Dresser Industries, Inc.
601 Jefferson
Houston, TX 77002
713/750-2092

Stig Rasmussen
Project Manager
A/S Niro Atomizer
305 Gladsaxevej DK 2860
Soeborg Denmark
01-691011

Steve Rees
Marketing Manager
Clean Air Eng., Inc.
207 N. Woodwork Lane
Palatine, IL 60067
312/991-3300

James L. Renner
Chemical Engineer
Colorado-Ute Electric Assn.
P.O. Box 1149
Montrose, CO 81402
303-249-4501

Robert L. Reveley
Vice President
WAHLCO, INC.
3600 W. Segerstrom Ave.
Santa Ana, CA 92704
714-979-7300

James B. Rhodes
Marketing Mgr.
Du Pont Co.
Centre Rd. Bldg.
Wilmington, DE 19898
302/999-4601

Richard G. Rhudy
Proj. Mgr.
Electric Power Research Inst.
P.O. Box 10412
Palo Alto, CA 94303
415/855-2421

George A. Rinard
Mgr. Particulate Control Tech.
Denver Research Inst.
F Box 10127
Denver, CO 80210
303/753-2241

David Rinas
Mgr. Engineered Sales
Standard Havens Inc.
8800 East 63rd St.
Kansas City, MO 64133
816/737-0400

Gary H. Roberts
Project Engr.
New York State Electric & Gas
P.O. Box 29
Homer City, PA 15748
412/479-9011

Wayne J. Roberts
Coordinator, Monitoring & Samp.
Eastman Kodak Company
1669 Lake Avenue
Rochester, NY 14650
716/722-2363

Collin Robinson
Sales Mgr.
Tilghman Wheelabrator
P.O. Box 60 Altrincham
Cheshire Wa A 5 EP, England
011-44-61-928-6388

Edward C. Rosar
President
Industrial Resources, Inc.
300 Union Blvd. #520
Lakewood, CO 80228
303/986-4507

Norman A. Rosekrans
Reg. Sales Manager
Joy Mfg.
5775 Peachtree Dunwoody
Atlanta, GA 30342
404/256-2934

Donald L. Rowe
Project Engr.
Naval Surface Weapons Center
Code G51
Dahlgren, VA 22448
703/663-7641

Donald E. Rugg
Sr. Research Engr.
Denver Research Inst.
University Park - F Box 10127
Denver, CO 80210
303/871-2421

Donald H. Rullman
Vice President
Lurgi Corp.
666 Kinderkamack Rd.
River Edge, NJ 07661
201/967-4914

Reda A. Salib
Consulting Engr.
EBASCO Services, Inc.
160 Chubb Avenue
Lyndhurst, NJ 07738
201/460-5907

Robert E. Sandberg
Electrical Engr.
Mississippi Power Co.
P.O. Box 4079
Gulfport, MS 39501
601/868-0218

Anthony A. Santilli
President
San Kris Market Tech, Inc.
P.O. Box 261
Westbury, NY 11590
516-333-3444

Stephen K. Santoro
Engineering Mgr.
Cogeneration Mgmt., Inc.
474 Brookline Ave.
Boston, MA 02215
617/732-2354

Masayaki Sato
Research Assistant
Florida State Un.
Physics Dept.
Tallahassee, FL 32306
904/644-6246

Hubert Satterfield
Sales Mgr.
STI/Environecs, Inc.
3601 Moore Avenue
Santa Ana, CA 92704
714/957-6916

Rick Savoie
Sr. Technologist
Consumers Power Co.
1945 Parnall Rd.
Jackson, MI 49201
517/788-1608

Martin Schiller
President
CSI Engineering
P.O. Box 1515
Fairfield, CT 06432
203-372-8790

Morten Schioth
Engr.
F.L. Smidth & Co. A/S
Vigerslev Alle 77, DK-2500
Copenhagen-Valby, Denmark
(01) 30 11 66

Loran Schmidt
Senior Project Coord.
Cadre Envn. Systems
P.O. Box 47860
Atlanta, GA 30362
404/458-9527

Ralph Schoemer
Assist. Product Mgr.
Wheelabrator APC Division
600 Grant Street
Pittsburgh, PA 15219
412-288-7479

Fred Schuler
Sr. Project Engr.
Donaldson Co., Inc.
P.O. Box 1299
Minneapolis, MN 55440
612/887-3644

Robert J. Schwabe
Electrical Engineer
General Electric
1 River Road
Schenectady, NY 12301
518/385-8308

Ray Schwarten
President
Sonic Power Systems
P.O. Box 12785
Lenexa, KS 66212
913/888-1929

Leland H. Scott
Senior Engr.
Armco, Inc.
7000 Roberts
Kansas City, MO 64125
816/242-5851

Sankar Seetharama
Assist. Product Mgr.
Wheelabrator APC Division
600 Grant Street
Pittsburgh, PA 15219
412-288-7385

Richard Serrurier
Engineer
Southwestern Pub. Serv. Co.
P.O. Box 1261
Amarillo, TX 79170
806/378-2185

Raymond J. Shaffery
Director, Commercial Development
The Church & Dwight Co., Inc.
20 Kingsbridge Rd.
Piscataway, NJ 08854
201-855-1220

Navin D. Shah
Consultant
n/a
142 Sundance Court
Grand Junction, Co 81503
303/243-1503

James F. Sharman
Engineer
Public Service Co. of Colorado
5900 E. 39th Ave.
Denver, CO 80207
303/329-1150

Edward J. Shaughnessy
Assoc. Professor
Duke University
Dept. of Mech. Engineering
Durham, NC 27706
919/684-2832

Jack Shaughnessy
VP General Mfg.
Mikropul Corp.
10 Chatham Road
Summit, NJ 07901
201/273-6360

J. M. Shoults
Project Engineer
Texas Municipal Power Agency
P.O. Box 7000
Bryan, TX 77805
409/873-2013

Douglas V. Shuit
Electrical Engr.
Wisconsin Electric & Power
4801 E. Elm Rd.
Oakcreek, WI 531154
414/762-0325 X-217

Paul Sierer
Engr.
Philadelphia Electric Co.
2301 Market St., P.O. Box 8699
Philadelphia, PA 19101
215/841-5317

Fred Simmons
Mech. Engr.
Cadre Environmental Systems, Inc.
P.O. Box 47837
Atlanta, GA 30362
404/458-9521

Chris Skomorowski
Controller
Lydall, Inc.-Westex Div.
P.O. Box 109
Hamptonville, NC 27020
919-468-8522

Frank J. Skutta
Manager, Research & Planning
General Electric
200 N. 7th St.
Lebanon, PA 17042
717/274-7049

David G. Sloat
Sr. Emission Control Spec.
Sargent & Lundy
55 E. Monroe
Chicago, IL 60603
312-269-2784

Michael Smart
Dir. Prod. Dev. & Tech. Serv.
J.P. Stevens & Co., Inc.
P.O. Box 208
Greenville, SC 29602
803/239-4830

Walter R. Smit
Electrical Systems Engr.
Plains Electric G&T Coop Inc.
P.O. Box 6551
Albuquerque, NM 87197
505/884-1881

David E. Smith
Tech. Mgr.
FMC Corp.
2000 Market St.
Philadelphia, PA 19103
215/299-6000

Earl O. Smith
Project Manager
Black & Veatch
P.O. Box 8405
Kansas City, MO 64114
913-967-2643

Glenn Smith
Vice President
BHA
8800 E. 63rd St.
Kansas City, MO 64133
816/356-8400

Wallace B. Smith
Head, Physics Div.
Southern Research Inst.
P.O. Box 55305
Birmingham, AL 35255
205/323-6592

Gardiner Snyder
Service Supv.
General Electric Co.
1000 First Ave.
King of Prussia, PA 19406
215/962-6112

Juan Sohn
APC Mgr.
Whellabrator De Mexico
Apartado M-7472
Mexico 1 D.F.
1-905-560-5577

R. E. Sorvillo
Sr. Engr.
Northern Ind. Public Serv.
591 Marquette Mall
Michigan City, IN 46360
219/874-4231 X-343

Barry J. Southam
Mgr., Sales Engineering
WAHLCO, INC.
3600 W. Segerstrom Ave.
Santa Ana, CA 92704
714-979-7300

Leslie E. Sparks
Sr. Chemical Engr.
U.S. EPA
IERL, MD-61
Research Triangle Park, NC 27711
919/541-2458

Jim Spellman
Sr. Business Rep.
General Electric
8101 Stemmons Freeway
Texas 75247
214/688-6165

H. W. Spencer
Mgr. Advanced Tech.
Joy Manufacturing Co.
4565 Colorado Blvd.
Los Angeles, CA 90039
818/240-2300, X426

James J. Spivey
Section Head, Process Research
Research Triangle Inst.
P.O. Box 12194
Research Triangle Park, NC 27709
919/541-7272

William R. Stalker
Professional Engineer
n/a
126 Miller Ave.
Bridgewater, NJ 08807
201/526-9178

Howard Steiman
Senior Chemical Engineer
Boston Edison Co.
800 Boylston St., P-276
Boston, MA 02199
617/424-3298

John G. Stensland
Marketing Mgr.
FMC Corp.
1501 Woodfield Rd., Ste. 300 E.
Shaumburg, IL 60195
312/843-1700

Daniel Strein
Station Engr.
Pennlylvania Electric Co.
Homer City Sta., P.O. Box 29
Homer City, PA 15748
412/479-9011

James Stukel
Assoc. Dean & Dir. of Engr.
University of Illinois,Urbana-Champ
252 Admin. Bldg., 506 So. Wright St
Urbana, IL 61801
217/333-6963

Joseph J. Stuparich
Sr. Business Rep.
General Electric
3 Penn Center Plaza
Philadephia, PA 19102
215/241-5240

Herb Sturm
Div. V.P. Marketing Services
Midwestco Filter Media Resources
400 Battaile Dr.
Winchester, VA 22601
703/667-8

Thomas C. Sunter
Applications Engr.
C-E Air Preheater
P.O. Box 372
Wellsville, NY 14895
716/593-2700

Donald O. Swenson
Consulting Engr.
Black & Veatch Engr. & Arch.
1500 Meadow Lake Pkwy.
Kansas City, MO 64114
913/967-7426

Paul Swoboda
Project Engineer
Texas Municipal Power Agency
P.O. Box 7000
Bryan, TX 77805
409/873-2013

Michael F. Szabo
Group Supv.
PEDCO Environmental, Inc.
11499 Chester Rd.
Cincinnati, OH 45246
513/782-4700

Tom Tarnok
Product Manager
Joy Manufacturing Co.
4565 Colorado Blvd.
Los Angeles, CA 90039
818-240-2300

William E. Theisen
Mechanical Engineer
Nevada Power Co.
P.O. Box 230
Las Vegas, NV 89151
702/367-5670

Robert W. Tisone
Sr. Applications Engineer
Environmental Elements Corp.
3700 Koppers St.
Baltimore, MD 21227
301-368-7104

James K. Tompkins
Process Engr.
FMC Corp.
Box 8
Princeton, NJ 08540
609/452-2300 X-4039

Donald P. Tonn
Process Engr.
Babcock & Wilcox
20 S. Van Buren
Barberton, OH 44203
216/860-1986

Joseph M. Towarnicky
Staff Scientist
United McGill Corp.
2400 Fairwood Ave
Columbus, OH 43216
614/443-0192

John Trainor
Asst. Sales Mgr.
NWL Transformer
Rising Sun Road
Bordentown, NJ 08505
609-298-7300

Thomas N. Tucker
Area Supv.
S.W. Ohio Air Pollution Control
2400 Beekmon St.
Cincinnati, OH 45214
513/251-8777

A. V. Turchina
Engineer
Proctor & Gamble Co.
7162 Reading Rd.
Cincinnati, OH 45222
513/763-4365

Mohammad Vakili
Power Plant Engr.
Wisconsin Power & Light
222 W. Washington Ave.
Madison, WI 53703
608/252-3347

Douglas Van Osdell
Sr. Chemical Enginer
Research Triangle Inst.
P.O. Box 12194
Research Triangle Park, NC 27709
919-541-6785

A. T.M. Vandewalle
Projects Director
James Howden Australia P/L
97-103 Pacific Highway
North Sydney NSW 2060
02-929-4566

Andrew S. Viner
Chemical Engr.
Research Tringle Inst.
P.O. Box 12194
Research Triangle Park, NC 27709
919/541-6747

Noel H. Wagner
Sr. Project Engr.
Pennsylvania Power & Light Co.
2 N. 9th.
Allentown, PA 18101
215/770-5496

Bill Walker
President
Clean Air Engineering
207 Woodwork Lane
Palatine, IL 60067
312/991-3300

Frank H. Walker
Scientific Serv. Engr.
Electricity Comm. of New So. Wales
Hyde Park Tower, Cnr. Park & Elizab
Sydney, New So. Wales, Australia
268-8111

Alan Wall
Sales Mgr.
Fuller Power Corp.
6420 Hillcroft Rm. 503
Houston, TX 77081
713/771-3575

John Walter
Field Engr.
General Electric
1015 Locust
St. Louis, MO 63101
314/342-7695

Anthony Warburton
Sr. Engineer
Sierra Pacific Power Co.
P.O. Box 10100
Reno, NV 89520
702/789-4741

George Weber
President, Environmental Prod. Div.
Dresser Industries, Inc.
601 Jefferson
Houston, TX 77002
713/750-2092

Maurice W. Wei
Env. Engr. Mgr. Technology Dev.
Aluminum Co. of America
1501 Alcoa Bldg.
Pittsburgh, PA 15219
412/553-2085

A. W. Wesa
Principal Engr.
Detroit Edison
2000 Second Ave.
Detroit, MI 48226
313/237-8000

Melvin W. Westley
Sr. Technical Specialist
Dupont
Chestnut Run TSL
Wilmington, DE 19898
302/999-3243

Alan Whale
Sr. Product Engr.
Dresser Industries, Inc.
601 Jefferson
Houston, TX 77002
713/750-2092

Lloyd R. White
Process Dev. Spec.
3M Co.
3M Center, Bldg. 219-1s-01
St. Paul, MN 55144
612/736-9601

Ray Wilson
N/A
Southern Research Inst.
P.O. Box 895
Chattanhoochee, FL 32324
904/593-6273

Steve Wise
Sr. Sales Mgr.
Dresser Industries, Inc.
601 Jefferson
Houston, TX 77002
713/750-2092

Steve Wolf
Mechanical Engineer
Northern States Power
414 Nicollet Mall
Minneapolis, MN 55401
612/330-5624

Carole A. Wolff
Tech. Assist.
Illinois Pollution Contl. Bd.
309 W. Washington
Chicago, IL 60606
312/793-3620

Charles Wright
President
Filters for Industry
1340 E. Eighth St.
Tempe, AZ 85281
602/968-6447

Robert A. Wright
Mgr, Systems Engineering
Lucidyne, Inc.
4235 Ponderosa Ave.
San Diego, CA 92123
619-571-7032

T. Yoneda
Chief Engineer
Sinto Dust Collector
Toyoda Bldg. No 7-23, 4-Chome
Mei-EKI, Nagoya 450 Japan
412/288-7416

Paul Yosick
Regional Sales Mgr.
Flakt Inc.
10000 W. 75th St.
Merriam, KS 66204
913/262-6787

Earle F. Young, Jr.
Vice President
American Iron & Steel Inst.
1000 16th St. N.W.
Washington, D.C. 20036
202/452-7271

Ronald P. Young
Research Physicist
Southern Research Inst.
P.O. Box 55305
Birmingham, AL 35255-5305
205/323-6592

Shui-Chow Yung
Research Director
Air Pollution Tech., Inc.
5191 Santa Fe Street
San Diego, CA 92109
619-272-0050

George J. Ziegenhorn
Senior Environmental Engr.
ARCO Petroleum Products
400 E. Sibley Blvd.
Harvey, IL 60426
312/210-3359

Frank J. Zuccarini
Product Specialist
Nalco Chemical Co.
2901 Butterfield Rd.
Oak Brook, IL 60521
312/887-7500

T. E. Lippert
Westinghouse Electric Corporation
Research and Development Center
1310 Beulah Road
Pittsburgh, PA 15235
412/256-1395

Anna W. Wallace
Conference Coordinator
Research Triangle Institute
P. O. Box 12194
Research Triangle Park, NC 27709
919/541-6967